

***Tutti i fiori di tutti i domani sono nei semi di oggi***

*A papà, mamma ed Enrico*

*Con infinito amore*



**UNIVERSITÀ DEGLI STUDI DI NAPOLI**

**“FEDERICO II”**

**FACOLTA' DI FARMACIA**



Dottorato di Ricerca

in

"Scienza del Farmaco"

Ciclo XXIII 2007-2010

***“Chemical analysis of toxic microalgae from  
Mediterranean Sea”***

**Tutor**

Ch.ma Prof.ssa

Patrizia Ciminiello

**Candidata**

Dott.ssa

Emma Dello Iacovo

**Coordinatore**

Ch.ma Prof.ssa

Maria Valeria D'Auria

---

## Index

<b>Abstract</b> .....	pag 7
<b>Presentazione dell'attività di ricerca e dei risultati ottenuti</b> .....	pag 11
<b>Introduction</b> .....	pag 15
<b>Chapter 1</b> .....	<b>pag 17</b>
<b>1.1. Analytical methods</b> .....	pag 17
1.1.1. Mass Spectrometry .....	pag 17
1.1.2. Nuclear Magnetic Resonance .....	pag 30
<b>1.2. Analytical methods to detect biotoxins</b> .....	pag 32
1.2.1. Biological assays: mouse toxicity .....	pag 33
1.2.2. Instrumental assays: LC-MS .....	pag 34
<b>1.3. References</b> .....	pag 35
<b>Chapter 2</b> .....	<b>pag 37</b>
<b>2.1. Marine plankton</b> .....	pag 37
2.1.1. Classification .....	pag 38
2.1.2. Globalization and Increase of the algal blooms .....	pag 40
<b>2.2. Conclusions</b> .....	pag 42
<b>2.3. References</b> .....	pag 43
<b>Chapter 3</b> .....	<b>pag 45</b>
<b>3.1. Mediterranean harmful algal events: marine biotoxins</b> .....	pag 45
3.1.1. Distribution of algal toxins in Mediterranean Sea .....	pag 49
3.1.2. Saxitoxins .....	pag 50
3.1.3. Okadaic acid .....	pag 51
3.1.4. Yessotoxins .....	pag 53
3.1.5. Domoic acid .....	pag 54
3.1.6. Pectenotoxins .....	pag 56

---

3.1.7. Spirolides .....	pag 57
3.1.8. Palytoxins .....	pag 58
<b>3.2. Recent insights into the latest Mediterranean toxic outbreaks .....</b>	<b>pag 60</b>
3.2.1. Historical background .....	pag 60
3.2.2. Occurrence of Spirolides in phytoplankton and mussels from Ardiatic Sea .....	pag 61
3.2.3. <i>Ostreopsis spp.</i> Blooms and palytoxins outbreaks in the Mediterranean Sea .....	pag 63
<b>3.3. Conclusions .....</b>	<b>pag 67</b>
<b>3.4. References .....</b>	<b>pag 68</b>
<b>Chapter 4 .....</b>	<b>pag 81</b>
<b>4.1. Marine invertebrates contamination .....</b>	<b>pag 81</b>
4.1.1. Biotoxins in Italy .....	pag 82
4.1.2. Maximum content of the algal biotoxins in shellfish .....	pag 84
<b>4.2. References .....</b>	<b>pag 84</b>
<b>Chapter 5 .....</b>	<b>pag 87</b>
<b>Identification of four new ovatoxins from <i>Ostreopsis ovata</i></b>	
<b>5.1. Experimental .....</b>	<b>pag 87</b>
5.1.1. Reagents .....	pag 87
5.1.2. Batch culture of <i>Ostreopsis ovata</i> .....	pag 87
5.1.3. Extraction .....	pag 88
5.1.4. Liquid Chromatography-Mass Spectrometry .....	pag 88
<b>5.2. Results and Discussion .....</b>	<b>pag 89</b>
<b>5.3. Future Perspectives .....</b>	<b>pag 104</b>
<b>5.4. References .....</b>	<b>pag 104</b>
<b>Chapter 6 .....</b>	<b>pag 105</b>
<b>Monitoring of <i>Ostreopsis ovata</i> along the Campania coasts</b>	
<b>6.1. Experimental .....</b>	<b>pag 108</b>

6.1.1. Plankton extraction .....	pag 108
6.1.2. Preliminary experiments of shellfish extraction .....	pag 109
6.1.3. Edible shellfish extraction .....	pag 110
6.1.4. Liquid Chromatography-Mass Spectrometry .....	pag 110
<b>6.2. Results and Discussion .....</b>	<b>pag 111</b>
6.2.1. Plankton LC-MS analyses .....	pag 112
6.2.2. Edible shellfish LC-MS analyses .....	pag 116
6.2.3. 2007 LC-MS analyses .....	pag 116
6.2.4. 2008 LC-MS analyses .....	pag 118
6.2.5. 2009 LC-MS analyses .....	pag 122
6.2.6. 2010 LC-MS analyses .....	pag 127
<b>6.3. References .....</b>	<b>pag 130</b>
<b>Chapter 7 .....</b>	<b>pag 133</b>
<b>Toxin profile of cultured <i>Ostreopsis ovata</i> from Tyrrhenian and Ardiatic seas</b>	
<b>7.1. Experimental .....</b>	<b>pag 133</b>
7.1.1. Cultures of <i>O. ovata</i> .....	pag 133
7.1.2. DNA extraction, polymerase chain reaction amplification .....	pag 134
7.1.3. Sequence alignment and phylogenetic analyses .....	pag 135
7.1.4. Chemicals .....	pag 135
7.1.5. Extraction .....	pag 135
7.1.6. Liquid Chromatography-Mass Spectrometry .....	pag 136
<b>7.2. Results and Discussion .....</b>	<b>pag 136</b>
7.2.1. Growth rate and cell volume .....	pag 136
7.2.2. Determination of toxin content by LC-MS .....	pag 141
<b>7.3. Conclusions.....</b>	<b>pag 146</b>
<b>7.4. References .....</b>	<b>pag 147</b>
<b>Chapter 8 .....</b>	<b>pag 151</b>
<b>42-Hydroxy Palytoxin : a new palytoxin analog from Hawaiian <i>Palythoa</i> spp.</b>	
<b>8.1. Experimental .....</b>	<b>pag 153</b>
8.1.1. Extraction and isolation .....	pag 153

---

8.1.2. Liquid Chromatography-Mass Spectrometry .....	pag 154
8.1.3. Nuclear Magnetic Resonance experiments .....	pag 155
8.1.4. Functional studies .....	pag 155
<b>8.2. Results and Discussion .....</b>	<b>pag 157</b>
<b>8.3. References .....</b>	<b>pag 169</b>
<b>Chapter 9 .....</b>	<b>pag 175</b>
<b>27-hydroxy-13-desmethylspiroside C and 27-oxo-13,19-didesmethylspiroside C: two new spiroside from Adriatic <i>Alexandrium ostenfeldii</i></b>	
<b>9.1. Experimental .....</b>	<b>pag 177</b>
9.1.1. Chemicals .....	pag 177
9.1.2. Cultures of <i>A. ostenfeldii</i> .....	pag 177
9.1.3. Extraction and isolation .....	pag 178
9.1.4. Liquid Chromatography-Mass Spectrometry .....	pag 178
9.1.5. Nuclear Magnetic Resonance .....	pag 179
9.1.6. 27-hydroxy-13-desmethyl spiroside C .....	pag 179
9.1.7. 27-oxo-13,19-didesmethyl spiroside C .....	pag 180
<b>9.2. Results and Discussion .....</b>	<b>pag 180</b>
9.2.1. 27-hydroxy-13-desmethyl spiroside C: Structure determination .....	pag 181
9.2.2. 27-oxo-13,19-didesmethyl spiroside C: Structure determination .....	pag 184
<b>9.3. References .....</b>	<b>pag 184</b>

## Abstract

Marine plankton is constituted by microalgae existing either in unicellular forms or in colonies of cells. These invisible organisms play a key role in the aquatic ecosystem as they are the producers of organic material thus being the first ring of the aquatic food chain.

Algal proliferation in the plankton, commonly referred to as *algal bloom*, is a periodic phenomenon occurring in many countries across the world usually in coincidence with particular climatic and environmental events. Blooms due to microalgae producing biotoxins are known as “harmful algal blooms”, as they pose serious threats to human health. In fact, oysters, mussels, clams and in general bivalve organisms, while feeding by filtering seawater, can accumulate toxins in their edible tissues sometimes to such a level to harass unaware consumers. Hence it can be stated that bivalves constitute a crucial ring of the food chain responsible for transferring toxicity from the plankton onto humans.

During my PhD within Prof. Ciminiello’s research group, I investigated the toxic profile of the Mediterranean Sea where over the past decades a number of toxic microalgae have bloomed. In particular, I focused my attention on toxic outbreaks caused by microalgae belonging to the *Ostreopsis* genus, quite rife along the Italian coasts.

Harmful algal blooms linked to *Ostreopsis* spp. reached alarming proportions in the late July of 2005 and 2006, when many people required extended hospitalization for respiratory distress after exposure to marine aerosol along the beach and promenade of Genoa. During these toxic episodes Prof. Ciminiello’s research group succeeded in identifying a putative palytoxin - the most potent non-proteic toxin so far known ( $DL_{50} < 100$  nanograms/Kg) - as well as a new palytoxin analog, ovatoxin-a, as the two main compounds responsible for the human poisoning. This was achieved by setting up a new analytical method for detecting palytoxin based on association of liquid chromatography with mass spectrometry (LC-MS). In the wake of this research on *Ostreopsis* spp. I carried out in-depth studies on *O. ovata* toxic profile succeeding in identifying four new palytoxin-like compounds, named ovatoxin-b, -c, -d, and, -e by High Resolution (HR)LC-MS and MS/MS experiments on a hybrid Linear Ion Trap (LTQ) Orbitrap XL<sup>TM</sup> FTMS operating up to 100,000 of resolution power. On the basis of the MS data in our hands we could also give some preliminary information about their structures; however NMR mono- and bi-dimensional experiments are needed to definitively assign their chemical architecture.



Since over the last years the restating of the *O. ovata* summer blooms has raised serious concerns to both human health and economy, from October 2006 a commission appointed by the Ministero della Salute has been in charge of investigating and monitoring *Ostreopsis* phenomenon along the whole Italian coasts to the aim of evaluating risks to human health and preventing any possible human intoxication. So, from the summer of 2007 on, a program of monitoring in the frame of the project “Monitoraggio *Ostreopsis ovata* litorale costiero Regione Campania” was started by ARPA Campania in collaboration with Stazione Zoologica A. Dohrn, Istituto Zooprofilattico Sperimentale del Mezzogiorno, and with Dipartimento di Chimica delle Sostanze Naturali, where I carried out my PhD. Therefore, every summer from 2007 to 2010, during the *O. ovata* blooms I carried out LC-MS analyses on samples of both mussels and sea-urchins, collected along the Campania coasts, once proven positive to the mouse bioassay. For many Campania sites, for which our analyses showed toxin contents above the EFSA (European Food Safety Authority)-established tolerance limits (30 µg/Kg), mussel harvesting was banned. Such a ban was lifted only when our analyses highlighted toxin amounts in the investigated samples well below the above official limits.

Considering the deep sanitary and economic impact due to the *Ostreopsis* outbreaks, I also tried to set up a suitable purification procedure for ovatoxin-a – which accounts for 50% of the total toxin content - with the purpose of obtaining sufficient amount of pure compound for investigating its toxicology as well as its mechanism of action. The best results were obtained by extracting ovatoxin-a from algal pellets with methanol and methanol/water 1:1, followed by partition of the water extract with chloroform, and then by a medium pressure chromatographic separation employing a reverse stationary phase and a UV instrument as detector, and eventually by a high pressure chromatographic separation using LTQ Orbitrap XL FTMS as detector. In this frame I also analyzed *O. ovata* cultures coming from the Adriatic (Ancona) and the Tyrrhenian Seas (Latina) in collaboration with the University of Bologna. Pellet samples and culture mediums were collected in both exponential and stationary cellular growth phases, extracted, and finally analyzed by LC-MS to the aim of evaluating the toxins production in the different Italian strains and at the different growth levels. Our studies showed that the Adriatic strain is richer in toxins than the Tyrrhenian one, and the toxins content during the stationary growth phase is higher than that of the exponential phase.

In the field of this research on palytoxins, I also studied extracts from soft corals belonging to the *Palythoa* genus collected in Hawaii. In particular, I carried out LC-MS analyses on a triple quadrupole mass spectrometer at unit resolution, with addition of NaCl and KCl to the

mobile phase to induce adduct ions production. LC-MS experiments were also recorded on a time of flight instrument, operating at high resolution. The whole of the above studies allowed us to individuate a new palytoxin analogue whose molecular formula ( $C_{129}H_{224}N_3O_{55}$ ) appeared to contain an oxygen atom more than palytoxin ( $C_{129}H_{224}N_3O_{54}$ ). NMR mono- and bi-dimensional experiments on the new palytoxin analogue identified it as 42-OH palytoxin.

Another subject of my research was the investigation of the toxin profile of *Alexandrium. ostenfeldii*, a dinoflagellate producing spirolides, fast acting toxins with an unusual 7-membered spiro-linked cyclic imine moiety. Beyond the fact that once injected intraperitoneally into a mouse spirolides give rise to neurologic symptoms, their human toxicity is largely unknown. *A. ostenfeldii* samples collected in the Adriatic Sea were extracted and analyzed by LC-MS/MS that highlighted the presence of some unreported spirolides on the basis of their characteristic fragmentation pattern. Finally, NMR studies allowed to characterize two of the new spirolides as 27-OH-13-desmetil spirolide C and 27-oxo-13,19-didesmetil spirolide C.



## **Presentazione dell'attività di ricerca svolta e dei risultati ottenuti**

Le microalghe sono organismi vegetali, unicellulari o coloniali, costitutivi del plankton marino; solo una piccola parte di esse, è in grado di produrre tossine e, quando si instaurano particolari condizioni climatiche e ambientali, esse possono proliferare massivamente, generando serie conseguenze per la salute umana. Infatti, gli organismi marini eduli, che si nutrono per filtrazione delle acque del mare e accumulano a livello dei loro tessuti digestivi queste tossine, diventano l'anello della catena alimentare responsabile del trasferimento della tossicità dal plankton all'uomo. Tale fenomeno ha assunto negli ultimi anni vasta risonanza anche in Italia, a causa delle gravi conseguenze che esso comporta sia sul piano propriamente sanitario che su quello economico.

Durante il corso di dottorato, la mia attività di ricerca si è focalizzata sullo studio di fioriture di microalghe nocive, in particolare di microalghe tropicali appartenenti al genere *Ostreopsis*, un fenomeno venuto prepotentemente alla luce negli ultimi anni lungo le coste italiane, che ha ottenuto vasta risonanza da parte dei media.

Nelle estati 2005 e 2006, infatti, lungo le coste liguri, si sono verificati degli eventi tossici, durante i quali numerose persone, in seguito ad esposizione ad aerosol marino tossico, manifestarono i sintomi di una severa intossicazione di tipo respiratorio. In quell'occasione, il gruppo di ricerca della Prof.ssa Ciminiello, presso cui ho svolto il mio dottorato, riuscì a identificare una palitossina e un suo nuovo analogo, l'ovatossina-a, quali agenti responsabili delle intossicazioni, attraverso la messa a punto di un nuovo metodo basato sulla combinazione della cromatografia liquida e della spettrometria di massa (LC-MS).

La palitossina è una macromolecola a struttura complessa, ritenuta la più potente tossina non proteica a tutt'oggi nota (Dose Letale<sub>50</sub> <100 nanogrammi/Kg), individuata ripetutamente in paesi tropicali come responsabile di sindromi di avvelenamento talvolta letali.

E' in tale contesto che si inserisce il mio lavoro di ricerca, riguardante principalmente lo studio di composti palitossino-simili. In questi anni, col gruppo della Prof.ssa Ciminiello, ho condotto analisi di estratti tossici di *O. ovata* e attraverso esperimenti HRLC-MS e MS/MS su Orbitrap, uno spettrometro di massa ibrido trappola lineare- trappola orbitale FTMS, capace di operare fino a risoluzione di 100000, sono riuscita ad identificare quattro nuovi composti palitossino-simili, denominati ovatossina-b,-c,-d ed -e.

Dai dati ottenuti dagli esperimenti di massa registrati, sono emerse varie ipotesi strutturali; naturalmente saranno necessari studi NMR per determinare la struttura chimica delle nuove ovatossine.

Nel corso degli ultimi anni, il reiterarsi delle fioriture di *O. ovata*, ha generato grande interesse da parte delle istituzioni per i problemi sanitari ed economici ad esse connessi e nell'ottobre 2006 il Ministero della Salute ha istituito una commissione di indagine che ha emanato delle linee guida, allo scopo di valutare il rischio legato a tali fioriture tossiche e tutelare l'ambiente, gli alimenti e la salute dei consumatori.

In conseguenza di ciò, nell'estate 2007 la Regione Campania ha attivato un piano di monitoraggio del fenomeno "*Ostreopsis*" da attuarsi durante il periodo di fioritura della microalga *Ostreopsis*, che va da giugno ad ottobre. Di tale piano fanno parte l'ARPA Campania, la Stazione Zoologica Anton Dohrn, l'Istituto Zooprofilattico Sperimentale del Mezzogiorno e il Dipartimento di Chimica delle Sostanze Naturali, presso cui ho svolto il mio lavoro di ricerca. Durante le fioriture estive di tale microalga, dal 2007 al 2010, ho condotto analisi LC-MS su estratti di campioni di mitili, ricci e plankton, raccolti lungo le coste campane e risultati tossici al saggio sul topo. Nei siti di raccolta, per i quali le analisi LC-MS hanno mostrato un contenuto di tossine superiore ai limiti di tollerabilità (30 µg/Kg) stabiliti dall'EFSA (Autorità Europea per la Tutela degli Alimenti), è stato indetto il divieto di raccolta per autoconsumo di mitili; tale divieto è stato revocato soltanto quando le nostre analisi hanno registrato un livello di tossine inferiore ai suddetti limiti.

Dato l'elevato interesse sanitario ed economico che scaturisce dal fenomeno *Ostreopsis*, mi sono anche interessata della purificazione dell'ovatossina-a, allo scopo di ottenere una quantità sufficiente per condurre gli studi farmacologici su effetti tossicologici e meccanismo d'azione. L'ovatossina-a rappresenta circa il 50% del quantitativo totale di tossine negli estratti di *O. ovata*; è stato necessario, innanzitutto, condurre studi relativi alle procedure di purificazione di tale tossina, che ne consentivano un recupero efficiente. I migliori risultati ottenuti per l'estrazione dai pellet algali prevedono la sospensione dei campioni in metanolo e sonicazione; si procede poi ad una seconda estrazione in metanolo/acqua 1:1. Gli estratti vengono quindi riuniti, e ripartiti con cloroformio.

L'estratto acquoso così ottenuto viene poi purificato prima mediante cromatografia liquida a fase inversa a media pressione, con rivelatore UV e successivamente mediante HPLC, utilizzando come rivelatore lo spettrometro di massa ibrido LTQ Orbitrap XL FTMS.

Un ulteriore aspetto del mio lavoro sull'*O. ovata* si è inserito nell'ambito di una collaborazione con l'Università di Bologna e ha riguardato uno studio di colture tossiche ottenute da vari

ceppi di tale microalga, provenienti dal Mar Adriatico (Ancona) e Tirreno (Latina). Mi sono occupata dell'estrazione e dell'analisi LC-MS sia di campioni di pellet cellulari raccolti in fase di crescita sia esponenziale che stazionaria, sia delle rispettive acque di coltura, per misurarne il contenuto in tossine nei diversi ceppi e ai vari livelli di crescita. Il ceppo adriatico è risultato più ricco in tossine rispetto a quello tirrenico e durante la fase stazionaria di crescita si è registrata una produzione di tossine maggiore rispetto alla fase esponenziale.

Un altro aspetto del mio lavoro ha riguardato lo studio di un composto palitossino-simile, proveniente da estratti di soft corals del genere *Palythoa*, raccolti lungo le coste di Maui, Hawaii, dai quali la palitossina fu isolata per la prima volta. Analisi LC-MS su uno spettrometro di massa a triplo quadrupolo a risoluzione unitaria, con aggiunta di NaCl e KCl alla fase mobile per indurre la formazione di ioni addotto, e l'utilizzo di uno strumento a tempo di volo ad alta risoluzione, hanno permesso di individuare la formula molecolare del nuovo composto ( $C_{129}H_{224}N_3O_{55}$ ), che possiede un atomo di ossigeno in più rispetto alla palitossina ( $C_{129}H_{224}N_3O_{54}$ ). Approfonditi studi NMR mono e bidimensionali hanno poi permesso di identificare il nuovo composto come 42-OH palitossina.

Un altro filone di ricerca al quale mi sono dedicata ha riguardato lo studio di colture di *Alexandrium ostenfeldii*, dinoflagellato produttore di spirolidi. Si tratta di tossine a rapida azione, il cui farmacoforo potrebbe essere un'inconsueta immina ciclica a sette termini spirolegata. La tossicità sull'uomo resta ancora sconosciuta, ma nel topo, per iniezione intraperitoneale, tali tossine provocano sintomi neurologici. Campioni di *A. ostenfeldii* sono stati raccolti nel Mar Adriatico, lungo le coste dell'Emilia Romagna ed estratti presso i nostri laboratori. Il confronto delle analisi LC-MS degli estratti tossici, con quelle di spirolidi noti, utilizzati come riferimento, ha evidenziato la presenza negli spettri dei campioni incogniti di due nuovi spirolidi, che presentavano un pattern di frammentazione caratteristico di questa classe di composti, ma con diverso rapporto  $m/z$ . Studi NMR hanno poi permesso di identificare i due nuovi composti, come 27-OH-13-desmetil spirolide C e 27-oxo-13,19-didesmetil spirolide C.



## **Introduction**

Oceans cover approximately 70% of the earth's surface and life on earth has its origin in the sea. Marine ecosystems are often characterized by a high biological diversity. This corresponds to a high chemical diversity: to date about 19,000 products of marine origin have been described and hundreds of new compounds are being discovered every year.

Bioactive natural products have been isolated from marine invertebrates such as sponges, tunicates, mollusks, and bryozoans as well as from marine microorganisms such as cyanobacteria, bacteria, and fungi.

Soft bodies of many marine invertebrates, together with their sedentary or slow-moving life, style pose the need for chemical defenses. Secondary metabolites serve as chemical weapons and are highly potent inhibitors of physiological processes in the prey, predators or competitors. Targets of these compounds include ion channels, various enzymes, microtubule structures and DNA.

Currently, marine natural products play a major role in biomedical research and drug development, either directly as drugs or as lead compounds in drug synthesis. Many marine compounds have already undergone clinical trials with regard to their healing properties. Potential anti-inflammatory, anti-cancer, anti-infective activities and other properties have been discovered.

Many marine invertebrates live in symbiosis or association with microorganisms (bacteria, cyanobacteria and fungi), while some others, such as filter feeding animals, feed on microorganisms, which are either symbiotic, just associated or serve as food. Numerous natural products from marine invertebrates show striking structural similarities with known metabolites of microbial origin suggesting that microorganisms are either involved in their biosynthesis or the true sources of bioactive compounds. In some cases, there is strong evidence for this hypothesis but the complexity of associations in marine organisms makes it extremely difficult to definitively state the biosynthetic origin of many marine natural products. So there is still a lot of work to do: new species and new marine natural products await to be discovered. The biochemical and pharmacological activities of the new compounds as well as the real producing organisms have to be characterized. The continuous supply for those that are suitable as (potential) drugs must be ensured without destroying marine ecosystems. This poses many challenges for life scientists but also great chances for discovery of new drugs against cancer and other diseases.





## Chapter 1

### 1.1. Analytical methods

#### 1.1.1. Mass Spectrometry

Mass Spectrometry is an analytical technique, particularly used in organic chemistry, which allows to measure molecular masses of unknown compounds and thus to determine their elementary formula, even at trace levels (such as NMR, UV, etc).

Unlike other spectroscopic techniques, mass spectrometry is a destructive analytical technique (any molecule get destroyed after the analysis), that is not based on the interaction between radiations and matter. Any molecule has first to be ionized and transferred to gas phase in the ion source and then it is transmitted to the mass analyzer where its mass properties are measured.

In order to obtain a mass spectrum, ions in a gas-phase, must be produced; they are subsequently accelerated, by an electric field, until they get to a specific speed and they are transferred to the mass analyzer, which separate different masses; ions on the base of their mass/charge ( $m/z$ ) ratio finally, ions having different  $m/z$  value are sequentially detected. during the time the compounds with a charge and with a mass are sequentially detected. All mass analyzers need a high vacuum ( $10^{-3}$ - $10^{-10}$  torr) to operate.

Every molecule able to ionize and maintain its ions in gas-phase, can be studied by mass spectrometry on the base of the different chemical features of the analyte and different kinds of ionization sources can be used.

#### Ionization Source

The ionization source has a key role in mass spectrometry, because it determines number, nature and abundance of the ion species contained in a mass spectrum.

For this reason many techniques are used; some allows to analyze only positive ions, others negative ions too. In addition, some ionization techniques operate at high energy and bring to a hard fragmentation (HARD TECHNIQUES); some others operate at low energy producing only few ions and very limited fragmentation (SOFT TECHNIQUES). The most used techniques are:

1. Electron impact (E.I.)
2. Chemical ionization (C.I.)
3. Fast atom bombardment (F.A.B.)

4. Matrix assisted laser desorption ionization (M.A.L.D.I.)

5. Atmospheric pressure ionization (API), including Electrospray (ESI) and Atmospheric pressure chemical ionization (APCI).

Depending on the chemical properties of a molecule, any of the above techniques can be chosen. The current MS instrumentation offers a large number of ion sources even interconvertible.

The chemical structures of the molecules I studied, needed the using of the ESI (Electro Spray Ionization) ionization technique. In particular, liquid chromatography-mass spectrometry experiments were carried out.

### **Liquid chromatography-mass spectrometry (LC-MS)**

The combination of liquid chromatography (LC) and mass spectrometry (MS) is a very useful technique for detection of organic compounds contained in trace amounts in complex matrices. Initially, this coupling appeared quite difficult to accomplish for the apparent incompatibility between LC and MS.

#### **HPLC**

- It works in liquid phase
- It works at 25-50°C
- No practical restrictions about the compounds to analyze
- No practical restrictions about the molecular weight
- It uses inorganic buffers

#### **MS**

- It works in gas phase
- It works at 100-350°C
- It needs samples having some volatility
- Molecular weight limited by the analyzer
- No inorganic buffers can be used

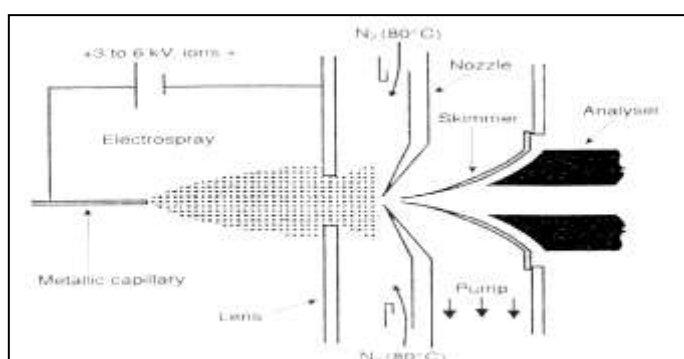
A number of different approaches to make possible the LC-MS coupling have been developed, the most successful being the *Atmospheric Pressure Ionization* (API). In API the ionization occurs at atmospheric pressure, then the ions are introduced in the system at high vacuum of the mass analyzer and are guided by opportune electric fields. ESI is a variant of the API.

In Ion Spray Ionization (ISI) the nebulization is assisted by a nebulizer gas (air or nitrogen), that produces a more directional spray, a stronger compatibility with the water, as well as the possibility of using higher flows. The whole of these characteristics make ISI very suitable to coupling LC-MS. However, it's often useful splitting the flow coming from the LC before

connecting to the source, to the aim of obtaining an improvement of the signal/noise ratio and without altering the sensitivity, because the ESI depends on the analyte concentration and not on its absolute amount. Finally, it exists a type of ESI at high flow (Turbo Ion Spray), allowing an increase of the evaporation speed of the solvent, by the intaking, of a secondary gas (air or nitrogen). This also allows to operate at flows of 1 mL/min, with no need for splitting.

### Electrospray Ionization (ESI)

ESI is a technique largely used for the analysis of water-soluble, polar or even charged biomolecules; it is used to accomplish the combination of liquid chromatography and mass spectrometry. The sample is introduced in the ion source as a solution of the analyte in a volatile solvent (methanol, water, acetonitrile, or a mixture of them), containing low levels of a weak acid or base. The solution is pushed across a capillary needle, charged at a high potential ( $\pm 3$ -5 kvolt) opposite to the potential of the sampling plate. As the solution comes out of the needle, it forms a spray made of a number of microdroplets of solvent, containing ions of the analytes. Generally, atmospheric pressure ionization spontaneously occurs under such conditions, but it can be increased by addition of opportune additives. An auxiliary gas (generally  $N_2$ ) can be introduced in the ion source in order to facilitate the solvent evaporation. Evaporation results in redaction of droplets until the electrostatic repulsion of ions (all positive or negative depending on the applied voltage), exceeds the superficial tension of the droplet; this droplet “blows” creating a current of nude ions, which are attracted through the sampling plate toward the analyzer. ESI can produce either positive (protonated) ions or negative (deprotonated) ions according to the potential applied to the needle (positive or negative respectively).



In so obtained, ions are then evaporated basing on their  $m/z$  ratio by the analyzer and then transmitted to the detector. The final result is a mass spectrum in which the main peaks are due to the molecular ion, taking one or more charges (multicharged species) and its adducts with the solvent or the salts ( $\text{Na}^+$ ,  $\text{K}^+$ ,  $\text{NH}_4^+$  in the positive ions mode and  $\text{Cl}^-$ ,  $\text{HCOO}^-$  in the negative ions mode). The presence of these adducts is useful in identifying molecular ion of unknown compounds, but a quantitative analysis should be avoided, since it can decrease sensitivity.

### Analyzers

Mass analyzer is the device of the mass spectrometer that operates selection of the ions formed in the ionization source, on the base of the  $m/z$  ratio. Different  $m/z$  ions arrive at the detector in different times, appearing at different values in the mass spectrum. Similarly to ionization sources, several types of analyzers exist having different characteristics and performances.

The analyzers can be classified, basing on the way they accomplish ion selection in:

1. Magnetic Deflection
2. Triple Quadrupole
3. Ion Trap
4. Time of Flight (TOF)
5. Ionic Cyclotronic Resonance (FT ICR)
6. Orbitrap Ion Trap

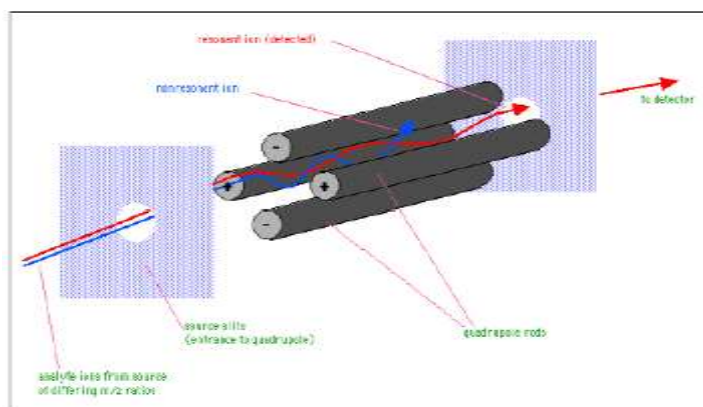
My research work has been carried out by using the following analyzers: Triple Quadrupole, Ion Trap, Time of Flight and Orbitrap, that I'll describe in detail in the following paragraphs.

### Quadrupole

Quadrupolar mass filters are constituted by four bars. A difference of potential is applied to the opposite bars of the quadrupole; this difference of potential is caused by a continuous and an alternate currents. The ions formed in ion source and accelerated by ion lens, enter in the quadrupole and go on through it with a constant speed along a parallel to poles direction ( $z$  direction); during their transit, they start complex oscillations along  $x$  and  $y$  directions thanks to concurrent application of continuous current (DC) and radio frequency current (RF) on the poles.

Each ion has its proper stable oscillation, that let it cross the quadrupole without banging into the poles; this oscillation strictly depends on the ion  $m/z$  ratio. For this reason, under the

conditions set in a MS experiment, only some ions, having a precise  $m/z$  value, will cross the whole length of the quadrupole filter. All the others will take unstable oscillations and will bang into the poles, getting lost. Since each  $m/z$  ion corresponds to a particular RF/DC ratio, the mass scan is carried out by varying both RF and DC, in time, but maintaining their ratio constant.



*Quadrupole Analyzer*

### **Quadrupole: data acquisition mode**

The main acquisition modes used in LC-MS experiments I performed on quadrupole, are:

- *Full scan MS (FSMS)*
- *Product ion scan (MS/MS)*
- *Selected Ion Monitoring (SIM)*
- *Selected Reaction Monitoring (SRM) and Multiple Reaction Monitoring (MRM)*

### ***Full scan MS***

*Full Scan MS* is an experiment in which the analyzer sequentially transfers all the ions produced in the source, to the detector, in a mass range selected by the operator. In a LC-MS experiment the resulting chromatogram is due to the *Total Ion Current (TIC)* for the retention time. Although this acquisition mode provides many information, it isn't selective if we are trying, to detect a known analyte in a complex mixture. In fact, the TIC appears as one only unsolved group of overlapping peaks. Also, since the sensitivity that a quadrupolar system has to detect a mass is directly proportional to the time that the detector spends on that mass (dwell time), the acquisition in *Full Scan MS* mode is little appropriate to research and detect substances contained at trace levels in complex matrices.

Instead, in the case of the ion trap analyzers the *Full Scan* spectra can be recorded with no a loss of sensitivity<sup>1</sup>. In fact, thanks to the store function of the trap, the sensitivity can get

higher, by collecting ions for longer period of time. The problem of the selectivity is solved by extracting, during the data processing, the target ions, that are so revealed as *extracted ion chromatogram* (XIC), namely a graphic in which the intensity of the target ion, versus the retention time reported.

### ***Selected Ion Monitoring (SIM)***

SIM is a MS experiment at single stage, in which one or a few ions of particular  $m/z$  ratio are monitored. In SIM among all the ions produced in the ion source, only those having the selected  $m/z$  ratio are isolated in the analyzer, which has the role of filter and let reach the detector, producing a SIM trace in which the selected ions intensities are “continuously” recorded versus the retention time. No data are acquired for the other ions. Since only a few ions of selected  $m/z$  are monitored, the SIM modality, in a single or triple quadrupole instrument, generally has a higher sensitivity than the *Full MS* spectrum; in fact, the detector spends on each ion a definitely longer dwell time than in the *Full Scan* mode; so, a big increase in both sensitivity and selectivity is obtained, to the detriment of the number of derivable information. The decrease, in the background noise and the subsequent increase of the signal/noise (S/N) ratio make this acquisition mode suitable for detection and quantification of substances present at trace levels on complex matrices. SIM identification of a known compound in a complex matrix occurs when:

- Its retention time is the same as that of the pure standard;
- At least 2 ion currents characteristic for the analyte, concurrently appear;
- the areas (or the heights) of the 2-3 ion signals selected for the analyte are in the same ratio as ions contained in the FS spectrum (or within the experimental deviation limits). The ion peaks are at least three times higher than ground noise<sup>2</sup> (S/N=3).

### ***Product Ion Scan (MS/MS)***

This is a 2-stage MS experiment. An ion with a certain  $m/z$  value (precursor ion), is selected and isolated during the first stage of the analysis; subsequently, it's excited and fragmented by collision with a gas (N<sub>2</sub>, Ar, or He). During the second step of the analysis, all the product ions contained in the mass range selected, are separated on the basis of their  $m/z$  ratio and detected. In a triple quadrupole analyzer, the ion selected, transmitted from Q1 collides in a collision cell (Q2) with the collision gas (N<sub>2</sub>), giving characteristic product ions. Q3 works in

*Full Scan MS*, separating all the product ions on the basis of their  $m/z$  ratio and producing a spectrum of fragmentation for the selected ion in Q1 mass.

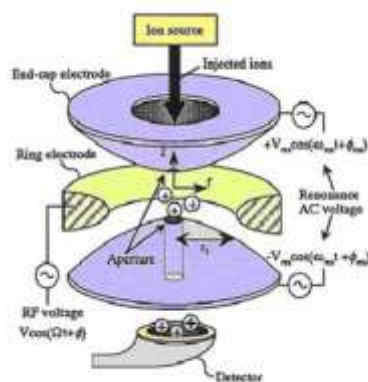
### ***Selected Reaction Monitoring (SRM)***

SRM is a 2-stage MS experiment, in which one or more set of transitions precursor ion > product ion are monitored. In the SRM acquisition mode on a triple quadrupole analyzer the ions produced in the ion source are stored in the first quadrupole (Q1) (first step) and here the selected precursor ions are isolated and transmitted to the second quadrupole (Q2), or collision cell. These ions are fragmented in Q2 by a collision gas (argon, nitrogen, or helium), producing a number of product ions. The product ions are stored in the third quadrupole (Q3) (second step), where only those selected as characteristic of the analyte are isolated and transmitted to the detector, producing a SRM mass spectrum. No data are acquired for all the other ions. Similarly to SIM, the SRM allows the rapid and sensitive analysis of compounds contained at trace levels in complex mixtures, because only a limited number of product ions, characteristic of the analyte, is monitored. As a consequence, the sensitivity and selectivity of the SRM experiments in a triple quadrupole MS instrument is definitely higher than in the Product ion scan (MS/MS) experiments. Generally, more than one transition for each analyte is monitored and so the experiment is also named *Multiple Reaction Monitoring* (MRM).

### **Ion Trap**

In the ion trap analyzers the bars of the filter have a spherical disposition, while in the quadrupole the selected ions go straight to the detector, the ion trap temporarily keeps in itself all the selected ions and subsequently releases them toward the detector, by varying the electric field. So, all or selected ions, formed in the ion source, can be trapped for variable times. Helium is introduced in the ion trap to support this process, by decreasing the kinetic energy of the ions; it makes all the ions to stay in the centre of the trap and far from the walls. Besides “preserving” the ions, it’s possible to make the path of the ions at growing  $m/z$  ratios unstable; so, these ions come out from the trap and go toward the detector.





*Ion Trap Analyzer*

Generally, the ion traps are very versatile and provide a good sensitivity and have relatively low initial costs.

### **Ion Trap: data acquisition mode**

The main acquisition modes used in LC-MS experiments I performed on Ion Trap, are:

- *Full scan MS*
- *Product ion scan (MS<sup>n</sup>)*
- *Selected Ion Monitoring (SIM)*

These experiments were described above.

### **Tandem Mass Spectrometry**

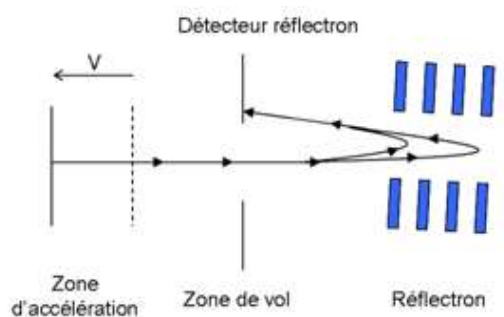
A tandem mass spectrometer is constituted by two analyzers laid in series. The first analyzer (MS1) has the function of selecting (filtering) the desired ion among the various ions present in a spectrum. The selected ion (precursor or parent ion) subsequently collides into a collision cell (MS2) with a collision gas (N<sub>2</sub>, He, Ar) originating a number of fragment ions (product ions); the so obtained fragment ions are separated by a third analyzer (MS3) on the basis of their *m/z* ratio. In this way structural information on an unknown molecule can be gained.

MS Instruments equipped of a tandem MS are the triple quadrupole (in which the fragmentation happens as above described) and the ion trap, in which the three events above reported (solution, fragmentation, selection) happen in one only place, the ion trap.



ratio of the particle (heavier particles reach lower speeds). From this time and the known experimental parameters one can find the  $m/z$  ratio of the ion.

The kinetic energy distribution in the direction of ion flight can be corrected by using a reflectron. The reflectron uses a constant electrostatic field to reflect the ion beam toward the detector. The more energetic ions penetrate deeper into the reflectron, and take a slightly longer path to the detector. Less energetic ions of the same  $m/z$  ratio penetrate a shorter distance into the reflectron and, correspondingly, take a shorter path to the detector. The flat surface of the ion detector (typically a microchannel plate, MCP) is placed at the point where ions with different energies reflected by the reflectron hit a surface of the detector at the same time counted with respect to the onset of the extraction pulse in the ion source. A point of simultaneous arrival of ions of the same mass and charge but with different energies is often referred as time-of-flight focus. An additional advantage to the re-TOF arrangement is that twice the flight path is achieved in a given length of instrument.



Continuous ion sources (most commonly electrospray ionization, ESI) are generally interfaced to the TOF mass analyzer by "orthogonal extraction" in which ions introduced into the TOF mass analyzer are accelerated along the axis perpendicular to their initial direction of motion. Orthogonal acceleration combined with collisional ion cooling allows separating the ion production in the ion source and mass analysis. In this technique, very high resolution can be achieved for ions produced in MALDI or ESI sources. Before entering the orthogonal acceleration region or the pulser, the ions produced in continuous (ESI) or pulsed (MALDI) sources are focused (cooled) into a beam of small diameter by collisions with a residual gas in RF multipole guides. A system of electrostatic lenses mounted in high vacuum region before the pulser makes the beam parallel to minimize its divergence in the direction of acceleration. The combination of ion collisional cooling and orthogonal acceleration TOF has provided significant increase in resolution of modern TOF MS from few hundred to several tens of thousand without compromising the sensitivity.

## TOF: data acquisition mode

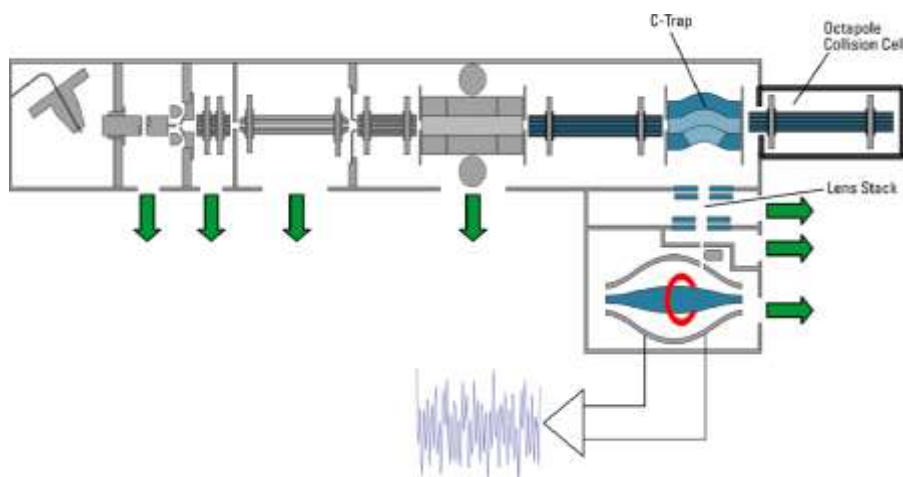
The main acquisition mode used in LC-MS experiments I performed on TOF, is:

- *Full scan MS*

These experiment was described above.

## LTQ Orbitrap XL

It's a hybrid linear ion trap LTQ Orbitrap XL™ Fourier Transform MS (FTMS) equipped with an ESI ION MAX™ source (Thermo-Fisher, San José, CA, USA).



### *LTQ Orbitrap XL*

In this spectrometer the ions are stored in the Linear Ion Trap (LTQ), then they are axially ejected and trapped in the C-trap. MS/MS experiments can be carried out by transfer in the HCD cell and return to the C-trap. Precursor ions originating from the LTQ or fragment ions originating from the HCD cell are squeezed into a small cloud in the C-trap and are injected into the Orbitrap, where they are electrostatically trapped, while rotating round the central electrode and performing axial oscillation. The oscillating ions induce an image current into the two outer halves of the orbitrap, which can be detected using a differential amplifier. Using Fourier Transformation, the transient can be converted from the Time domain to the Frequency domain. Each frequency can be assigned to a specific  $m/z$  and finally a spectrum is obtained.

From the diagram above it is obvious that the Orbitrap is only used as an accurate mass detection system. All advanced operations such as isolation and fragmentation take place in the LTQ and subsequently the ions are transferred into the Orbitrap in order to measure their accurate mass.

## The Orbitrap

The Orbitrap consists of two electrodes: a central electrode called “the spindle”, around which ions are forced to move in a spiral and an outer electrode, which is split in half by an insulating ceramic ring.

The Orbitrap doesn't use an RF or a magnet to hold the ions inside. Instead, ions moving towards the Orbitrap are trapped in an electrostatic field created both by the spindle and the outer electrodes. The electrostatic attraction towards the central electrode is compensated by a centrifugal force that arises from the initial tangential velocity of ions: very much like a satellite on orbit. Potential barriers created by the end electrodes confine the ions axially, while one can control the frequencies of oscillations by shaping the electrodes appropriately. This is why the Orbitrap has its current shape. Although the principle of trapping the ions in the Orbitrap is straight forward, the difficulty lies in getting the ions in the system. If the ions entered a static electric field, they would zoom past it, in the way a comet flies through the solar system. To avoid this from happening, the field inside the Orbitrap is not static and the principle of electrodynamic squeezing is employed. As the ions enter the field in a tangent, they are squeezed towards the central electrode by increasing its voltage. In addition in the axial direction the ions are forced to go away from the narrow parts of the Orbitrap and move towards the wider area in the centre. This initiates axial oscillations without the need for further excitation. The increase on the voltage then stops and the ion trajectory becomes a stable spiral. As the frequency of rotation for each  $m/z$  value depends on parameters such as the ion energy, position and angle, rotating rings of ions are finally formed. The lighter ions that enter the Orbitrap first, are squeezed closer to the central electrode than the heavier ions. Also since the ions stay concentrated within  $1 \text{ mm}^3$  only for a short time, space charge effects have no time to develop.

The axial component of the ion oscillations is independent of initial energy, angles and positions and can be detected as an image current on the two halves of the outer electrode encapsulating the Orbitrap. A Fourier transform is then employed to obtain oscillation frequencies for ions with different masses, resulting in an accurate reading of their  $m/z$  and high mass resolution.

Vacuum in the Orbitrap is created by three turbomolecular pumps but there are only two gauges in order to monitor the pressure. The last gauge, although shown in the software, is not installed in the instruments. The temperature of the Orbitrap is also controlled and has to be stable in order for the system to operate properly. The acceptable temperature is 26 degrees.

## C-trap

Based on the topics discussed above, the success of the Orbitrap depends to a big extent on the ability to trap the ions and allow them to start spinning around the central electrode. However, a step of equal importance is the introduction of ion packages into the system, as it ensures that both the trapping and the spinning can take place successfully. Hence the C-trap device was developed.

Ions accumulated in the LTQ are transferred *via* an octapole into the C-trap. The C-trap is an RF-only quadrupole, bent into a C shape. The C-trap ensures that short ion packages containing loads of ions are injected into the Orbitrap. After trapping the ions in the C-trap, the RF on the rods is ramped down and DC voltages are applied to the rods, creating a field across the trap that ejects along lines converging to the pole of curvature, which coincides with the Orbitrap entrance. Essentially the ions are trapped, pushed and pulled into the Orbitrap with the help of the C-trap. This is the key of interfacing the Orbitrap with another analyzers.

The C-trap is filled with N<sub>2</sub> as a dampening gas and the pressure inside is 10<sup>-3</sup> torr, which is a lot lower than the 10<sup>-5</sup> torr of the LTQ. The pressure in the Orbitrap is 10<sup>-10</sup> which is 7 orders of magnitude higher than the C-trap. In order to avoid excess of nitrogen transfer between the two various components due to pressure difference, it is essential for the ions enter the Orbitrap from the C-trap off-axis. Therefore, a series of deflectors and lenses are employed for successful transfer and to account for the difference in pressure. High energy collision fragmentations (soft HCD) are possible in the C-trap using the nitrogen in Orbitrap Classic systems. The precursor is isolated in the LTQ and transferred into the C-trap as normal. Then high voltages are applied on the rods of the C-trap forcing the ions into multiple collisions with the nitrogen atoms. High energy fragmentation occurs with no low-mass cut off in the spectra. In new Orbitrap systems, HCD is carried out in a separate collision cell as described below.

## Octapole Collision Cell

In the LTO Orbitrap Discovery and the LTQ Orbitrap XL, an octapole is integrated with the C-trap. This allows high energy collisions to take place resulting in MS/MS spectra with no low mass cut-off. Various user-selectable gases can also be employed, although light gases cannot be used.

In order to perform MS/MS experiments, the precursor ions are isolated in the LTQ, they are transferred into the C-trap and from there they are accelerated into the octapole collision cell.

In the collision cell, DC offset voltages are applied in the same way as in a triple quadrupole instrument. This results in the kinetic energy of the ions to increase and for the ions to undergo collisions with the gas that fills the cell. The gas most commonly used is Nitrogen. Dissociation occurs after only a small number of collisions between the ions and the gas and MS/MS fragmentation patterns resembling those obtained from triple quadrupole systems are collected. HCD in the octapole collision cell works well both for small molecules and peptides and proteins and generates results valuable for the purposes of structure elucidation. Once fragment ions are formed in the collision cell, they are then transferred back into the C-trap using a potential gradient and from then on the usual process of ion transfer from the C-trap to the Orbitrap takes place.

### **LTQ Orbitrap: data acquisition mode**

The main acquisition modes used in LC-MS experiments I performed on LTQ Orbitrap, are:

- *Full scan* MS
- *Product ion scan* (MS<sup>n</sup>)

These experiments were described above.

### **1.1.2. Nuclear Magnetic Resonance**

The most important spectroscopic technique used for structure elucidation of the isolated secondary metabolites is nuclear magnetic resonance (NMR). In addition to standard <sup>1</sup>H and <sup>13</sup>C NMR spectra, a large use of 2D NMR experiments are made. They are superior to their 1D NMR counterparts both for the shorter acquisition times and for the easier assignment of nuclei resonating in crowded regions of the spectra (signal overlapping is much less likely in two dimensions than in one).

### **COSY<sup>3</sup> (COrrrelation SpettroscopY)**

The COSY (Correlation SpectroscopY) experiment is one of the simplest and yet most useful 2D NMR experiment. It allows determination of the connectivity of a molecule by identifying which protons are scalarly coupled. In spite of the many modifications which have been proposed along the years, the very basic sequence composed of two  $\pi/2$  pulses separated by the evolution period  $t_1$  is still the best choice if one is simply dealing with the presence or the absence of a given coupling, but not with the value of the relevant coupling constant.

**TOCSY<sup>4</sup> (Total Correlation SpectroscopY)**

The TOCSY (Total Correlation SpectroscopY) experiment is a 2D NMR experiment very useful in the analysis of molecules composed of many separate spin systems, such as oligosaccharides or peptides. The TOCSY spectrum shows correlation peaks between nuclei that may be not directly coupled, but are still within the same spin system. The appearance of a TOCSY spectrum resembles in all aspects a COSY; the difference is that the cross peaks in a COSY result from coupled spins, whereas in the TOCSY spectra they arise from coherence transfer through a chain of spin-spin couplings, and therefore any pair of protons within a spin system may give rise to a peak. The range of the coherence transfer (i.e. through how many couplings the coherence may be transferred) increases with increasing mixing times ( $\Delta$ ), but a mixing time too long may reduce sensitivity.

**HSQC (Heteronuclear Single Quantum Correlation) and HMQC<sup>5</sup> (Heteronuclear Multiple Quantum Correlation)**

These two experiments are 2D NMR heteronuclear correlation experiments, in which only one-bond proton-carbon couplings ( $^1J_{CH}$ ) are observed. In principle, the HSQC experiment is superior to HMQC in terms of selectivity and additionally allows DEPT-style spectral editing. However, the sequence is longer and contains a larger number of  $\pi$  pulses, and is therefore much more sensitive to instrumental imperfections than HMQC.

**HMBC<sup>6</sup> (Heteronuclear Multiple Bond Correlation)**

The HMBC experiment is a heteronuclear two- and three-bond  $^1H$ - $^{13}C$  correlation experiment; its sequence is less efficient than HSQC because the involved  $^{2,3}J_{CH}$  couplings are smaller (3-10Hz). Moreover, while  $^1J_{CH}$  are all quite close to each other,  $^{2,3}J_{CH}$  can be very different, making impossible to optimize the experiment for all couplings. As a result, in most HMBC spectra not all of the correlation peaks which could be expected from the structure of the molecule are present.

**ROESY<sup>7</sup> (Rotating-frame Overhauser SpectroscopY)**

The ROESY (Rotating-frame Overhauser SpectroscopY) experiment is a chemical shift homonuclear correlation which can detect ROEs (Rotating-frame Overhauser Effect). ROE is similar to NOE, being related to dipolar coupling between nuclei, and depending on the geometric distance between the nuclei. While NOE is positive for small molecules and negative for macromolecules, ROE is always positive. Therefore, the ROESY experiment is



particularly useful for mid-size molecules, which would show a NOE close to zero. The ROESY sequence is similar to the TOCSY sequence, and unwanted TOCSY correlation peaks may be present in the ROESY spectra. Fortunately, these unwanted peaks can be easily recognized, because their phase is opposite compared to ROESY correlation peaks. It is important to acquire ROESY spectrum in phase-sensitive mode for a correct interpretation of the spectrum.

## 1.2. Analytical methods to detect biotoxins

Marine biotoxins are produced by aquatic microorganisms and can contaminate freshwater, shellfish and fish; they represent a serious concern for human and animal health.

Biotoxins represent a true challenge for the analytical chemist, who is interested to detect them because of their great structural variety and the large range of polarity and molecular weights they present. So we need analytical methods allowing the detection of biotoxins in a very large variety of biological matrices are needed. These methods have to be applicable to:

- freshwater monitoring;
- screening of shellfishes in aquaculture before their collection;
- studies of quantitative screening, and/or quality confirming of shellfish and fish before marketing;
- detailed analysis of the toxic profile in the plankton and shellfish, the production of toxins from the plankton, the intaking, the metabolism and the elimination of toxins from shellfish.

Unfortunately there isn't one only method meeting all the above requirements. Generally the analytical methods are divided in two groups: biological assays and chemical-methods.

The biological assays include the mouse toxicity assay, the toxicity assays in vitro, the biochemical assays of inhibition of phosphatase or receptorial assays, the immunological assays ELISA and RIA. They are very rapid, sensitive and present relatively low costs, but they don't give detailed information on the nature of individual toxins responsible for toxicity.

For this reason sensitive, precise and specific instrumental methods are needed. Instrumental analytical methods include TLC (*Thin Layer Chromatography*), GC (*Gas Chromatography*), LC (*Liquid Chromatography*), CE (*Capillary electrophoresis*), and MS (*Mass Spectrometry*). Other methods have been developed and they plan the derivatization of the biotoxins by appropriate reagents and their subsequent detection or others, hiphenated techniques, needing

the coupling of two among the above mentioned instrumental methodologies (GC-MS, CE-MS, e LC-MS).

### **1.2.1. Biological assays: mouse toxicity**

Marine biotoxin monitoring in shellfish is carried out by mouse bioassays, as indicated in Gazzetta Ufficiale Italiana<sup>2</sup> for the diarrhetic-shellfish-poisoning (DSP) toxins and the paralytic-shellfish-poisoning (PSP) toxins.

**Mouse bioassay for the DSP-toxins.** This method is based on intraperitoneal injection of a shellfish extract in Swiss race adult mice, weighing 18-20 g. The presence of toxins generates general indisposition and death. This assay is carried out on 20 g of epatopancreas (weigh of dripped sample) of mussels, extracted with 100 mL of acetone homogenized and kept for 2 minutes at room temperature. The obtained mixture is then filtered or centrifuged and extracted twice more with 50 mL of acetone. The three extracts are combined, evaporated and the residue is suspended in 10-15 mL of distilled water, that is, finally, extracted with 50 mL of ethyl ether. The ethereal extract, after the solvent evaporation, is suspended in 4 ml of a physiological solution of Tween 60 at 1% and intraperitoneally inoculated in three mice (dose of 1 mL per mouse), to the aim of ascertaining the toxicity. This test is considered positive if 3 mice die within 5 hours after the injection; if, instead, the mice die within 24 hours or they survive, the test is considered negative, because the quantity of toxins, if present, does not represent a real risk for consumer health.

**Mouse bioassay for the PSP-toxins.** This method is based on the intraperitoneal injection of shellfish extract in Swiss race adult mice, weighing 18-20 g. The presence of toxins causes paralysis and death within few minutes from the inoculation. This assay is carried out on 100-150 g of shellfishes (weigh of dripped sample), that are first blended and then (weighing 100 g) extracted with 100 mL of HCl 0.1 N. The pH is measured after the extraction and it must be lower than 4 (it's preferable about 3). The mixture is boiled for 5 minutes and the pH is measured again (it has to be 2-4 and not higher than 4.5); HCl 5 N or NaOH 0.1 N can be added to adjust pH. The volume has to be adjusted to 200 mL with water. The mixture is then centrifuged and the supernatant, is injected intraperitoneally in three mice (the dose is 1 mL per mouse). This test is considered positive if the mouse dies within 5-7 minutes after the injection.

### **1.2.2. Instrumental assays: LC-MS**

Among the instrumental methods used to detect biotoxins, a very important place is occupied by liquid chromatography-mass spectrometry coupling techniques (LC-MS).

LC-MS is a very useful instrument for qualitative and quantitative toxins detection in plankton and mussels, in identifying new toxins and research about toxins metabolism in edible shellfish.<sup>8</sup>

Analytical methods based on HPLC-MS coupling have been developed for the principal marine biotoxins classes: domoic acid and other ASP-toxins, okadaic acid and other DSP-toxins, saxitoxin and other PSP-toxins, brevetoxin, spirolides and ciguatoxin. In fact, this is the only technique which is valid for all the toxins analysis and satisfies the needs of laboratories interested in both monitoring and marine biotoxins research. HPLC-MS coupling gives, in fact:

- Possibility of universal detection
- High sensibility, with limits of detection in the order of parts per billion
- High selectivity and specificity
- Minimum sample's clean-up
- Possibility of examining labile and very structurally different toxins
- Accurate and precise quantification
- Large range of linear answer
- Possibility of di automation
- High productivity
- Quickness in developing analytical methods
- Legal acceptability in confirmation studies
- Structural information for new toxins, known toxins analogues and metabolites identification.

The high initial cost of HPLC-MS systems and the necessity of specialized staff in using HPLS-MS systems represent the principal difficulties for many laboratories, even if recently less expensive instruments, easy to be used, versatile and of reduced dimensions have been introduced, reducing, in this way, these problems.

### 1.3. References

1. Quilliam, M.A.; Hess, P.; Dell'Aversano, C. In: *Mycotoxins and Phycotoxins in Perspective at the Turn of the Century*, Eds: W.J. deKoe, R.A. Samson, H.P. van Egmond, J. Gilbert and MMM. Sabino, 2001, pp. 383.
2. *Gazzetta Ufficiale della Repubblica Italiana*, 18-9-1990, 218, p. 8.
3. Bax A.; "Two Dimensional Nuclear Magnetic Resonance in Liquids", Delft University Press, Dordrecht, 1982.
4. Davis D.G., Bax A.; *J. Am. Chem. Soc.*, 1985, 107, p. 2820.
5. Davis D.G., Bax A.; *J. Mag. Res.*, 1986, 67, p. 565.
6. Bax A., Summers M.F.; *J. Am. Chem. Soc.*, 1986, 108, p.2093.
7. Davis D.G., Bax A.; *J. Mag. Res.*, 1985, 37, p. 207.
8. Quilliam M. A.; *Applications of LC-MS in Environmental Chemistry*, Elsevier Science Publ. BV, Amsterdam, 1996, p 415. b) Quilliam M. A.; *Harmful Algae Proc. VIII International Conference on Harmful Algae*, Vigo Spain, 1997, p 509.



## Chapter 2

### 2.1. Marine plankton

Plankton represents a major constituent of the living organisms of the oceans. It's constituted by living species that can't oppose themselves to the currents movement, but they get carried away from currents and from this comes the name: from the Greek *planktos*, that means "errant". In particular, the plankton is constituted by microalgae, which can live isolated (unicellular forms) or in groups of little colonies of cells and depending on the species grow in biomass, by raising both in dimension and quantity. These organisms, quite invisible, play a key role in the aquatic ecosystem; in fact, they produce organic material and represent, therefore, the first ring of the aquatic food chain. They, also, produce a large quantity of oxygen. The growth speed is due to both species and environmental conditions. Microalgae can double their number in 24 hours if they belong to a rapid growth species or double their number in a week or 10 days if they belong to a slow growth species. Many phytoplanktonic species are able to adapt themselves to unfavorable conditions.

The unicellular organism is able to perceive the environmental changes and become active, therefore it possesses a perception system for the fluctuations happening in its habitat and it's able to react to them. The most part of the planktonic organisms, (except the dinoflagellates), haven't flagells and would be trending to leave slowly a sediment toward the bottom. In the water, the phytoplankton floating should be only slow fall movement, but this isn't true because its movement is regulated by the specific weight, the fiction resistances and the active movement of the flagells. This explains many characteristics of planktonic algae: the presence of oils as reserve, the forming of appendices and protuberances on the cellular walls, the cellular aggregation to make chainlets and also the observation that the appendices favoring the flotation are bigger in hot waters (with a lower viscosity) than in cold waters. To cross the gravity effect and stay in the euphotic area some phytoplanktonic organisms have structures capable of reducing their specific weight and favoring their flotation.

The algae proliferation in the plankton, defined *algal bloom*, is a periodic phenomenon, happening in different countries of the world in conjunction with particular climatic and environmental events, among which the upwelling, that consists in the happening of upward currents of water, rich of nutrients and represents the principal cause of the "coloured water" all over the world.<sup>1</sup> The cellular density can be so high that the waters turn red ("red tides"), but also green or brown. In particular, phenomena associated to toxic and/or harmful algal

proliferation<sup>2,3</sup> are defined “harmful algal bloom” and can become a serious threat for human health. In fact, microalgae, besides herbivorous fishes, represent the principal source of feeding for those all organisms, as oysters, mussels, clams and in general bivalve organisms that feed themselves by filtering sea water. These organisms, by their “filter-feeding” activity, accumulate phytotoxins in their edible tissues, during the periods in which the harmful algae blooms appear in areas where the mussels are cultivated.<sup>4-6</sup>

The mussels are among the most consumed marine seafood in the world and in case of harmful algal bloom, they represent the ring of the food chain that is responsible for transferring toxicity from the plankton to the humans. One of the first poisoning accidents, due to the ingestion of contaminated edible shellfish during an algal bloom, was recorded in 1793, when the Captain George Vancouver landed at the British Columbia and many members of his crew died, after paralysis, because they had eaten shellfish collected in an area, today known as “Poison Cove”. The Captain, subsequently, observed as the aborigines considered very dangerous eating shellfish when the sea water appeared “coloured”. Only after many years, the substances responsible of that poisoning were identified and they were named PSP (*paralytic shellfish poisoning*); these compounds are toxins so potent that only 500 µg, easily accumulable in only 100 gr of shellfishes, can be fatal for a man. From then on, many episodes, due to PSP-toxins or other marine toxins, have been recorded in north America and worldwide, till today and over 2000 cases of human poisoning (fatal in 15% of the cases) are recorded every year in the globe for the fish and shellfish consume.<sup>7</sup> It’s evident that these phenomenons produce, hygienic-sanitary harms for popolation as well as economic damages for the fishing industry, the shellfish farmers and the fishermen, that have to block their activity during the full period of toxicity.

### **2.1.1. Classification**

There isn’t a definitive evaluation about the total number of species constituting phytoplankton, because every time new species are discovered. Actually, 10,000 species are known and divided in five big classes:

- *Chlorophyta* (green algae)
- *Chrysophita* (yellow algae and diatoms)
- *Pyrrhophyta* (dinoflagellates)
- *Euglenophyta*
- *Cyanophyta* (blue-green algae or cianobacteria)

About 300 of the above mentioned marine phytoplankton species,<sup>8</sup> are actually considered responsible of the characteristic reddish coloring of the sea surface, defined red tides, and only about thirty species are considered capable of producing secondary toxic metabolites called “phytotoxins”, that intoxicate men through the ingestion of contaminate seafood. The toxic species belong mostly to diatoms and dinoflagellates taxa. The other taxa are less represented, both qualitatively and quantitatively and their presence is due to particular conditions; by way of example, the presence of the silicoflagellates is recorded during the most cold months, the coccolithophorids are mainly pelagic, the cloroficeae and the euglenoficeae prefer estuarial conditions.

The harmful algal blooms, depending on the effects they produce, can be classified in:<sup>9</sup>

a) blooms of species causing only a water discoloration with a reduction of visibility and of quality of seawater; they can grow and cause, fish and aquatic invertebrates mortality, due to depletion of oxygen. Many dinoflagellates species, such as *Gonyaulax polygramma*, *Noctiluca scintillans*, *Srippsiella trochoidea* and diatoms such as *Skeletonema costatum*, belong to this group;

b) blooms of species producing potent toxins, which can reach humans through the food chain, causing a variety of gastrointestinal and neurologic damages. These toxins are classified in:

- PSP (*Paralytic Shellfish Poisoning*), produced by dinoflagellates coming from the classes of *Alexandrium*, *Pyrodinium* and *Gymnodinium*, as well as by some cyanobacteria.
- DSP (*Diarrhetic Shellfish Poisoning*), produced by dinoflagellates from the classes of *Dinophysis*, *Prorocentrum*, and *Protoceratium*.
- ASP (*Amnesic Shellfish Poisoning*), biosynthesized by some diatoms, as *Pseudonitzschia multiseriata*, *P. pseudodelicatissima*, *P. australis*, etc.
- CIGUATERA-toxins, produced by the dinoflagellates *Gambierdiscus toxicus*, and *Ostreopsis spp.*
- Toxins produced by the cyanobacteria, as *Anabaena circinalis*, *Microcystis aeruginosa*, *Nodularia spumigena*, etc.;

c) blooms of species that aren't toxic for humans, but in different way, can damage fish and invertebrates, as, for example, the diatom *Chaetoceros convolutus*, the dinoflagellate *Gymnodinium mikimotoi*, the prymnesiofite *Prymnesium parvum* and the raphidofite *Chattonella antiqua*;



d) blooms of species producing toxins that are carried in the aerosol, from the bloom area to the coast: NSP-toxins (*Neurotoxic Shellfish Poisoning*), produced by the dinoflagellate *Gymnodinium breve*.

### **2.1.2. Globalization and increase of the algal blooms**

Even if the harmful algal blooms are a natural phenomenon, occurring since the ancient times, in the last decades they are showing an increase in frequency, intensity and geographic distribution.<sup>10-12</sup> For example, the dinoflagellates *Alexandrium tamarense* and *Alexandrium catenella*'s blooms, till the 1970 happened only in the temperate seas of Europa, North America and Japan;<sup>8</sup> while since 1990 on, these episodes have spread all over the southern hemisphere, South Africa, Australia, New Zealand, India and Philippines seas.

The increase in number of the algal blooms signaled, and the increase of the cases of food poisoning, seems due to several causes:

a) *Increase of the phenomenon of sea eutrophication.* The phenomenon of marine coastal eutrophication is the result of enrichment in nutrients (essentially nitrates and phosphates) contained in the water. This phenomenon is explained on the base of both natural and anthropogenic causes.<sup>13</sup> The principal characteristic that distinguishes these two kind of eutrophication is the time of arrival. In fact, the natural eutrophication is a long run process, entering in a range of 1,000-10,000 years. The anthropogenic eutrophication, happening more frequently in the coastal areas because of the contribution of eutrophic substances, as phosphates and nitrates at the hands of the man, it occurs in very short times, in a range of about 10 years. These eutrophic substances are highly nutritious for algae, that in presence of these compounds, start a huge growing and produce, by chlorophyllian photosynthesis, big quantity of oxygen. Soon after the algae are died, they are attacked by aerobic bacteria, which oxidize them, releasing carbon dioxide. The oxygen amount, spent by the bacteria, is higher if there's much organic substance to be decomposed. In this way, the oxygen amount in the water, considerably decreases and this impairs the animals life, above all in the closed basins as lakes and in shallow sea with low hydrodinamism, such as Adriatic Sea.

The first and most important index of evaluation of the phenomenons of natural and anthropogenic eutrophication is given by sea water quality: an abnormal growth of microalgae and/or the increase of the phytoplankton biomass, determines a phenomenon called «discolored waters» and «red tide» as previously reported. In the European coasts the «colored waters» are due to «exceptional algal blooms» (exceptional algal blooms containing more than 10<sup>6</sup> cells/Liter and 50 mg/m<sup>3</sup> of chlorophyll), while there are also «seasonal

blooms» not determining visible phenomena because they are due to unicellular algal species, not exceeding 103 cells/Liter of water. But, while some plankton aren't influenced by the enrichment in nutrients of the coastal waters, as *Gymnodinium breve*, and *Alexandrium*, many other species seem to be stimulated in their growing, by domestic, industrial and agricultural dumping. The significant increase of the *Phaeocystis poucheti* blooms, found for the first time in 1978 in German seas, is the best known example of this phenomenon.<sup>14</sup>

Many risks are associated to the episodes of seas eutrophication, so Hong-Kong, Japan and several European countries decided to reduce the phosphates and nitrates dumping at least of the 50% in the next years: these efforts, however, result vain, if these initiatives are isolated and if, namely, the neighbouring countries continue to pollute seas.

b) The increased scientific knowledge of toxic species. News about algal blooms, associated to harms for human health and for shellfish and fish industry, occupy a more and more important space on the newspapers, on television and in the scientific literature. Therefore, the number of researchers interested to marine waters and monitoring the toxic species blooms, is growing up. A good example is represented by the *Alexandrium minutum*, which was known to occur only in Egypt<sup>15</sup> till 1988, but just a few years ago it was also found in Australia, Ireland, France, Spain, Portugal, Italy, Turkey, Thailand, New Zealand and Japan.<sup>16-17</sup>

Also with the increasing of the problems due to the indiscriminate fishing along the coastal waters, many countries are evaluating the advantages of the fishes and shellfishes breeding. These activities, by a more severe control of the seas, allow to discover the presence of unknown toxic species. In fact, wherever scientific and sanitary communications about the PSP, DSP, NSP and ASP-toxins have increased.

c) The deforestation and industrial development. The progressive increase of the intaking in the marine environment of the urban, industrial, agricultural and zootechnical effluents, contribute to harmful algae development. In Sweden, for example, experimental evidences show that the fluvial waters, drained from the agricultural soils rich in nitrose and phosphorus, stimulate some cianobacteria to proliferate, while the waters coming from the woods, favor the growth of other species, as the *Prorocentrum minimum*.<sup>18</sup>

d) Climatic changes. Most the scientific community considers the green house effect and the oceans heating up, as able favor some microalgae development and the migration of some species from a geographic area to another. For example, some fossils testify as the progenitors of the dinoflagellate *Pyrodinium bahamense*, which is, actually, typical only of some areas, in the past had a geographic distribution much larger; also, we can't exclude that in the next future, the *Pyrodinium* will return to proliferate, for example, in the Australian seas, where it

flourished a long time ago.<sup>19</sup> Many coincidences were, also, observed between the proliferation of the *Pyrodinium* in the Philippines and in Indonesia, with particular climatic events, as the ENSO (El Nino-Southern Oscillation).<sup>20</sup> The strong event ENSO happened between 1991 and 1994 and the increasing dinoflagellates blooms in the same period tend to confirm this hypothesis.

e) Occasional vectors of microalgae from a geographic area to another. Ship ballast waters are vectors of marine plankton worldwide. This problem appeared very serious already in the 80's, when some toxic not indigenous dinoflagellates, were introduced in the mussels breeding areas, along the Australian coasts, causing disastrous economic consequence.<sup>21</sup> In order to reduce the risks associated to the transport of dangerous species through ballast waters, in November 1991, the International Maritime Organization ratified a policy still optional, as the prohibition of taking on board water during the toxic species blooms in the harbors, or the possibility to treat the ballast water with heat, electric shocks or chemical agents (Cl<sub>2</sub>, H<sub>2</sub>O<sub>2</sub> etc.).<sup>22</sup>

## 2.2. Conclusions

Actually, the research on the toxic species is growing up thanks to a high number of scientists interested in this topic; in fact the effects on the public health and economy are becoming a real emergency worldwide. Surely, the increasing interest in using the coastal waters in the fish and shellfish breeding, is bringing the scientists to a better knowledge of the toxic algal species.

The countries not involved in both phenomenons of intoxications from marine foods and pollution of coastal waters, are trying to prevent the introduction of new toxic marine algae species.

It's also very important, that people responsible of checking coastal waters were conscious that an increase of the nutrients, coming from agricultural activities or deforestation or industry, could result into an increase of toxic planktonic species. Finally, studies carried out on the climatic fluctuations (El Nino, green house effect, ozone depletion) can provide information about the changes or the increase of the toxic algae in the seas.

However, many International programs aim to study and manage an adequate way the toxic algal blooms and their repercussions on both environment and economy and above all on the human health.

### 2.3. References

1. Ade, P.; Funari, E.; Poletti, R.; *Ann Ist Super Sanità* 2003, 39(1), p. 53.
2. Anderson D.M. *Le Scienze*, 1994, 314, p.74.
3. Hallegraeff G.M., Anderson D.M., Cembella A.D. (Ed.) *Manual on harmful marine microalgae*. Paris : UNESCO 1995.
4. Anderson D.M., *Sci. Am.* 1994, 271 , p 52.
5. Anderson D.M., *Nature*, 1997, 338, p.513.
6. Yasumoto T., Murata M., *Chem. Rev*, 1993, 93, p1897.
7. Dale B.; Yentsch C. M.; *Oceanus* 1978, 21, p. 41.
8. Sournia A., Chretiennot-Dinet M. J., Ricard M. J. *Plancton Res.* 1991, 13, p. 1093.
9. *Manual on harmful marine microalgae*, UNESCO, 1995.
10. Anderson D.M., Okaichi T., Remoto T., (ed.). *Red tides: biology, environmental science and technology*. New york. Elsevier Science Publishing Co.; 1989, p. 11.
11. Cosper E.M., Carpenter E.J., Bricelj V.M., (ed.). *Novel phytoplankton blooms: causes and impacts of recurrent brown tides and other unusual blooms*. Berlin; Springer Verlag; 1989, p. 449.
12. Hallegraeff G.M., *Phycologia*, 1993, 32, p. 77.
13. *Eutrophication in the Mediterranean Sea*, UNESCO, 1988.
14. Lancelot C., Billens G., Sournia A., Weisse T., Colijn F., Veldhuis M., Davies A., Wassman P.; *Ambio* 1987, 16, p. 38.
15. Halim, Y. *Vie et Milieu* 1960, 11, p. 102.
16. Hallegraeff G. M., Bolch C. J., Blackburn S. I., Oshima Y.; *Bot. Mar.* 1991, 34, p. 575.
17. Yuki K.; *Jap. J. Phycol.* 1994, 42, p. 425.
18. Graneli E., Moreira M. O.; *J. Exp. Mar. Biol. Ecol.* 1960, 136, p.89.
19. McMinn A.; *Micropaleontology* 1989, 35, p. 1.
20. Maclean J. L.; *Mar. Poll. Bull.* 1989, 20, p. 304.
21. Hallegraeff G. M., Bolch, C. J.; *J. Plankton Res.* 1992, 14, p. 1067.
22. Bolch C. J., Hallegraeff G. M.; *J. Mar. Env. Eng.* 1993, 1, p. 23.

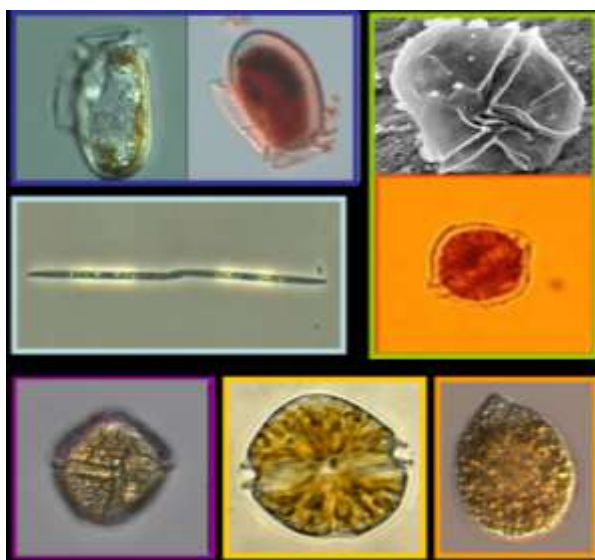


## Chapter 3

### 3.1. Mediterranean harmful algal events: marine biotoxins

Marine toxins from harmful algae are listed among the most important causative agents of poisoning episodes occasionally involving seafood consumers.<sup>1-3</sup> Out of the thousands of species of microscopic algae lying at the base of the marine food chain there are several dozens, which produce very potent toxins (Figure 1).

These toxins normally occur in small quantities and do not pose any serious problem to public health. Proliferations of harmful algae may mostly happen as massive "red tides" or blooms of cells capable of discoloring seawater. However, sometimes dilute and/or inconspicuous concentrations of harmful cells get noticed only because of the harm caused by the highly potent toxins they produce.



**Figure 1.** Most occurring harmful algae in the Mediterranean basin: a) *Dinophysis fortii* (left-blue); *Dinophysis acuminata* (right-blue); b) *Pseudonitschia pungens* (gray); c) *Protoceratium reticulatum* (violet); d) *Alexandrium ostenfeldii* (yellow); e) *Ostreopsis ovata* (orange); f) *Alexandrium tamarense* (top-green); *Alexandrium minutum* (bottom-green).

Well documented is the process through which shellfish can accumulate marine biotoxins in their edible tissues from harmful algae; it is also known that other organisms, such as reef fish, crabs and tunicates, can be affected by proliferation of toxic plankton. Therefore, harmful algal toxins can find their way through the different levels of the food chain ending up on the table of unaware consumers, thus provoking a variety of gastrointestinal and

neurological illnesses. Moreover, toxins can also cause alterations of marine trophic structure through adverse effects on larvae and other life history stages of commercial fishery species.<sup>4,5</sup>

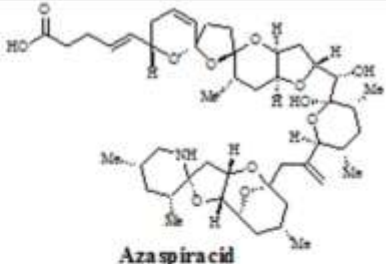
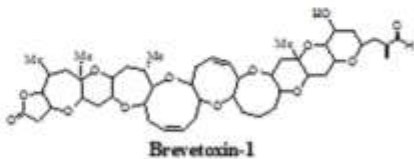
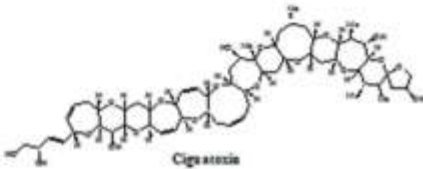
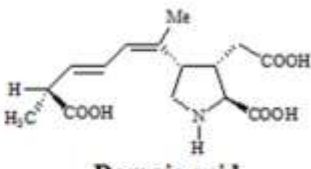
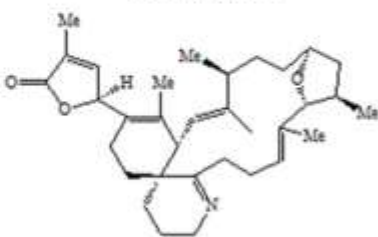
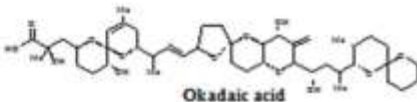
In addition to those toxins passed along to consumers through the food chain, particular phytoplankton blooms can directly affect humans accidentally exposed to toxic algae through swimming or breathing aerosols. It is also to be underlined that other harmful algal proliferations can induce severe ecological disruption through widespread killing of sea life including marine mammals and seabirds.<sup>6,7</sup>

The extent of harmful algal blooms has changed considerably over the last decades. If in the past only a few regions were affected in scattered locations, now virtually every coastal state is threatened by toxic outbreaks, in many cases even over large geographic areas and by more than one toxic algal species. Even though the causes for this apparent expansion are still largely unknown, the explosive growth of toxic plankton is sometimes clearly intertwined with changes in weather conditions. Important contributing causes may also be found in variations in upwelling, temperature, transparency, turbulence or salinity of seawater, as well as in concentration of dissolved nutrients, wind and surface illumination.<sup>8</sup>

It is not clear why some micro-algal species produce toxic compounds, secondary metabolites playing no explicit role in the internal economy of the producer organisms. These toxins are probably used as a tool for competing for space, fighting predation or as a defense against the overgrowth of other organisms.<sup>9</sup>

A wide diversity of marine algal toxins has been discovered so far, but those of major significance can be gathered into eleven classes reported in Table 1.

Table 1. Algal Toxins.

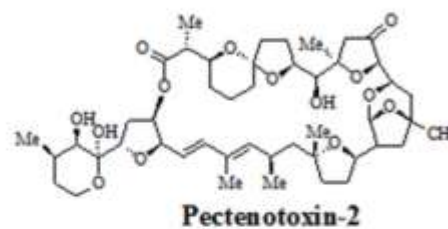
TOXINS CLASS	MAIN ALGAL SOURCE	TOXICITY	STRUCTURE OF A REPRESENTATIVE
<i>Azaspiracids</i>	<i>Protoperidinium crassipes</i>	Neurotoxic	 <p style="text-align: center;"><b>Azaspiracid</b></p>
<i>Brevetoxins</i>	<i>Karenia brevis</i>	Neurotoxic	 <p style="text-align: center;"><b>Brevetoxin-1</b></p>
<i>Ciguatoxins</i>	<i>Gambierdiscus toxicus</i>		 <p style="text-align: center;"><b>Ciguatera</b></p>
<i>Domoic Acid</i>	<i>Pseudo-nitzschia</i> species	Amnesic	 <p style="text-align: center;"><b>Domoic acid</b></p>
<i>Gymnodimines</i>	<i>Karenia selliformis</i>		 <p style="text-align: center;"><b>Gymnodimine</b></p>
<i>Okadaic acids</i>	<i>Dinophysis</i> species <i>Prorocentrum lima</i>	Diarrhetic Tumor Promoter	 <p style="text-align: center;"><b>Okadaic acid</b></p>



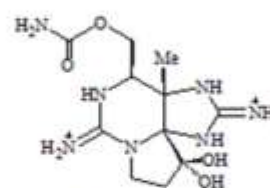
*Palytoxins*      *Ostreopsis* species      **Neurotoxic  
Tumor  
Promoter**



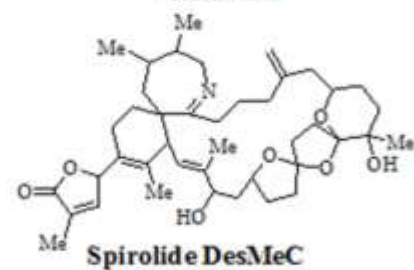
*Pectenotoxins*      *Dinophysis* species      **Diarrhetic**



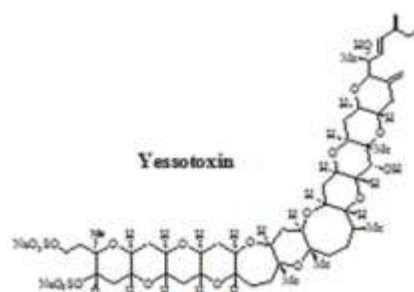
*Saxitoxins*      *Alexandrium* species      **Paralytic**



*Spirolides*      *Alexandrium  
ostenfeldii*



*Yessotoxins*      *Protoceratium  
reticulatum*



Phytoplankton marine toxins rank among the most potent and extremely dangerous toxins in the world. For some of them, doses in the range of micrograms per kilogram may be lethal to humans. In fact, small quantities of contaminated seafood are able to kill a normal, healthy, adult human. Alongside these extremely potent biotoxins, there are also dozens of less potent toxins, which can be all the more accumulated to such a high level to still cause harm to humans.

Unfortunately, poisonous seafood neither looks nor tastes different from uncontaminated seafood, and cooking or other culinary treatment do not destroy toxins.

Therefore, fish and shellfish farms infested by toxic algal species need to run costly monitoring programs for checking the occurrence of toxic algae in seafood. Whenever these are present, regular tests for toxins in seafood products need to be attentively carried out. As toxicity is the only common factor among the diverse phycotoxins isolated so far, it is no wonder that live-animal toxicity assay is currently the most widely used method for toxin detection in regulatory settings. At the moment, the most common test is the mouse bioassay. This test is carried out by injecting a sample extract into intraperitoneal cavity of a 20 g mouse that is observed for a given stretch of time in order to determine symptoms and time-to-death generally correlated to the amount of toxin present.<sup>10</sup>

### ***3.1.1. Distribution of algal toxins in the Mediterranean Sea***

Due to its geographical features, the Mediterranean basin is home to a large variety of living species, some of which endemic and unknown elsewhere. Survival of this biodiversity depends strongly on conservation of its necessary biotope. Unfortunately, many indicators have clearly shown a declining quality of the Mediterranean seawater and sediments, as testified by the alarming surge of harmful algal blooms over the last two decades.<sup>11</sup> These toxic episodes occurred basically across the whole Mediterranean basin with disquieting frequency and intensity. Figure 2, alongside the geographical location of the toxic outbreaks, details also the chemical nature of the major causative toxins, whose levels in seafood have frequently edged and sometimes exceeded guideline values.

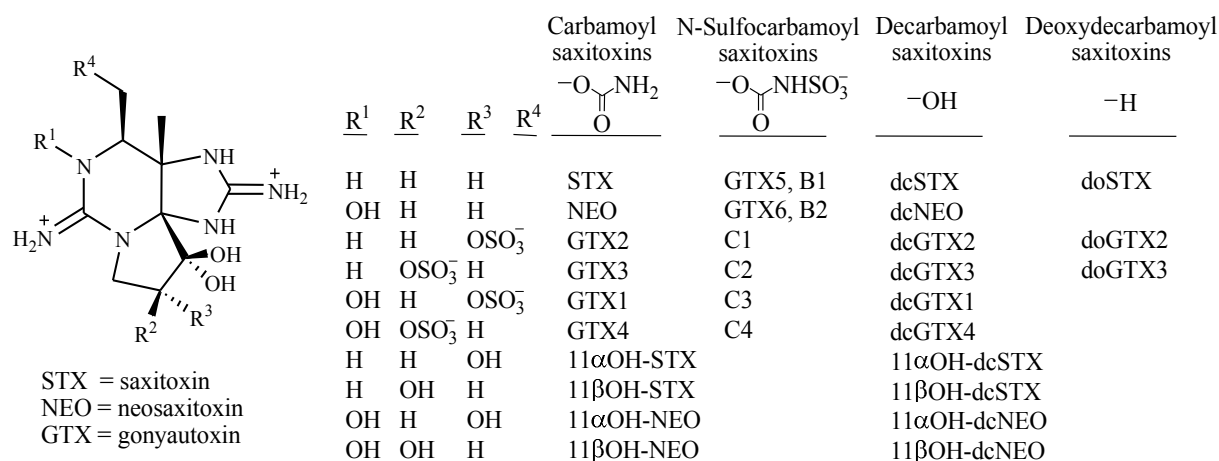


**Figure 2.** Major reported toxic outbreaks in the Mediterranean basin over the past two decades.

In particular, the Northern Adriatic Sea - which shows a peculiar and complex toxin profile - has been plagued by okadaic acids, yessotoxins and lately also by spirolides;<sup>12</sup> French, Spanish, and North African coasts have mainly been interested by the occurrence of saxitoxins;<sup>11</sup> while relatively simpler appears the Greek toxic profile, where only okadaic acid has been detected this far.<sup>13</sup> Very recently, a new, most alarming, threat have been impending over the Mediterranean Sea where the tropical alga *Ostreopsis* spp. is rife.<sup>14,15</sup> Over the past years, such an alga has been causing severe sanitary emergencies and economic losses due to its production of palytoxins<sup>16,17</sup> brought ashore through the marine aerosol.<sup>18</sup>

### 3.1.2. Saxitoxins

Saxitoxin and its analogues (Figure 3) are potent water-soluble neurotoxins that block voltage-gated sodium channel on excitable cells. Currently over 29 congeners of saxitoxin are known.<sup>19</sup> They represent a suite of heterocyclic guanidines, whose structures vary by different combination of hydroxyl and sulfate substitutions at four sites on the molecule. Based on substitutions at R4, saxitoxins can be subdivided into four groups: the carbamoyl-, sulfo-carbamoyl-, decarbamoyl-, and deoxydecarbamoyl-saxitoxins. Substitution at R4 results in substantial changes in toxicity, with the carbamoyl toxins being the most potent.



**Figure 3.** Chemical structure of saxitoxin and its analogues.

These compounds - responsible for the syndrome known as Paralytic Shellfish Poisoning (PSP) - are toxic at submicromolar concentrations and represent a severe public health risk.

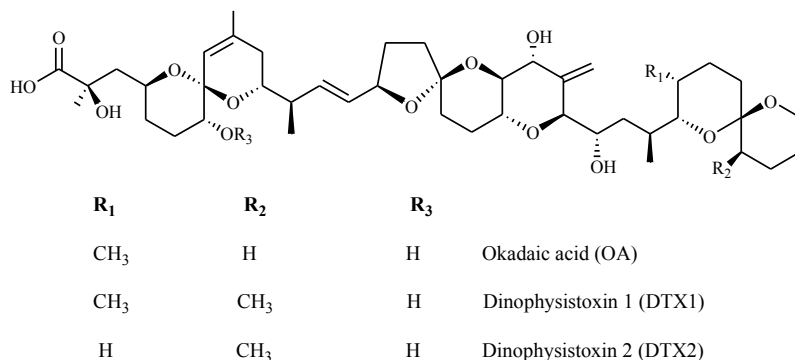
A number of dinoflagellate species are known to produce saxitoxins: *Alexandrium* (formerly *Gonyaulax* or *Protogonyaulax*), *Gymnodinium* and *Pyrodinium spp.*;<sup>20</sup> most of these dinoflagellates have not been shown to be directly toxic to fish or shellfish. By far, most cases of human PSP intoxications are caused by the consumption of shellfish that have accumulated saxitoxins after filtration of toxic marine dinoflagellates.

PSP symptoms develop fairly rapidly, within 0.5 to 2 hours after ingestion of shellfish, depending on the amount of toxin consumed.<sup>20</sup> In humans the peripheral nervous system is affected, with symptoms ranging from tingling of the tongue and lips, followed by a numbness spreading towards the extremities, to vomiting, pain, diarrhea, loss of coordination and breathing difficulty. In severe cases, ataxia, muscle weakness, and respiratory paralysis can occur. Without intervention, symptoms can turn into coma or death from suffocation. When respiratory support is provided within 12 hours of exposure, recovery usually is complete, with no lasting side effects. In unusual cases, because of the weak hypotensive action of the toxins, death may occur from cardiovascular collapse despite respiratory support. PSP is prevented by large-scale monitoring programs (assessing toxin levels in mussels, oysters, scallops, clams) and rapid closures to harvest of suspect or demonstrated toxic areas.

### 3.1.3. Okadaic acid

Okadaic acid (OA) is the parent compound of a group of polyether toxins – consisting of at least eight congeners - responsible for the Diarrhetic Shellfish Poisoning (DSP) syndrome, associated with seafood consumption and characterized by an acute gastrointestinal

disturbance.<sup>21</sup> Okadaic acid, dinophysistoxin 1<sup>22</sup> and dinophysistoxin 2<sup>23</sup> (Figure 4) are the primary congeners involved in shellfish poisoning, with the other congeners believed either precursors or shellfish-modified products of the active toxins.



**Figure 4.** Chemical structure of okadaic acid and some of its analogues.

The toxins are produced both by several *Dinophysis* species including *Dinophysis acuta*, *D. fortii*, *D. acuminata*, *D. norvegica*, *D. mitra*,<sup>24</sup> and *D. caudata*,<sup>25</sup> and by benthic species such as *Prorocentrum lima*.<sup>26,27</sup> The toxins are accumulated by several bivalves, which filter the seawater containing the toxic phytoplankton and cause human poisoning after ingestion.

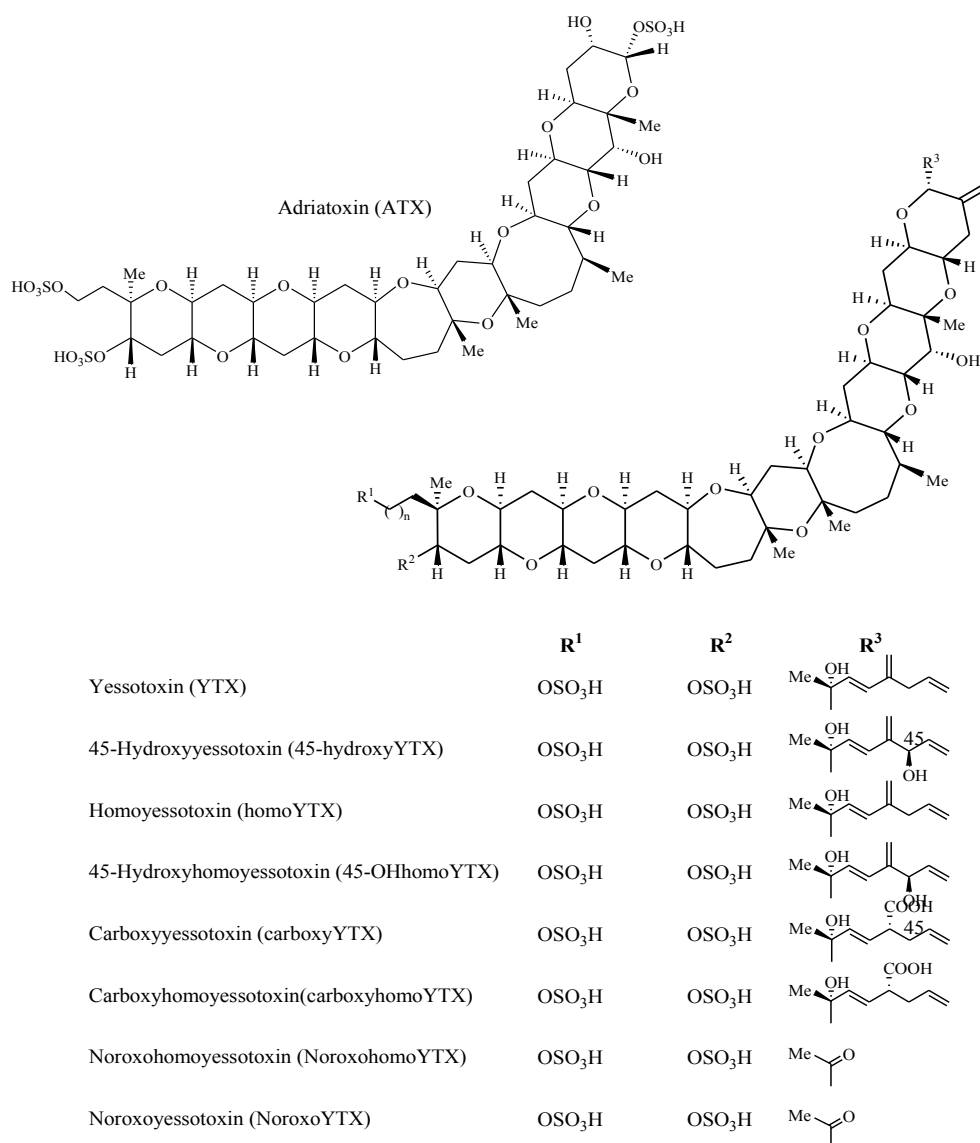
Oral assumption of OAs can lead to gastrointestinal distresses, often beginning within 30 minutes after consumption of contaminated shellfish. The main DSP symptom is represented by diarrhea, often associated with other disturbances such as nausea, vomiting and abdominal pain.<sup>28</sup> No human casualty has been to date reported in literature due to any case of DSP poisoning, although sometimes considerable morbidity has resulted in hospitalization. The clinical symptoms of Diarrhetic Shellfish Poisoning may have been often mistaken for those of bacterial gastric infections and the problem may be much more widespread than currently thought. The treatment, if necessary, is only supportive to replace fluid and electrolyte losses. OA is a potent tumor promoter<sup>29</sup> and chronic exposure to it may promote tumor formation in the digestive system.

The mechanism of action underlying diarrhetic as well as tumor-promoting activity is explained mainly by their potent inhibitory action against ser/thr protein phosphatases.<sup>30,31</sup> Inhibitory activity is specific for classes PP2A and PP1, whilst PP2B is inhibited only at high concentrations of OA and PP2C is practically insensitive.

### 3.1.4. Yessotoxins

Yessotoxins (YTXs) represent a group of polycyclic ether molecules (Figure 5). The parent compound of this class of marine toxins is yessotoxin (YTX), a disulphated polyether first reported as a contaminant of the scallop *Patinopecten yessoensis*.<sup>32</sup>

Yessotoxin in shellfish results from ingestion of toxic algae. The first species reported as a YTX producer is the dinoflagellate *Protoceratium reticulatum*.<sup>33</sup> However, more recent studies have shown that yessotoxin is also produced by the closely related species *Lingulodinium polyedrum*<sup>34</sup> and *Gonyaulax spinifera*.<sup>35</sup>



**Figure 5.** Chemical structure of yessotoxins from the Adriatic Sea.

YTX represents the dominant toxin in algal cultures; there is, however, a report in which the major toxin of *P. reticulatum* cultures is homoYTX.<sup>36</sup> This conflicting result, which is

indirectly confirmed by the toxin profiles in some contaminated shellfish,<sup>37-39</sup> can be attributed to a genetic variability of the producer species inducing a slight modification of the genes involved in the YTX biosynthesis. Some YTX analogues present in large quantities in contaminated shellfish - 45-hydroxyYTX, carboxyYTX, noroxoYTX, and/or their homoanalogues - are supposed to derive from oxidative modification of the absorbed\_YTX or homoYTX within the mollusk.<sup>40</sup>

Yessotoxin and its analogues were at beginning included within the Diarrhetic Shellfish Poisoning (DSP) group because they are not distinguishable from okadaic acids on the basis of the mouse bioassay-based standard procedure.<sup>10</sup> However, their toxic activities are significantly different; in fact, YTX and its analogues do not induce diarrhea, whereas their cardiotoxic effects have been demonstrated in mice after intraperitoneal (i.p.) and oral exposure to very high doses of YTX.<sup>41</sup> For these reasons, YTXs are not included in the list of DSP toxins anymore. YTX is highly toxic towards mice when administered after i.p. injection, while its oral toxicity is at least tenfold lower.<sup>42</sup>

Although no human intoxication caused by consumption of shellfish contaminated by YTXs has been reported, the widespread occurrence of these compounds in shellfish, sometimes at high levels, arouses an increasing interest in studying YTX toxicity. Nonetheless, no one has so far succeeded in proposing a unitary model for its mechanism of action. The chemical structure of YTX resembles that of brevetoxins, which are known to interfere with the voltage-sensitive sodium channel;<sup>43</sup> this finding suggested a possible interaction between YTX and cellular ion channels. Recently, however, it has been observed that YTX doesn't interact with sodium channels nor induces any competitive displacement of brevetoxins from site five of sodium channels.<sup>44</sup> It has been proposed that YTX may interact with calcium channels inducing an uptake of calcium in human lymphocytes.<sup>45,46</sup> Finally, studies on immune cells point to phosphodiesterases as an intracellular target for YTX.<sup>47</sup>

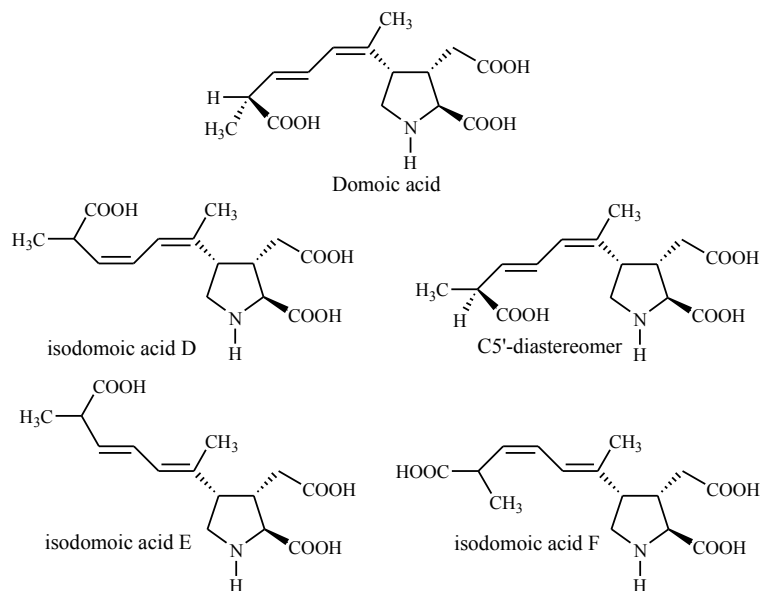
### **3.1.5. Domoic acid**

Domoic acid (DA) is a water soluble excitatory tricarboxylic aminoacid (Figure 6), structurally resembling the excitatory neuro-transmitter glutamic acid. It has been recognized as the causative toxin of Amnesic Shellfish Poisoning (ASP) syndrome.<sup>48</sup>

Domoic acid is produced by *Pseudo-nitzschia pungens* f. *multiseries*, a diatom widely distributed in coastal waters all around the world.<sup>49</sup> Several further species of *Pseudo-nitzschia* (*P. australis*, *P. pseudo-delicatissima*, *P. galaxiae*) have been found to produce

domoic acid, although some species are not always toxic and there is a considerable variability in toxicity.<sup>50-52</sup>

Up to date, several congeners of domoic acid have been identified, among which three geometrical isomers, isodomoic acids D, E, and F and the C5'-diastereomer have been found in small amounts in both the producing diatom and shellfish tissue<sup>53</sup> (Figure 6).



**Figure 6.** Chemical structure of domoic acid and its stereoisomers.

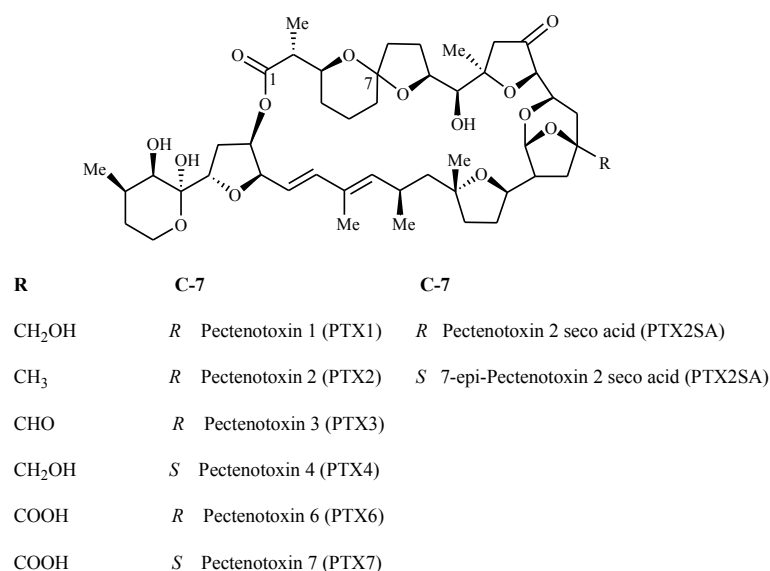
Due to their structural analogies, domoic acid and glutamic acid share the same mechanism of action, even though domoic acid shows a far stronger receptor affinity. More in details, domoic acid binds predominantly to *N*-methyl-D-aspartate (NMDA) receptors in the central nervous system, thus causing depolarization of neurons. As a consequence, the permeability to calcium ions increases, thus inducing cell dysfunction and even death. This provokes lesions in those areas of the brain where glutaminergic pathways are heavily concentrated, particularly in the CA1 and CA3 regions of the hippocampus responsible for learning and memory processes.<sup>54</sup>

The clinical symptoms of ASP include abdominal cramps, vomiting, diarrhea, incapacitating headaches, disorientation and short-term memory loss. In the worst-case scenario patients are victims of seizures, coma, profuse respiratory secretions, unstable blood pressure and also death.<sup>55</sup>



### 3.1.6. Pectenotoxins

Pectenotoxins (PTXs) are lipophilic macrocyclic polyethers, whose chemical structures resemble okadaic acid in having cyclic ethers and a carboxyl group in the molecule. Unlike okadaic acid, the carboxyl moiety in many pectenotoxins is in a form of macrocyclic lactone (Figure 7).



**Figure 7.** Chemical structure of pectenotoxins.

A number of PTXs have been isolated or identified in a range of source organisms.<sup>56</sup> The PTXs in shellfish originate from dietary microalgae. This far, only the genus *Dinophysis* (e.g. *D. acuta*, *D. fortii*, *D. acuminata*, and *D. caudata*) has been implicated in contamination of shellfish with PTXs.<sup>56</sup> However, only PTX-2 and the *seco* acids of PTX-2 (PTX-2SA and *epi*-PTX-2SA) have been isolated from phytoplankton, while the other compounds have been detected only in shellfish samples. Therefore, it has been supposed that many of these PTXs are products of shellfish metabolism, produced after ingestion of PTX-contaminating algae.<sup>56,57</sup>

Similarly to yessotoxins, also pectenotoxins have been grouped at the beginning together with DSP toxins because of their co-extractability with okadaic acids. However, animal studies have indicated that pectenotoxins are much less toxic than the latter ones through oral route and that they do not induce diarrhea.<sup>58</sup> Additionally, many DSPs have been found to be potent phosphatase inhibitors,<sup>59</sup> but PTX-1 and PTX-6 were found to be inactive against PP-1 and PP2A.<sup>60</sup> Therefore, they are currently considered as a separate group.

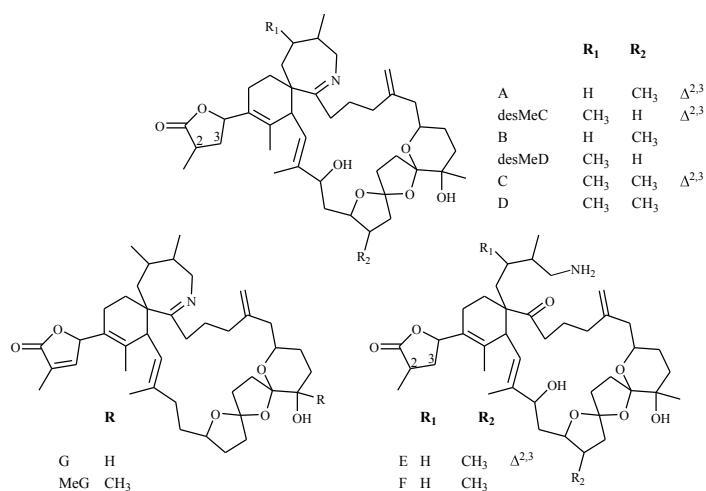
Since PTXs often co-occur with other phycotoxins in shellfish, no toxic episodes in humans could be unequivocally related to them and therefore there is no information about their toxicity to humans.

It has been shown that PTXs are potently cytotoxic<sup>61</sup> and cause necrosis to hepatocytes.<sup>62</sup> Nothing is known of the chronic toxicology of PTXs or the potential implications to public health in the long term.

### 3.1.7. Spirolides

Spirolides constitute a group of toxins featuring a spiro-linked tricyclic ether ring system and an unusual 7-membered spiro-linked cyclic imine moiety (Figure 8).

The causative micro-organism producing spirolide toxins has been unequivocally identified as the dinoflagellate *Alexandrium ostenfeldii*.<sup>63,64</sup> Chemical studies performed on strains of *A. ostenfeldii* from several geographical areas have individuated a considerable number of spirolide toxins differing in slight structural details.<sup>65-70</sup>



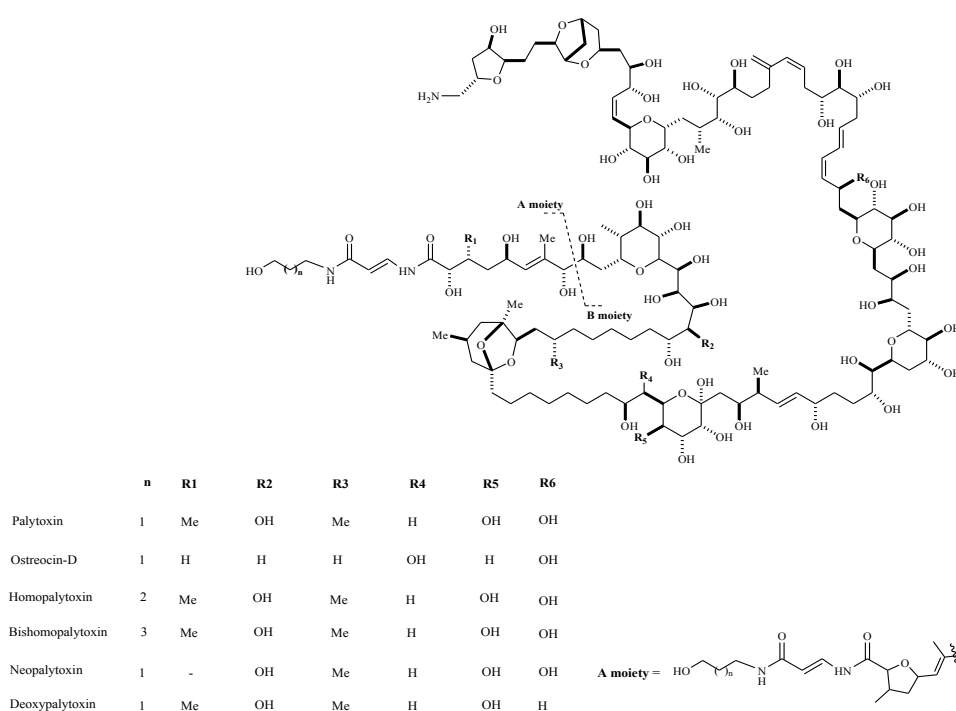
**Figure 8.** Chemical structure of spirolides.

Spirolides induce a fast lethal toxic effect when i.p. administered to both mice and rats, and are less toxic by oral administration. Spirolide toxicity on humans still remains unknown, although gastric distress and tachycardia were diagnosed in shellfish consumers in coincidence with the occurrence of spirolides in Canadian mollusks. The unique cyclic imine moiety seems to be the pharmacophore responsible for the fast-acting syndrome induced in mice when spirolides are i.p. administered ( $LD_{50} = 40 \mu\text{g}/\text{kg}$ ).<sup>71</sup> In fact, two hydrolysis derivatives of the cyclic imine functionality, namely spirolide E and spirolide F, reported by Hu *et al.* in 1996 are inactive in the mouse bioassay.<sup>66</sup>

### 3.1.8. Palytoxins

Palytoxin (Figure 9) is a complex polyhydroxylated water-soluble compound and one of the most potent non-protein marine toxins known so far.

It was first isolated in 1971 by the soft coral *Palythoa toxica*<sup>72</sup> but its gross structure was elucidated only 10 years later by two groups independently, namely Moore's<sup>73</sup> and Hirata's group.<sup>74</sup> In 1982, Kishi and co-workers disclosed the complete stereochemistry of the natural isomer of palytoxin isolated from *Palythoa tuberculosa*,<sup>75</sup> which was confirmed a few years later by the total synthesis of palytoxin.<sup>76</sup>



**Figure 9.** Structure of palytoxin and its analogues.

Although palytoxin has been isolated worldwide from zoanthids belonging to the genus *Palythoa*, its origin has long been controversial. Recently, dinoflagellates belonging to the genus *Ostreopsis* have been suggested as probable biogenetic origin of palytoxin.<sup>77,78</sup> Support to this hypothesis is provided by identification of putative palytoxin as the causative toxin of cases of clupectoxism occurred during *O. siamensis* blooms<sup>79</sup> and, most importantly, by identification of a number of palytoxin-like compounds from various *Ostreopsis* spp., namely:

- ostreocin-D (from *O. siamensis*), whose complete structure (Figure 9) was assigned as 42-hydroxy-3,26-didemethyl-19,44-dideoxypalytoxin, basing on NMR data,<sup>77,80</sup> and

verified by negative-ion fast-atom bombardment collision-induced dissociation tandem mass spectrometry.<sup>81</sup>

- b) mascarenotoxins<sup>82</sup> (from *O. mascarenensis*) purified and identified as palytoxin-like compounds basing on comparison of their mass spectrum profiles and fragmentation patterns with those of a reference standard of palytoxin.
- c) ovatoxin-a (from *O. ovata*),<sup>17</sup> whose LC/MS/MS structure determination is described below.

Other analogues of palytoxin, namely homo-, bishomo-, neo-, and deoxy-palytoxin (Figure 9) were isolated from the soft coral *Palythoa tuberculosa*<sup>83</sup> but they have not yet proved to be produced by *Ostreopsis* spp.

Palytoxin exhibits high toxicity in mammals with intravenous LD<sub>50</sub> ranging between 25 and 450 ng/kg.<sup>84</sup> Although no data is available on toxicity of palytoxin by oral administration, studies on rats demonstrated that toxicity by intra-gastric administration is significantly lower with an LD<sub>50</sub> > 40 µg/kg.<sup>84,85</sup>

Despite palytoxin high lethality to terrestrial animals, some marine animals appear not to be affected by the toxin, namely crabs,<sup>86</sup> filefish,<sup>87</sup> triggerfish,<sup>88</sup> and mackerel.<sup>89</sup> Such animals accumulate palytoxin and enable it to enter the human food chain. Some fatal human poisonings attributed to palytoxin have been reported worldwide.<sup>90,91</sup> Symptoms of intoxication include vasoconstriction, hemorrhage, ataxia, muscle weakness, ventricular fibrillation, pulmonary hypertension, ischemia, and death. Palytoxin binds to the Na<sup>+</sup>, K<sup>+</sup>-ATPase and converts this pump into an open channel.<sup>92-95</sup>

In the late '80s, palytoxin was also identified as a skin tumor promoter.<sup>96,97</sup> In contrast to TPA (12-*O*-tetradecanoylphorbol-13-acetate), palytoxin induces neither ornithine decarboxylase in mouse skin nor HL-60 cell adhesion. Furthermore, palytoxin neither binds to protein kinase C in vitro nor increases ornithine decarboxylase activity in the mouse skin. On the basis of such evidence, palytoxin is classified as a non-TPA-type tumor promoter.<sup>98</sup>

Detection and quantitation of palytoxin in biological samples can be accomplished by both analytical means and biological assays. However, it is often necessary to use a combination of methods to confirm the presence of the toxin. The simplest way to detect palytoxin is the mouse bioassay (LD<sub>50</sub> = 450 ng/kg).<sup>99</sup> Alternative assays take advantage of palytoxin functional properties and include in vitro cytotoxicity,<sup>100</sup> delayed haemolysis,<sup>101</sup> and antibody-based haemolysis neutralization tests.<sup>102</sup> All these assays are extremely sensitive but, in most regulatory situations, positive results require further confirmation by instrumental methods.

Recently, a precolumn derivatization method has been proposed for the separation and quantification of palytoxin; it takes advantage of the presence of one amino terminal group in the palytoxin molecule and uses the 6-aminoquinolyl-N-hydroxysuccinimidyl carbamate as derivatization reagent.<sup>103</sup>

A new method for detection of palytoxin based on liquid chromatography with electrospray ionization and tandem mass spectrometric detection (LC-ESI-MS) has been recently developed by my research group.<sup>16</sup>

## 3.2. Recent insights into the latest Mediterranean toxic outbreaks

### 3.2.1. Historical background

Across the Mediterranean basin, toxic outbreaks due to harmful algal blooms have been spreading with an ever increasing incidence over the past decades. Towards the late '80s - when for the first time in Italy some cases of gastroenteritis were related to the presence of producers of DSP toxins both in seawater and shellfish<sup>104</sup> – Prof. Ciminiello's group undertook a research line aimed at investigating the occurrence of marine biotoxins in Italian seas, contributing to provide insightful details on the complex and peculiar Mediterranean toxin profile.

As mentioned above, when in the late '80s DSP-producers, (e.g. *Dinophysis fortii*, *D. sacculus*, and *D. tripos*<sup>105</sup>), bloomed in the Adriatic Sea, this research group succeeded in isolating and unambiguously identifying okadaic acid from a bulky batch of contaminated shellfish.<sup>104</sup> This afforded the very first experimental evidence of the occurrence of DSP-toxins in the Mediterranean Sea. Since then, OAs have been the main Adriatic marine biotoxins through the mid '90s.<sup>106-108</sup>

Around 1995, in fact, discrepant results deriving from mouse bioassays and analytical HPLC-based methodologies suggested the presence in Adriatic mussels of toxins other than okadaic acids. This assumption was also prompted by a concomitant proliferation of a new dinoflagellate, *Protoceratium reticulatum*, in the Northern Adriatic Sea. Through analyzing a huge amount of toxic mussels (about 300 kg), for the first time in Italy we could isolate yessotoxin (YTX, Figure 5) in addition to only trace quantity of OA.<sup>109</sup>

Successively, beside relatively large amount of 45-hydroxyYTX,<sup>110</sup> two new analogues, homoYTX and 45-hydroxyhomoYTX,<sup>111</sup> were also isolated from Italian mussels.

Over the following years, our continuous studies on toxic shellfish led us to isolate and fully characterize a number of new YTX analogues, namely adriatoxin (ATX),<sup>112</sup>

carboxyessotoxin (carboxyYTX),<sup>113</sup> carboxyhomoyessotoxin (carboxyhomoYTX) [<sup>114</sup>], and 42,43,44,45,46,47,55-heptanor-41-oxohomoYTX (noroxohomoYTX)<sup>115</sup> (Figure 5).

From 1995 on, yessotoxins have played a dominant role in Adriatic mussel poisoning, while okadaic acids have slowly subsided until virtually disappearing around the turn of the new millennium.

### **3.2.2. Occurrence of Spirolides in phytoplankton and mussels from the Adriatic Sea**

The spreading of domoic acid producing species in the Adriatic Sea further compounds sanitary problems associated to shellfish contamination in that area already plagued by the presence of yessotoxins and DSP-toxins. To make the picture even more alarming, a new threat to human health is now impending over the Adriatic Sea: the toxic dinoflagellate *Alexandrium ostenfeldii*.

Ever since November 2003, high concentrations of *A. ostenfeldii* cells have been detected along the Northern Adriatic coasts (Italy), and in concomitance with these toxic outbreaks we started analyzing the toxin profile of Adriatic *A. ostenfeldii* cultures<sup>116</sup> as well as that of mussels grown in areas massively infested by this dinoflagellate.

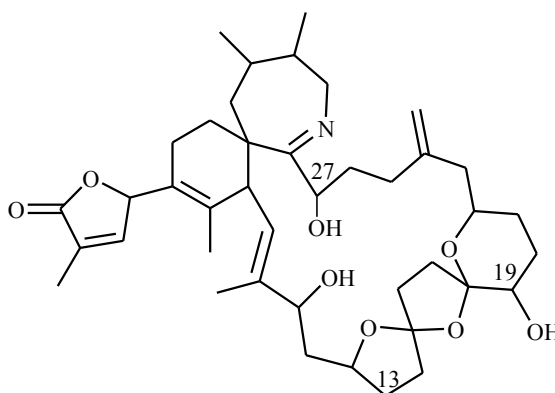
In literature, *Alexandrium* strains are reported to produce different classes of marine biotoxins depending on its geographical provenience. In Canadian strains high levels of spirolides have been described,<sup>64</sup> whilst strains from New Zealand have been proven to produce PSP-toxins.<sup>117</sup> Even more complex is the toxin profile of certain *A. ostenfeldii* populations detected in Scandinavia, where both spirolides and PSP-toxins have been found.<sup>118</sup> On the basis of these reports, Prof. Ciminiello's group searched the occurrence of both spirolides and PSP-toxins in samples of toxic mussels and in cultures of *A. ostenfeldii* from the Adriatic Sea. This study characterized the Adriatic *A. ostenfeldii* as an organism producing several spirolides but none of the major PSP-toxins.<sup>116</sup>

Chemical studies performed on strains of *A. ostenfeldii* from several geographical areas have individuated a considerable number of spirolide toxins differing in slight structural details.<sup>65,67-70</sup> Among the isolated compounds, 13-desmethyl spirolide C represents the major component of the spirolide content of all the *A. ostenfeldii* strains analyzed this far.<sup>68</sup>

Some preliminary studies performed on Adriatic *A. ostenfeldii* cultures in Ciminiello's laboratories proved that 13-desmethyl spirolide C was the main toxin produced by the dinoflagellate in accordance with what already reported in literature.<sup>116</sup> Alongside this major already known spirolide, the analysis highlighted the occurrence of a complex mixture of other, potentially new, spirolides. Unfortunately, the small amount of available material kept

Prof. Ciminiello's group from fully assigning the structures of these new spirolides. Therefore, large scale culturing of *A. ostentfeldii* was carried out in order to isolate the new derivatives in amount sufficiently large for NMR investigation.

Starting from such greater quantity of *A. ostentfeldii* culture a much higher number of spirolides than that reported in a previous study, were detected. Some of the detected derivatives corresponded to those described by other authors on the basis of  $[M+H]^+$  ions and fragmentation patterns,<sup>68-70</sup> while some others appeared to have been never reported before. Among them, three major spirolides were identified: the recently described 13,19-didesmethyl spirolide C<sup>70</sup> and 13-desmethyl spirolide C<sup>67</sup> (Figure 8), as well as a compound at  $m/z$  694.5 which appeared a potentially new spirolide. Consequently, its structural determination was achieved by employing both MS- and NMR-based experiments, which led to define it as 27-OH-13,19-didesmethyl spirolide C<sup>119</sup> (Figure 10).



**Figure 10.** Chemical structure of 13,19-didesmethyl-27-hydroxy spirolide C from Adriatic *A. ostentfeldii*.

A number of minor spirolides were also detected by HRLC-MS experiments,<sup>136</sup> and investigated by NMR.

Besides the analysis of Adriatic *A. ostentfeldii* cultures, Ciminiello's group has also investigated the toxin content of shellfish samples collected along the Adriatic coastline in coincidence with the occurrence of high concentrations of *A. ostentfeldii* in seawater. Studies carried out on these toxic samples provided almost the same conclusions afforded by investigating the Adriatic *A. ostentfeldii* cultures. In particular, LC-MS analyses clearly highlighted the occurrence of 13,19-didesmethyl spirolide C and 13-desmethyl spirolide C as major component of the spirolide content (*data not published*).

### 3.2.3. *Ostreopsis* spp. blooms and palytoxins outbreaks in the Mediterranean Sea

Dinoflagellates belonging to *Ostreopsis* genus have been blooming along the Mediterranean coastlines since the late '90s. The first documented cases occurred in summers 1998, 2000 and 2001 along North-western Tuscanian coasts,<sup>120</sup> when massive blooms of *O. ovata* resulted in extensive benthonic biocenosis sufferings. Concurrently, most of the emerging rocks and pebbly sea-bottom as well as seaweeds were covered by a reddish-brown jelly film teeming with *Ostreopsis ovata*.<sup>121</sup> Human sufferings were occasionally recorded during these events and in following summers when an *Ostreopsis* population bloomed along the Apulian coasts.<sup>122</sup>

In summer 2005, the phenomenon broke out with alarming proportion along the Ligurian coasts and caught the attention of both national and international media. Hundreds of people required medical attention after exposure to marine aerosol during recreational or working activities on the beach and promenade of Genoa (Italy). The symptoms shown by all the patients included high fever associated to serious respiratory distress such as watery rhinorrhea, dry or mildly productive cough, bronchoconstriction with mild dyspnea and wheezes. Some people described a metallic taste of the water. At the same time, an environmental suffering involving mostly epibenthos, both sessile (cirripeds, bivalves, gastropods) and mobile (echinoderms, cephalopods, little fishes), was observed. A careful look at the marine plankton brought to the light that an unusual proliferation of the tropical microalga *O. ovata* ( $1.8 \times 10^6$  cells/L) was occurring along the investigated coastal areas during the toxic outbreak. Most symptoms in humans disappeared as the population of *O. ovata* started fading away.

The Prof. Ciminiello's research group analyzed a plankton sample collected off Genoa coasts during the toxic outbreak. The aqueous-methanol extract of the sample was proved to induce mice death within 30 min after intra-peritoneal injection. Initially, the presence in the extract of the following phycotoxins was investigated by liquid chromatography-mass spectrometry (LC-MS):<sup>123,124,125</sup> a) okadaic acid, spirolides, yessotoxins, saxitoxins, and domoic acid, that are commonly found in the Mediterranean Sea;<sup>126</sup> b) brevetoxins that, although never reported in the Mediterranean Sea, are usually associated with poisonings due to marine aerosols.<sup>127</sup> None of the above toxins was detected in the plankton sample.<sup>16</sup>

Since some *Ostreopsis* species are regarded as producers of palytoxin-like compounds (Figure 9), the need arose to set up a new method based on liquid chromatography-mass spectrometry coupling for detection of palytoxin to investigate whether the *O. ovata* blooming during the Genoa endemic disease was producing the toxin.



LC-MS/MS has great potential for rapid, sensitive and unambiguous identification of palytoxin in contaminated material. In fact, the capability of ESI to produce multiply charged molecules under mild conditions has accessed detection of a high MW compound such as palytoxin ( $C_{129}H_{223}N_3O_{54}$ ) by extending the mass range for  $m/z$ -limited mass spectrometers.

A full-MS spectrum in positive ion mode was obtained by direct infusion of the toxin standard in a mixture of acetonitrile-water (1:1, v/v) both eluents containing 30 mM acetic acid. Basing on full-MS spectra, the following ions were selected for selected ion monitoring (SIM) experiments:  $m/z$  1340.7  $[M+2H]^{2+}$ , 1331.7  $[M+2H-H_2O]^{2+}$ , and 906.1  $[M+2H+K]^{3+}$ . Whatever was the precursor ion used, either bi-charged or tri-charged, the fragmentation pattern of palytoxin produced in the product ion spectra contained an intense ion at  $m/z$  327, which arises from the cleavage between the carbons 8 and 9 of the toxin molecule and the additional loss of a molecule of water.<sup>83</sup> Thus, the following transitions Q1  $\rightarrow$  Q3 at  $m/z$  values of 1340.7  $\rightarrow$  327.1, 1331.7  $\rightarrow$  327.1, and 906.1  $\rightarrow$  327.1 were selected for multiple reaction monitoring (MRM) experiments, which permit better selectivity and better signal-to-noise ratios than SIM.

The best LC conditions which allowed determination of palytoxin in a 15 min analysis are the following.

<b>COLUMN:</b>	5 $\mu$ m Gemini C-18, 150 x 2.00 mm, (Phenomenex, Torrance, CA, USA)
<b>MOBILE PHASE:</b>	A = water with 30 mM acetic acid
	B = acetonitrile/water (95:5, v/v) with 30 mM acetic acid
<b>ELUTION:</b>	Gradient = 20-100 % B over 10 min and hold 4 min
<b>FLOW:</b>	200 $\mu$ l/min
<b>TEMPERATURE :</b>	room temperature (21 $^{\circ}$ C)

Under the used conditions, limits of detection (LOD, S/N = 3) and quantitation (LOQ, S/N = 10) in MRM mode were calculated to be 25 and 84 ng/ml for matrix-free palytoxin, respectively; while they resulted to be 38 and 127 ng/ml for matrix-matched palytoxin, respectively.

Basing on the newly developed method for detection of palytoxin Ciminiello's group analyzed the plankton extract and detected a peak in MRM chromatogram which matched perfectly in retention time, fragmentation and ion ratios those of a reference sample injected under the same experimental conditions. This indicated that putative palytoxin was contained in the plankton extract at levels of 3.30  $\mu$ g which matched with the mouse bioassay results.

Due to the complex stereo-structure of palytoxin this research group referred to the detected compound as putative palytoxin rather than palytoxin, as the possibility that the compound is a palytoxin isomer cannot be excluded on the base of the obtained LC-MS results.<sup>16</sup>

Following this event, in 2006 the presence of *O. ovata* was monitored along the Ligurian coasts in order to prevent further human sufferings. Indeed, a remarkable proliferation of *O. ovata* was detected in the Mediterranean sea from July through August 2006. Bathing was forbidden in several Italian coastal areas and, thus, the number of people suffering from the toxic outbreak was significantly limited in comparison to the 2005 event.

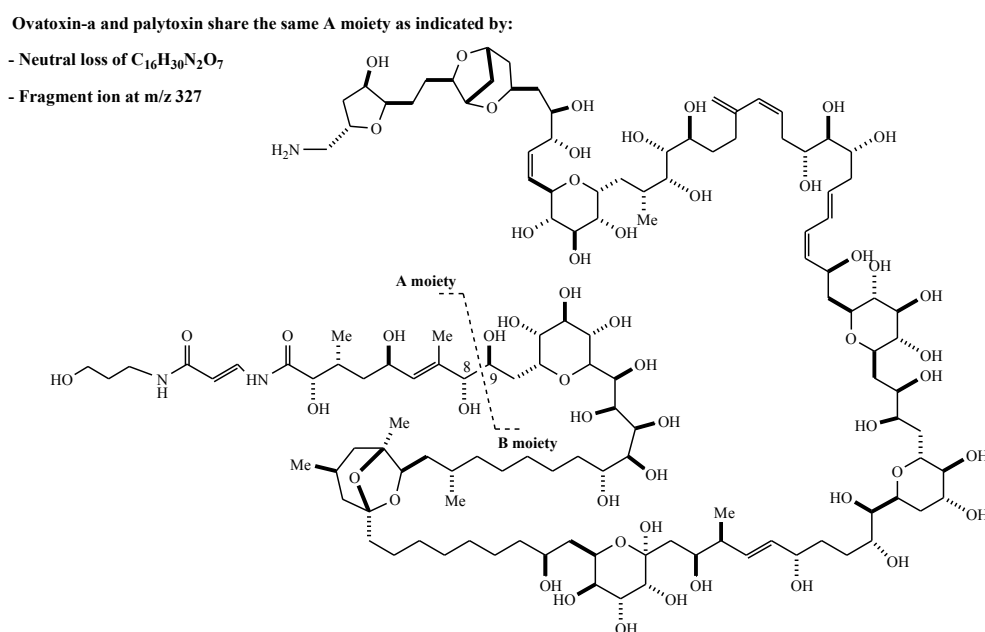
Four plankton samples were collected in summer 2006 along the Ligurian coasts in the area of Genoa and La Spezia and they were analyzed by the newly developed method for detection of palytoxin.<sup>16</sup> The obtained results paralleled those obtained on the 2005 plankton samples with levels of putative palytoxin in the range 0.09-0.40 pg/cell. The presence of putative palytoxin was shown in all the samples by peaks which closely matched those of a reference sample of palytoxin in retention time, fragmentation and ion ratios.

In order to look for additional palytoxin analogues in the samples, a more detailed and comprehensive MS investigation was carried out by using different MS instrumentation. Initially, full scan mass spectra were recorded on both an ESI triple quadrupole MS and an ESI-ion trap-MS. A different degree of front end fragmentation, likely due to different geometry of ionization sources and ionization parameters used, was observed on the two instruments. However, an accurate comparison between the obtained MS spectra and palytoxin standard's indicated the presence in the sample of a palytoxin-like molecule that didn't correspond either to palytoxin itself or to any known palytoxin analogue. It was named ovatoxin-a.<sup>17</sup>

The exact mass of ovatoxin-a and its fragments were established by high resolution spectra obtained in LC-MS and LC-product ion MS modes using a linear ion trap hybrid FTMS instrument. The mono-charged ion cluster in the HRMS spectrum of ovatoxin-a presented a mono-isotopic ion peak  $[M+H]^+$  at  $m/z$  2647.4868 which allowed to infer the molecular formula  $C_{129}H_{223}N_3O_{52}$  ( $\Delta = -3.918$  ppm) to the molecule. Further confirmation for such elemental composition was provided by the exact masses of bi-charged (mono-isotopic ion peak at  $m/z$  1335.2429 for  $C_{129}H_{224}N_3NaO_{52}$ ,  $\Delta = -0.174$  ppm) and tri-charged (mono-isotopic ion peak at  $m/z$  890.4937 for  $C_{129}H_{225}N_3NaO_{52}$ ,  $\Delta = -4.657$  ppm) ions. Ovatoxin-a presented two oxygen atoms less than palytoxin ( $C_{129}H_{223}N_3O_{54}$ ). The LC-HR product ion spectrum obtained by selecting the mono-charged ion of ovatoxin-a as precursor ion contained

abundant peaks due to subsequent losses of two, three, and four water molecules from the  $[M+H]^+$  ion and a structurally interesting fragment ion at  $m/z$  2286.2864 (mono-isotopic ion at  $m/z$  2285.2825) due to loss of 362.2043 amu from the precursor ion, corresponding to a  $C_{16}H_{30}N_2O_7$  ( $\Delta = -2.765$  ppm) neutral fragment.

In the same experimental conditions, the LC-HR product ion spectrum of palytoxin standard paralleled that of ovatoxin-a in the presence of ions due to multiple water losses and of an ion ( $m/z$  2318.2749) due to neutral loss of 362.2036 amu ( $C_{16}H_{30}N_2O_7$ ). The neutral fragment  $C_{16}H_{30}N_2O_7$  originates from cleavage between carbons 8 and 9 and corresponds to A moiety of palytoxin with an additional molecule of water. Thus, structural differences between ovatoxin-a and palytoxin likely lie in the rest of the molecule (part structure B in Figure 11).



**Figure 11.** Structure of palytoxin and indication of the structural features common to ovatoxin-a.

On the basis of molecular formula (ovatoxin-a presents two oxygen atoms less than palytoxin), fragmentation pattern, and chromatographic behaviour, the structure of ovatoxin-a appeared to be strictly related to palytoxin's. However, on the account of data reported on bio-activity of palytoxin analogues, even slight structural differences could significantly affect and differentiate the toxicology of the two compounds. By way of example, ostreocin D, whose structure is very similar to palytoxin's, presents a very different cytotoxic (2.5 pM for ostreocin D versus 0.2 pM for palytoxin) and hemolytic activity (39.5 nM for ostreocin D

versus 1.5 nM for palytoxin) from those of palytoxin.<sup>80,128</sup> Thus, isolation of ovatoxin-a is most necessary both to elucidate its chemical structure and evaluate its toxicology.

Quantitative analyses were carried out by assuming for palytoxin and ovatoxin-a a similar molar response as a consequence of the evident structural similarities between the two compounds. The calculated amount of ovatoxin-a in the analyzed sample were in the range 1.26-3.11 pg/cell, suggesting that ovatoxin-a was by far the predominant palytoxin-like compound in the 2006 plankton. Application of the developed method for detection of palytoxin and ovatoxin-a to the analysis of cultures of *O. ovata* indicated it as the producing organism of both compounds detected in natural plankton. Quantitative analyses afforded a putative palytoxin and a ovatoxin-a contents of 0.55 pg/cell and 3.85 pg/cell, respectively. Interestingly, the two compounds appeared to be produced approximately in the same ratio observed in natural plankton.<sup>17</sup>

In summer 2007, *O. ovata* bloomed again in Italy along the whole Tirrenian coasts, from Liguria to Sicily, and in some sites of the Adriatic coasts, in Apulia and Friuli Venezia Giulia. About 80 people reported serious respiratory distress after exposure to toxic marine aerosols along the coasts of Bari (Apulia).

Very recently, an episode of shellfish contamination due to palytoxin-like compounds from *Ostreopsis* species has been reported along the coastal waters of the North Egean Sea (Greece). Studies were carried out by testing toxicity of the samples by mouse bioassay and delayed hemolytic activity.<sup>129</sup>

### 3.3 Conclusions

Toxins studies, carried out over the past 20 years have afforded significant insights into the problem of marine biotoxins infesting the Italian coastline.

Unlike other marine environments across the world, probably due to its geographical and morphological features, the Adriatic Sea shows a pretty unique, complex, and, above all, continuously changing toxin profile. In fact, if from the late '80s through the mid '90s okadaic acids have been the main Adriatic toxins, from 1995 onward, yessotoxins have dominated the toxic content of this sea. Successively, around the beginning of the 3<sup>rd</sup> millennium, desulfoyessotoxins have proven the most abundant toxic compounds detected in Adriatic mollusks; while lately spirolides have been posing health risks to seafood consumers. To make the picture even more complex, also domoic acid has recently entered the Adriatic toxin profile. Even though detected so far at concentrations lying below its regulatory limit, this latter toxin must be attentively monitored as it could any time be rising at alarming levels.

In such a dangerous context, a frequent and in-depth chemical analysis of toxic plankton and contaminated seafood is strongly needed. In fact, routine monitoring based on mouse bioassays alone suffers from at least two main drawbacks:

- 1) only already known biotoxins can be individuated, and no information is given on any other new toxic compound possibly occurring in toxic plankton or mollusks;
- 2) critical misunderstandings in assessing toxin content of a sample can arise, as demonstrated in the case of okadaic acids and desulfoyessotoxins whose identity cannot be established on the basis of the official mouse bioassay alone.

Besides all of the above hazards, very recently another most dangerous threat has been impending over the Mediterranean Sea: the spreading of the tropical alga *O. ovata*. The investigation of Prof. Ciminiello's group on Mediterranean *O. ovata* has brought to light the presence of a new palytoxin-like compound, named ovatoxin-a, alongside minor amounts of a putative palytoxin. In this field, the next step of this lab will be the isolation and full characterization of ovatoxin-a. This is a prerequisite to evaluate its toxicity and assess whether it represents a serious threat to human beings. The potential of ovatoxin-a of entering the human food chain should be also investigated. In particular, scientific efforts should zero in on singling out edible marine organisms capable of accumulating ovatoxin-a, as well as assessing the extent of the accumulation process.

Another crucial issue entwined with *O. ovata* deals with the release of palytoxins into the marine aerosol, inducing fastidious symptoms – i.e. respiratory distress and conjunctivitis-in humans. To this regard it is fundamental studying the environmental factors, such as weather conditions and geographical morphology, favoring the onset of the toxic aerosols, as they cause grave damages to the tourism industry, such an essential component of the Italian economy.

### 3.4. References

1. G.M. Hallegraeff, A review of harmful algal blooms and their apparent global increase, *Phycologia*, 1993, 32, 79-99.
2. C.P. Soames-Mraci, Shellfish poisoning: public health risks, quality assurance and analytical detection, *Chemistry in Australia*, 1995, December, 22-25.
3. J. Tibbetts, Toxic Tides, *Environmental Health Perspectives*, 1998, 106, A326-A331.
4. S.E. Shumway, A review of the effects of algal blooms on shellfish and aquaculture, *J World Aquacult. Soc.*, 1990, 21, 65-104.

5. F.E. Ahmed, Naturally occurring seafood toxins, *Journal of Toxicology, Toxin Reviews*, 1991, 10, 263-287.
6. D.M. Anderson in *Red Tides: Biology Environmental Science and Toxicology* (eds. T. Okaichi, D.M. Anderson and T. Nemoto), Elsevier, New York, 1989, pp. 11-16.
7. T. Smayda in *Food Chains, Yields, Models, and Management of Large Ecosystems* (eds. K.L.M.A. Sherman and B.D. Gold), Westview Press, Boulder, 1992, pp. 275-307.
8. D.J. Bower, R.J. Hart, P.A. Matthews and M.E.H. Howden, Nonprotein neurotoxins, *Clin. Toxicol.*, 1981, 18, 813-843.
9. L.M. Botana, M. Rodriguez-Vieytes, A. Alfonso and M.C. Louzao, in *Handbook of food analysis - residues and other food component analysis*, Vol. 2 (ed. L.M.L. Nollet), Marcel Dekker Inc., New York, 1996, pp. 1147-1169.
10. L.M. Botana, in *Seafood and Freshwater Toxins – Pharmacology, Physiology, and Detection*, 2<sup>nd</sup> Edition (ed. L.M. Botana), CRC Press Taylor & Francis Group, Boca Raton, FL, 2008, pp. 149-161.
11. FAO Food and Nutrition Papers 80, 2004, pp. 1-295, <http://www.fao.org/docrep/007/y5486e/y5486e00.htm>.
12. P. Ciminiello and E. Fattorusso, in *Progress in Molecular and Subcellular Biology - Subseries Marine Molecular Biotechnology*, Vol. 43 (eds. G. Cimino, and M. Gavagnin), Springer-Verlag Berlin, Heidelberg, 2006, 53-82.
13. P. Ciminiello, C. Dell'Aversano, E. Fattorusso, M. Forino, S. Magno, F. Santelia and M. Tsoukatou, Investigation of the toxin profile of Greek *Mytilus galloprovincialis* by liquid chromatography –mass spectrometry, *Toxicon*, 2006, 47, 174-181.
14. G. Sansoni, B. Borghini, G. Camici, M. Casotti, P. Righini and C. Rustighi, Fioriture algali di *Ostreopsis ovata* (Gonyaulacales: Dinophyceae): un problema emergente. *Biologia Ambientale*, 2003, 17, 17-23.
15. A. Penna, M. Vila, S. Fraga, M.G. Giacobbe, F. Andreoni, P. Riobò and C. Vernesi, Characterization of *Ostreopsis* and *Coolia* (Dinophyceae) isolates in the Western Mediterranean sea based on morphology, toxicity and internal transcribed spacer 5.8S rDNA sequences. *Journal of Phycology*, 2005, 41, 212-225.
16. P. Ciminiello, C. Dell'Aversano, E. Fattorusso, M. Forino, G.S. Magno, L. Tartaglione, C. Grillo and N. Melchiorre, The Genoa 2005 outbreak. Determination of putative palytoxin in Mediterranean *Ostreopsis ovata* by a new liquid chromatography tandem mass spectrometry method, *Anal. Chem.*, 2006, 78, 6153-6159.

17. P. Ciminiello, C. Dell'Aversano, E. Fattorusso, M. Forino, L. Tartaglione, C. Grillo and N. Melchiorre, Putative palytoxin and its new analogue, ovatoxin-a, in *Ostreopsis ovata* collected along the Ligurian coasts during the 2006 toxic outbreak, *J. Am. Soc. Mass Spectrom.*, 2008, 19, 111-120.
18. P. Durando, F. Ansaldi, P. Oreste, P. Moscatelli, L. Marensi, C. Grillo, R. Gasparini and G. Icardi, *Ostreopsis ovata* and human health: epidemiological and clinical features of respiratory syndrome outbreaks from a two-year syndromic surveillance, 2005-06, in north-west Italy, *Euro Surveill.*, 2007, 12 (6).
19. Y. Shimizu, Chemistry and mechanism of action, *Food Science and Technology*, 2000, 103, 151-172.
20. S. Hall, G. Strichartz, E. Moczydowski, A. Ravindran and P.B. Reichardt, in *Marine toxins: origin, structure and molecular pharmacology* (eds. S. Hall and G. Strichartz), American Chemical Society, Washington, DC., 1990, pp. 29-65.
21. T. Yasumoto and M. Murata, Marine Toxins, *Chem. Rev.*, 1993, 93, 1897-1909.
22. M. Murata, M. Shimatani, H. Sugitani, Y. Oshima and T. Yasumoto, Isolation and structural elucidation of the causative toxin of the diarrhetic shellfish poisoning, *Bull. Jpn. Soc. Sci. Fish.*, 1982, 48, 549-552.
23. T. Hu, J. Doyle, D. Jackson, J. Mart, E. Nixon, S. Pleasance, M.A. Quilliam, J.A. Walter and J.L.C. Wright, Isolation of a new diarrhetic shellfish poison from Irish mussels, *J. Chem. Soc. Chem. Commun.*, 1992, 30, 39-41.
24. J.S. Lee, T. Igarashi, S. Fraga, E. Dahl, P. Hovgaard, and T. Yasumoto, Determination of diarrhetic shellfish toxins in various dinoflagellate species, *J. Appl. Phycol.*, 1989, 1, 147-152.
25. G. Eaglesham, S. Brett, B. Davis and N. Holling, Detection of pectenotoxin-2 and pectenotoxin-2 seco acid in phytoplankton and shellfish from the Ballina region of New South Wales, Australia, *X International IUPAC Symposium on Mycotoxins and Phycotoxins*, Brazil, 2000, p. 40.
26. L.L. Rhodes and M. Syhre, Okadaic acid production by a New Zealand *Prorocentrum lima* isolate, *New Zealand J. Mar. Freshwat. Res.*, 1995, 29, 367-370.
27. I. Bravo, M.L. Fernandez, I. Ramilo and A. Martinez, Toxin composition of the toxic dinoflagellate *Prorocentrum lima* isolated from different locations along the Galician coast (NW Spain), *Toxicon*, 2001, 39, 1537-1545.
28. K. Terao, E. Ito, T. Yanagi and T. Yasumoto, Histopathological studies on experimental marine toxin poisoning. 1. Ultrastructural-changes in the small-intestine and liver of

- suckling mice induced by dinophysistoxin-1 and pectenotoxin-1, *Toxicon*, 1986, 24, 1141-1151.
29. H. Fujiki and M. Suganuma, Tumor promotion by inhibitors of protein phosphatases 1 and 2A: the okadaic acid class of compounds, *Adv. Cancer Res.*, 1993, 61, 143-194.
  30. A. Takai, M. Murata, K. Torigoe, M. Isobe, G. Mieskes and T. Yasumoto, Inhibitory effect of okadaic acid derivatives on protein phosphatases. A study on structure-affinity relationship, *Biochem. J.* 1992, 284, 539-544.
  31. K. Sasaki, M. Murata, T. Yasumoto, G. Mieskes and A. Takai, Affinity of okadaic acid to type-1 and type-2A protein phosphatases is markedly reduced by oxidation of its 27-hydroxyl group, *Biochem. J.*, 1994, 298, 259-262.
  32. M. Murata, M. Kumagai, J.S. Lee and T. Yasumoto, Isolation and structure of yessotoxin, a novel polyether compound implicated in diarrhetic shellfish poisoning, *Tetrahedron Lett.*, 1987, 28, 5869-5872.
  33. M. Satake, L. MacKenzie and T. Yasumoto, Identification of *Protoceratium reticulatum* as the biogenetic origin of yessotoxin, *Nat. Toxins*. 1997, 5, 164-167.
  34. B. Paz, P. Riobo, M.L. Fernandez, S. Fraga and J.M. Franco, Production and release of yessotoxins by the dinoflagellates *Protoceratium reticulatum* and *Lingulodinium polyedrum* in culture, *Toxicon*, 2004, 44, 251-258
  35. L. Rhodes, P. McNabb, M. de Salas, L. Briggs, V. Beuzenberg and M. Gladstone, Yessotoxin production by *Gonyaulax spinifera*, *Harmful Algae*, 2006, 5, 148-155.
  36. M. Konishi, X. Yang, B. Li, C.R. Fairchild and Y. Shimizu, Highly cytotoxic metabolites from the culture supernatant of the temperate dinoflagellate *Protoceratium cf. reticulatum*, *J. Nat. Prod.*, 2004, 67, 1309-1313.
  37. M. Satake, A. Tubaro, J-S. Lee and T. Yasumoto, Two new analogs of yessotoxin, homoyessotoxin and 45-hydroxyhomoyessotoxin, isolated from mussels of the Adriatic Sea, *Nat. Toxins*, 1997, 5, 107-110.
  38. P. Ciminiello, E. Fattorusso, M. Forino, R. Poletti and R. Viviani, Structure determination of carboxyhomoyessotoxin, a new yessotoxin analog isolated from Adriatic mussels, *Chem. Res. Toxicol.*, 2000, 3, 770-774.
  39. P. Ciminiello, E. Fattorusso, M. Forino and R. Poletti, 42,43,44,45,46,47,55-Heptanor-41-oxohomoyessotoxin, a new biotoxin from mussels of the northern Adriatic Sea, *Chem. Res. Toxicol.*, 2001, 14, 596-599.
  40. J. Aasen, I.A. Samdal, C.O. Miles, E. Dahl, L.R. Briggs and T. Aune, Yessotoxins in Norwegian blue mussels (*Mytilus edulis*): uptake from *Protoceratium reticulatum*,



- metabolism and depuration. *Toxicon*, 2005, 45, 265-272.
41. K. Terao, E. Ito, M. Oarada, M. Murata and T. Yasumoto, Histopathological studies on experimental marine toxin poisoning: 5. The effects in mice of yessotoxin isolated from *Patinopecten yessoensis* and of a desulfated derivative, *Toxicon* 1990, 28, 1095-1104.
  42. H. Ogino, M. Kumagai, T. Yasumoto, Toxicologic evaluation of yessotoxin, *Nat. Toxins*, 1997, 5, 225–229.
  43. J.M. Huang, C.H. Wu and D.G. Baden, Depolarizing action of a red-tide dinoflagellate brevetoxin on axonal membranes, *J. Pharmacol. Exp. Ther.*, 1984, 229, 615–621.
  44. M. Inoue, M. Dirama, M. Satake, K. Sugiyama and T. Yasumoto, Inhibition of brevetoxins binding to voltage-gated sodium channel by gambierol and gambieric acid-A, *Toxicon*, 2003, 41, 469-474.
  45. L.A. de la Rosa, A. Alfonso, N. Vilarino, M.R. Vieytes and L.M. Botana, Modulation of cytosolic calcium levels of human lymphocytes by yessotoxin, a novel marine phycotoxin, *Biochem. Pharmacol.*, 2001, 61, 827-833.
  46. A. de la Rosa, A. Alfonso, N. Vilarino, M.R. Vieytes, T. Yasumoto and L.M. Botana, Maitotoxin-induced calcium entry in human lymphocytes: modulation by yessotoxin, Ca(2+) channel blockers and kinases, *Cell. Signal.*, 2001, 13, 711-716.
  47. A. Alfonso, L.A. de la Rosa, M.R. Vieytes, T. Yasumoto and L.M. Botana, Yessotoxin a novel phycotoxin, activates phosphodiesterases activity. Effect of yessotoxin on cAMP levels in human lymphocytes, *Biochem. Pharmacol.*, 2003, 65, 193-208.
  48. J.L.C. Wright, R.K. Boyd, A.S.W. de Freitas, M. Falk, R.A. Foxall, W.D. Jamieson, M.V. Laycock, A.W. McCulloch, A.G. McInnes, P. Odense, V.P. Pathak, M.A. Quilliam, M.A. Ragan, P.G. Sim, P. Thibault, J.A. Walter, M. Gilgan, D.J.A. Richard, D. Dewar, Identification of domoic acid, a neuroexcitatory amino acid, in toxic mussels from eastern Prince Edward Island, *Can. J. Chem.*, 1989, 67, 481-490.
  49. S.S. Bates, C.J. Bird, A.S.W de Freitas, R. Foxall, M. Gilgan, L.A. Hanic, G.R. Johnson, A.W. McCulloch, P. Odense, R. Pocklington, M.A. Quilliam, P.G. Sim, J.C. Smith, D.V. Subba Rao, E.C.D. Todd, J.A. Walter and J.L.C. Wright, Pennate diatom *Nitzschia pungens* as the primary source of domoic acid, a toxin in shellfish from eastern Prince Edward Island, *Can. J. Fish. Aq. Sci.* 1989, 46, 1203-1215.
  50. D.L. Garrison, S.M. Conrad, P.P. Eilers and E.M. Waldron, Confirmation of domoic acid production by *Pseudo-nitzschia australis* (Bacillariophyceae) cultures, *J. Phycol.* 1992, 28, 604-607.

51. J.L. Martin, K. Haya, L.E. Burridge and D.J. Wildish, *Nitzschia pseudodelicatissima* - a source of domoic acid in the Bay of Fundy, eastern Canada, *Marine Ecol. Progress Series*, 1990, 67, 177-182.
52. F. Cerino, L. Orsini, D. Sarno, C. Dell'Aversano, L. Tartaglione and A. Zingone, The alternation of different morphotypes in the seasonal cycle of the toxic diatom *Pseudonitzschia galaxiae*, *Harmful Algae*, 2005, 4, 33-48.
53. J. Clayden, B. Read and K.R. Hebditch, Chemistry of domoic acid, isodomoic acids, and their analogs, *Tetrahedron*, 2005, 61, 5713-5724.
54. F.W. Bernam and T.F. Murray, Domoic acid neurotoxicity in cultured cerebellar granule neurons is mediated predominantly by NMDA receptors that are activated as a consequence of excitatory amino acid release, *J. Neurochem.*, 1997, 69, 693-703.
55. A. Quilliam and J.L.C. Wright, The amnesic shellfish poisoning mystery, *Anal. Chem.*, 1989, 61, 1053-1060.
56. T. Suzuki, in *Seafood and Freshwater Toxins – Pharmacology, Physiology, and Detection*, 2<sup>nd</sup> Edition (ed. L.M. Botana), CRC Press Taylor & Francis Group, Boca Raton, FL, 2008, pp. 343-359.
57. T. Yasumoto, M. Murata, J.S. Lee and K. Torigoe, in *Mycotoxins and Phycotoxins*, (eds. S. Natori, K. Hashimoto and Y. Ueno), Elsevier, Amsterdam, 1989, 375-382.
58. L. Edebo, S. Lange, X.P. Li, S. Allenmark and F. Jennische, in *Mycotoxins and Phycotoxins*, (eds. S. Natori, K. Hashimoto and Y. Ueno), Elsevier, Amsterdam, 1989, 437-444.
59. J.C. Gonzalez, F. Leira, O.I. Fontal, M.R. Vieytes, F.F. Arevalo, J.M. Vieites, M. Bermudez-Puente, S. Muniz, C. Salgado, T. Yasumoto and L.M. Botana, Inter-laboratory validation of the fluorescent protein phosphatase inhibition assay to determine diarrhetic shellfish toxins: intercomparison with liquid chromatography and mouse bioassay, *Anal. Chim. Acta*, 2002, 466, 233-246.
60. A. Lun, D.Z. Chen, J. Magoon, J. Worms, J. Smith and C.F. Holmes, Quantification of Diarrhetic Shellfish Toxins by identification of novel protein phosphatase inhibitors in marine phytoplankton and mussels, *Toxicon*, 1993, 31, 75-83.
61. J.H. Jung, C.J. Sim and C.O. Lee, Cytotoxic compounds from a two-sponge association, *J. Nat. Prod.*, 1995, 58, 1722-1726.
62. M. Ishige, N. Satoh and T. Yasumoto, Pathological studies on the mice administered with the causative agent of diarrhetic shellfish poisoning (okadaic acid and pectenotoxin-2), *Bull. Hokkaido Inst. Public Health*, 1988, 38, 15-19.

63. A.D. Cembella, M.A. Quilliam, N.I. Lewis, A.G. Bauder and J.L.C. Wright, in *Harmful Algae*, (eds. B. Reguera, J. Blanco, M.L. Fernandez and T. Wyatt), Xunta de Galicia and Intergovernmental Oceanographic Commission of UNESCO, 1998, pp. 481-484.
64. A.D. Cembella, N.I. Lewis, M.A. Quilliam, Spirolide composition of micro-extracted pooled cells isolated from natural plankton assemblages and from cultures of the dinoflagellate *Alexandrium ostenfeldii*, *Nat. Toxins*, 1999, 7, 197-206.
65. T. Hu, J.M. Curtis, Y. Oshima, M.A. Quilliam, J.A. Walter, W.M. Watson-Wright and J.L.C. Wright, Spirolides B and D, two novel macrocycles isolated from the digestive glands of shellfish, *J. Chem. Soc., Chem. Commun.*, 1995, 20, 2159-2161.
66. T. Hu, J.M. Curtis, J.A. Walter and J.L.C. Wright, Characterization of biologically inactive spirolides E and F: identification of the spirolide pharmacophore, *Tetrahedron Lett.*, 1996, 37, 7671-7674.
67. T. Hu, I.W. Burton, A.D. Cembella, J.M. Curtis, M.A. Quilliam, J.A. Walter and J.L.C. Wright, Characterization of spirolides A, C, and 13-desmethylC, new marine toxins isolated from toxic plankton and contaminated shellfish, *J. Nat. Prod.*, 2001, 64, 308-312.
68. L.Sleno, M.J. Chalmers and D.A. Volmer, Structural study of spirolide marine toxins by mass spectrometry. Part II. Mass spectrometric characterization of unknown spirolides and related compounds in a cultured phytoplankton extract, *Anal. Bioanal. Chem.*, 2004, 378, 977-986.
69. J. Aasen, S.L. MacKinnon, P. LeBlanc, J.A. Walter, P. Hovgaard, T. Aune, M.A. Quilliam, Detection and identification of spirolides in Norwegian shellfish and plankton, *Chem. Res. Toxicol.*, 2005, 18, 509-515.
70. S.L. MacKinnon, J.A. Walter, M.A. Quilliam, A.D. Cembella; P. LeBlanc, I.W. Burton, W.R. Hardstaff and N.I. Lewis, Spirolides isolated from Danish strains of the toxigenic dinoflagellate *Alexandrium ostenfeldii*, *J. Nat. Prod.*, 2006, 69, 983-987.
71. D. Richard, E. Arsenault, A. Cembella and M.A. Quilliam, in *Harmful Algal Blooms 2000* (eds. G.M. Hallegraeff, S.I. Blackburn, C.J. Bolch, R.J. Lewis), Intergovernmental Oceanographic Commission of UNESCO, Paris, 2001, pp. 383-386.
72. R.E. Moore and P.J. Scheuer, Palytoxin: a new marine toxin from a coelenterate, *Science*, 1971, 172, 495-498.
73. R.E. Moore and G. Bartolini, Structure of palytoxin, *J. Am. Chem. Soc.*, 1981, 103, 2491-2494.
74. D. Uemura, K. Ueda, Y. Hirata, H. Naoki and T. Iwashita, Further studies on palytoxin. II. Structure of palytoxin, *Tetrahedron letters*, 1981, 22, 2781-2784.

75. J.K. Cha, W.J. Christ, J.M. Finan, H. Fujioka, Y. Kishi, L.L. Klein, S.S. Ko, J. Leder, W.W. McWhorter, Jr, K.P. Pfaff, M. Yonaga, D. Uemura and Y. Hirata, Stereochemistry of palytoxin. Part 4. Complete structure, *J. Am. Chem. Soc.*, 1982, 104, 7369-7371.
76. R.W. Armstrong, J.M. Beau, S.H. Cheon, W.J. Christ, H. Fujioka, W.H. Ham, L.D. Hawkins, H. Jin, S.H. Kang, Y. Kishi, M.J. Martinelli, W.W. McWhorter, Jr., M. Mizuno, M. Nakata, A.E. Stutz, F.X. Talamas, M. Taniguchi, J.A. Tino, K. Ueda, J. Uenishi, J.B. White, M. Yonaga, Total synthesis of palytoxin carboxylic acid and palytoxin amide, *J. Am. Chem. Soc.*, 1989, 111, 7530-7533.
77. M. Usami, M. Satake, S. Ishida, A. Inoue, Y. Kan, and T. Yasumoto, Palytoxin analogs from the dinoflagellate *Ostreopsis siamensis*, *J. Am. Chem. Soc.*, 1995, 117, 5389-5390.
78. S. Taniyama, A. Osamu, T. Masamitsu, N. Sachio, T. Tomohiro, M. Yahia and N. Tamao, *Ostreopsis* sp., a possible origin of palytoxin (PTX) in parrotfish *Scarus ovifrons*. *Toxicon* 2003, 42, 29-33.
79. Y. Onuma, M. Satake, T. Ukena, J. Roux, S. Chanteau, N. Rasolofonirina, M. Ratsimaloto, H. Naoki and T. Yasumoto, Identification of putative palytoxin as the cause of clupeotoxism, *Toxicon*, 1999, 37, 55-65.
80. T. Ukena, M. Satake, M. Usami, Y. Oshima, H. Naoki, T. Fujita, Y. Kan and T. Yasumoto, Structure elucidation of ostreocin D, a palytoxin analog isolated from the dinoflagellate *Ostreopsis siamensis*, *Biosci. Biotechnol. Biochem.*, 2001, 65, 2585-2588.
81. T. Ukena, M. Satake, M. Usami, Y. Oshima, T. Fujita, H. Naoki and T. Yasumoto, Structural confirmation of ostreocin-D by application of negative-ion fast-atom bombardment collision-induced dissociation tandem mass spectrometric methods, *Rapid Commun. Mass Spectrom.*, 2002, 16, 2387-2393.
82. S. Lenoir, L. Ten-Hage, J. Turquet, J.P. Quod, C. Bernard and M.C. Hennion, First evidence of palytoxin analogues from an *Ostreopsis mascarenensis* (Dinophyceae) benthic bloom in southwestern Indian Ocean, *J. Phycol.*, 2004, 40, 1042-1051.
83. D. Uemura, Y. Hirata, T. Iwashita and H. Naoki, Studies on palytoxins, *Tetrahedron* 1985, 41, 1007-1017.
84. J.S. Wiles, J.A. Vick and M.K. Christensen, Toxicological evaluation of palytoxin in several animal species, *Toxicon*, 1974, 12, 427-433.
85. J.A. Vick and J.S. Wiles, The mechanism of action and treatment of palytoxin poisoning, *Toxicol. Appl. Pharmacol.*, 1975, 34, 214-223.

86. T. Yasumoto, D. Yasumura, Y. Ohizumi, M. Takahashi, A.C. Alcala and L.C. Alcala, Palytoxin in two species of xanthid crab from the Philippines, *Agric. Biol. Chem.*, 1986, 50, 163-167.
87. Y. Hashimoto, N. Fusetani and S. Kimura, Aluterin, a toxin of filefish *Alutera scripta*, probably originating from a zoantharian *Palythoa tuberculosa*, *Bull. Jpn. Soc. Scient. Fish.*, 1969, 35, 1086-1093.
88. M. Fukui, M. Murata, A. Inoue, M. Gawel and T. Yasumoto, Occurrence of palytoxin in the triggerfish *Melichtys vidua*, *Toxicon*, 1987, 25, 1121-1124.
89. A.M. Kodama, Y. Hokama, T. Yasumoto, M. Fukui, S.J. Manea and N. Sutherland, Clinical and laboratory findings implicating palytoxin as cause of ciguatera poisoning due to *Decapterus macrosoma* (mackerel), *Toxicon*, 1989, 27, 1051-1053.
90. A.C. Alcala, L.C. Alcala, J.S. Garth, D. Yasumura and T. Yasumoto, Human fatality due to ingestion of the crab *Demania reynaudii* that contained a palytoxin-like toxin, *Toxicon*, 1988, 26, 105-107.
91. T. Noguchi, D.F. Hwang, G. Arakawa, K. Daigo, S. Sato, H. Ozaki, N. Kawai, M. Ito and K. Hashimoto, in *Progress in Venom and Toxin Research* (eds. P. Gopalakrishnakone and C.K. Tan), National University, Singapore, 1987, pp. 325–335.
92. S. Weidmann, Effects of palytoxin on the electrical activity of dog and rabbit heart, *Experientia*, 1977, 33, 1487-1489.
93. H. Bottinger and E. Habermann, Palytoxin binds to and inhibits kidney and erythrocyte  $\text{Na}^+$ ,  $\text{K}^+$ -ATPase, *Naunyn Schmiedebergs Arch. Pharmacol.*, 1984, 325, 85-87.
94. H. Bottinger, L. Beress and E. Habermann, Involvement of  $(\text{Na}^+ + \text{K}^+)$ -ATPase in binding and actions of palytoxin on human erythrocytes, *Biochim. Biophys. Acta*, 1986, 861, 165-176.
95. C. Li, O. Capendeguy, K. Geering and J-D. Horisberger, A third  $\text{Na}^+$ -binding site in the sodium pump, *Proc. Natl. Acad. Sci. Usa*, 2005, 102, 12706-12711.
96. E.V. Wattemberg, Palytoxin: exploiting a novel skin tumor promoter to explore signal transduction and carcinogenesis, *Am. J. Physiol. Cell Physiol.*, 2007, 292, C24-C32.
97. E.V. Wattemberg, D. Uemura, K.L. Byron, M.L. Villereal, H. Fujiki and M.R. Rosner, Structure-activity studies of the norphorbol tumor promoter palytoxin in carcinogenesis, *Cancer Research*, 1989, 49, 5837-5842.
98. H. Fujiki, M. Suganuma, M. Nakayasu, H. Hakii, T. Horiuchi, S. Takayama and T. Sugimura, Palytoxin is a non-12-*O*-tetradecanoylphorbol-13-acetate type tumor promoter in two-stage mouse skin carcinogenesis, *Carcinogenesis*, 1986, 7, 707-710.

99. Y. Onuma, M. Satake, T. Ukena, J. Roux, S. Chanteau, N. Rasolofonirina, M. Ratsimaloto, H. Naoki and T. Yasumoto, Identification of putative palytoxin as the cause of clupectoxism, *Toxicon*. 1999, 37, 55-65.
100. T. Yasumoto, M. Fukui, K. Sasaki and K. Sugiyama, Determinations of marine toxins in foods, *J. AOAC Int.*, 1995, 78, 574-582.
101. E. Habermann, G. Ahnert-Hilger, G.S. Chatwal and L. Beress, Delayed hemolytic action of palytoxin. General characteristics, *Biochim. Biophys. Acta*, 1981, 649, 481-486.
102. G.S. Bignami, A rapid and sensitive hemolysis neutralization assay for palytoxin, *Toxicon*. 1993, 31, 817-820.
103. P. Riobò, B. Paz and J.M. Franco, Analysis of palytoxin-like in *Ostreopsis* cultures by liquid chromatography with precolumn derivatization and fluorescence detection, *Anal. Chim. Acta*, 2006, 566, 217-223.
104. E. Fattorusso, P. Ciminiello, V. Costantino, S. Magno, A. Mangoni, A. Milandri, R. Poletti, M. Pompei and R. Viviani, Okadaic Acid in Mussels of Adriatic Sea, *Mar. Poll. Bull.* 1992, 24, 234-237.
105. L. Boni, L. Mancini, A. Milandri, R. Poletti, M. Pompei and R. Viviani, in *Marine coastal eutrophication. Proc Inter Conf Bologna, 21-24 March 1990* (eds. R.A., Vollenweider, R. Marchetti, R. Viviani), Elsevier, Amsterdam, 1992, pp 419-426.
106. Zhao, G. Lembeze, G. Cenci, B. Wall and T. Yasumoto, in *Toxic Phytoplankton Blooms in the Sea*, Vol. 3 (eds. T.J. Smayda, and Y. Shimizu), Elsevier, New York, 1993, pp. 587-592.
107. J. Zhao, G. Cenci, E. Di Antonio and T. Yasumoto, Analysis of diarrhetic shellfish toxins in mussels from the Adriatic coast of Italy, *Fish. Sci.*, 1994, 60, 687-689.
108. R. Draisci, L. Lucentini, L. Riannetti, P. Boria and A. Stacchini, Detection of diarrhetic shellfish toxins in mussels from Italy by ionspray liquid chromatography-mass spectrometry, *Toxicon*, 1995, 33, 1591-1603.
109. P. Ciminiello, E. Fattorusso, M. Forino, S. Magno, R. Poletti, M. Satake, R. Viviani and T. Yasumoto, Yessotoxin in mussels of the northern Adriatic Sea, *Toxicon*, 1997, 35, 177-183.
110. P. Ciminiello, E. Fattorusso, M. Forino, S. Magno, R. Poletti and R. Viviani, Isolation of 45-hydroxyessotoxin from mussels of the Adriatic Sea, *Toxicon*, 1999, 37, 689-693.
111. M. Satake, A. Tubaro, J-S. Lee and T. Yasumoto, Two new analogs of yessotoxin, homoyessotoxin and 45-hydroxyhomoyessotoxin, isolated from mussels of the Adriatic Sea, *Nat. Toxins*, 1997, 5, 107-110.

112. P. Ciminiello, E. Fattorusso, M. Forino, S. Magno, R. Poletti and R. Viviani, Isolation of adriatoxin, a new analog of yessotoxin from mussels of the Adriatic Sea, *Tetrahedron Letters*, 1998, 39, 8897-8900.
113. P. Ciminiello, E. Fattorusso, M. Forino, R. Poletti and R. Viviani, A new analogue of yessotoxin, carboxyessotoxin, isolated from Adriatic Sea Mussels, *Eur. J. Org. Chem.*, 2000, 291-295.
114. P. Ciminiello, E. Fattorusso, M. Forino, R. Poletti and R. Viviani, Structure Determination of Carboxyhomoyessotoxin, a New Yessotoxin Analog Isolated from Adriatic Mussels, *Chem Res Toxicol.*, 2000, 13, 770-774.
115. P. Ciminiello, E. Fattorusso, M. Forino and R. Poletti, 42,43,44,45,46,47,55-Heptanor-41-oxohomoyessotoxin, a New Biotxin from Mussels of the Northern Adriatic Sea, *Chem Res Toxicol.*, 2001, 14, 596-599.
116. P. Ciminiello, C. Dell'Aversano, E. Fattorusso, G.S. Magno, L. Tartaglione, M. Cangini, M. Pompei, F. Guerrini, L. Boni and R. Pistocchi, Toxin profile of *Alexandrium ostenfeldii* (Dinophyceae) from the Northern Adriatic Sea revealed by liquid chromatography-mass spectrometry, *Toxicon*, 2006, 47, 597-604.
117. L. Mackenzie, D. White, Y. Oshima and J. Kapa, The resting cyst and toxicity of *Alexandrium ostenfeldii* (Dinophyceae) in New Zealand, *Phycologia*, 1996, 35, 148-155.
118. A.D. Cembella, N.I. Lewis and M.A. Quilliam, The marine dinoflagellate *Alexandrium ostenfeldii* (Dinophyceae) as the causative organism of spirolide shellfish toxins, *Phycologia* 2000, 39, 67-74.
119. P. Ciminiello, C. Dell'Aversano, E. Fattorusso, M. Forino, L. Grauso, L. Tartaglione, F. Guerrini and R. Pistocchi, Spirolide toxin profile of Adriatic *Alexandrium ostenfeldii* cultures and structure elucidation of 27-hydroxy-13,19-didesmethylspirolide C, *J. Nat. Prod.*, 2007, 70, 1878-1883.
120. G. Sansoni, B. Borghini, G. Camici, M. Casotti, P. Righini and C. Rustighi, Fioriture algali di *Ostreopsis ovata* (Gonyaulacales: Dinophyceae): un problema emergente, *Biologia Ambientale*, 2003, 17, 17-23.
121. A. Penna, M. Vila, S. Fraga, M.G. Giacobbe, F. Andreoni, P. Riobò and C. Vernesi, Characterization of *Ostreopsis* and *Coolia* (Dinophyceae) isolates in the Western Mediterranean sea based on morphology, toxicity and internal transcribed spacer 5.8S rDNA sequences, *J. Phycol.*, 2005, 41, 212-225.

- 
122. M. Gallitelli, N. Ungaro, L.M. Addante, V. Procacci, N. Gentiloni and C. Sabbà, Respiratory illness as a reaction to tropical algal blooms occurring in a temperate climate, *JAMA*, 2005, 293, 2599-2600.
123. M.A. Quilliam, P. Hess and C. Dell'Aversano, in *Mycotoxins and phycotoxins in perspective at the turn of the millennium* (eds. W.J. deKoe, R.A. Samson, H.P. Van Egmond, J. Gilbert and M. Sabino), W.J. deKoe, Wageningen, The Netherlands, 2001, 383-391.
124. C. Dell'Aversano, P. Hess and M.A. Quilliam, Hydrophilic Interaction Liquid Chromatography-Mass Spectrometry for the analysis of Paralytic Shellfish Poisoning Toxins, *J. Chromatogr. A.*, 2005, 1081, 190-201.
125. P. Ciminiello, C. Dell'Aversano, E. Fattorusso, M. Forino, G.S. Magno, L. Tartaglione, M.A. Quilliam, A. Tubaro and R. Poletti, Hydrophilic interaction liquid chromatography-mass spectrometry (HILIC-MS) for determination of domoic acid in Adriatic shellfish, *Rapid Commun. Mass Spectrom.*, 2005, 19, 2030-2038.
126. P. Ciminiello and E. Fattorusso, Shellfish toxins-Chemical studies on Northern Adriatic mussels, *Eur. J. Org. Chem.*, 2004, 12, 2533-2551.
127. Furey, J. Garcia, K. O'Callaghan, M. Lehane, M.F. Amandi and K.J. James, Brevetoxins: structures, toxicology, and origin, *Phycotoxins*, 2007, 19-46.
128. D. Uemura, Bioorganic Studies on Marine Natural Products—Diverse Chemical Structures and Bioactivities, *The Chemical Record*, 2006, 6, 235-248.
129. K. Aligizaki, P. Katikou, G. Nikolaidis and A. Panou, First episode of shellfish contamination by palytoxin -like compounds from *Ostreopsis* species (Aegean Sea, Greece), *Toxicon*, 2008, 51, 418-427.





## Chapter 4

### 4.1. Marine invertebrates contamination

Bivalve shellfish, gastropods, crabs, lobsters and other marine invertebrates store biotoxins by either direct filtration of sea water (as filter feeding shellfish), or ingestion of contaminated organisms, as the carnivore and sweeper invertebrates.

The level of contamination is specific for each species and generally, it's directly correlated to the concentration of toxic microalgal cells in the plankton.<sup>1</sup>

First of all, level of contamination depends on the season and the sea temperature:<sup>2</sup> in fact, low temperatures appears to delay the toxins elimination, although the real mechanism by which temperature influences the toxins accumulate and elimination, isn't really known.<sup>3</sup> Secondly, it depends on the part of the organism in which toxins are stored: toxins in the gastrointestinal tract are eliminated more quickly than those stored to other tissues.

Little is known about the mechanism of toxins retention in carnivore gastropods and crabs. On the contrary, much is known, is about bivalve shellfish, thanks also to the wide diffusion of shellfish seafood.

It's known, for example, that mussels store PSP-toxins more quickly than whatever other species, but at the same time they can also eliminate them very quickly; instead, oysters accumulate toxic substances more slowly, but they stay contaminated for a longer time.<sup>4-5</sup> Scallops, then, can retain toxins for a time longer than two years.

Some species of bivalves, as *Mercenaria mercenaria*, can avoid phycotoxin contamination.<sup>6</sup> In fact, in 1972 during an *Alexandrium tamarense* bloom along the Massachusetts coasts, fishing was banned because of the strong contamination by PSP-toxins. Also, in that circumstance, assays on shellfish samples were carried out and revealed toxin amounts of 3000-5000 µg per 100 g of shellfish, with the maximum grade of contamination in being recorded mussels. Instead, no samples of *Mercenaria mercenaria* or of oysters resulted toxic. Subsequent studies demonstrated that *Mercenaria mercenaria*, in presence of *A. tamarense*, at first draws back its siphon and then isolates itself from the surrounding environment, by closing the seashell valve, until the seawater comes back pure. We can't exclude the possibility that this organism has this same reaction also in presence of other dinoflagellates.

In addition to PSP-toxins, also other toxic substances are accumulated in filter feeding shellfish, representing a big risk for public health.

DSP-toxins, as okadaic acid, DTX, PTX and yessotoxin, associated to the presence of *Dinophysis spp.* and *Prorocentrum spp.*, are easily stored by shellfish but there isn't much information about the contamination length. In 1993 Marcaillou-Le Baut *et al.* compared the decontamination speed from DSP-toxins, in mussels samples, cultivated in aquaculture and in laboratory, showing that decontamination happens more quickly in the natural environment than in laboratory. This suggests that the quality of the food available for mussels during the detoxification is a factor which determines the speed of elimination of the toxins.

More recently, it was demonstrated that also domoic acid and its analogs are easily accumulated by filtering organisms. In 1987 a mysterious and serious intoxication due to the ingestion of cultivated *Mytilus edulis*, happened in Canada. The symptoms of the poisoning included vomiting, diarrhea, mental confusion, loss of memory, disorientation and coma. Three old patients died and other victims reported permanent neurologic damages. Domoic acid was individuated as the agent responsible for intoxication and the term amnesic shellfish poisoning (ASP) was coined to indicate the group of these clinical symptoms.

In conclusion, we can affirm that the differences in the storing and retention of toxins depend on the nature of both the contaminating and the contaminated organism, but also on other factors that are not clear yet. We should consider all these elements when we have to choose species to cultivate in aquaculture and the place they must be locate where position them, to reduce damages due to harmful algal blooms.

#### **4.1.1. Biotoxins in Italy**

The increasing of dinoflagellates blooms and the consequent episodes of poisoning due to ingestion of contaminated shellfish, have been recorded in Italy since 1980, causing they breed serious concerns for the public health. There are, also, economic damages for the fishing industry, in fact, all the activities which are connected to fishing and mussels aquaculture, are subjected to a sudden stop, when the toxicity appears.

The area, which is responsible for the 90% of the Italian production of mussels is located along the North Adriatic coasts<sup>13</sup> and just in these areas accidents of poisoning by DSP-toxins were recorded since 1989:<sup>14</sup> *Dinophysis fortii* were found in the digestive glands of mussels collected in the coastal waters of Emilia Romagna and the isolation of an extract containing some not-identified DSP-toxins, suggested that several cases of diarrhea in the mussels consumers weren't due to bacterial or viral contamination, but to DSP-toxins poisoning. This pathogenesis, brought to the light by the Centro di Ricerche Marine di Cesenatico, was

afterward observed in the coastal areas of Marche, Veneto, Abruzzo and Friuli-Venezia Giulia.<sup>15</sup>

This research demonstrated that the DSP-toxins levels, contained in the mussels from the coastal areas of Emilia Romagna, were so high that the sale of shellfish had to be suspended for eight months. Also, on going toxicity, from June 1990 to January 1991, indicated that it wasn't an occasional problem, and it was necessary to face both the economic and health risks, already faced in other countries of the European Community.

A large number of European countries established limits of tolerance for DSP-toxins, which can be applied to both the mussels produced in the national territory and the imported ones; however these levels are diverse in the different countries, because they weren't established, for example, by international organizations, as the *World Health Organization*. In the meanwhile in different European states, Italy including, surveillance programs for DSP-toxins were introduced; they provide systematic analyses of sea water, phytoplankton, and shellfish, to the aim of detecting cells of *Dinophysis* spp. and of other toxins producing species.

In this area of interest, Prof. Ciminiello's research group undertook, in 1992, a study about marine biotoxins, carried out by periodic analyses of mussels, which were cultivated along the Italian coasts, during the highest algal blooms.

So, it was possible to establish that the hepatopancreas of the toxic *Mytilus galloprovincialis*, collected in the first 90's, contained a remarkable amount of okadaic acid, identified by NRM spectroscopy techniques, more than 100  $\gamma$  per 600 gr of hepatopancreas. This result represented the first sure evidence of DSP-toxins along the Italian coasts.

In the following years, the toxicity due to okadaic acid was gradually replaced by the yessotoxins one. In that occasion, yessotoxin<sup>16a</sup> was isolated together with its structurally known analogues, but never found in Italy before, as homo-YTX, 45-OH-homo-YTX,<sup>16b</sup> 45-OH-YTX,<sup>16c</sup> and some structurally new derivatives never isolated before, as adriatoxin,<sup>16d</sup> carboxy-YTX,<sup>16e</sup> and carboxy-homo-YTX.<sup>16f</sup>

The okadaic acid had already been identified in shellfish from West Europe in 1985 together with its analogue DTX > 1;<sup>17</sup> instead, yessotoxin had appeared in the Norwegian mussels in 1988 together with other substances of acid nature.<sup>18</sup> PTXs were kept under control less because of the absence of routinary methods of detection.<sup>19</sup>

In addition to DSP-toxins, which represent the principal source of the mussels contamination in the Adriatic Sea, also PSP- toxins were detected during some analyses carried out in 1994, raising all the problems associated to the poisoning that this kind of toxins can breed.

By HPLC FLD analyses, Prof. Ciminiello's research group detected the presence of two PSP-toxins, gonyautoxin 2 (GTX 2) and gonyautoxin 3 (GTX 3.). The responsible organism of the mussels contamination wasn't clarified, although, among the dinoflagellates species, which are considered PSP-toxins producers, only two were detected in the Adriatic Sea: *Alexandrium tamarense* and *Alexandrium minutum*. A bloom of the first reported species happened along the Emilia Romagna coasts in 1982,<sup>21</sup> without causing toxic phenomenon. About, instead, *Alexandrium minutum*, although studies on its toxicity in the Adriatic Sea<sup>22</sup> haven't been carried out yet, from analyses carried out on Australian strains, it results as the producer of only GTX 1 and GTX 4.<sup>23</sup> The absence of C toxins, STX and NEO in the analyzed Italian samples allows to suppose that just *Alexandrium minutum* is the probable source of PSP-toxins in the Adriatic Sea.<sup>20</sup>

#### 4.1.2. Maximum content of the algal biotoxins in shellfish

The European Union proposed some official health regulations, tolerance limits and methods of analysis for the toxins responsible of food poisoning due to the consumption of shellfish. In particular, the Ministero della Salute Italiano ratified by a decree in May 2002, the following maximum content of algal biotoxins, as well as the methods for their detection:

“The maximum content of okadaic acid is set at 160µg of equivalents okadaic acid/kg”.

“The maximum content of yessotoxin is set at 1mg of equivalents yessotoxin/kg”.

“The maximum content of PSP is set at 800µg of equivalents saxitoxin/kg”.

“The maximum content of ASP in the edible parts of the mussels (full body or edible parts separately) mustn't be more than 20µg of domoic acid per gram according to the HPLC analysis method”.

#### 4.2. References

1. Sribhibhadh, A.; *Thesis*, Univ. of Washington, 1963.
2. Prakash, A.; Medcof, J. C.; Tennant, A. D.; *Bull. Fish. Res. Bd. Canada*, 1971, 177, p. 87.
3. Madenwald, N. D.; *Toxic Dinoflagellates*, 1985, p. 479.
4. Desbiens, M.; Cembella, A. D.; *Proceedings of the 6<sup>th</sup> International Conference on Toxic Marine Phytoplankton*, Nantes, 1994.
5. Shumway, S. E.; Sherman, S. A.; Cembella, A. D.; Selvin, R.; *Natural Toxins*, 1994, 2, p. 236.
6. Shumway, S. E.; Cucci, T. L.; *Aquat. Toxicol.*, 1987, 10, p. 9.

7. Kodama, M.; Ogata, T.; Sato, S.; Inoguchi, N.; Shimizu, M.; Daido, H.; *Toxicon*, 1989, 27, p. 55.
8. Thurberg, F. P.; *Aquatic Application of Ozone*, 1975, p. 50.
9. Blogoslowski, W.; Brown, C.; Rhodes, E.; Broadhurst, M.; *Proc. First Inter. Symp. On Ozone for Water and Wastewater Treatment*, New York, 1975, p. 684.
10. Dawson, M. A.; Thurberg, F. P.; Blogoslowski, W.; Sasner, J. J.; Ikawa, M.; *Proc. Fourth Food-Drug from the Sea Conference*, Washington, 1976, p. 152.
11. Blogoslowski, W.; Stewart, M. E.; *Mar. Biol.*, 1978, 45, p. 261.
12. Shumway, S. E.; Sherman-Caswell, S.; Hurst, J. W.; *J. Shellfish Res.*, 1988, 7, p. 643.
13. Ciminiello, P.; Fattorusso, E.; Forino, M.; Magno, S.; Poletti, R.; Satake, M.; Viviani, R.; Yasumoto, T.; *Toxicon*, 1997, 35, p. 177.
14. Boni, L.; Mancini, L.; Milandri, A.; Poletti, R.; Pompei, M.; Viviani, R.; *International Conference on Marine Toxins*, Bologna, 1990.
15. Fattorusso, E.; *Tossine in alimenti marini*, Napoli, 1993.
16. (a) Fattorusso, E.; Ciminiello, P.; Costantino, V.; Magno, S.; Mangoni, A.; Milandri, A.; Poletti, R.; Pompei, M.; Viviani, R.; *Mar. Poll. Bull.* 1992, 24, 234. (b) Ciminiello, P.; Fattorusso, E.; Forino, M.; Magno, S.; Poletti, R.; Satake, M.; Viviani, R.; Yasumoto, T.; *Toxicon* 1997, 35, 177. (c) Ciminiello, P.; Fattorusso, E.; Forino, M.; Magno, S.; Poletti, R.; Viviani, R.; *Toxicon* 1999, 37, 689. (d) Ciminiello, P.; Fattorusso, E.; Forino, M.; Magno, S.; Poletti, R.; Viviani, R.; *Tetrahedron Lett.* 1998, 39, 8897. (e) Ciminiello, P.; Fattorusso, E.; Forino, M.; Poletti, R.; Viviani, R.; *Eur. J. Org. Chem.* 2000, 2, 291. (f) Ciminiello, P.; Fattorusso, E.; Forino, M.; Poletti, R.; Viviani, R.; *Chem. Res. Toxicol.* 2000, 13, 770.
17. Dahl, E.; Yndestad, M.; *Toxic Dynoflagellates*, 1985, p. 495.
18. Lee, J.; Tangen, K.; Dahl, E.; Hovgaard, P.; Yasumoto, T.; *Nippon Suisan Gakkaishi*, 1988, 54, p. 1953.
19. Krogh, P.; *Report of the Scientific Veterinary Committee on DSP in Europe*. 1990.
20. Ciminiello, P.; Fattorusso, E.; Magno, S.; Oshima, Y.; Poletti, R.; Viviani, R.; Yasumoto, T.; *Marine Pollution Bulletin*, 1995, 30, p. 733.
21. Boni, L.; *Inf. Bot. It.*, 1983, 15, p. 18.
22. Honsell, G.; *Toxic Phytoplankton Bloom in the Sea*, 1993, p. 127.
23. Oshima, Y.; Hirota, M.; Yasumoto, T.; Hallegraeff, G.; Blackburn, S.; Steffensen, D.; *Nippon Suisan Gakkaishi*, 1989, 55, p. 925.



## Chapter 5

### Identification of four new ovatoxins from *Ostreopsis ovata*

In my research work on *Ostreopsis ovata* toxins, I carried out a high resolution (HR)LC-MS and MS<sup>2</sup> investigation of an *O. ovata* culture extract, which: i) confirmed the presence of small amounts of putative PLTX; ii) confirmed OVTX-a as the major component of *O. ovata* toxin profile; iii) highlighted the presence of four new palytoxin-like compounds, that we have named ovatoxin-b (OVTX-b), OVTX-c, OVTX-d, and OVTX-e. Elemental formulae, very close to palytoxin's, have been assigned to the new ovatoxins and information has been gained about their structural features.

#### 5.1. Experimental

##### 5.1.1. Reagents

All organic solvents were of distilled-in-glass grade (Carlo Erba, Milan, Italy). Water was distilled and passed through a MilliQ water purification system (Millipore Ltd., Bedford, MA, USA). Glacial acetic acid (Laboratory grade) was purchased from Carlo Erba. Analytical standard of palytoxin was purchased from Wako Chemicals GmbH (Neuss, Germany) and dissolved in methanol/water (1:1, v/v).

##### 5.1.2. Batch culture of *Ostreopsis ovata*

A strain of *O. ovata*<sup>1</sup> was isolated by the capillary pipette method<sup>2</sup> from water samples collected along the Adriatic coasts of Italy (Marche region, Numana sampling site, strain OOAN0601), in October 2006. The sample was collected in proximity of the seaweeds *Cystoseira* sp. and *Alsidium corallinum*. After an initial growth in microplates, the cells were cultured at 20°C under a 16:8 h L:D cycle (ca. 90  $\mu\text{mol m}^{-2} \text{s}^{-1}$  from cool white lamp); cultures were established in natural seawater, at salinity of 32 psu, adding nutrients at a five-fold diluted f/2 concentration,<sup>3</sup> with addition of selenium. Cell counts were made in settling chambers by the Utermöhl method.<sup>4</sup> Cell pellets from a total culture volume of 500 mL (4,336,578 cells) were collected at stationary phase on the 21<sup>th</sup> day of growth first by gravity filtration through Whatman GF/F filters and stored at -80°C.



### 5.1.3. Extraction

Cell pellets of Adriatic *O. ovata* culture were added of 20 mL of a methanol/water (1:1, v/v) solution and sonicated for 6 min in pulse mode, while cooling in ice bath. The mixture was centrifuged at 7500 rpm for 20 min, the supernatant was decanted and the pellet was washed twice with 5 mL of methanol/water (1:1, v/v). The extracts were combined and the volume was adjusted to 30 mL with extracting solvent. The obtained mixture was analyzed directly by LC-MS (10  $\mu$ L injected).

### 5.1.4. Liquid chromatography-mass spectrometry (LC-MS)

High resolution (HR)LC-MS experiments were carried out on an Agilent 1100 LC binary system (Palo Alto, CA, USA) coupled to a hybrid linear ion trap LTQ Orbitrap XL<sup>TM</sup> Fourier Transform MS (FTMS) equipped with an ESI ION MAX<sup>TM</sup> source (Thermo-Fisher, San José, CA, USA). Chromatographic separation was accomplished by using a 3  $\mu$ m gemini C18 (150  $\times$  2.00 mm) column (Phenomenex, Torrance, CA, USA) maintained at room temperature and eluted at 0.2 mL/min with water (eluent A) and 95% acetonitrile/water (eluent B), both containing 30 mM acetic acid. A slow gradient elution was used: 20-50% B over 20 min, 50-80% B over 10 min, 80-100% B in 1 min, and hold 5 min. This gradient system allowed a sufficient chromatographic separation of most palytoxin-like compounds, namely: putative PLTX (Rt = 10.78 min), OVTX-a (Rt = 11.45 min), OVTX-b (Rt = 11.28 min), OVTX-c (Rt = 10.90 min), OVTX-d and OVTX-e (Rt = 11.07 min).

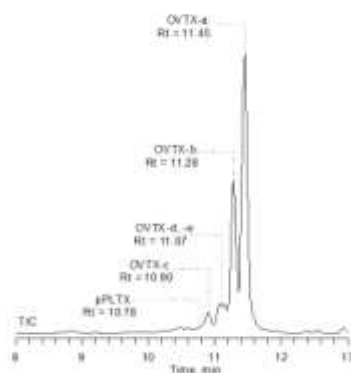
HR full MS experiments (positive ions) were acquired in the range normal ( $m/z$  800-1400) and high ( $m/z$  2000-3000) at a resolving power of 100,000 and 15,000 respectively. The LTQ Orbitrap XL<sup>TM</sup> MS was calibrated just before the analyses by using a mixture of caffeine, MRFA (L-methionyl-arginyl-phenylalanyl-alanine acetate  $\times$  H<sub>2</sub>O) and Ultramark 1621 for the normal mass range and PPG 2007 for the high mass range. The following source settings were used in all HRLC-MS experiments: a spray voltage of 4 kV, a capillary temperature of 290°C, a capillary voltage of 22 V, a sheath gas and an auxiliary gas flow of 35 and 1 (arbitrary units). The tube lens voltage was set at 110 V and 250 V in the experiments acquired in mass range normal and high, respectively. HRMS<sup>2</sup> data were acquired at a 60,000 resolving power setting by selecting as precursor the  $[M+2H+K]^{3+}$  ion at  $m/z$  906.8 (PLTX),  $m/z$  896.2 (OVTX-a),  $m/z$  910.8 (OVTX-b),  $m/z$  916.1 (OVTX-c), and  $m/z$  901.4 (OVTX-d and OVTX-e). A collision energy of 25%, an activation Q of 0.250, and an activation time of 30 msec were used.

Calculation of elemental formulae of ions contained in HRMS and HRMS<sup>2</sup> spectra was performed by using the mono-isotopic ion peak of each ion cluster. A mass tolerance of 7 ppm was used.

PLTX standards at five levels of concentration (25, 12.5, 6.25, 3.13, and 1.6 ng/mL) were used to generate a calibration curve that was employed in quantitative analyses. Calibration points were the result of triplicate injection. Extracted ion chromatograms (XIC) for PLTX and each OVTX were obtained by selecting the most abundant ion peaks of both  $[M+2H-H_2O]^{2+}$  and  $[M+2H+K]^{3+}$  ion clusters. Chromatographic peak areas were compared to peak area of palytoxin standard by using the calibration curve equation  $y=14976.5356x+38344.3111$  ( $R^2 = 0.9982$ ).

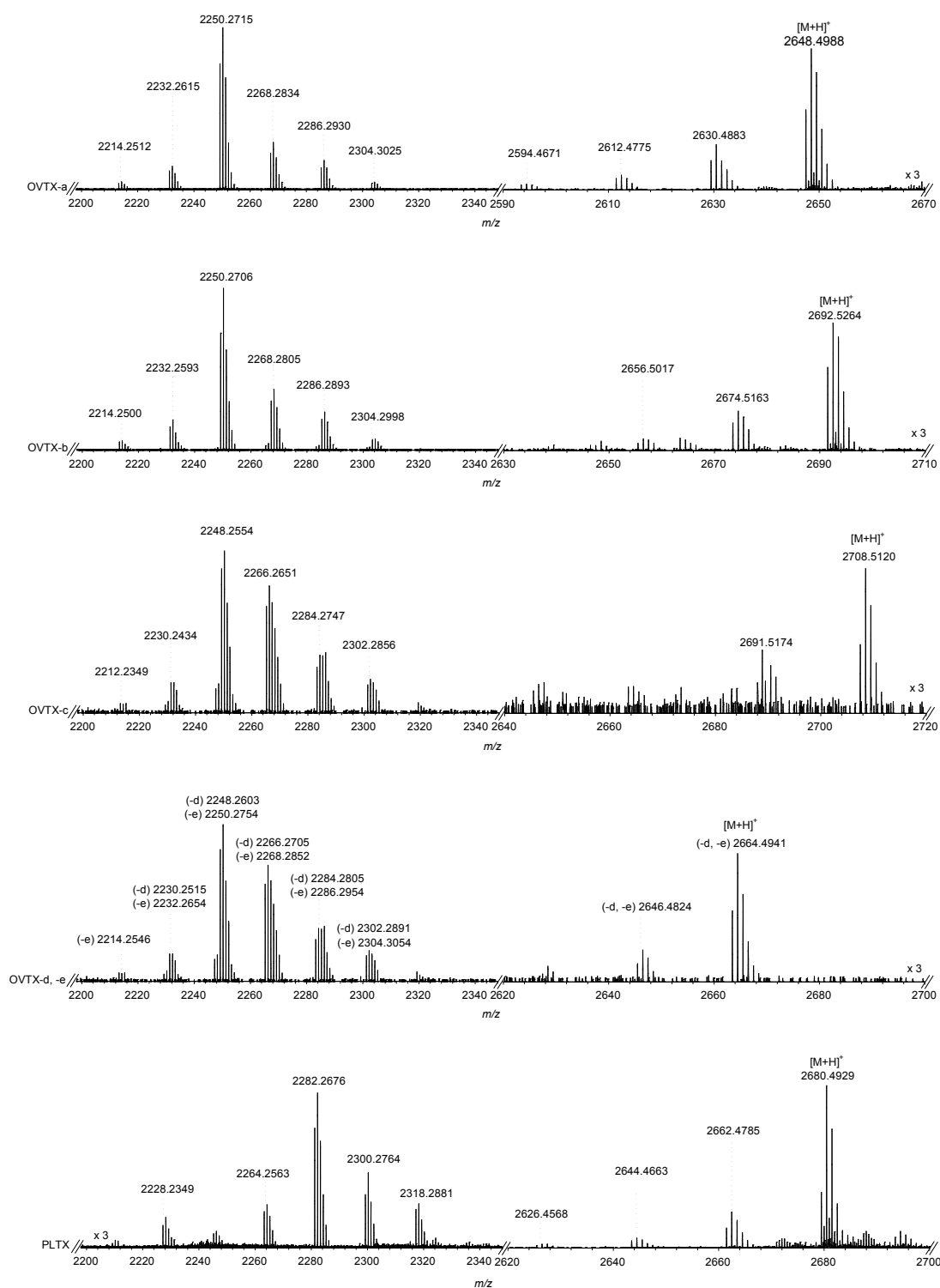
## 5.2. Results and Discussion

Cell pellets of an Adriatic *O. ovata* culture collected at the end of the stationary growth phase were extracted as reported in the experimental and the crude extract was used for characterization of the algal toxin profile by HRLC-MS and MS<sup>2</sup> experiments. A sufficient, although incomplete, chromatographic separation of the major components of the extract was accomplished using a slow gradient elution (Figure 1).

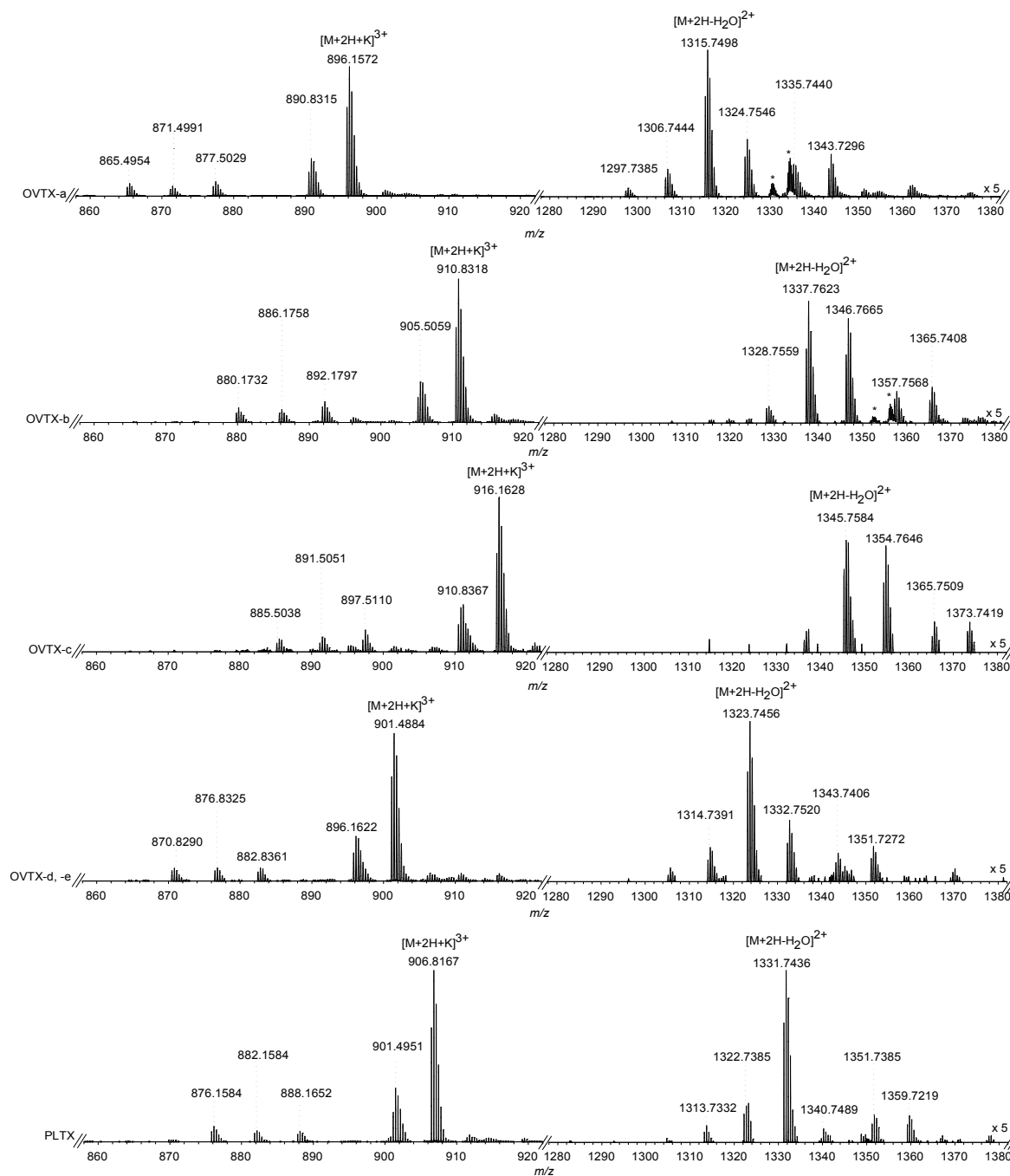


**Figure 1.** Total ion chromatogram (TIC) of the *O. ovata* culture extract containing putative PLTX, OVTX-a, -b, -c, -d, and-e. LC-MS analysis was carried out in full MS positive ion mode in the mass range 800-1400 amu, by using the chromatographic conditions reported in the experimental.

HR full MS spectra were acquired on a hybrid linear ion trap FTMS instrument both in the high ( $m/z$  2000-3000) and normal ( $m/z$  800-1400) mass range (Figure 2 and 3, respectively).



**Figure 2.** HR Full MS spectra (positive ions) in the mass range 2000-3000 amu of ovatoxins contained in the *O. ovata* culture extract and of a PLTX standard. The most intense ion of each ion cluster is indicated together with ion assignment.



**Figure 3.** HR Full MS spectra (positive ions) in the mass range 800-1400 amu of ovatoxins contained in the *O. ovata* culture extract and of a PLTX standard. The most intense ion of each ion cluster is indicated together with ion assignment. \* = impurity.

In the former range, the presence of mono-charged ions due to  $[M+H]^+$  of putative PLTX and ovatoxins emerged together with  $[M+H-nH_2O]^+$  ( $n = 1-3$ ) ions and diagnostic fragment ions in

the region 2200-2350 amu. In the normal mass range, each palytoxin-like compound presented bi-charged ion peaks due to  $[M+H+K]^{2+}$ ,  $[M+H+Na]^{2+}$ , and  $[M+2H]^{2+}$ , as well as tri-charged ions, due to  $[M+2H+K]^{3+}$  and  $[M+2H+Na]^{3+}$ ; ions due to multiple water losses from the  $[M+2H]^{2+}$  and  $[M+3H]^{3+}$  ions were also present. It is to be noted that the MS spectrum of PLTX itself shows a complex ion profile with several adduct and fragment ion clusters, the pattern depending on the used ionization and MS parameters.

Elemental composition assignment to the observed ions was complicated by the high value of their exact masses which resulted in a number of possible elemental formulae ascribable to the mono-isotopic ion peaks. A key role in dispelling any doubt about elemental formula of each compound was played by a cross-checked interpretation of its mono-, bi-, and tri-charged ions (Table 1).

**Table1.** HRMS data of palytoxin (PLTX), putative PLTX, and ovatoxin-a (OVTX-a), OVTX-b, OVTX-c, OVTX-d, and OVTX-e, obtained from full MS spectra acquired in the high ( $m/z$  2000-3000) and normal ( $m/z$  800-1400) mass range. Assignment of molecular formulae to the mono-isotopic ion peaks of mono-, bi- and tri-charged ions, relative double bonds (RDB) equivalent, and error (ppm).

	PLTX	Putative PLTX <sup>a</sup>	OVTX-a	OVTX-b	OVTX-c	OVTX-d	OVTX-e
<b>MONO-CHARGED IONS</b>							
[M+H] <sup>+</sup>	2679.4893	2679.4721	2647.4979	2691.5233	2707.5173	2663.4905	2663.4905
Formula	C <sub>129</sub> H <sub>224</sub> N <sub>3</sub> O <sub>54</sub>	C <sub>129</sub> H <sub>224</sub> N <sub>3</sub> O <sub>54</sub>	C <sub>129</sub> H <sub>224</sub> N <sub>3</sub> O <sub>52</sub>	C <sub>131</sub> H <sub>228</sub> N <sub>3</sub> O <sub>53</sub>	C <sub>131</sub> H <sub>228</sub> N <sub>3</sub> O <sub>54</sub>	C <sub>129</sub> H <sub>224</sub> N <sub>3</sub> O <sub>53</sub>	C <sub>129</sub> H <sub>224</sub> N <sub>3</sub> O <sub>53</sub>
RDB, Δ ppm	19.5, 0.907	19.5, -5.512	19.5, 0.325	19.5, 0.017	19.5, -0.321	19.5, -0.546	19.5, -0.546
[M+H-H <sub>2</sub> O] <sup>+</sup>	2661.4744		2629.4844	2673.5112		2645.4797	2645.4797
Formula	C <sub>129</sub> H <sub>222</sub> N <sub>3</sub> O <sub>53</sub>		C <sub>129</sub> H <sub>222</sub> N <sub>3</sub> O <sub>51</sub>	C <sub>131</sub> H <sub>226</sub> N <sub>3</sub> O <sub>52</sub>		C <sub>129</sub> H <sub>222</sub> N <sub>3</sub> O <sub>52</sub>	C <sub>129</sub> H <sub>222</sub> N <sub>3</sub> O <sub>52</sub>
RDB, Δ ppm	20.5, -0.715		20.5, -0.789	20.5, -0.557		20.5, -0.639	20.5, -0.639
[M+H-2H <sub>2</sub> O] <sup>+</sup>	2643.4629		2611.4721	2655.5029		2627.4702	2627.4702
Formula	C <sub>129</sub> H <sub>220</sub> N <sub>3</sub> O <sub>52</sub>		C <sub>129</sub> H <sub>220</sub> N <sub>3</sub> O <sub>50</sub>	C <sub>131</sub> H <sub>224</sub> N <sub>3</sub> O <sub>51</sub>		C <sub>129</sub> H <sub>220</sub> N <sub>3</sub> O <sub>51</sub>	C <sub>129</sub> H <sub>220</sub> N <sub>3</sub> O <sub>51</sub>
RDB, Δ ppm	21.5, -1.074		21.5, -1.459	21.5, 0.292		21.5, -0.238	21.5, -0.238
[M+H-3H <sub>2</sub> O] <sup>+</sup>	2625.4487		2593.4686	2637.4915			
Formula	C <sub>129</sub> H <sub>218</sub> N <sub>3</sub> O <sub>51</sub>		C <sub>129</sub> H <sub>218</sub> N <sub>3</sub> O <sub>49</sub>	C <sub>131</sub> H <sub>222</sub> N <sub>3</sub> O <sub>50</sub>			
RDB, Δ ppm	22.5, -2.466		22.5, 1.255	22.5, -0.023			
[M+H-A moiety] <sup>+</sup>	2335.2944		2303.2983	2303.2947	2319.2917	2319.2954	2303.2988
Formula	C <sub>113</sub> H <sub>196</sub> NO <sub>48</sub>		C <sub>113</sub> H <sub>196</sub> NO <sub>46</sub>	C <sub>113</sub> H <sub>196</sub> NO <sub>46</sub>	C <sub>113</sub> H <sub>196</sub> NO <sub>47</sub>	C <sub>113</sub> H <sub>196</sub> NO <sub>47</sub>	C <sub>113</sub> H <sub>196</sub> NO <sub>46</sub>
RDB, Δ ppm	16.5, 0.971		16.5, -1.738	16.5, -3.301	16.5, -2.379	16.5, -0.784	16.5, -1.521
[M+H-A moiety-H <sub>2</sub> O] <sup>+</sup>	2317.2842		2285.2893	2285.2866	2301.2830	2301.2871	2285.2913
Formula	C <sub>113</sub> H <sub>194</sub> NO <sub>47</sub>		C <sub>113</sub> H <sub>194</sub> NO <sub>45</sub>	C <sub>113</sub> H <sub>194</sub> NO <sub>45</sub>	C <sub>113</sub> H <sub>194</sub> NO <sub>46</sub>	C <sub>113</sub> H <sub>194</sub> NO <sub>46</sub>	C <sub>113</sub> H <sub>194</sub> NO <sub>45</sub>
RDB, Δ ppm	17.5, 1.136		17.5, -1.067	17.5, -2.248	17.5, -1.587	17.5, 0.194	17.5, -0.192

[M+H-A moiety-2H <sub>2</sub> O] <sup>+</sup>	2299.2734	2267.2793	2267.2759	2283.2710	2283.2776	2267.2808
Formula	C <sub>113</sub> H <sub>192</sub> NO <sub>46</sub>	C <sub>113</sub> H <sub>192</sub> NO <sub>44</sub>	C <sub>113</sub> H <sub>192</sub> NO <sub>44</sub>	C <sub>113</sub> H <sub>192</sub> NO <sub>45</sub>	C <sub>113</sub> H <sub>192</sub> NO <sub>45</sub>	C <sub>113</sub> H <sub>192</sub> NO <sub>44</sub>
RDB, Δ ppm	18.5, 1.043	18.5, -0.826	18.5, -2.326	18.5, -2.229	18.5, 0.662	18.5, -0.165
[M+H-A moiety-3H <sub>2</sub> O] <sup>+</sup>	2281.2634	2249.2693	2249.2671	2265.2622	2265.2668	2249.2725
Formula	C <sub>113</sub> H <sub>190</sub> NO <sub>45</sub>	C <sub>113</sub> H <sub>190</sub> NO <sub>43</sub>	C <sub>113</sub> H <sub>190</sub> NO <sub>43</sub>	C <sub>113</sub> H <sub>190</sub> NO <sub>44</sub>	C <sub>113</sub> H <sub>190</sub> NO <sub>44</sub>	C <sub>113</sub> H <sub>190</sub> NO <sub>43</sub>
RDB, Δ ppm	19.5, 1.298	19.5, -0.582	19.5, -1.560	19.5, -1.467	19.5, 0.563	19.5, 0.841
[M+H-A moiety-4H <sub>2</sub> O] <sup>+</sup>	2263.2522	2231.2578	2231.2556	2247.2502	2247.2551	2231.2620
Formula	C <sub>113</sub> H <sub>188</sub> NO <sub>44</sub>	C <sub>113</sub> H <sub>188</sub> NO <sub>42</sub>	C <sub>113</sub> H <sub>188</sub> NO <sub>42</sub>	C <sub>113</sub> H <sub>188</sub> NO <sub>43</sub>	C <sub>113</sub> H <sub>188</sub> NO <sub>43</sub>	C <sub>113</sub> H <sub>188</sub> NO <sub>42</sub>
RDB, Δ ppm	20.5, 1.028	20.5, -1.006	20.5, -1.992	20.5, -2.118	20.5, 0.063	20.5, 0.876
[M+H-A moiety-5H <sub>2</sub> O] <sup>+</sup>	2245.2415	2213.2493	2213.2446	2229.2393	2229.2480	2213.2498
Formula	C <sub>113</sub> H <sub>186</sub> NO <sub>43</sub>	C <sub>113</sub> H <sub>186</sub> NO <sub>41</sub>	C <sub>113</sub> H <sub>186</sub> NO <sub>41</sub>	C <sub>113</sub> H <sub>186</sub> NO <sub>42</sub>	C <sub>113</sub> H <sub>186</sub> NO <sub>42</sub>	C <sub>113</sub> H <sub>186</sub> NO <sub>41</sub>
RDB, Δ ppm	21.5, 0.976	21.5, -0.081	21.5, -2.205	21.5, -2.285	21.5, 1.617	21.5, 0.145
[M+H-A moiety-6H <sub>2</sub> O] <sup>+</sup>	2227.2310	2195.2385	2195.2351	2211.2319		
Formula	C <sub>113</sub> H <sub>184</sub> NO <sub>42</sub>	C <sub>113</sub> H <sub>184</sub> NO <sub>40</sub>	C <sub>113</sub> H <sub>184</sub> NO <sub>40</sub>	C <sub>113</sub> H <sub>184</sub> NO <sub>41</sub>		
RDB, Δ ppm	22.5, 1.013	22.5, -0.189	22.5, -1.738	22.5, -0.873		

**BI-CHARGED IONS**

[M+H+K] <sup>2+</sup>	1359.2194	1343.2262	1365.2393	1373.2346	1351.2231	1351.2231
Formula	C <sub>129</sub> H <sub>224</sub> KN <sub>3</sub> O <sub>54</sub>	C <sub>129</sub> H <sub>224</sub> KN <sub>3</sub> O <sub>52</sub>	C <sub>131</sub> H <sub>228</sub> KN <sub>3</sub> O <sub>53</sub>	C <sub>131</sub> H <sub>228</sub> KN <sub>3</sub> O <sub>54</sub>	C <sub>129</sub> H <sub>224</sub> KN <sub>3</sub> O <sub>53</sub>	C <sub>129</sub> H <sub>224</sub> KN <sub>3</sub> O <sub>53</sub>
RDB, Δ ppm	19.0, -4.130	19.0, -2.903	19.0, -2.861	19.0, -4.416	19.0, -3.298	19.0, -3.298
[M+H+Na] <sup>2+</sup>	1351.2377	1335.2435	1357.2540	1365.2510	1343.2411	1343.2411
Formula	C <sub>129</sub> H <sub>224</sub> N <sub>3</sub> NaO <sub>54</sub>	C <sub>129</sub> H <sub>224</sub> N <sub>3</sub> NaO <sub>52</sub>	C <sub>131</sub> H <sub>228</sub> N <sub>3</sub> NaO <sub>53</sub>	C <sub>131</sub> H <sub>228</sub> N <sub>3</sub> NaO <sub>54</sub>	C <sub>129</sub> H <sub>224</sub> N <sub>3</sub> NaO <sub>53</sub>	C <sub>129</sub> H <sub>224</sub> N <sub>3</sub> NaO <sub>53</sub>
RDB, Δ ppm	19.0, -0.255	19.0, 0.277	19.0, -1.649	19.0, -1.974	19.0, 0.381	19.0, 0.381
[M+2H] <sup>2+</sup>	1340.2462	1340.2479	1324.2534	1346.2655	1354.2620	1332.2484
Formula	C <sub>129</sub> H <sub>225</sub> N <sub>3</sub> O <sub>54</sub>	C <sub>129</sub> H <sub>225</sub> N <sub>3</sub> O <sub>54</sub>	C <sub>129</sub> H <sub>225</sub> N <sub>3</sub> O <sub>52</sub>	C <sub>131</sub> H <sub>229</sub> N <sub>3</sub> O <sub>53</sub>	C <sub>131</sub> H <sub>229</sub> N <sub>3</sub> O <sub>54</sub>	C <sub>129</sub> H <sub>225</sub> N <sub>3</sub> O <sub>53</sub>
RDB, Δ ppm	19.0, -0.651	19.0, 0.617	19.0, 0.938	19.0, 0.174	19.0, -0.534	19.0, -0.912
[M+2H-H <sub>2</sub> O] <sup>2+</sup>	1331.2417	1331.2417	1315.2480	1337.2595	1345.2566	1323.2439

Formula	$C_{129}H_{223}N_3O_{53}$	$C_{129}H_{223}N_3O_{53}$	$C_{129}H_{223}N_3O_{51}$	$C_{131}H_{227}N_3O_{52}$	$C_{131}H_{227}N_3O_{53}$	$C_{129}H_{223}N_3O_{52}$	$C_{129}H_{223}N_3O_{52}$
RDB, $\Delta$ ppm	20.0, -0.068	20.0, -0.068	20.0, 0.855	20.0, -0.361	20.0, -0.625	20.0, -0.327	20.0, -0.327
$[M+2H-2H_2O]^{2+}$	1322.2360		1306.2429	1328.2542	1336.2548	1314.2397	1314.2397
Formula	$C_{129}H_{221}N_3O_{52}$		$C_{129}H_{221}N_3O_{50}$	$C_{131}H_{225}N_3O_{51}$	$C_{131}H_{225}N_3O_{52}$	$C_{129}H_{221}N_3O_{51}$	$C_{129}H_{221}N_3O_{51}$
RDB, $\Delta$ ppm	21.0, -0.384		21.0, 1.000	21.0, -0.377	21.0, 1.977	21.0, 0.494	21.0, 0.494
$[M+2H-3H_2O]^{2+}$	1313.2303		1297.2334	1319.2498		1305.2328	1305.2328
Formula	$C_{129}H_{219}N_3O_{51}$		$C_{129}H_{219}N_3O_{49}$	$C_{131}H_{223}O_{50}N_3$		$C_{129}H_{219}N_3O_{50}$	$C_{129}H_{219}N_3O_{50}$
RDB, $\Delta$ ppm	22.0, -0.705		22.0, -2.244	22.0, 0.289		22.0, -0.742	22.0, -0.742

**TRI-CHARGED IONS**

$[M+2H+K]^{3+}$	906.4851	906.4861	895.8225	910.4976	915.8286	901.1533	901.1533
Formula	$C_{129}H_{225}KN_3O_{54}$	$C_{129}H_{225}KN_3O_{54}$	$C_{129}H_{225}KN_3O_{52}$	$C_{131}H_{229}KN_3O_{53}$	$C_{131}H_{229}KN_3O_{54}$	$C_{129}H_{225}KN_3O_{53}$	$C_{129}H_{225}KN_3O_{53}$
RDB, $\Delta$ ppm	18.5, -0.737	18.5, 0.366	18.5, 0.009	18.5, -0.326	18.5, -1.021	18.5, -0.921	18.5, -0.921
$[M+2H+Na]^{3+}$	901.1592	901.1603	890.4968	905.1717	910.5017	895.8281	895.8281
Formula	$C_{129}H_{225}N_3NaO_{54}$	$C_{129}H_{225}N_3NaO_{54}$	$C_{129}H_{225}N_3NaO_{52}$	$C_{131}H_{229}N_3NaO_{53}$	$C_{131}H_{229}N_3NaO_{54}$	$C_{129}H_{225}N_3NaO_{53}$	$C_{129}H_{225}N_3NaO_{53}$
RDB, $\Delta$ ppm	18.5, -2.133	18.5, -0.912	18.5, -1.174	18.5, -1.713	18.5, -3.502	18.5, -1.545	18.5, -1.545
$[M+3H-H_2O]^{3+}$	887.8308	887.8268	877.1687	891.8452	897.1757	882.5019	882.5019
Formula	$C_{129}H_{224}N_3O_{53}$	$C_{129}H_{224}N_3O_{53}$	$C_{129}H_{224}N_3O_{51}$	$C_{131}H_{228}N_3O_{52}$	$C_{131}H_{228}N_3O_{53}$	$C_{129}H_{224}N_3O_{52}$	$C_{129}H_{224}N_3O_{52}$
RDB, $\Delta$ ppm	19.5, 0.579	19.5, -3.926	19.5, 1.927	19.5, 3.124	19.5, 1.836	19.5, 3.685	19.5, 3.685
$[M+3H-2H_2O]^{3+}$	881.8273		871.1649	885.8421	891.1729	876.4982	876.4982
Formula	$C_{129}H_{222}N_3O_{52}$		$C_{129}H_{222}N_3O_{50}$	$C_{131}H_{226}N_3O_{51}$	$C_{131}H_{226}N_3O_{52}$	$C_{129}H_{222}N_3O_{51}$	$C_{129}H_{222}N_3O_{51}$
RDB, $\Delta$ ppm	20.5, 0.608		20.5, 1.621	20.5, 3.621	20.5, 2.658	20.5, 3.507	20.5, 3.507
$[M+3H-3H_2O]^{3+}$	875.8238		865.1615	879.8395	885.1697	870.4941	870.4941
Formula	$C_{129}H_{220}N_3O_{51}$		$C_{129}H_{220}N_3O_{49}$	$C_{131}H_{224}N_3O_{50}$	$C_{131}H_{224}N_3O_{51}$	$C_{129}H_{220}N_3O_{50}$	$C_{129}H_{220}N_3O_{50}$
RDB, $\Delta$ ppm	21.5, 0.636		21.5, 1.773	21.5, 4.693	21.5, 3.040	21.5, 2.867	21.5, 2.867

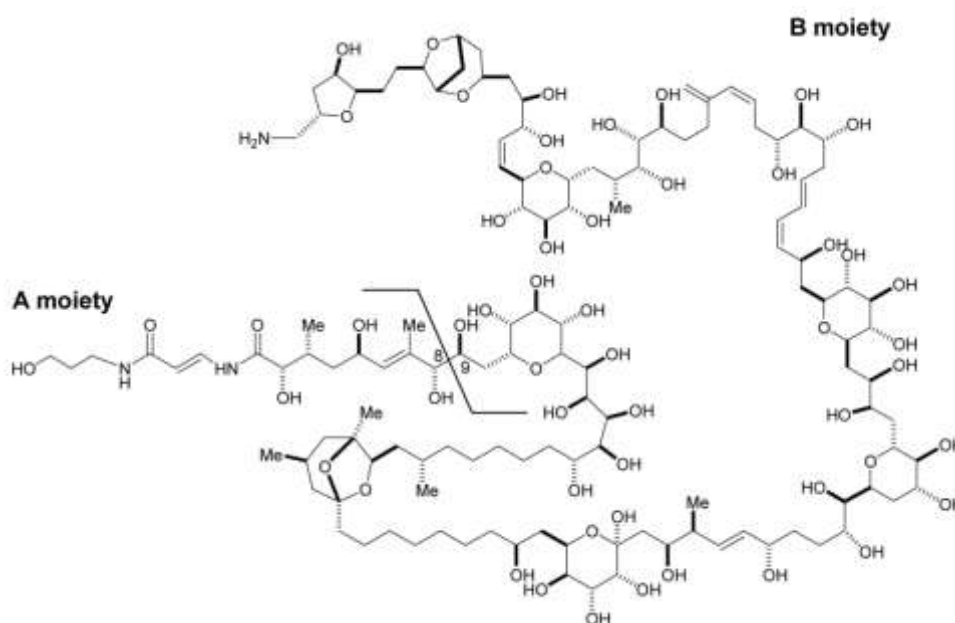
<sup>a</sup> The presence of a small amount of putative PLTX in the *O. ovata* extract results in a very poor spectrum in the high mass range where only the  $[M+H]^+$  ion could be individuated.



A comparison of molecular formulae of the ovatoxins with PLTX's ( $[M+H]^+$  at  $m/z$  2679.4893,<sup>5</sup>  $C_{129}H_{224}N_3O_{54}$ ) indicated that: i) OVTX-a ( $[M+H]^+$  at  $m/z$  2647.4979,<sup>5</sup>  $C_{129}H_{224}N_3O_{52}$ ) presents two O atoms less than PLTX, as already ascertained in our previous study;<sup>6</sup> ii) OVTX-b ( $[M+H]^+$  at  $m/z$  2691.5233,<sup>5</sup>  $C_{131}H_{228}N_3O_{53}$ ) presents two C, four H and one O atoms more than OVTX-a; iii) OVTX-c ( $[M+H]^+$  at  $m/z$  2707.5173,<sup>5</sup>  $C_{131}H_{228}N_3O_{54}$ ) presents two C, four H and two O atoms more than OVTX-a; iv) OVTX-d and OVTX-e ( $[M+H]^+$  at  $m/z$  2663.4905,<sup>5</sup>  $C_{129}H_{224}N_3O_{53}$ ) present one O atom more than OVTX-a.

Undoubtedly, a full structural elucidation of ovatoxins can be unambiguously carried out only on the basis of NMR experiments. However, NMR is a technique at least  $10^6$  times less sensitive than MS, requiring  $\mu\text{g}$  to  $\text{mg}$  amounts of pure material for successful identification of such complex molecules. Currently, pure material is not available in such amount, so we tried to gain preliminary information on the structure of ovatoxins by investigating both their fragmentation and collision induced dissociation (CID) behaviour in HR full MS and HRMS<sup>2</sup> spectra, respectively.

It is noteworthy that cleavage between carbons 8 and 9 of the PLTX molecule is highly favoured (Figure 4), and divide the molecule in two moieties, A and B.<sup>7</sup> Ions associated to both moieties are formed in the full MS spectrum of PLTX as well as in its MS<sup>2</sup> spectra whatever is the precursor ion used (mono-, bi-, or tri-charged ions).<sup>7,8</sup> Many palytoxin-like compounds, such as ostreocin-d,<sup>9</sup> mascarenotoxins,<sup>10</sup> 42-OH-palytoxin,<sup>11</sup> and ovatoxin-a,<sup>6</sup> present the above MS behaviour.



**Figure 4.** Structure of palytoxin.

On the basis of our previous experience on ovatoxin-a, we tried to gain structural information on the new compounds initially analyzing the fragment ions due to  $[M+H-A \text{ moiety}-nH_2O]^+$  ( $n = 0-6$ ) present in the mass range 2200-2350 amu of the HR full MS spectrum of each ovatoxin (Figure 3).

Absolute  $m/z$  values of such ions in OVTX-b spectrum were practically superimposable to OVTX-a's suggesting that the two compounds share part structure B at least in elemental composition.

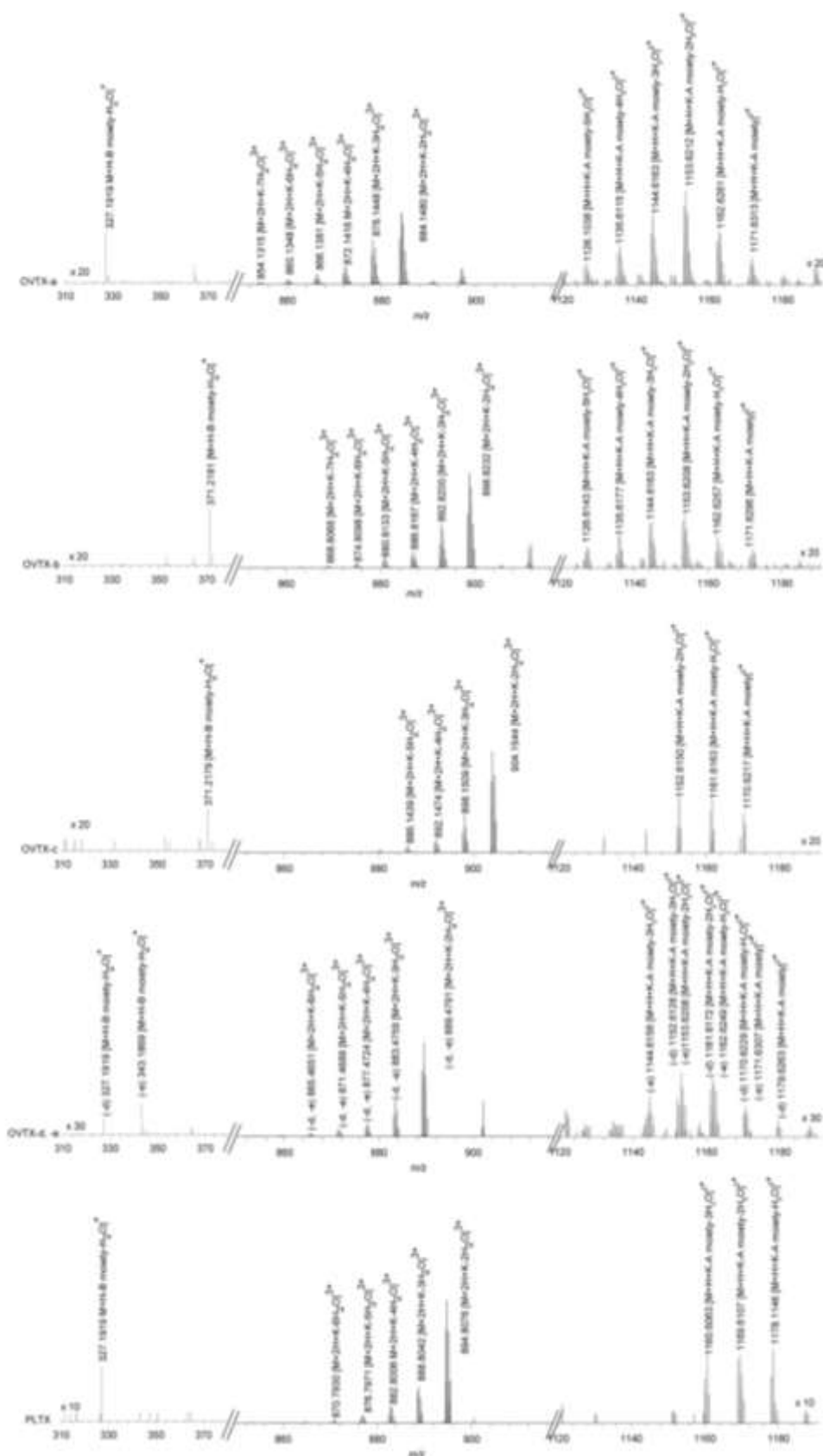
As for OVTX-c, -d and -e, identification of the mono-isotopic ion peak for each ion cluster was hampered by their heavy overlapping, likely due to incomplete chromatographic separation. Thus, basing only on full MS results, an unambiguous assignment of elemental formula to each fragment ion was prevented. Fortunately, this drawback was overcome through interpretation of HRMS<sup>2</sup> spectra of the  $[M+2H+K]^{3+}$  ions of ovatoxins (Figure 5), that paralleled palitoxin's in containing: i) abundant tri-charged ion peaks due to subsequent losses of water molecules (2 to 7) from the relevant precursor ion, ii) a diagnostic mono charged  $[M+H-B \text{ moiety}-H_2O]^+$  ion in the region 300-400 amu, and iii) diagnostic bi-charged ions due to  $[M+H+K-A \text{ moiety}-nH_2O]^{2+}$  ( $n = 0-5$ ); among them the  $[M+H+K-A \text{ moiety}-2H_2O]^{2+}$  ion was the most abundant. From the whole of these data we could individuate the elemental composition of moiety A and B for all the ovatoxins; this represents a first step in structural assignment of these very complex molecules.

MS<sup>2</sup> spectrum of the  $[M+2H+K]^{3+}$  ion at  $m/z$  896.2 of OVTX-a contained an  $[M+H-B \text{ moiety}-H_2O]^+$  ion at  $m/z$  327.1919<sup>5</sup> ( $C_{16}H_{27}N_2O_5$ ,  $\Delta = 1.380$  ppm) and a bi-charged  $[M+H+K-A \text{ moiety}-2H_2O]^{2+}$  ion at  $m/z$  1153.1194<sup>5</sup> ( $C_{113}H_{192}KNO_{44}$ ,  $\Delta = -2.399$ ) in addition to seven abundant peaks due to subsequent losses of water molecules from the precursor ion. These data confirmed our previous hypothesis<sup>6</sup> that OVTX-a presents the same part structure A as PLTX and two oxygen atoms less in the B moiety (Figure 5).

MS<sup>2</sup> spectrum of the tri-charged ion at  $m/z$  910.8 of OVTX-b contained, in addition to six abundant peaks due to subsequent losses of water molecules from the precursor ion, an  $[M+H-B \text{ moiety}-H_2O]^+$  ion at  $m/z$  371.2181<sup>5</sup> ( $C_{18}H_{31}N_2O_6$ ,  $\Delta = 1.177$  ppm) and an  $[M+H+K-A \text{ moiety}-2H_2O]^{2+}$  ion at  $m/z$  1153.1189<sup>5</sup> ( $C_{113}H_{192}KNO_{44}$ ,  $\Delta = -2.832$  ppm). A comparison of OVTX-b vs OVTX-a data (Figure 5) indicates that A moiety of OVTX-b contains additional  $C_2H_4O$  atoms (ion at  $m/z$  371.2181,<sup>13</sup>  $C_{18}H_{31}N_2O_6$  vs  $m/z$  327.1919,<sup>5</sup>  $C_{16}H_{27}N_2O_5$ ), whereas part structure B is identical (ion at  $m/z$  1153.1189<sup>13</sup> vs 1153.1194,<sup>5</sup>  $C_{113}H_{192}KNO_{44}$ ) at least in elemental composition.

MS<sup>2</sup> spectrum of tri-charged ion at  $m/z$  916.1 of OVTX-c contained, in addition to 4 abundant peaks due to subsequent losses of water molecules from the precursor ion, an  $[M+H-B \text{ moiety}-H_2O]^+$  ion at  $m/z$  371.2179<sup>13</sup> ( $C_{18}H_{31}N_2O_6$ ,  $\Delta = 0.638$  ppm) and an  $[M+H+K-A \text{ moiety}-2H_2O]^{2+}$  ion at  $m/z$  1161.1173<sup>5</sup> ( $C_{113}H_{192}KNO_{45}$ ,  $\Delta = -2.001$  ppm). These data compared to those of OVTX-a (Figure 5) indicated that OVTX-e presents additional  $C_2H_4O$  atoms in the A moiety ( $m/z$  371.2179,<sup>5</sup>  $C_{18}H_{31}N_2O_6$  vs 327.1919,<sup>5</sup>  $C_{16}H_{27}N_2O_5$ ) and an extra oxygen atom in the B moiety ( $m/z$  1161.1173,<sup>5</sup>  $C_{113}H_{192}KNO_{45}$ , vs 1153.1194,<sup>5</sup>  $C_{113}H_{192}KNO_{44}$ ).

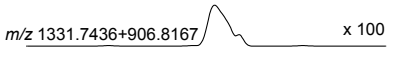

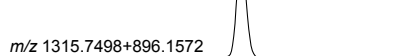


MS<sup>2</sup> spectrum of the  $[M+2H+K]^{3+}$  ion at  $m/z$  901.4 highlighted the presence of two structural isomers, OVTX-d and -e. It presented, in addition to 6 abundant peaks due to subsequent losses of water molecules from the precursor ion, two diagnostic mono charged  $[M+H-B \text{ moiety}-H_2O]^+$  ions at  $m/z$  327.1919<sup>5</sup> ( $C_{16}H_{27}N_2O_5$ ,  $\Delta = 1.380$  ppm) and  $m/z$  343.1869<sup>5</sup> ( $C_{16}H_{27}N_2O_6$ ,  $\Delta = 1.565$  ppm), assigned to OVTX-d and OVTX-e, respectively; the region 1100-1200 amu contained overlapped bi-charged ion clusters where the most intense ions  $[M+H+K-A \text{ moiety}-2H_2O]^{2+}$  could be individuated at  $m/z$  1161.1157<sup>5</sup> ( $C_{113}H_{192}KNO_{45}$ ,  $\Delta = -3.379$  ppm) and  $m/z$  1153.1179<sup>5</sup> ( $C_{113}H_{192}KNO_{44}$ ,  $\Delta = -3.700$  ppm) for ovatoxin-d and -e, respectively. A comparison of the above data with OVTX-a's (Figure 5) indicated that OVTX-d presents the same A moiety as OVTX-a (327.1919,<sup>5</sup>  $C_{16}H_{27}N_2O_5$ ), and one additional oxygen atom in the B moiety ( $m/z$  1161.1157,<sup>5</sup>  $C_{113}H_{192}KNO_{45}$  vs 1153.1194,<sup>5</sup>  $C_{113}H_{192}KNO_{44}$ ). As for OVTX-e vs OVTX-a, the former contains one additional oxygen atom in the A moiety ( $m/z$  343.1869,<sup>5</sup>  $C_{16}H_{27}N_2O_6$  vs 327.1919,<sup>5</sup>  $C_{16}H_{27}N_2O_5$ ) and the same B moiety ( $m/z$  1153.1179<sup>5</sup> vs 1153.1194,<sup>5</sup>  $C_{113}H_{192}KNO_{44}$ ).



**Figure 5.** HRMS<sup>2</sup> spectra (positive ions) of the  $[M+2H+K]^{3+}$  ion of OVTX-a (precursor  $m/z$  896.2), OVTX-b (precursor  $m/z$  910.8), OVTX-c (precursor  $m/z$  916.1), OVTX-d and -e (precursor  $m/z$  901.4) and PLTX standard (precursor  $m/z$  906.8).

In order to gain information about the relative abundance of putative PLTX and ovatoxins in the *O. ovata* culture, extracted ion chromatograms (XIC) were obtained from the HR full MS experiment by summing the most abundant peaks of both  $[M+2H-H_2O]^{2+}$  and  $[M+2H+K]^{3+}$  ion clusters for each compound. The resulting chromatographic peak areas were compared to that of palytoxin standard injected under the same conditions. Quantitative analyses were carried out by assuming that ovatoxins show the same molar response as PLTX. This is quite reasonable taking into account that they are very large and complex molecules presenting small differences in structural details as evidenced by their very similar elemental composition and chromatographic behaviour. A calibration curve for palytoxin standard at five levels of concentration was used to calculate putative PLTX and ovatoxins content. Table 2 summarizes the obtained quantitative results and shows the XIC of each compound.

**Table 2.** Quantitative results obtained from the HR LC-MS spectrum of the *O. ovata* culture (normal mass range). Extracted ion chromatograms (XIC) were obtained by summing the most abundant peaks of  $[M+2H-H_2O]^{2+}$  and  $[M+2H+K]^{3+}$  ion clusters for each compound. Results are expressed as pg/cell and percentage (%) on the total toxin content. Elemental formula of each compound (M) and relevant A and B moiety are reported.

Toxin	Rt (min)	Extracted Ion Chromatogram (XIC)	pg/cell	%	Elemental formula		
					M	A moiety	B moiety
Putative PLTX	10.78		0.2	0.06	$C_{129}H_{223}N_3O_{54}$	$C_{16}H_{28}N_2O_6$	$C_{113}H_{195}NO_{48}$
OVTX-a	11.45		17.9	54.4	$C_{129}H_{223}N_3O_{52}$	$C_{16}H_{28}N_2O_6$	$C_{113}H_{195}NO_{46}$
OVTX-b	11.28		9.4	28.5	$C_{131}H_{227}N_3O_{53}$	$C_{18}H_{32}N_2O_7$	$C_{113}H_{195}NO_{46}$
OVTX-c	10.90		1.6	4.86	$C_{131}H_{227}N_3O_{54}$	$C_{18}H_{32}N_2O_7$	$C_{113}H_{195}NO_{47}$
OVTX-d + OVTX-e	11.07		4.0	12.1	$C_{129}H_{223}N_3O_{53}$	(-d) $C_{16}H_{28}N_2O_6$ (-e) $C_{16}H_{28}N_2O_7$	(-d) $C_{113}H_{195}NO_{47}$ (-e) $C_{113}H_{195}NO_{46}$

The whole of the above data indicates a toxin profile of *O. ovata* more complex than that highlighted from our previous investigations. This has to be taken into account when monitoring programs of either plankton or contaminated seafood are carried out. Particularly, the presence of OVTX-b, -c, -d, and -e should also be considered since the whole of these new ovatoxins represents about 46% of the total toxin content of the investigated extract. In addition, much attention should be paid when LC-MS experiments are performed on MS instruments operating at unit resolution, even when multiple reaction monitoring (MRM) experiments are performed. In fact, the proximity of  $m/z$  values of a number of ions (either bi- or tri-charged) of PLTX and ovatoxins (Table 1), that can be used as precursor ions, and the presence of the same fragment ion  $[M+H-B \text{ moiety-H}_2\text{O}]^+$  at  $m/z$  327.2 for PLTX, OVTX-a and -d and at  $m/z$  371.2 for OVTX-b and -c could lead to incorrect assessment of individual toxins. Studies aiming to overcome these drawbacks are currently in progress in our lab.

### 5.3. Future Perspectives

Ovatoxin-a represents the 50% of the total toxins content in the *O. ovata* cultures, so my research group is carrying out experiments of purification in order to develop an effective isolation procedure for this toxin. The chemical structural elucidation of ovatoxin-a would enrich our knowledge on Mediterranean Sea's toxic profile. Furthermore the isolation of this toxin represents the basis for the study of its exact mechanism of action by pharmacological assays.

After a number of preliminary studies, my research group gained the best results by extracting algal pellets as follows:

addition of methanol to cell pellets and sonication for 6 min in pulse mode, while cooling in ice bath; a second extraction is then carried out by adding a methanol/water solution. The extracts are combined and concentrated, and the obtained mixture is extracted by an equal volume of chloroform.

The obtained aqueous extract is separated on a combiflash C18 chromatographic column, by using the following gradient:

<b>Time</b>	<b>% 1-propanol</b>	<b>% Water 0.1% HCOOH</b>
0	40%	60%
60 min	70%	30%
160 min	90%	10%

Several stationary and mobile phases were tested in HPLC purification to the aim of evaluating the percentage recovery of toxins. Pure palytoxin standard solution was employed in such an experiment. Table 3 shows the results of this study.

**Table 3.** HPLC purification results.

Column	Stationary phase	Mobil phase	% recovery of palytoxin standard
Grace	Mixed mode RP-C18/Cation 100A 5 $\mu$ 250mm x 4.6mm	NaH <sub>2</sub> PO <sub>4</sub> 20mM : CH <sub>3</sub> CN (7:3); pH=4.6	4%
Shodex	RP/Cation 8 x 75 mm	NaH <sub>2</sub> PO <sub>4</sub> 20mM : EtOH (7:3); pH=5.8	56%
Biosep-sec-s-2000	Molecular exclusion; 300 x 4.60 mm	H <sub>2</sub> O : EtOH (75:25)	16%
Gemini	C 18; 5 $\mu$ 250 x 3.00 mm	H <sub>2</sub> O : CH <sub>3</sub> CN Gradient: from 20% CH <sub>3</sub> CN to 95 % CH <sub>3</sub> CN (in 26 min)	64%

In conclusion, the best column for the final purification of ovatoxin-a is the Gemini (C 18; 5 $\mu$  250 x 3.00 mm), eluted by a gradient of water (A eluent) and acetonitrile/water 95:5 both added of 30 mM acetic acid (B eluent) as follows :

Time	% A ELUENT	% B ELUENT
0	80%	20%
40 min	0%	100%

We use a hybrid linear ion trap LTQ Orbitrap XL<sup>TM</sup> Fourier Transform MS (FTMS) equipped with an ESI ION MAX<sup>TM</sup> source (Thermo-Fisher, San Josè, CA, USA) as detector, coupled to an Agilent 1100 LC binary system (Palo Alto, CA, USA).

#### 5.4. References

1. Fukuyo Y. *Bull. Jpn. Soc. Sci. Fish.* 1981; 47: 967.
2. Hoshaw RW, Rosowski JR. *Handbook of Phycological Methods: Culture Methods and Growth Measurements.* Cambridge University Press: New York, 1973.
3. Guillard RRL. *Culture of Marine Invertebrates Animals.* Plenum Press: New York, 1975.
4. Utermöhl H. *Mitt. Int. Verein. Limnol.* 1958; 9: 1.



5. mono-isotopic ion peak
6. Ciminiello P, Dell'Aversano C, Fattorusso E, Forino M, Tartaglione L, Grillo C, Melchiorre N. *J. Am. Soc. Mass Spectrom.* 2008; 19: 111.
7. Uemura D, Hirata Y, Iwashita T, Naoki H. *Tetrahedron.* 1985; 41: 1007.
8. Ciminiello P, Dell'Aversano C, Fattorusso E, Forino M, Magno GS, Tartaglione L, Grillo C, Melchiorre N. *Anal. Chem.* 2006; 78: 6153.
9. Unpublished MS data obtained using a reference sample of ostreocin-d. The Authors wish to thank prof. T. Yasumoto for providing the sample.
10. Lenoir S, Ten-Hage L, Turquet J, Quod JP, Bernard C, Hennion MC. *J. Phycol.* 2004; 40: 1042.
11. Ciminiello P, Dell'Aversano C, Dello Iacovo E, Fattorusso E, Forino M, Grauso L, Tartaglione L, Florio C, Lorenzon P, De Bortoli M, Tubaro A, Poli M, Bignami G. *Chem. Res. Toxicol.* 2009; 22: 1851.

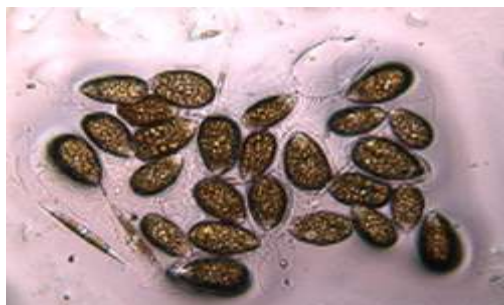
## Chapter 6

### Monitoring of *Ostreopsis ovata* along the Campania coasts: quali-quantitative analysis of palytoxin-like compounds

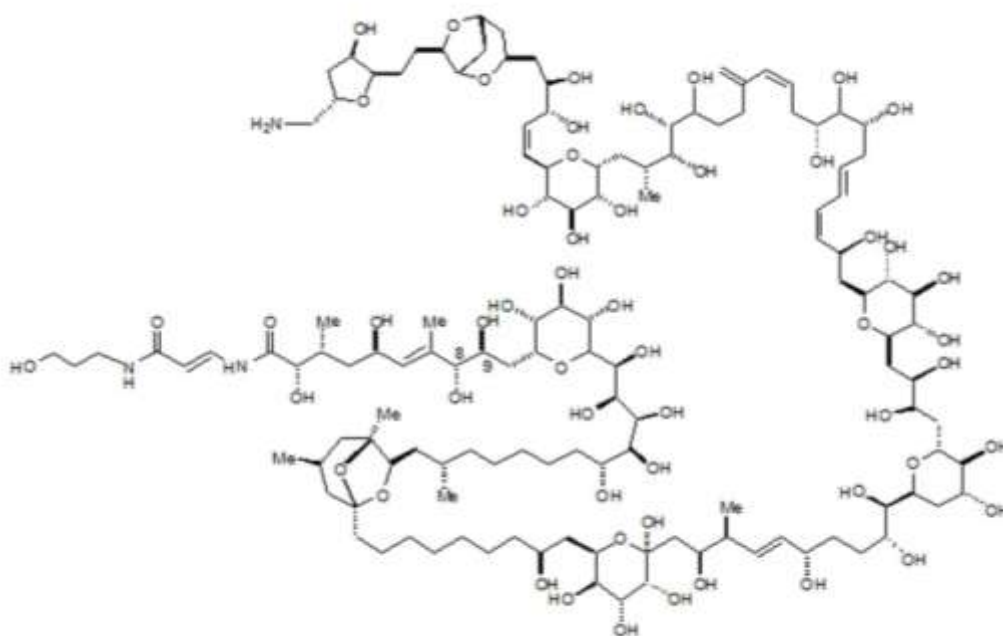
Over the past few years a new threat due to harmful algal blooms has been impending over the Mediterranean Sea: tropical microalgae belonging to *Ostreopsis* genus have spread along the Italian coasts<sup>1</sup>, mostly in the Tyrrhenian Sea, causing serious concerns to both environment and public health. In fact, concurrently to the algal blooms, environmental sufferings involving mostly epibenthos were observed and symptoms of rhinorrhoea, conjunctivitis, dermatitis, cough, dyspnoea, wheezes and severe fever arose in people exposed to marine aerosols.

Such a phenomenon was recorded for the first time during the summer 1998 along the north-western Tuscany coasts<sup>1</sup>, but it reached alarming proportions in late July 2005, when about 200 people exposed to marine aerosols along the beach and promenade of Genoa required extended hospitalization. Respiratory distress observed in humans was concurrent with a massive bloom of *Ostreopsis ovata* (Figure 1) along Genoa coasts and disappeared when the *O. ovata* population decreased.

These toxic episodes caught the attention of the media both national and international. The Agenzia Regionale per la Protezione dell'Ambiente Liguria (ARPAL) carried out a plankton analysis, which highlighted the presence of this tropical microalga in high concentrations.



**Figure 1.** The microalga *Ostreopsis ovata* isolated in Genoa gulf.



**Figure 2.** Structure of palytoxin.

Palytoxin (Figure 2) is the most potent non-proteic toxin so far known ( $DL_{50} < 100$  nanograms/Kg), repeatedly individuated in tropical countries as responsible agent of poisoning syndromes, sometimes lethal. It's a macromolecule with a complex structure and it's very difficult to be detected, because of the high number of modifications it can have in the environment and in the host organism.

The presence of microalgal species producing palytoxin has impact on:

- 1) balneability and attending of coastal areas for effect of the toxin in water and in marine aerosols;
- 2) toxicity of the ichthyic products which enter in contact with the microalga.

The consequences of the latter phenomenon are very well known in tropical countries, where every year palytoxin or its analogues become responsible of poisoning syndromes, sometimes lethal, known as *clupeotoxism*. In particular, some ichthyic products, as pilchards, anchovies and crabs can accumulate these toxins in high concentrations, without being subjected to their effects; so they become the ring of the food chain, which allows the transfer of the toxicity from the microalga to man.

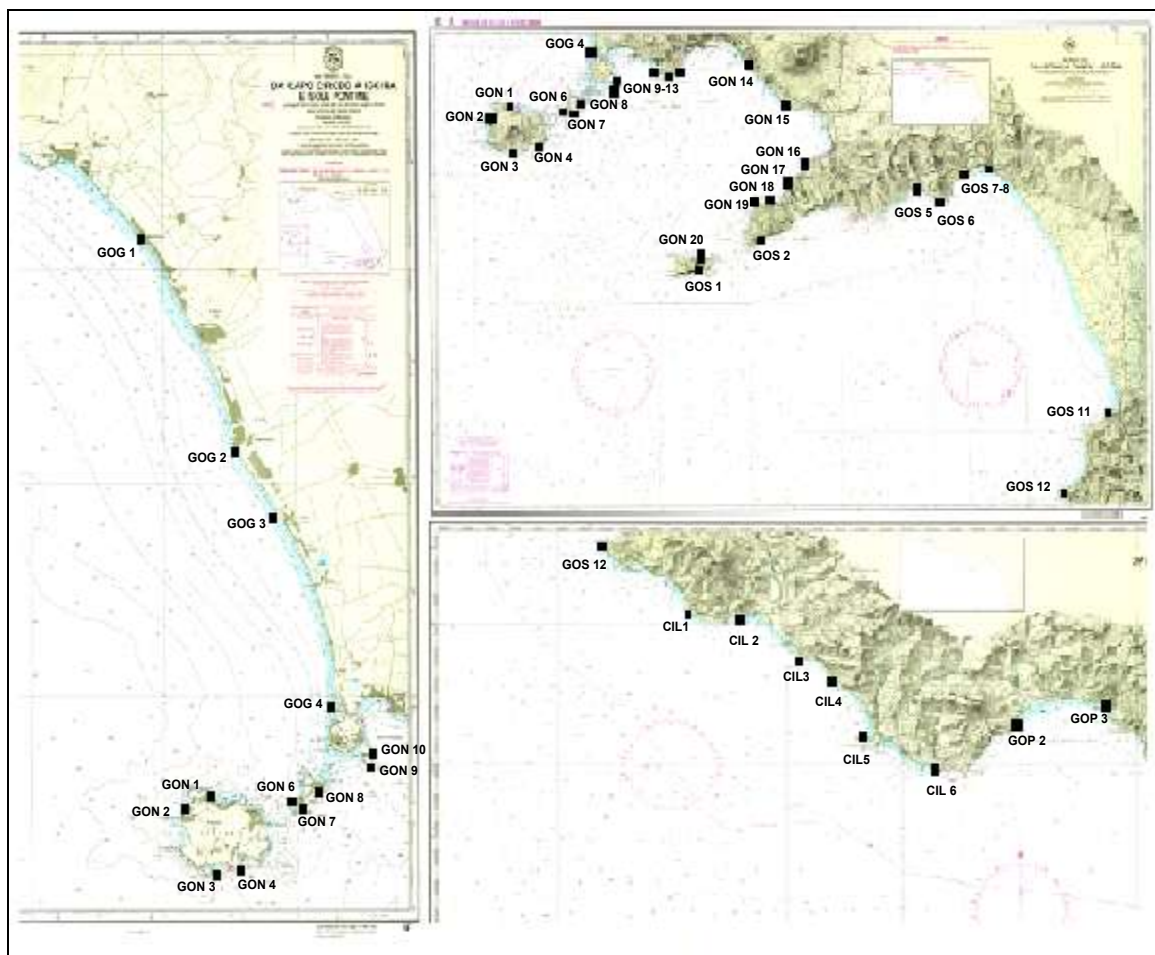
During the last years, the restateing of the *O. ovata* Summer blooms, is arousing serious concerns to both human health and economy; so from October 2006 a commission of the Ministero della Salute is in charge of investigating and monitoring *Ostreopsis* phenomenon

---

along the whole Italian coasts to the aim of evaluating risks to human health<sup>2</sup> and preventing any possible human intoxication.

A year later, during the summer 2007, high concentrations of *Ostreopsis spp.* were detected along the Tyrrhenian coasts, from Liguria to Sicily, and Adriatic, from Apulia to Friuli Venezia Giulia (except Romagna and Veneto). A massive bloom of *O. ovata* was also recorded along the Campania coasts. So, a program of monitoring in the frame of the project “Monitoraggio *Ostreopsis ovata* litorale costiero Regione Campania” was started by ARPA Campania in collaboration of Stazione Zoologica A. Dohrn, Istituto Zooprofilattico Sperimentale del Mezzogiorno, and with Dipartimento di Chimica delle Sostanze Naturali, where I carried out my PhD. This program of monitoring allowed us to individuate the presence of *Ostreopsis* species, producing palytoxins in many areas of the Gulf of Naples and the Gulf of Salerno.

Samples of plankton and shellfish (mussels and sea-urchins) were collected in many areas along the South-Latium and Campania coasts and its islands (Figure 3) and analyzed in our laboratories to investigate the presence of palytoxin-like compounds by the new developed LC-MS method.<sup>3,4</sup> The obtained results are here described.



**Figure 3.** Sites of collection of the samples of plankton and mussels.

## 6.1. Experimental

Samples of plankton and shellfish collected along the Tyrrhenian coasts of South-Latium and Campania.<sup>3,4</sup> were extracted and analyzed by the new LC-MS method for the detection of palytoxin.

### 6.1.1. Plankton extraction

For every sample of plankton, volume (about 0.9-1 L) and pH (about 7.5-7.8) were measured; successively, the samples were sonicated for 4 min twice. This step is very important to break the microalgal cells which are still undamaged in the sample, to the aim of pouring all the cells content in the growth media (sea water) around. Then, the obtained mixture was centrifuged at 6500 revolutions per minute (rpm) for 10 min to the aim of separating the sea water (containing the toxins) from the cell pellets. The obtained mixture was analyzed directly by LC-MS (5  $\mu$ L injected). The supernatant was extracted by an equal volume of 1-butanol trice. The butanol layer was evaporated under vacuum, filtered by centrifugation in Ultra-Free

(0.45  $\mu\text{m}$ ) at 5500 rpm for 10 min, dissolved in methanol/water (1:1, v/v) and then analyzed by LC-MS (5  $\mu\text{L}$  injected).

Considering that palytoxin's coefficient of partition between 1-butanol and water is about 0.21, palytoxin recovery in the butanolic extract after 3 partitions water/butanol is estimated to be 45.5%, while the 54.5% of palytoxin remains in water unrecovered, after the extraction. We have to take into consideration the palytoxin's recovery for a correct evaluation of the palytoxin content in each sample extracted. Further studies are actually being carried out in our laboratories to the aim of evaluating other extraction procedures to obtain higher recoveries of palytoxin.

### ***6.1.2. Preliminary experiments of shellfish extraction***

Preliminary experiments were carried out in collaboration with Istituto Zooprofilattico in order to evaluate which was the best method of extraction of palytoxin for the analysis of the shellfish samples:

- 1) extraction of the edible tissue using a methanol/water 1:1 solution;
- 2) extraction of the edible tissue as reported by the Italian Law plans for the analysis of the DSP-toxins in the mussels (protocol 2).

In the first case, three aliquots each one of 1 g of homogenized pulp of mussels were contaminated by adding 20  $\mu\text{g}$  of palytoxin standard and separately extracted with 3 mL of methanol/water 1:1 trice. Every extract (final volume = 10 mL), containing 0.1 g of edible tissue/mL, was directly analyzed by LC-MS. The same kind of extraction was carried out on an aliquot of uncontaminated mussels. The toxin recovery was calculated by comparing the LC-MS results of the contaminated samples to that of standard solutions of palytoxin at four levels of concentration (2.5, 0.83, 0.27, 0.09 and 0.03  $\mu\text{g mL}^{-1}$ ).

In the second case, three aliquots each one of 1 g of homogenized pulp of mussels were contaminated by adding 20  $\mu\text{g}$  of palytoxin standard and separately extracted with 3 mL of acetone and 3 mL of methanol. Each extract, so obtained, was concentrated at rotavapor. The residue was dissolved in 10 mL of methanol/water 6:4 and shared out with 5 mL of dichloromethane. An aliquot of each dichloromethane extract (corresponding to  $\frac{1}{4}$  of the total volume) was evaporated and the residue was dissolved in 500 $\mu\text{L}$  of methanol/water 1:1 and analyzed by LC-MS. Each hydromethanolic extract (final volume = 12.5 mL), containing 0.08 g of edible tissue  $\text{mL}^{-1}$ , was directly analyzed by LC-MS. The same type of extraction was carried out on an aliquot of uncontaminated pulp of mussels. The toxin recovery was

evaluated by comparing LC-MS results of the contaminated samples to palytoxin standard solutions at four concentration levels (2.5, 0.83, 0.27, 0.09 and 0.03  $\mu\text{g mL}^{-1}$ ).

### **6.1.3. Edible shellfish extraction**

On the base of results obtained by these preliminary experiments, samples of mussels and sea-urchins were extracted by Istituto Zooprofilattico as reported by Italian Law for DSP-toxins analysis in mussels (protocol 2). An aliquot of each methanol/water 6:4 extract, corresponding to the fourth part of the total extract (50 mL from 200 mL of total extract), and to 25 g of edible tissue was sent to our laboratories for the chemical analysis. This was carried out on each aliquot, by injecting in LC-MS system 5  $\mu\text{L}$  of the total extract (corresponding to 0.5 g of edible tissue  $\text{mL}^{-1}$ ) and a 1:5 dilution (corresponding to 0.1 g of edible tissue  $\text{mL}^{-1}$ ). In no sample the investigated toxins appeared. So, every sample was concentrated to 3 mL (corresponding to about 8 g of edible tissue  $\text{mL}^{-1}$ ) and analyzed by L-MS again.

### **6.1.4. Liquid chromatography-mass spectrometry (LC-MS)**

During Summer 2007, 2008 and 2009 LC-MS analyses were carried out by using a mass spectrometer API 2000 equipped of Turbo ion-spray® source and triple quadrupole analyzer coupled to a chromatographic system Agilent HP 1100 provided of binary pump, degasser, autosampler and thermostat of vials compartment. The used chromatographic conditions in LC-MS experiments are reported below:

*Column:* 3 $\mu\text{m}$  Gemini C18 (150  $\times$  2.00 mm)

*Mobile phase:* A = water, B = 95% acetonitrile/water, both phases 30 mM acetic acid

*Gradient elution:* t = 0 min, 20% B; t = 20 min, 100% B; t = 21 min, 100% B

*Flow:* 0.2 mL/min

*Temperature:* room temperature (about 21°C)

*Injection volume:* 5  $\mu\text{L}$

In these conditions palytoxin and ovatoxin-a co-elute at 6.45 min and are separated on the basis of their different (precursor ion) > (fragment ion) mass transitions, which are monitored in multiple reaction monitoring (MRM) experiments. The monitored (precursor ion) > (fragment ion) transitions for palytoxin (Figure 2) are:

$m/z$  1340 > 327 corresponding to  $[\text{M}+2\text{H}]^{2+}$  >  $[\text{fragment C8-C9} - \text{H}_2\text{O}]^+$

$m/z$  1331 > 327 corresponding to  $[M+2H-H_2O]^{2+} > [\text{fragment C8-C9} - H_2O]^+$

The monitored (precursor ion) > (fragment ion) transitions for ovatoxin-a are:

$m/z$  1324 > 327 corresponding to  $[M+2H]^{2+} > [\text{fragment C8-C9} - H_2O]^+$

$m/z$  1315 > 327 corresponding to  $[M+2H-H_2O]^{2+} > [\text{fragment C8-C9} - H_2O]^+$

In the quantitative analysis, the emerging peaks areas for the most abundant transitions at  $m/z$  1331 > 327 and  $m/z$  1315 > 327 were compared to the peaks areas corresponding to palytoxin standard solutions of similar concentration, injected in the same experimental conditions.

During Summer 2010 high resolution (HR)LC-MS experiments were carried out on the same Agilent 1100 LC binary system (Palo Alto, CA, USA), but coupled to a hybrid linear ion trap (LTQ) Orbitrap XL<sup>TM</sup> Fourier Transform MS (FTMS) equipped with an ESI ION MAX<sup>TM</sup> source (Thermo-Fisher, San José, CA, USA). The used chromatographic conditions in LC-MS experiments are reported below:

*Column:* 3 $\mu$ m Gemini C18 (150  $\times$  2.00 mm)

*Mobile phase:* A = water, B = 95% acetonitrile/water, both phases 30 mM acetic acid

*Gradient elution:* 20-50% B over 20 min, 50-80% B over 10 min, 80-100% B in 1 min, and hold for 5 min

*Flow:* 0.2 mL/min

*Temperature:* room temperature (about 21°C)

*Injection volume:* 5  $\mu$ L

This gradient system allowed a sufficient chromatographic separation of most palytoxin-like compounds, namely: putative PLTX (Rt = 10.78 min), OVTX-a (Rt = 11.45 min), OVTX-b (Rt = 11.28 min), OVTX-c (Rt = 10.90 min), OVTX-d and OVTX-e (Rt = 11.07 min).

## 6.2. Results and Discussion

During 2007, 2008 and 2009 LC-MS analyses of samples of plankton and edible shellfish were carried out in multiple reaction monitoring (MRM) in positive ions mode. The (precursor ion) > (fragment ion) transitions for palytoxin (Figure 2) (C<sub>129</sub>H<sub>223</sub>O<sub>54</sub>N<sub>3</sub>, MW=2679.5) were obtained by monitoring the precursor bicharged ions  $[M+2H]^{2+}$  at  $m/z$  1340 and  $[M+2H-H_2O]^{2+}$  at  $m/z$  1331 connected to the fragment ion at  $m/z$  327, due to fragmentation of the molecule in C8-C9 and subsequent H<sub>2</sub>O loss.

High resolution mass spectrometry studies, previously reported in a recently published article of ours on *Journal of the American Society for Mass Spectrometry*,<sup>4</sup> indicated that ovatoxin-a



presents a molecular weight of 2647.5 (monoisotopic at  $m/z$  2647.4868) corresponding to the elementary formula  $C_{129}H_{223}O_{52}N_3$ ; therefore, it contains 2 oxygen atoms less than palytoxin ( $C_{129}H_{223}O_{54}N_3$ , MW=2679.5). Also, different evidences showed that, probably, palytoxin and ovatoxin-a share the same little structural moiety, coming from the molecular fragmentation in C8-C9, which originates the fragment at  $m/z$  327. In consequence, the monitored transitions for ovatoxin-a in MRM experiments are:  $m/z$  1324 > 327 corresponding to  $[M+2H]^{2+}$  >  $[\text{fragment C8-C9} - H_2O]^+$  and  $m/z$  1315 > 327 corresponding to  $[M+2H-H_2O]^{2+}$  >  $[\text{fragment C8-C9} - H_2O]^+$

Before carrying out the samples analyses, the minimum levels of detection and quantitation of the LC-MS method used were evaluated. In fact, these limits change during the time on the base of the instrument clearing and maintenance conditions. For this palytoxin standard solutions were analyzed in MRM (positive ions mode) at four different concentration levels: 2.5, 0.83, 0.27, 0.09 and 0.03  $\mu\text{g mL}^{-1}$  in triplicate. From these experiments the limit of quantitation of palytoxin was estimated to be 60 ng/mL, corresponding to 0.3 ng injected on column.

During Summer 2010, instead, HR full MS experiments (positive ions) on LTQ Orbitrap FTMS spectrometer were acquired in both the range  $m/z$  800-1400 and  $m/z$  2000-3000 at a resolving power of 15,000 and 100,000 respectively; so we could evaluate the presence of palytoxin, ovatoxin-a and also the new ovatoxin-b, -c, -d, and -e in the samples.

### 6.2.1. Plankton LC-MS analyses

In 2007, 2008 and 2009 plankton extracts and standard solutions were analyzed in triplicate in the same day. In the quantitative analysis, the peak areas for the most abundant transitions at  $m/z$  1331 > 327 (for palytoxin) and  $m/z$  1315 > 327 (for ovatoxin-a) were compared to the peak areas corresponding to palytoxin standard's at similar concentration, injected in the same experimental conditions. The equation of the calibration curve was used for the quantitative analysis. Unfortunately a pure ovatoxin-a standard isn't available, so the ovatoxin-a amount was evaluated supposing that in the used ionization conditions, it gives the same molar response than palytoxin.

The quantitative results of the LC-MS analysis on plankton samples during Summer 2007 are shown in Table 1 and the collection sites are graphically represented in Figure 6. Since the injection volumes was 5  $\mu\text{L}$  and the extract volume of each sample is 5 mL, the samples which resulted negative, could, actually, contain palytoxin in lower quantity than 300 ng.

**Table 1.** LC-MS results of the plankton samples collected along the Tyrrhenian coasts during Summer 2007.<sup>a</sup>

n.d.= absent or present in lower quantities than the limit of detection (LOD) of the used method.

&lt;LOQ = present in lower quantities than the limit of quantitation (LOQ) of the used method.

Collection Points	Date	Site	cells/L	cells/g alga	pH	Volume (L)	palytoxin				ovatoxin-a			
							Total µg	µg/L	pg/cell	µg/g	Total µg	µg/L	pg/cell	µg/g
Rocce Verdi-Gaiola	11/07/2007	Rocce verdi	6090000	266950	7.50	3	8.7	2.90	0.48	0.13	81.90	27.30	4.48	1.20
GOG01(B)	09/03/2007	Baia Domizia	0	0	7.15	1.1	n.d.	n.d.	n.d.	n.d.	n.d.	n.d.	n.d.	n.d.
GOG02	03/08/2007	Foce Volturno	0	0	7.38	1.05	n.d.	n.d.	n.d.	n.d.	n.d.	n.d.	n.d.	n.d.
GOG03	03/08/2007	Pineta Mare	0	0	7.34	1.05	n.d.	n.d.	n.d.	n.d.	n.d.	n.d.	n.d.	n.d.
GOG04	03/08/2007	Foce Fusaro	0	0	7.57	1.1	n.d.	n.d.	n.d.	n.d.	n.d.	n.d.	n.d.	n.d.
GON01(b)	06/08/2007	Ischia-Lacco ameno	99000	absent	7.56	1.1	n.d.	n.d.	n.d.	n.d.	< LOQ	< LOQ	< LOQ	< LOQ
GON02(b)	06/08/2007	Ischia-Forio	110000	2004	7.8	1.1	n.d.	n.d.	n.d.	n.d.	< LOQ	< LOQ	< LOQ	< LOQ
GON03a	06/08/2007	Ischia-S.Angelo	191400	9274	7.46	1.1	n.d.	n.d.	n.d.	n.d.	< LOQ	< LOQ	< LOQ	< LOQ
GON04(a)	06/08/2007	Ischia-Capo Grosso	48400	2125	7.75	1.15	n.d.	n.d.	n.d.	n.d.	n.d.	n.d.	n.d.	n.d.
GON05(b)	20/08/2007	Ischia-S.Pietro	manca	absent	8.39	0.99	n.d.	n.d.	n.d.	n.d.	n.d.	n.d.	n.d.	n.d.
GON06a	06/08/2007	Procida-Vivara	39600	683	7.38	1.15	n.d.	n.d.	n.d.	n.d.	n.d.	n.d.	n.d.	n.d.
GON0(7a)	06/08/2007	Procida-Solchiaro	193600	13128	7.92	1.15	n.d.	n.d.	n.d.	n.d.	n.d.	n.d.	n.d.	n.d.
GON08(a)	06/08/2007	Procida-Corricella	191400	14779	7.97	1.1	n.d.	n.d.	n.d.	n.d.	<LOQ	< LOQ	< LOQ	< LOQ
GON09	07/08/2007	Miseno-Faro	363000	24621	7.7	1.03	<LOQ	< LOQ	< LOQ	< LOQ	3.9	3.77	10.40	0.26
GON10	07/08/2007	Miseno-Punta Pennata	1375000	49340	7.37	1.04	<LOQ	< LOQ	< LOQ	< LOQ	2.90	2.79	2.03	0.10
GON11	07/08/2007	Nisida	4609000	194996	7.43	2	2.40	1.20	0.26	0.05	16.7	8.35	1.81	0.35

Chapter 6

GON12	07/08/2007	Gaiola	1623600	92750	7.65	1.05	1.52	1.45	0.89	0.08	5.55	5.28	3.25	0.30
GON13	07/08/2007	Rocce Verdi	3612400	88776	7.41	1.03	1.77	1.71	0.47	0.04	14.67	14.27	3.95	0.35
GON14	07/08/2007	Portici	0	0	7.95	1.07	n.d.	n.d.	n.d.	n.d.	n.d.	n.d.	n.d.	n.d.
GON 15	07/08/2007	Torre del Greco	169400	8144	7.88	0.88	n.d.	n.d.	n.d.	n.d.	0.945	1.09	6.44	0.052
GON16	07/08/2007	Banco di S.Croce	77000	4445	7.92	1.05	<LOQ	<LOQ	<LOQ	<LOQ	0.88	0.84	10.88	0.05
GON17(a)	13/08/2007	P.ta Gradelle	33000	5248	8	1.1	n.d.	n.d.	n.d.	n.d.	n.d.	n.d.	n.d.	n.d.
GON17(b)	13/08/2007	P.ta Gradelle	66000	44	7.63	1.05	<LOQ	<LOQ	<LOQ	<LOQ	0.81	0.77	11.69	0.001
GON18	13/08/2007	Sorrento	814000	24404	7.39	1.1	<LOQ	<LOQ	<LOQ	<LOQ	3.43	3.12	3.83	0.09
GON19	13/08/2007	Capo Massa	70400	5815	7.32	1.05	n.d.	n.d.	n.d.	n.d.	n.d.	n.d.	n.d.	n.d.
GON20	13/08/2007	Capri-Marina Grande	129910	2637	7.2	1.05	n.d.	n.d.	n.d.	n.d.	0.92	0.88	6.74	0.02
GOS01	13/08/2007	Capri-Marina Piccola	6600	123	8.14	1.05	n.d.	n.d.	n.d.	n.d.	n.d.	n.d.	n.d.	n.d.
GOS02	13/08/2007	P.ta Campanella- nerano	187000	2400	7.47	1.05	n.d.	n.d.	n.d.	n.d.	<LOQ	<LOQ	<LOQ	<LOQ
GOS05	08/08/2007	Minori	212630	1933	7.95	1	n.d.	n.d.	n.d.	n.d.	n.d.	n.d.	n.d.	n.d.
GOS06	08/08/2007	C.po d'Orso	70400	762	7.43	1	n.d.	n.d.	n.d.	n.d.	n.d.	n.d.	n.d.	n.d.
GOS07	08/08/2007	Vietri	363000	7116	7.92	1.07	n.d.	n.d.	n.d.	n.d.	<LOQ	<LOQ	<LOQ	<LOQ
GOS08	08/08/2007	p.zza Della Concordia	266200	7746	8.33	1	n.d.	n.d.	n.d.	n.d.	0.58	0.58	2.18	0.02
GOS11	08/08/2007	Agropoli	94600	914	7.89	1.95	n.d.	n.d.	n.d.	n.d.	n.d.	n.d.	n.d.	n.d.
GOS12	08/08/2007	P.ta Licosa	52800	432	7.45	1.03	n.d.	n.d.	n.d.	n.d.	n.d.	n.d.	n.d.	n.d.
CIL01	16/08/2007	Acciaroli	24640	98	7.48	1.05	n.d.	n.d.	n.d.	n.d.	n.d.	n.d.	n.d.	n.d.
CIL02	16/08/2007	Pioppi	378400	7450	7.12	1.05	n.d.	n.d.	n.d.	n.d.	2.83	2.70	7.12	0.05
CIL03	16/08/2007	Torre del Telegrafo	0	0	7.22	1.1	n.d.	n.d.	n.d.	n.d.	n.d.	n.d.	n.d.	n.d.
CIL04	16/08/2007	Pisciotta	45100	641	7.5	1.05	n.d.	n.d.	n.d.	n.d.	n.d.	n.d.	n.d.	n.d.
CIL05	16/08/2007	Palinuro	19250	17	6.77	0.9	n.d.	n.d.	n.d.	n.d.	n.d.	n.d.	n.d.	n.d.
CIL06	16/08/2007	Marina di Camerota	380600	7145	7.54	0.9	n.d.	n.d.	n.d.	n.d.	1.86	2.07	5.43	0.04
GOP02(a)	16/08/2007	Scario	0	0	7.51	1.05	n.d.	n.d.	n.d.	n.d.	n.d.	n.d.	n.d.	n.d.

Chapter 6

GOP02(b)	16/08/2007	Scario	0	0	7.44	1.05	n.d.	n.d.	n.d.	n.d.	n.d.	n.d.	n.d.	n.d.
GOP03	16/08/2007	Sapri	19800	116	7.1	1.05	n.d.	n.d.	n.d.	n.d.	n.d.	n.d.	n.d.	n.d.
Praiano (GOS04)	04/08/2007	Gavitella 2 (G2)	1298000	29711	7.43	0.55	<LOQ	<LOQ	<LOQ	<LOQ	2.59	4.71	3.63	0.11
Praiano (GOS04)	05/08/2007	Praia/Pirata 1	1386000	670259	7.43	1.1	1.36	1.24	0.89	0.60	9.10	8.27	5.97	4.00
Praiano (GOS04)	05/08/2007	Praia/Pirata 2	2574000	131831	7.32	1.1	2.13	1.94	0.75	0.10	14.70	13.36	5.19	0.68
GOS04(a)	08/08/2007	Gavitella ovest	2772000	170164	7.63	0.9	4.50	5.00	1.80	0.31	35.4	39.33	14.19	2.41
GOS04(b)	08/08/2007	Praia Africana	58080	175	7.84	1.1	n.d.	n.d.	n.d.	n.d.	<LOQ	<LOQ	<LOQ	<LOQ
GOS04(c)	08/08/2007	Praia Paradise	880000	95869	7.22	1.05	1.85	1.76	2.00	0.19	4.55	4.33	4.92	0.47
Praiano (GOS04)	20/08/2007	Gavitella est	198000	17058	7.2	0.9	<LOQ	<LOQ	<LOQ	<LOQ	3.12	3.47	17.51	0.30
Rocce verdi(GON13)	26/07/2007	Rocce verdi Asparagopsis	638000	24494	7.4	1.05	n.d.	n.d.	n.d.	n.d.	3.54	3.37	5.28	0.13
S. Nicola	04/08/2007	San Nicola Arcella	rarissime	0	7.96	1	n.d.	n.d.	n.d.	n.d.	n.d.	n.d.	n.d.	n.d.
Sapri	05/08/2007		0	0	7.75	1.05	n.d.	n.d.	n.d.	n.d.	n.d.	n.d.	n.d.	n.d.

<sup>a</sup>The toxins amount, reported in the table, is corrected considering the 56% of recovery during the extraction procedure.



**Figure 4.** Sites of collection of plankton, with indication about the samples containing palytoxin and ovatoxin-a (red), only ovatoxin-a (orange) and palytoxin and ovatoxin-a absent or present in lower amounts than the limit of detection of the used method (gray).

### 6.2.2. Edible shellfish LC-MS analyses

As for edible shellfish, not existing a reference method for palytoxin analysis in seafood, in collaboration with Istituto Zooprofilattico, preliminary experiments of contamination were carried out to the aim of evaluating which extraction method to be used: the methanol/water 1:1 extraction or the extraction expected by Italian Law for DSP-toxins analysis in mussels (protocol 2). The recovery, calculated by comparing the LC-MS results of the contaminated samples to the palytoxin standard solutions, was in the range 58%-72% (average 65%) and 49%-61% (average 56%) for methanol/water 1:1 extraction and the law method respectively.

### 6.2.3. 2007 LC-MS analyses

On the basis of the results of the preliminary experiments, some mussels and sea-urchins samples were extracted at Istituto Zooprofilattico as reported in the law protocol and tested by mouse bioassay. An aliquot of each extract resulted positive at mouse bioassay, was sent to our laboratories for the chemical analysis. The analysis was carried out as reported for the plankton analysis, by injecting in LC-MS system 5  $\mu$ L of each extract (corresponding to about 0.5 g of edible tissue/mL) and then a dilution 1:5 of them (corresponding to about 0.1 g of edible tissue/mL). Since only in Gaiola and Rocce Verdi samples traces of ovatoxin-a were

recorded, all the samples were concentrated to 1.5-3 mL (corresponding to about 5-9 g of edible tissue/mL) and analyzed by LC-MS again.

In the most part of the analyzed samples, palytoxin and ovatoxin-a resulted present (Table 2). In the samples collected at Rocce Verdi and Gaiola in July the 26th 2007 and Miseno-Faro and Gaiola in August the 7th 2007 the ovatoxin-a and/or palytoxin's concentrations determined by LC-MS analyses, appeared significant and allowed to hypothesize a potential risk for human health. In the samples GON19, GON20 and GOS01 no one of the monitored toxins was detected. This let suppose that palytoxin and ovatoxin-a, if present, were contained in the samples, in lower quantity than the limit of detection of the used method, or, as an alternative, that the positivity of the mouse bioassay for these samples, was due to other toxins and/or products of decomposition. In the remaining samples, palytoxin and/or ovatoxin-a resulted present in lower quantity than the limit of quantification of the used method.

**Table 2.** LC-MS results of the mussels and sea-urchins samples collected along the Tyrrhenian coasts during the Summer 2007.<sup>a</sup>

n.d.= absent or present in lower quantities the limit of detection (LOD) of the used method.

<LOQ = present in lower quantities than the limit of quantitation (LOQ) of the used method.

Collection Points	Date	Site	Matrix	palytoxin µg/Kg	ovatoxin-a µg/Kg
Gaiola	26/07/2007	Gaiola	Mussels	15.68	94.59
Rocce Verdi	26/07/2007	Rocce Verdi	Mussels	14.19	132.55
Pirata	25/08/2007	Pirata	Mussels	n.d.	<LOQ
GON04	07/08/2007	Ischia	Sea-urchins	n.d.	<LOQ
GON09	07/08/2007	Misero-Faro	Mussels	n.d.	57.73
GON10	07/08/2007	Misero- Punta Pennata	Mussels	n.d.	<LOQ
GON11	03/08/2007	Nisida	Sea-urchins	n.d.	<LOQ
GON12	07/08/2007	Gaiola	Sea-urchins	<LOQ	37.86
GON18	13/08/2007	Sorrento	Sea-urchins	n.d.	<LOQ
GON19	13/08/2007	Capo Massa	Sea-urchins	n.d.	n.d.
GON20	13/08/2007	Capri-Marina Grande	Sea-urchins	n.d.	n.d.
GOS01	13/08/2007	Capri-Marina Piccola	Sea-urchins	n.d.	n.d.
GOS08	08/08/2007	p.zza Della Concordia	Mussels	n.d.	<LOQ

<sup>a</sup> The toxins amount, reported in the table, is corrected considering the 56% of recovery during the extraction procedure.

Every year, this plane of monitoring along the Campania coasts is generally carried out from July to October/November.

#### 6.2.4. 2008 LC-MS analyses

In Table 3 the results of LC-MS analyses, carried out during summer 2008, are shown for the sites in which the situation appeared the least risky for human health.

**Table 3.** Results of LC-MS analyses of samples of mussels and sea-urchins collected along the Campania coasts from June to November 2008.

n.d.= absent or present in lower quantities than the limit of detection (LOD) of the used method.

Collection Points	Date	Site	Matrix	palytoxin µg/kg	ovatoxin-a µg/kg
Point 10	18/07/2008	Ischia Lacco Ameno	Sea- urchins	n.d.	161
Point 10	29/07/2008	Ischia Lacco Ameno	Sea- urchins	n.d.	n.d.
Point 29	15/07/2008	Vietri sul Mare	Sea- urchins	n.d.	161
Point 29	31/07/2008	Vietri sul Mare (Hotel Fuenti)	Sea- urchins	n.d.	n.d.
Point 30	04/08/2008	Porto infreschi	Sea- urchins	n.d.	n.d.
Point 30	13/08/2008	Porto infreschi	Sea- urchins	n.d.	n.d.
Point 30	25/08/2008	Porto infreschi	Sea- urchins	n.d.	n.d.
Point 8	07/08/2008	Ischia Sant'Angelo	Sea- urchins	n.d.	n.d.
Point 8	21/08/2008	Ischia Sant'Angelo	Sea- urchins	n.d.	n.d.
Ischia Lacco Ameno	30/06/2008	Ischia Lacco Ameno	Sea- urchins	n.d.	n.d.
Point 22	31/07/2008	Praiano- Positano	Sea- urchins	n.d.	n.d.
Massa Lubrense	31/07/2008	Massa Lubrense	Mussels	n.d.	n.d.
Torre del Greco	21/08/2008	Torre del Greco	Mussels	n.d.	n.d.
Point 7	21/08/2008	Casamicciola	Sea- urchins	n.d.	n.d.
Vico Equense (Gradelle)	22/08/2008	Vico equense (Gradelle)	Mussels	n.d.	n.d.
Point 25	25/08/2008	Punta Licosa	Sea- urchins	n.d.	n.d.
Point 28	25/08/2008	Pioppi	Sea- urchins	n.d.	n.d.

In the samples collected in Ischia's sea, except a sample of sea-urchins collected at middle July 2008, which resulted positive for ovatoxin-a, LC-MS analyses didn't highlight the presence of palytoxin and ovatoxin-a.



For the samples of sea-urchins and/or mussels, collected along the South Cilento's coasts (Pioppi and Porto infreschi), the Sorrento's peninsula (Vico Equense and Massa Lubrense), and Amalfi's coast (Praiano, Vietri sul mare, and Punta Licosa) the LC-MS analyses resulted negative for both the toxins. In this case too, the negative results didn't mean that palytoxin and ovatoxin-a were absent; they could have been present, but in lower quantities than the limit of detection of the used LC-MS method (LOD=18 ng/mL, 18 ng/0.5g edible tissue).

Table 4 shows the LC-MS results about the samples collected in the sites of the gulf of Naples, where the situation appeared so complex as to need more frequent samplings and analyses, in July and August 2008. The toxins amount shown in Table 4, are measured and corrected by considering the 56% recovery, during the extraction procedure.

**Table 4.** Results of LC-MS analyses of the samples of mussels collected in the gulf of Naples from June to November 2008 and resulted rich in toxins.

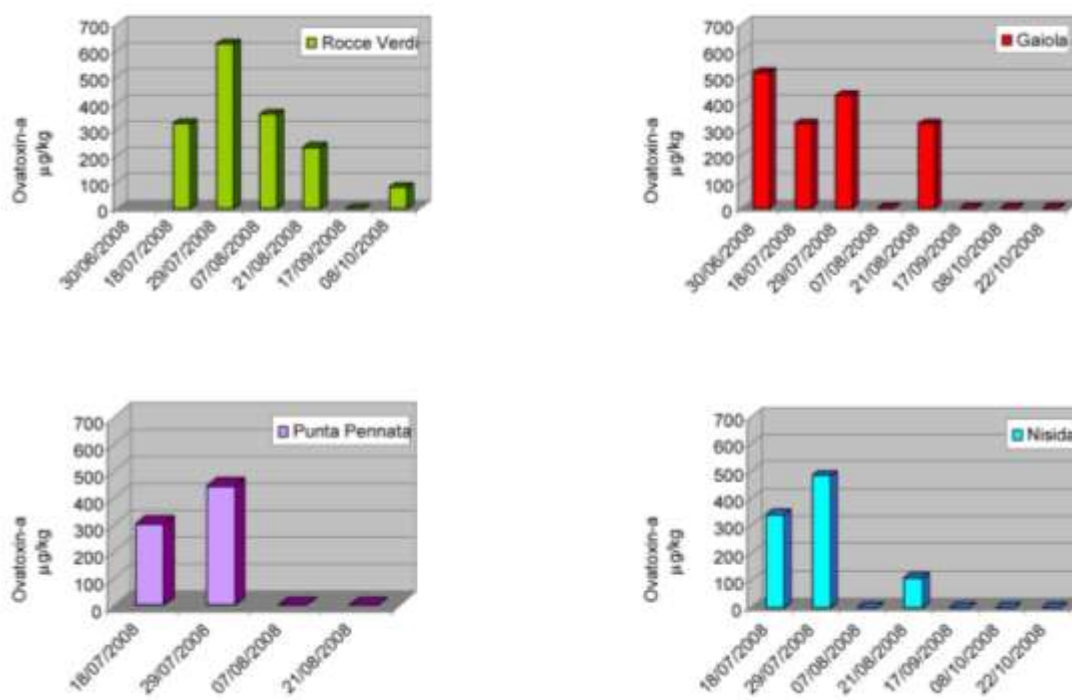
n.d.= absent or present in lower quantities than the limit of detection (LOD) of the used method.

traces= present in lower quantities than the limit of quantitation (LOQ) of the used method.

Collection Points	Date	Site	Matrix	Palytoxin µg/kg	Ovatoxin-a µg/kg
Gaiola	30/06/2008	Gaiola	Mussels	n.d.	518
Gaiola	18/07/2008	Gaiola	Mussels	n.d.	321
Gaiola	29/07/2008	Gaiola	Mussels	n.d.	428
Gaiola	07/08/2008	Gaiola	Mussels	n.d.	traces
Gaiola	21/08/2008	Gaiola	Mussels	n.d.	321
Gaiola	17/09/2008	Gaiola	Mussels	n.d.	traces
Gaiola	08/10/2008	Gaiola	Mussels	n.d.	traces
Gaiola	22/10/2008	Gaiola	Mussels	n.d.	traces
Rocce Verdi	30/06/2008	Rocce Verdi	Mussels	n.d.	n.d.
Rocce Verdi	18/07/2008	Rocce Verdi	Mussels	n.d.	321
Rocce Verdi	29/07/2008	Rocce Verdi	Mussels	n.d.	625
Rocce Verdi	07/08/2008	Rocce Verdi	Mussels	n.d.	357
Rocce Verdi	21/08/2008	Rocce Verdi	Mussels	n.d.	232
Rocce Verdi	17/09/2008	Rocce Verdi	Mussels	n.d.	traces
Rocce Verdi	08/10/2008	Rocce Verdi	Mussels	n.d.	82
Nisida	18/07/2008	Nisida	Mussels	n.d.	339
Nisida	29/07/2008	Nisida	Mussels	n.d.	482
Nisida	07/08/2008	Nisida	Mussels	n.d.	traces
Nisida	21/08/2008	Nisida	Mussels	n.d.	107
Nisida	17/09/2008	Nisida	Mussels	n.d.	traces
Nisida	08/10/2008	Nisida	Mussels	n.d.	traces
Nisida	22/10/2008	Nisida	Mussels	n.d.	traces
Punta Pennata	18/07/2008	Punta Pennata	Mussels	n.d.	303
Punta Pennata	29/07/2008	Punta Pennata	Mussels	n.d.	446
Punta Pennata	07/08/2008	Punta Pennata	Mussels	n.d.	traces
Punta Pennata	21/08/2008	Punta Pennata	Mussels	n.d.	traces

For the sites Gaiola, Rocce Verdi, Nisida, and Punta Pennata, sometimes the presence of ovatoxin-a was recorded at concerning concentration levels.

In Figure 5 the toxic profile of ovatoxin-a concentrations versus the collection dates is displayed for the sites in which the highest toxins levels were recorded (Rocce Verdi, Gaiola, Punta Pennata, and Nisida).



**Figure 5.** Values of the toxins concentration for the dates of collection, for 4 of the sites included in the 2008 program of monitoring.

In particular, in the samples collected at Gaiola in June 30<sup>th</sup>, and at Punta Pennata, Rocce Verdi, Nisida and Gaiola, in July 18<sup>th</sup>, and 29<sup>th</sup>, the recorded ovatoxin-a's concentrations appeared very significant and induced to hypothesize risks for human health. In fact, the concentrations of ovatoxin-a were upper than the limit of tolerance for palytoxins (100-200 µg/Kg of seafood), emerged from a first evaluation carried out during the 1st Meeting of Working Group on Palytoxins organized by the Community Reference Laboratory for Marine Biotoxins.

#### 6.2.5. 2009 LC-MS analyses: results

In Table 5 the LC-MS results about the samples of mussels and sea-urchins, collected along the Campania coasts from June to November 2009 are reported.

**Table 5.** Results of the LC-MS analyses in samples of mussels and sea-urchins collected along the Campania coasts from June to November 2009.

n.d.= absent or present in lower quantities the limit of detection (LOD) of the used method (11 µg/Kg).

traces= present in lower quantities than the limit of quantitation (LOQ) of the used method (37 µg/Kg).

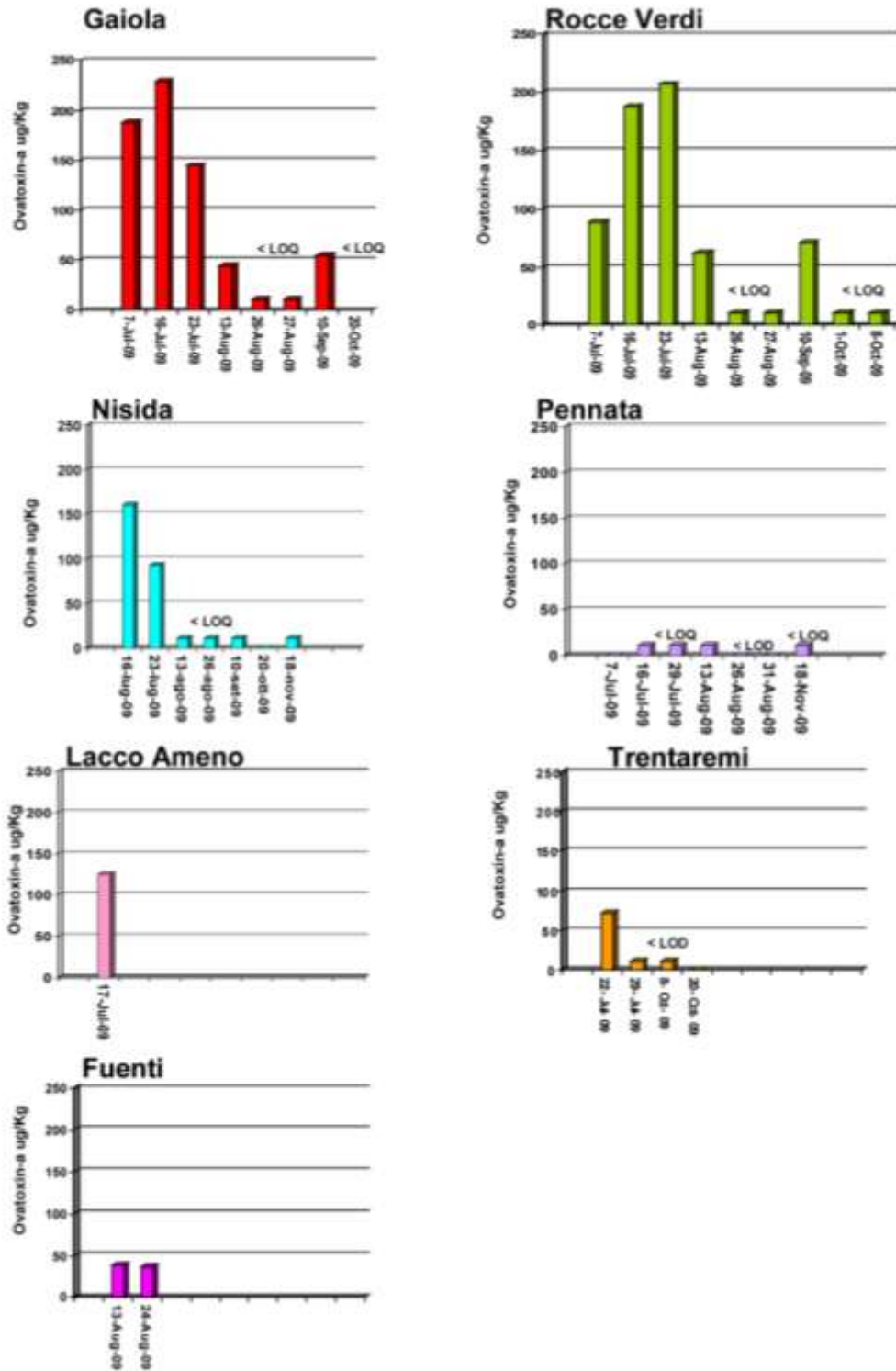
Collection Points	Date	Matrix	LC/MS results		LC/MS result corrected of the 56% recovery	
			PLTX ug/kg	OVTX-a ug/kg	PLTX ug/kg	OVTX-a ug/kg
Gaiola	7/07/2009	Mussels	nd	105.34	nd	188.11
Gaiola	16/07/2009	Mussels	traces	128	traces	228.57
Gaiola	23/07/2009	Mussels	nd	81	traces	144.64
Gaiola	13/08/2009	Mussels	nd	25	nd	44.64
Gaiola	26/08/2009	Mussels	nd	traces	nd	traces
Gaiola IZSM	27/08/2009	Mussels	nd	traces	nd	traces
Gaiola	10/09/2009	Mussels	traces	31	tracce	55
Gaiola	20/10/2009	Mussels	nd	traces	nd	traces
Rocce Verdi	7/07/2009	Mussels	nd	49.41	nd	88.23
Rocce Verdi	16/07/2009	Mussels	traces	105	tracce	187.50
Rocce Verdi	23/07/2009	Mussels	traces	116	tracce	207.14
Rocce Verdi	13/08/2009	Mussels	nd	35	nd	62.50
Rocce Verdi	26/08/2009	Mussels	nd	traces	nd	traces
Rocce Verdi	10/09/2009	Mussels	traces	40	tracce	71
Rocce Verdi	1/10/2009	Mussels	traces	traces	tracce	traces
Rocce Verdi	8/10/2009	Mussels	nd	traces	nd	traces
Rocce Verdi	18/11/2009	Mussels	nd	traces	nd	traces
Nisida	16/07/2009	Mussels	nd	90	nd	160.71
Nisida	23/07/2009	Mussels	nd	52	tracce	92.86
Nisida	13/08/2009	Mussels	nd	traces	nd	traces

Nisida	26/08/2009	Mussels	nd	traces	nd	traces
Nisida	10/09/2009	Mussels	traces	traces	tracce	traces
Nisida	20/10/2009	Mussels	nd	nd	nd	nd
Nisida	18/11/2009	Mussels	nd	traces	nd	traces
Pennata	7/07/2009	Mussels	nd	nd	nd	nd
Pennata	16/07/2009	Mussels	nd	traces	nd	traces
Pennata	29/07/2009	Mussels	nd	traces	nd	traces
Punta Pennata ARPAC	13/08/2009	Mussels	nd	traces	nd	traces
Punta Pennata	26/08/2009	Mussels	nd	nd	nd	nd
Punta Pennata IZSM	31/08/2009	Mussels	nd	nd	nd	nd
Pennata	18/11/2009	Mussels	nd	traces	nd	traces
Sorrento	16/07/2009	Sea-urchins	nd	32	nd	57.14
Sorrento	1/09/2009	Sea-urchins	nd	traces	nd	traces
Sorrento	9/09/2009	Sea-urchins	nd	traces	nd	traces
Trentaremi	22/07/2009	Mussels	nd	40	nd	71.43
Trentaremi	29/07/2009	Mussels	nd	traces	nd	traces
Trentaremi	8/10/2009	Mussels	nd	traces	nd	traces
Trentaremi	20/10/2009	Mussels	nd	nd	nd	nd
Praiano	13/07/2009	Sea-urchins	nd	nd	nd	nd
Praiano	4/08/2009	Mussels	nd	nd	nd	nd
Praiano	18/08/2009	Sea-urchins	nd	nd	nd	traces
Porto Infreschi	22/07/2009	Sea-urchins	nd	nd	nd	nd
Porto Infreschi	11/08/2009	Sea-urhins	nd	traces	nd	traces
Porto Infreschi	28/09/2009	Sea-urchins	nd	nd	nd	nd
Resto	16/07/2009	Sea-urchins	nd	nd	nd	nd
Lacco Ameno	17/07/2009	Sea-urchins	traces	70	tracce	125.00

Castel dell'Ovo	8/10/2009	Mussels	nd	traces	nd	traces
Castel dell'Ovo	20/10/2009	Mussels	nd	traces	nd	traces
Fuenti	13/08/2009	Mussels	nd	21.49	nd	38.38
Fuenti IZSM	24/08/2009	Mussels	nd	21	nd	37.50
Ischia OS7	30/07/2009	Sea-urchins	nd	traces	nd	traces
Lungomare Fiume Irno IZSM	24/08/2009	Mussels	nd	44	nd	78.57
Lungomare Salerno IZSM	24/08/2009	Mussels	nd	traces	nd	traces
Ischia OS-10	25/08/2009	Sea-urchins	nd	nd	nd	nd
Ischia OS-7	25/08/2009	Sea-urchins	nd	nd	nd	nd
Casamicciola	8/10/2009	Sea-urchins	nd	traces	nd	traces
S. Pietro	20/10/2009	Sea-urchins	nd	nd	nd	nd

In all the samples palytoxin resulted absent or present in lower quantities than the limit of detection of the used method. In the samples collected in July and August, ovatoxin-a resulted at times present in higher quantities than the limits of tolerance established for palytoxins (100-200  $\mu\text{g}/\text{Kg}$  of food). In the samples collected in September, October and November, instead, ovatoxin-a resulted present in traces or at lower levels than the alert threshold.

The shellfish samples, collected at Gaiola and Rocce Verdi contained the highest amounts of ovatoxin-a with maximum levels, which were higher than 200  $\mu\text{g}/\text{Kg}$  in the middle July 2009 samplings. In the same period, shellfishes collected at Nisida contained 160  $\mu\text{g}/\text{Kg}$  of ovatoxin-a, while at Lacco Ameno the only sampling carried out contained 125  $\mu\text{g}/\text{Kg}$ . Lower quantities (about 70  $\mu\text{g}/\text{Kg}$ ) were detected at Sorrento and Trentaremi, while at Punta Pennata, for all the samplings, the detected toxins levels were lower than the limit of detection (LOD =11  $\mu\text{g}/\text{Kg}$ ) or quantification (LOQ=37  $\mu\text{g}/\text{kg}$ ) of the used LC-MS method. In figure 6 the trend of the toxic profile of the shellfishes, in connection with the dates of sampling, is reported.



**Figure 6.** Values of the toxins concentrations for the dates of collection, for some of the sites included in the program of monitoring.

### 6.2.6. 2010 LC-MS analyses

From 2010 on, LC-MS analyses have been carried out by LTQ Orbitrap XL and in the extracted samples the presence of both palytoxin and ovatoxins (-a, -b, -c, -d and -e) was detected; so the analyses results were expressed as total amount of palytoxins.

Also, EFSA (European Food Safety Authority) established, for palytoxins, the alert threshold at 30 µg/kg of tissue.

In table 6 the results of LC-MS analyses about the sites, in which the situation appeared the least risky for human health, are showed.

**Table 6.** Results of LC-MS analyses of mussels and sea-urchins samples collected along the Campania coasts from June to November 2010.

n.d.= absent or present in lower quantities than the limit of detection (LOD) of the used method.

Date	Site	Matrix	LC/MS Results	LC/MS Results corrected of the 56% recovery
			Total palytoxins ug/kg	Total palytoxins ug/kg
05/07/2010	Punta Gradelle	Mussels	71	126
05/07/2010	Sorrento	Sea-urchins	9	16
08/07/2010	Gaiola	Mussels	traces	traces
08/07/2010	Nisida	Mussels	traces	traces
08/07/2010	Lacco Ameno	Sea-urchins	traces	traces
19/07/2010	S. Pietro	Sea-urchins	nd	nd
15/07/2010	Sorrento	Fish gastric content	13,5	24
22/07/2010	Punta Gradelle	Mussels	34,22	61
20/07/2010	Punta Pennata	Mussels	traces	traces
20/07/2010	Rocce Verdi	Mussels	traces	traces
22/07/2010	Sorrento	Sea-urchins	27,65	49
20/07/2010	Trentaremi	Mussels	107,28	192
20/07/2010	Gaiola	Mussels	12,07	22



20/07/2010	Nisida	Mussels	tracce	traces
23/07/2010	Porto Infreschi	Sea-urchins	54,82	98
29/07/2010	Sorrento	Sea-urchins	traces	traces
29/07/2010	Baia di Ieranto	Sea-urchins	traces	traces
29/07/2010	Capri Marina Grande	Sea-urchins	39,59	71
29/07/2010	Capri Marina Piccola	Sea-urchins	15,47	28
29/07/2010	Spiaggia Cimitero	Sea-urchins	traces	traces
29/07/2010	Castello Aragonese	Sea-urchins	traces	traces
02/08/2010	Trentaremi	Mussels	85,6	153
03/08/2010	Porto Infreschi	Sea-urchins	121,03	216
03/08/2010	Lacco Ameno	Sea-urchins	15,71	28
03/08/2010	S. Pietro	Sea-urchins	15,48	28
12/08/2010	Trentaremi	Mussels	16	28
12/08/2010	Gaiola	Mussels	33	58
12/08/2010	Rocce Verdi	Mussels	75	133
12/08/2010	Punta Pennata	Mussels	traces	traces
12/08/2010	Nisida	Mussels	nd	nd
16/08/2010	Praiano	Mussels	traces	traces
16/08/2010	Baia di Ieranto	Sea-urchins	nd	nd
16/08/2010	Capri Marina Grande	Sea-urchins	29	52
18/08/2010	Porto Infreschi	Sea-urchins	21	37
02/09/2010	Trentaremi	Mussels	12	21
02/09/2010	Gaiola	Mussels	nd	nd
01/09/2010	Rocce Verdi	Sea-urchins	traces	traces
02/09/2010	Bagni Elena	Mussels	10	17
05/09/2010	Erchie	Mussels	46	82
05/09/2010	Fuenti	Mussels	39	69

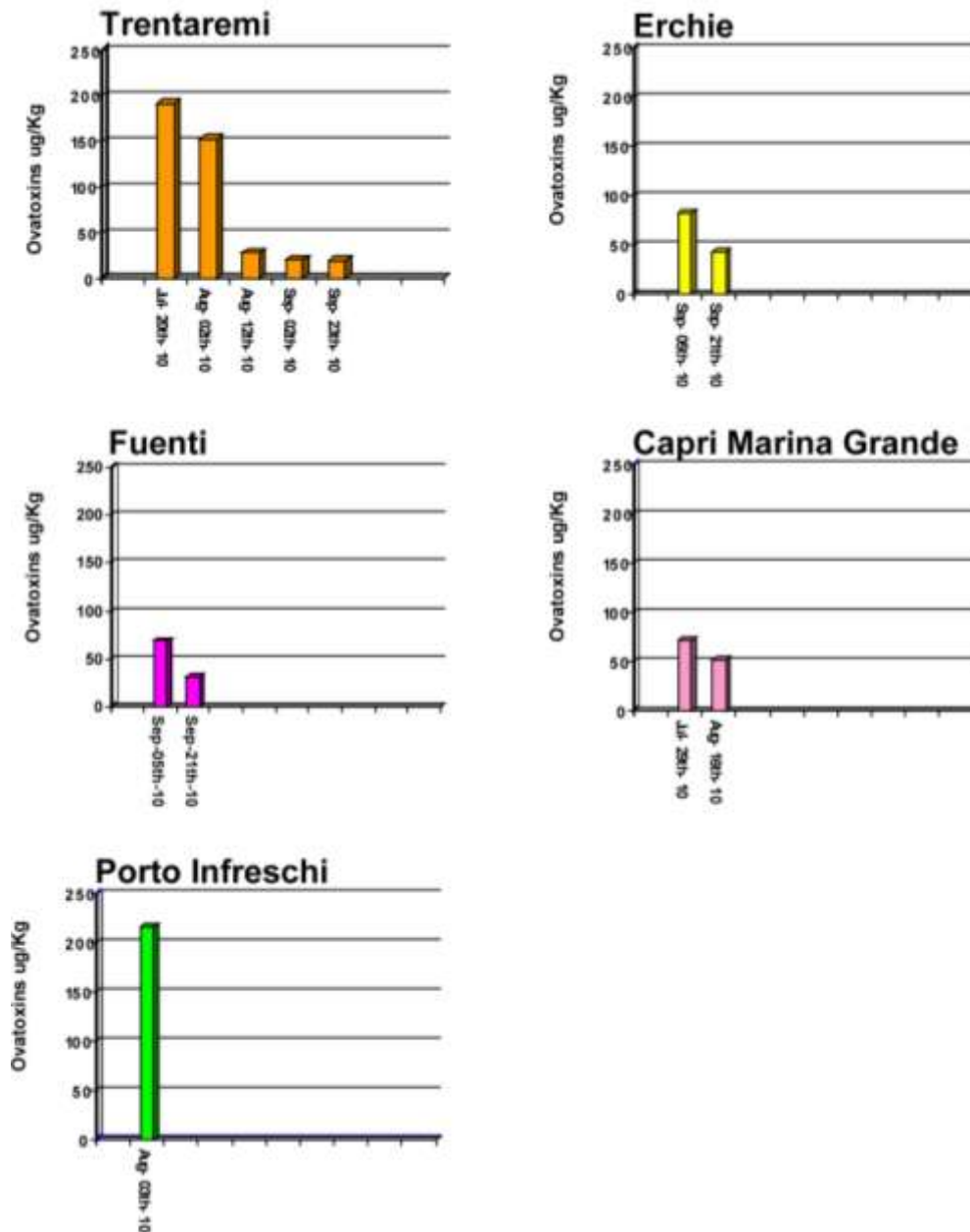
15/09/2010	Praiano ARPAC	Mussels	nd	nd
21/09/2010	Baia Hotel Salerno IZSM	Mussels	nd	nd
21/09/2010	Casamicciola ARPAC	Sea-urchins	nd	nd
21/09/2010	Erchie IZSM	Fish intestine	nd	nd
21/09/2010	Erchie IZSM	Mussels	24	42
21/09/2010	Fuenti IZSM	Mussels	17	31
21/09/2010	Fuenti IZSM	Fish intestine	nd	nd
23/09/2010	Porto Infreschi ARPAC	Sea-urchins	nd	nd
23/09/2010	Trentaremi ARPAC	Mussels	11	20
23/09/2010	Bagni Elena	Mussels	6,4	11
23/09/2010	Gaiola	Mussels	traces	traces
23/09/2010	Nisida	Mussels	nd	nd
21/09/2010	Rocce Verdi	Mussels	7	13

In the samples collected at Punta Gradelle (Vico Equense), except 2 samples of mussels collected in July 5<sup>th</sup>, and 22<sup>th</sup>, 2010, which resulted positive for palytoxins (126 and 61 µg/Kg respectively), LC-MS analyses didn't highlight the presence of these toxins in this site.

Samples of mussels, collected at Rocce Verdi and Gaiola, showed the toxins presence, as recorded the last years but the peak of the toxicity was recorded in August and not in July, as happened in the last years; also, in this same area (Posillipo) the samples collected at Trentaremi showed a high content of palytoxins.

Very interesting results came from samples collected at Erchie and Fuenti (Vietri sul mare), because the toxins presence in these sites had never been recorded before; the same happened for samples coming from Porto Infreschi (Marina di Camerota) (216 µg/Kg).

In Figure 7 the toxic profile of the mussels samples for the dates of sampling is displayed for some of the sites of the 2010 program of monitoring.



**Figure 7.** Values of the toxins concentrations versus the dates of sampling, for some of the sites included in the 2010 program of monitoring, in which a high toxins level was recorded.

### 6.3. References

1. G. Sansoni, B. Borghini, G. Camici, M. Casotti, P. Righini, C. Fustighi. Fioriture algali di *Ostreopsis ovata* (Gonyaulacales: Dinophyceae): un problema emergente. *Biologia Ambientale*, 17, 17-23, 2003.
2. I. Di Girolamo; E. Fattorusso; E. Funari; L. Gramaccioni; C. Grillo; G. Icardi; D. Mattei; R. Poletti; S. Scardala; E. Testai. Linee guida- Gestione del Rischio associato alle Fioriture di

*Ostreopsis ovata* nelle coste italiane. Enacted by Consiglio Superiore di Sanità-Ministero della Salute-May 24th 2007.

3. P. Ciminiello; C. Dell'Aversano; E. Fattorusso; M. Forino; G. S.Magno; L.Tartaglione; C. Grillo; N. Melchiorre. The Genoa 2005 outbreak. Determination of putative palytoxin in Mediterranean *Ostreopsis ovata* by a new liquid chromatography tandem mass spectrometry method. *Anal. Chem.* 78, 6153-6159, 2006.
4. P. Ciminiello, C. Dell'Aversano, E. Fattorusso, M. Forino, L. Tartaglione, C. Grillo, N. Melchiorre. Putative palytoxin and its new analogue, ovatoxin-a, in *Ostreopsis ovata* collected along the Ligurian coasts during the 2006 toxic outbreak . *J. Amer. Soc. Mass Spec.* 19, 111-120, 2008.



## Chapter 7

### Toxin profile of cultured *Ostreopsis ovata* from the Tyrrhenian and Adriatic seas

Very recently, blooms of *O. ovata* have been reported from a number of Mediterranean sea sites located along Italian, Greek<sup>1</sup>, Spanish<sup>2</sup> and French<sup>3</sup> coastlines. To the best of our knowledge, only the toxin profile of the Ligurian *O. ovata* strain has been accurately investigated, whereas no data have been reported either on growth or toxin profile of *O. ovata* strains from other sites.

We carried out a work to the aim of characterising growth and toxin profile of two *O. ovata* strains collected along the Adriatic and the Tyrrhenian coasts of Italy in 2006 and grown in culture. Molecular analyses were performed to confirm the identification of the two strains and the morphometric characters of *O. ovata* cells were compared within different growth periods (exponential and stationary phase). LC-MS analyses were carried out to identify toxins produced by both Adriatic and Tyrrhenian *O. ovata* strains. Toxin production at the end of the stationary and exponential growth phases was quantitatively determined and toxin released in the growth medium was measured.

### 7.1. Experimental

#### 7.1.1. Cultures of *Ostreopsis ovata*

Two strains of *O. ovata*<sup>4</sup> were isolated by the capillary pipette method<sup>5</sup> from water samples collected either along the Tyrrhenian (Lazio region, Porto Romano sampling site, strain OOTL0602) or the Adriatic (Marche region, Numana sampling site, strain OOAN0601) coasts of Italy, in August and October 2006, respectively. The samples were collected in proximity of the seaweeds *Cystoseira* sp. and *Alsidium corallinum*. After an initial growth in microplates, the cells were cultured at 20°C under a 16:8 h L:D cycle (ca. 90  $\mu\text{mol m}^{-2} \text{s}^{-1}$  from cool white lamp); cultures were established in natural seawater, at salinity of 35, adding nutrients at a five-fold diluted f/2 concentration,<sup>6</sup> with addition of selenium.

Evaluation of growth profile of the two *O. ovata* strains in batch cultures was complicated by the presence of mucous aggregates which included cells and prevented a correct sampling. In order to overcome this problem, we set up the following counting method: 20 Erlenmeyer flasks, each containing 200 mL culture, were grown in parallel at the same conditions of temperature, light and nutrients. The flasks within the incubator were repeatedly randomized

during the experiment. Every other day, two out of the initial 20 flasks were treated with HCl to a final concentration of 4 mM. Acid addition proved to dissolve mucous aggregates without disrupting *O. ovata* cells or altering their shape and, thus, a homogenous sampling could be performed, as demonstrated by repeatable counting within the same flask. After counting, the two acidified flasks were discarded. Cell counts were made following the Utermöhl method and specific growth rate ( $\mu$ ,  $\text{day}^{-1}$ ) was calculated using the following equation:

where  $N_0$  and  $N_1$  are cell density values at time  $t_0$  and  $t_1$ .

Calculation of cell volume was made with the assumption of ellipsoid shape using the following equation (Sun and Liu, 2003):

$$V = (\pi/6) * a * b * c$$

where  $a$  = dorsoventral diameter (length),  $b$  = width,  $c$  = anteriorposterior diameter (height).

Algal toxin profile was determined by using a set of flasks which were partly collected after 10 days of growth (late exponential phase) and partly after 27 days (late stationary phase). Cell number estimation was obtained using culture flasks run in parallel and acidified as described above.

### **7.1.2. DNA extraction, polymerase chain reaction amplifications and sequencing**

Aliquots (90 mL) of *O. ovata* cultures, collected during the exponential growth phase, were centrifuged at  $6000 \times g$  for 10 min; the pellet was re-suspended in 420  $\mu\text{L}$  of Nuclease-Free water; the DNA was extracted with phenol-chloroform using the protocol described by Godhe et al. (2001). The quality and amount of genomic DNA was controlled on an agarose TBE gel and 10 fold-diluted to perform PCR reaction.

The terminal primers D1R<sup>7</sup> and 28-1483R<sup>8</sup> were used to amplify ca. 1400 bp of the nuclear-encoded LSU rDNA gene which included domains D1, D2, D3 and conserved core region,<sup>9,10</sup> applying PCR conditions reported by Daugbjerg et al.<sup>8</sup> and Hansen et al.<sup>11</sup>

The PCR products were purified using the ExoSAP-IT kit (usb) and nucleotide sequences were determined using the BigDye Terminator v1.1 cycle sequencing kit (Applied Biosystems); sequencing reactions were run in an ABI PRISM 310 Genetic Analyzer. The partial-length sequence of *O. ovata* LSU was obtained using both the PCR and two internal primers: D2C and D3B.<sup>12</sup>

### **7.1.3. Sequence alignment and phylogenetic analyses**

The partial LSU sequences of *O. ovata* were analysed with ProSeq v2.91.<sup>13</sup> In order to compare the Adriatic strains with strains from different locations, our sequences were aligned with those retrieved from the GenBank.

A multiple alignment of the D1-D2 sequences of *O. ovata* and other species of Dinophyta, retrieved from GenBank, was obtained using the ClustalX 1.83<sup>14</sup> program. In molecular systematics and phylogenetic analyses we applied the Kimura2-parameter model and the NJ method of reconstruction implemented in Mega 3.1 program.<sup>15</sup>

### **7.1.4. Chemicals**

All organic solvents were of distilled-in-glass grade (Carlo Erba, Milan, Italy). Water was distilled and passed through a MilliQ water purification system (Millipore Ltd., Bedford, MA, USA). Acetic acid (Laboratory grade) was purchased from Carlo Erba. Analytical standard of palytoxin was purchased from Wako Chemicals GmbH (Neuss, Germany). A reference sample of ovatoxin-a was obtained from a natural population of *O. ovata* collected along Genoa coasts in July 2006.<sup>16</sup>

### **7.1.5. Extraction**

Adriatic and Tyrrhenian *O. ovata* cells were collected by gravity filtration through GF/F Whatman (0.7 µm) filters at the end of the exponential (9,531,270 and 6,367,410 cells in the Adriatic and the Tyrrhenian sample, respectively) and the stationary (7,916,265 and 7,322,805 cells in the Adriatic and the Tyrrhenian sample, respectively) growth phases. Cell pellets and growth media for each strain were separately extracted. Each pellet was added of 30 mL of a methanol/water (1:1, v/v) solution and sonicated for 30 min in pulse mode, while cooling in ice bath. The mixture was centrifuged at 3000 g for 30 min, the supernatant was decanted and the pellet was washed twice with 30 mL of methanol/water (1:1, v/v). The extracts were combined and the volume was adjusted to 90 mL with extracting solvent. The obtained mixture was analyzed directly by LC-MS (5 µL injected). Growth media (945 mL each) were separately extracted with an equal volume of butanol for three times. The butanol layer was evaporated to dryness, dissolved in 5 mL of methanol/water (1:1, v/v) and analyzed directly by LC-MS (5 µL injected).



### 7.1.6. Liquid chromatography-mass spectrometry (LC-MS)

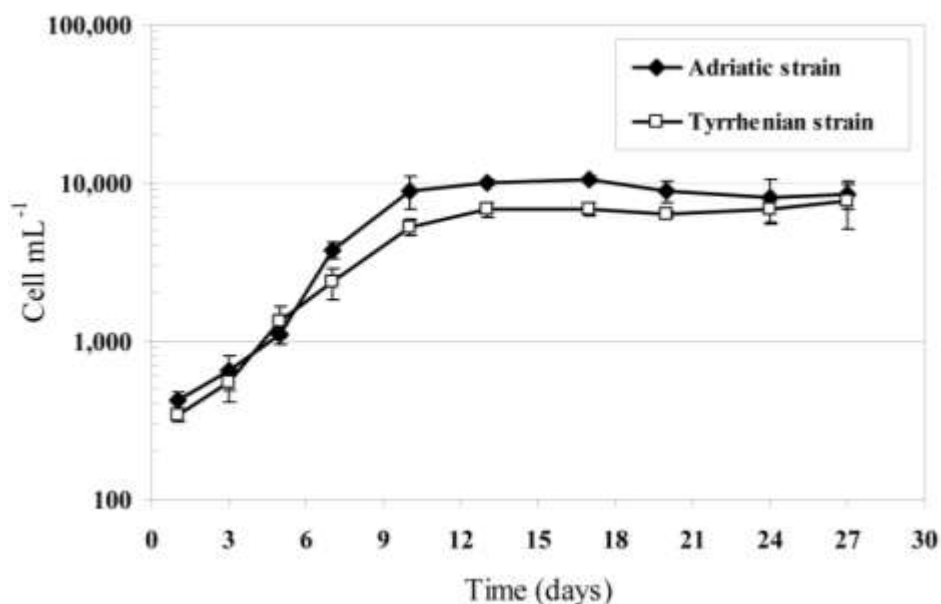
LC-MS experiments were performed on an API-2000 triple-quadrupole MS instrument (Applied Biosystems part of Life Technologies, Foster City, CA, USA) equipped with a Turbospray<sup>®</sup> (TSI) source coupled to an Agilent (Palo Alto, CA, USA) model 1100 LC, which included a solvent reservoir, in-line degasser, binary pump, and refrigerated autosampler. A 3  $\mu\text{m}$  gemini C18 (150  $\times$  2.00 mm) column (Phenomenex, Torrance, CA, USA) maintained at room temperature, was used in all experiments; it was eluted at 0.2 mL  $\text{min}^{-1}$  with water (eluent A) and 95% acetonitrile/water (eluent B), both containing 30 mM acetic acid. The following gradient elution was required: 20-100% B over 10 min and hold 4 min. MS detection was carried out in multiple reaction monitoring (MRM) mode (positive ions) by monitoring the transitions  $m/z$  1340.7  $\rightarrow$  327.1, 1331.7  $\rightarrow$  327.1 for palytoxin and the transitions  $m/z$  1324.7  $\rightarrow$  327.1, 1315.7  $\rightarrow$  327.1, for ovatoxin-a. The following source parameters were used: turbogas temperature = 0°C, ionspray voltage = 5500 V, declustering potential = 1 V, focusing potential = 390 V, entrance potential = 11 V (for  $m/z$  1331.7  $\rightarrow$  327.1 and 1315.7  $\rightarrow$  327.1) and 5 V (for  $m/z$  1340.7  $\rightarrow$  327.1 and 1324.7  $\rightarrow$  327.1), collision energy = 50 eV, cell exit potential = 10 V. The dwell time was set to achieve a total scan time of 1 sec. Palytoxin standards at four levels of concentration (2.0, 1.0, 0.5, and 0.25  $\mu\text{g mL}^{-1}$ ) were used to generate a calibration curve that was employed in quantitative analyses. Sum of MRM peak areas was used to express peak intensity. The average of duplicate measurements was used for plotting.

## 7.2. Results and Discussion

### 7.2.1. Growth rate and cell volume

The growth pattern of both Adriatic and Tyrrhenian *O. ovata* strains was investigated for 28 days, by measuring cell density every 2-3 days. Formation of cell aggregates, mainly occurring in the stationary growth phase, hampered accurate and reliable representative sampling of cultures. Thus, a new procedure was set up (see Experimental) consisting in the addition of hydrochloric acid to the two culture flasks selected every other day for counting; this allowed to dissolve mucous aggregates without disrupting *O. ovata* cells or altering their shape and to obtain a homogeneous sampling.

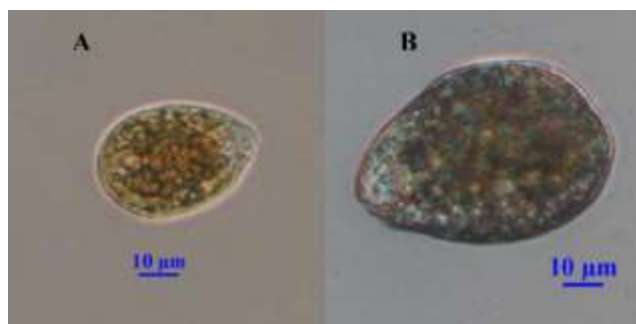
During the exponential phase both Adriatic and Tyrrhenian *O. ovata* strains showed low growth rates, namely 0.37 and 0.32  $\text{day}^{-1}$  for the Adriatic and the Tyrrhenian cultures, respectively (Figure 1).



**Figure 1.** Growth pattern of the two *Ostreopsis ovata* cultures.

In the stationary phase the Adriatic strain reached the maximum density of about 10,000 cells mL<sup>-1</sup>, which was higher than that observed for the Tyrrhenian strain (maximum concentration about 8,000 cells mL<sup>-1</sup>).

The two strains appeared highly different both in size and in shape (Figure 2).



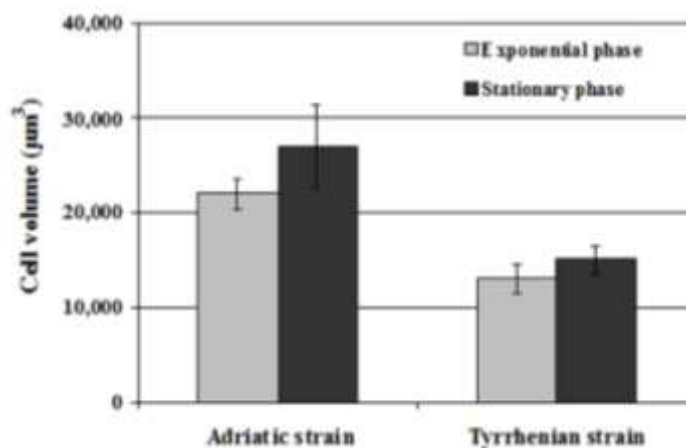
**Figure 2.** A light micrograph of *Ostreopsis ovata* cells stained with Lugol from a culture sample: (A) Tyrrhenian strain (B) Adriatic strain.

The two main dimensions appeared highly variable and mean values were higher for the Adriatic strain than for the Tyrrhenian one (Table 1).

**Table 1.** Morphometric characteristics of the two *Ostreopsis ovata* strains: minimum, maximum, mean values ( $\mu\text{m}$ ) and standard deviation of dorsoventral diameter (DV), anteriorposterior diameter (AP) and width (W).

morphometrical variability		width (W)	Dorsoventral diameter (DV)	Anteriorposterior diameter (AP)
		( $\mu\text{m}$ )		
<b>Adriatic</b> <i>O. ovata</i>	Mean	<b>37.3</b>	<b>57.2</b>	<b>24.5</b>
	St.dv.	5.4	7.5	2.3
	Max	50.7	75.4	39.3
	Min	18.3	28.6	15.3
<b>Tyrrhenian</b> <i>O. ovata</i>	Mean	<b>28.2</b>	<b>40.2</b>	<b>22.8</b>
	St.dv.	5.7	7.3	3.8
	Max	43.3	58.8	34.3
	Min	14.9	22.9	14.0

Cell volumes were calculated by measuring the cross section (anteriorposterior diameter, AP) in a statistically significant cell numbers ( $n \geq 50$ ). The mean biovolumes of the two strains were significantly different ( $p < 0.0001$ ), the Adriatic strain being nearly two-fold larger than the Tyrrhenian strain (Figure 3).

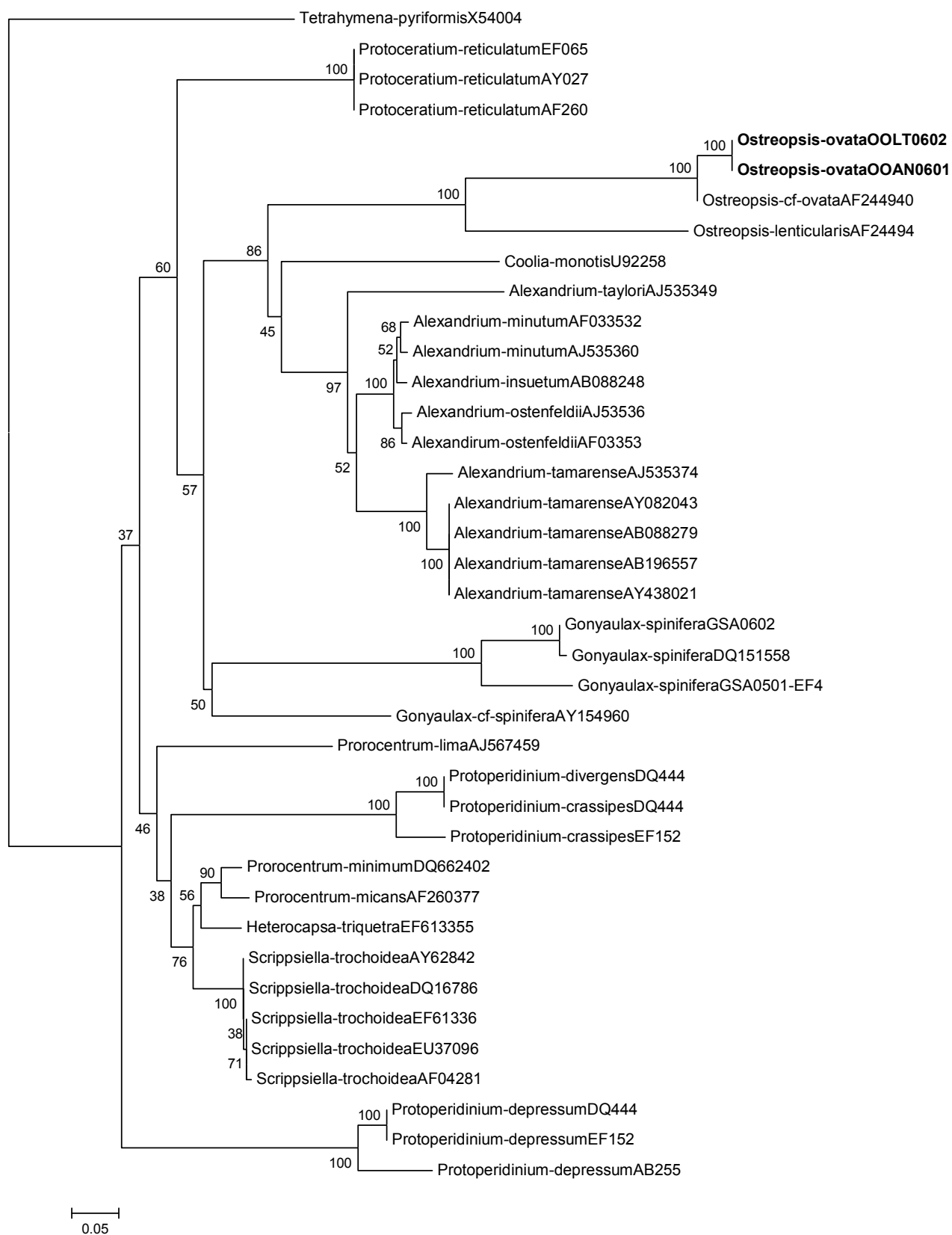


**Figure 3.** Cell volumes of the two strains of *Ostreopsis ovata*, in the exponential and stationary phases.

The cell volume did not significantly change during the progression from the exponential to the stationary growth phase, although the Tyrrhenian *O. ovata* cells progressively changed from an ellipsoid to a spherical shape. Measurements performed monthly for both strains highlighted a progressive decrease in cell volume (data not shown).

Despite the morphometric differences, the two strains appeared rather genetically uniform. The partial LSU rDNA gene was sequenced and resulted 1362 bp long for both isolates. Sequences are available in public database GenBank (submitted). The two Italian strains were homologues and differed also from each other by 25 variable nucleotide positions with a sequence divergence of 3.1%, calculated as number of variable nucleotides. Both differed from the corresponding sequence of a Malaysian strain (AF244940) of *O. cf ovata* available on GenBank.

In order to elucidate *O. ovata* phylogeny, a data matrix with the LSU sequences from various dinoflagellate species (mostly gonyaulacoid) was compiled. The phylogenetic tree based on D1 and D2 domains of the LSU rDNA (Figure 4) confirmed the similarity between the two Italian strains and the position of *O. ovata* strains into the *Ostreopsis* genus, which clustered with the other gonyaulacoid species considered.

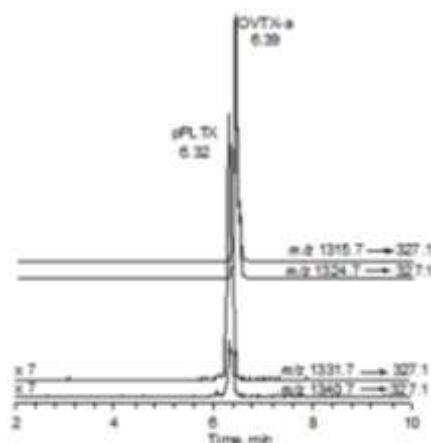


**Figure 4.** Phylogeny of *Ostreopsis ovata* and related Gonyaucales inferred from sequencing the D1 and D2 domains of 28S rDNA, obtained from a Kimura-2-parameter model using Neighbour Joining reconstruction; the bootstrap support has been calculated for 1000 replicates. Strains sequenced in this work are in bold.

### 7.2.2. Determination of toxin content by LC-MS

Pellets and growth media of the Adriatic and Tyrrhenian *O. ovata* strains were collected both at the end of the exponential and the stationary growth phases. They were separately extracted as reported in the experimental and the crude extracts were used for evaluation of toxin profile. It has to be noted that, since we were dealing with different matrices, two different extraction methods were used: cell pellets were suspended in methanol/water (1:1, v/v) and sonicated, whereas growth media were partitioned thrice with butanol. Chemical analyses were carried out on the aqueous methanol extracts of the pellets and on the butanol extracts of the growth media by the recently developed LC-MS method for determination of palytoxin-like compounds,<sup>16,17</sup> using an ESI-triple quadrupole MS instrument. On the basis of previous studies on Ligurian *O. ovata*, the presence of putative-palytoxin (pPLTX) and ovatoxin-a (OVTX-a) was investigated in all the extracts. Chromatographic separation was accomplished on a reversed phase column by using a mobile phase containing water/acetonitrile, 30 mM acetic acid and a gradient system which allowed the elution of PLTX and OVTX-a at 6.32 and 6.39 min, respectively. Multiple reaction monitoring (MRM) experiments were carried out by selecting two transitions (precursor ion  $\rightarrow$  product ion) for each toxin, namely  $[M+2H]^{2+} \rightarrow [A \text{ moiety}+H-H_2O]^+$  ( $m/z$  1340.7  $\rightarrow$  327.1 for PLTX and  $m/z$  1324.7  $\rightarrow$  327.1 for OVTX-a) and  $[M+2H-H_2O]^{2+} \rightarrow [A \text{ moiety}+H-H_2O]^+$  ( $m/z$  1331.7  $\rightarrow$  327.1 for PLTX and  $m/z$  1315.7  $\rightarrow$  327.1 for OVTX-a). The product ion at  $m/z$  327.1 arises from cleavage between the carbons 8 and 9 of PLTX (Uemura et al, 1985) and the additional loss of a water molecule; this ion dominates the product ion spectra of both palytoxin and ovatoxin-a whatever is the precursor ion used, either the  $[M+2H]^{2+}$  or the  $[M+2H-H_2O]^{2+}$  ion.

The presence of pPLTX and OVTX-a was demonstrated in all the analyzed samples by peaks eluting at the same retention times as PLTX (6.32 min) and OVTX-a (6.39 min), respectively. By way of example, the MRM traces of the Adriatic pellet extract (stationary phase) is reported in Figure 5.



**Figure 5.** LC-MS analysis in positive MRM mode of the Adriatic pellet extract (stationary phase). The MRM transitions  $[M+2H]^{2+} \rightarrow [A \text{ moiety}+H-H_2O]^+$  ( $m/z$  1340.7  $\rightarrow$  327.1 for palytoxin and  $m/z$  1324.7  $\rightarrow$  327.1 for ovatoxin-a) and  $[M+2H-H_2O]^{2+} \rightarrow [A \text{ moiety}+H-H_2O]^+$  ( $m/z$  1331.7  $\rightarrow$  327.1 for palytoxin and  $m/z$  1315.7  $\rightarrow$  327.1 for ovatoxin-a) were monitored. LC conditions are reported in the experimental. Both putative palytoxin (pPLTX) and ovatoxin-a (OVTX-a) were detected at 6.32 and 6.39 min, respectively.

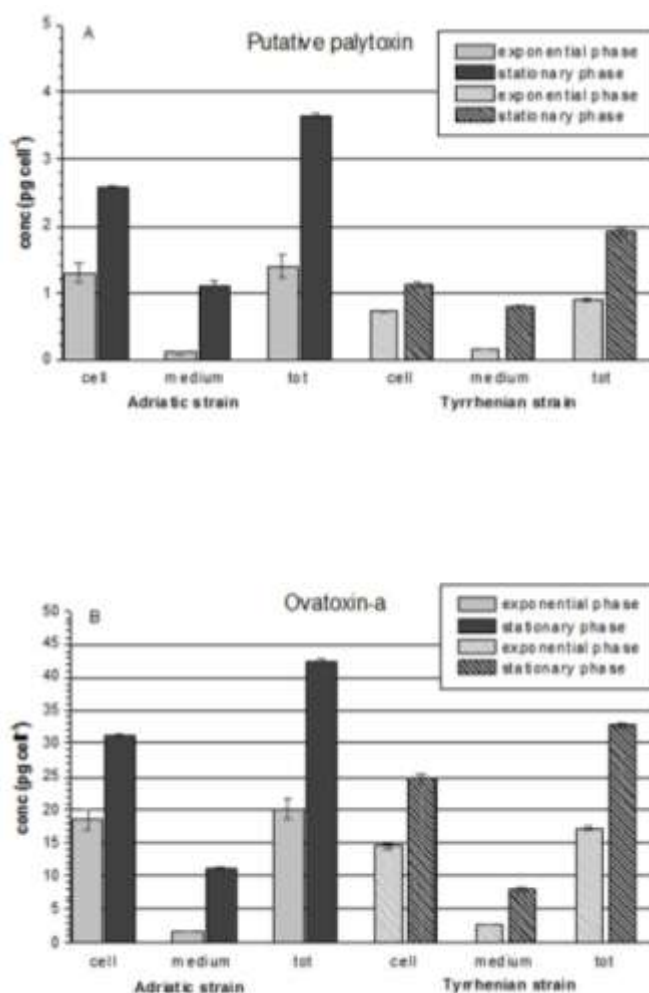
Extraction recovery was calculated for PLTX and showed to be 98% and 45% for pellets and growth media, respectively.<sup>17</sup> Since a pure standard of OVTX-a was not available and taking into account its structural similarity with PLTX, extraction recovery for OVTX-a was considered to be the same as PLTX's. Similarly, quantitative analyses were carried out assuming that the two molecules show the same molar response. Thus, a calibration curve for palytoxin standard at four levels of concentration was used to calculate both pPLTX and OVTX-a content in the analyzed samples. The obtained concentration values for both toxins were corrected basing on recovery percentages. In all cases, OVTX-a was present at levels significantly higher than pPLTX's. Both toxins were more abundant in the Adriatic *O. ovata* than in the Tyrrhenian strain, on a per cell basis, with slightly different OVTX-a/pPLTX ratios between the two strains (12 and 17 for the Adriatic and the Tyrrhenian *O. ovata*, respectively). Toxin concentrations ( $\text{pg cell}^{-1}$ ) for both strains were found to be higher at the end of the stationary growth stage than at the end of the exponential phase. The total toxin content, expressed as  $\mu\text{g per Liter}$  (Table 2), reached the highest values in the Adriatic strain (stationary phase).

**Table 2.** Putative Palytoxin (pPLTX) and Ovatoxin-a (OVTX-a) concentrations in the cells and in the extracellular medium of the two *Ostreopsis ovata* strains, expressed as  $\mu\text{g L}^{-1}$  culture and measured in both exponential and stationary phases. Values are reported as means  $\pm$  SD.

		Putative Palytoxin ( $\mu\text{g L}^{-1}$ )		Ovatoxin-a ( $\mu\text{g L}^{-1}$ )	
		Exponential phase	Stationary phase	Exponential phase	Stationary phase
<b>Adriatic</b> <i>O. ovata</i>	<b>cell</b>	12.99 $\pm$ 1.46	21.34 $\pm$ 0.35	186.19 $\pm$ 15.97	260.98 $\pm$ 2.13
	<b>medium</b>	1.01 $\pm$ 0.22	9.09 $\pm$ 0.69	15.92 $\pm$ 0.56	92.28 $\pm$ 2.44
	<b>total</b>	14.01 $\pm$ 1.67	30.43 $\pm$ 0.34	202.11 $\pm$ 16.53	353.26 $\pm$ 4.57
<b>Tyrrhenian</b> <i>O. ovata</i>	<b>cell</b>	4.88 $\pm$ 0.13	8.69 $\pm$ 0.31	97.51 $\pm$ 2.68	192.18 $\pm$ 5.30
	<b>medium</b>	1.10 $\pm$ 0.10	6.13 $\pm$ 0.07	18.69 $\pm$ 0.16	61.22 $\pm$ 2.10
	<b>total</b>	5.98 $\pm$ 0.23	14.82 $\pm$ 0.38	116.20 $\pm$ 2.52	253.40 $\pm$ 3.20

The concentration of each toxin expressed as pg per cell is reported in Figure 6.



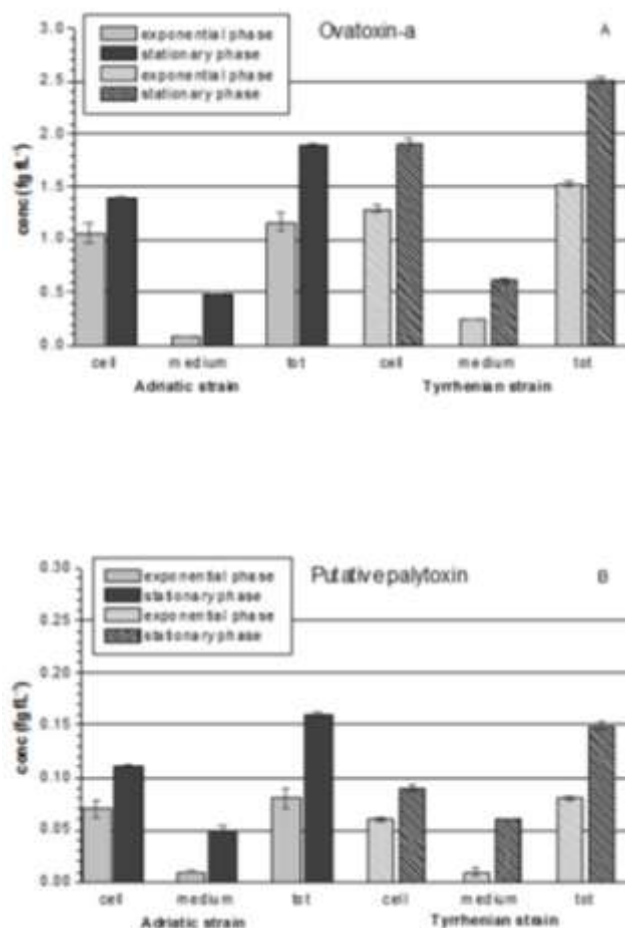


**Figure 6.** Total amount (pg cell<sup>-1</sup>) of (A) Ovatoxin-a (OVTX-a) and (B) Putative Palytoxin (pPLTX) produced by the two *Ostreopsis ovata* strains and measured in cell and medium fractions of cultures in the exponential and stationary phases.

During the stationary phase, the Adriatic *O. ovata* was found to produce 42.2 pg cell<sup>-1</sup> of OVTX-a and 3.6 pg cell<sup>-1</sup> of pPLTX, while the Tyrrhenian strain produced 32.7 and 1.9 pg cell<sup>-1</sup> of OVTX-a and pPLTX, respectively.

For both Adriatic and Tyrrhenian strains, the toxin content retained in cells was significantly higher than that released in growth medium. For the Adriatic strain, the percentage of pPLTX and OVTX-a released in the medium at the end of the exponential phase was 7% and 8%, respectively, while, at the end of the stationary phase it increased up to 30% and 26%, respectively. For the Tyrrhenian strain, the toxin release at the end of the exponential phase was higher than that observed in the Adriatic strain (22% for pPLTX and 16% for OVTX-a), and it further increased at the end of the stationary phase up to 42% for pPLTX and 24% for

OVTX-a. In the evaluation of the above results, it has to be considered that palytoxin is quite stable in solution and, thus, the high toxin amount measured at the end of the stationary phase could be likely due to toxin accumulation in growth medium during the whole cell lifecycle. Since the two *O. ovata* strains presented different cell sizes (the Adriatic *O. ovata* is 2-fold bigger than the Tyrrhenian strain), the toxin concentration was expressed also on a biovolume basis (Figure 7).



**Figure 7.** Total amount (fg fL<sup>-1</sup>) of (A) Ovatoin-a (OVTX-a) and (B) Putative Palytoxin (pPLTX) produced by the two *Ostreopsis ovata* strains and measured in cell and medium fractions of cultures in the exponential and stationary phases.

The total concentration of pPLTX (fg fL<sup>-1</sup>) was quite similar between the two strains, whatever growth stage was considered. On the contrary, OVTX-a concentration in the Tyrrhenian strain appeared to be significantly higher (1.533 and 2.508 fg fL<sup>-1</sup> for the exponential and the stationary phase, respectively) than in the Adriatic strain (1.156 and 1.891 fg fL<sup>-1</sup> for the exponential and the stationary phase, respectively).

### 7.3. Conclusions

Two *O. ovata* strains were collected in 2006 along the Adriatic and the Tyrrhenian coasts, respectively. The dimensions of both strains were similar to those found by other authors<sup>4,18,19,20,21,1,22</sup> and displayed a high variability, which resulted in two different size classes of the cells, as had been previously observed in field samples either in Greece and in Italy.<sup>1,23</sup> Cell dimensions of the two analyzed strains were similar to those found for *O. ovata* from different locations by other authors;<sup>4,18,19,20,21,1,22</sup> Cells of the Adriatic and the Tyrrhenian *O. ovata* strains were tear-shaped as most of the *O. ovata* strains reported so far. In particular, dimensions of the Adriatic *O. ovata* cells were similar to those of other strains collected at different Adriatic sites, namely in the Gulf of Trieste and along the Istrian coasts (Rovinj).<sup>22</sup> No relevant differences were observed between morphometric characters of our Tyrrhenian strain and those of other strains collected along the Tuscanian coasts.<sup>18</sup>

*O. ovata* and *O. siamensis* are very similar, the only distinct character being in the dorsoventral (DV)/anteroposterior (AP) diameters ratio which is higher for *O. siamensis* than for *O. ovata* (Penna et al., 2005). The two strains investigated in this work showed a DV/AP ratio close to 2 which allowed to identify the species as *O. ovata*. Molecular analyses of the nuclear-encoded LSU rDNA gene (D1, D2, D3 and conserved core region) ascribed both strains to the same species. In the phylogenetic tree, based on D1 and D2 domains of the LSU rDNA, the Adriatic and Tyrrhenian strains clustered with other selected gonyaulacoid species. They clustered also with *O. cf ovata* from Malaysia although the difference between the Mediterranean and the Asian strains was smaller than that emerging when the ITS-5.8S rDNA sequence was considered.<sup>21</sup> This result confirmed the great utility of ITS-5.8S rDNA in highlighting phylogenetic relationships; however, the D1 and D2 region of the LSU rDNA gene are widely employed for the construction of dinoflagellate phylogenetic trees and this work provides additional data on LSU sequences of *O. ovata* which until now were limited only to the Malaysian isolate. Data for the D3 and D3core domains of *O. ovata* were also obtained for the first time.

The Adriatic and Tyrrhenian *O. ovata* strains form mucus-cell aggregates, as previously reported for other cultured *O. ovata* strains<sup>24</sup> hampering a reliable cell counting. Acid addition to the culture enabled to break apart aggregates, thus allowing to estimate cell density. Despite this method requires the preparation of a large set of culture flasks it was necessary to obtain either a representative growth curve and an accurate counting for toxin quantification on a cell basis.

The toxin profiles of the Adriatic and Tyrrhenian *O. ovata* strains were characterised by the presence of putative palytoxin and ovatoxin-a. Both toxins had been previously observed in a Ligurian *O. ovata* strain by Ciminiello et al.,<sup>16</sup> at levels of 0.55 pg cell<sup>-1</sup> and 3.85 pg cell<sup>-1</sup> for pPLTX and OVTX-a, respectively. Toxin content of the Adriatic and Tyrrhenian strains measured at the end of the stationary phase resulted significantly higher than Ligurian strain's: pPLTX and OVTX-a were present at levels of 3.63 and 42.17 pg cell<sup>-1</sup> in the Adriatic strain, respectively, and at levels of 1.91 and 32.70 pg cell<sup>-1</sup> in the Tyrrhenian strain, respectively. Ligurian, Adriatic and Tyrrhenian *O. ovata* strains, although morphologically different, present a rather homogenous toxin profile characterized by the presence of ovatoxin-a as the major toxin produced by the alga; this could be used as chemical fingerprint of the species.

pPLTX and OVTX-a were detected also in the growth medium indicating a toxin release relatively low at the end of the exponential phase. Toxin concentration measured in growth medium at the end of the stationary phase increased, on a per liter basis, by three- to nine-fold compared to the exponential phase, suggesting a toxin accumulation in growth medium during the whole cell lifecycle. It has also to be noted that, at the end of an *O. ovata* bloom, when the dinoflagellate population is in the stationary phase, cell concentrations reach the maximum level but, at the same time, many cells break, resulting in a big amount of toxins released in the medium. A long lasting bloom could, thus, enhance the toxin content in the water, resulting in toxic effects towards marine organisms or people inhaling the aerosol.

The Adriatic strain, despite the large cell size, shows a higher growth rate and, on a biovolume basis, produces less palytoxins than the smaller Tyrrhenian strain. However, on a per liter basis, the Adriatic strain presents a higher toxin content than the Tyrrhenian strain, being potentially more dangerous.

#### 7.4. References

1. Aligizaki, K., Nikolaidis, G., 2006. The presence of the potentially toxic genera *Ostreopsis* and *Coolia* (Dinophyceae) in the North Aegean Sea, Greece. *Harmful Algae* 5, 717-730.
2. Masò, M., Vila, M., Alvare, P., 2005. *Ostreopsis* along the Catalan coast (NE Spain): ecological aspects and epidemiologic study. – International seminar “*Ostreopsis*: un problema per il Mediterraneo?” Genova, 5 dicembre 2005.
3. Lenoir, S., Krys, S., 2005. Studies on a tropical benthic *Ostreopsis* specie – AFSSA Agence Française de Sécurité Sanitaire des Aliments (Francia).

4. Fukuyo, Y., 1981. Taxonomical study on benthic dinoflagellates collected in coral reefs. *Bull. Jpn. Soc. Sci. Fish.* 47 (8), 967–978.
5. Hoshaw and Rosowski, 1973.
6. Guillard, R.R.L., 1975. Culture of phytoplankton for feeding marine invertebrates. In: Smith, W.L., Chanley, M.H. (Eds.), *Culture of Marine Invertebrates Animals*. Plenum Press, New York, pp. 26-60.
7. Scholin, C.A., Herzog, M., Sogin, M., Anderson, D.M., 1994. Identification of group and strain specific genetic markers for globally distributed *Alexandrium* (Dinophyceae). II. Sequence analysis of a fragment of the LSU rRNA genes. *J. Phycol.* 30, 999–1011.
8. Daugbjerg, N., Hansen, G., Larsen, J., Moestrup, Ø., 2000. Phylogeny of some of the major genera of dinoflagellates based on ultrastructure and partial LSU rDNA sequence data, including the erection of three new genera of unarmoured dinoflagellates. *Phycologia* 39, 302–317.
9. Ellegard, M., Daugbjerg, N., Rochon, A., Lewis, J., Harding, I., 2003. Morphological and LSU rDNA sequence variation within the *Gonyaulax spinifera*-*Spiniferites* group (Dinophyceae) and proposal of *G. elongata* comb. Nov. and *G. membranacea* comb. Nov. *Phycologia* 42, 151–164.
10. Lenaers, G., Maroteaux, L., Michot, B., Herzog, M., 1989. Dinoflagellates in evolution. A molecular phylogenetic analysis of large subunit ribosomal RNA. *J. Mol. Evol.* 29, 40-51.
11. Hansen, G., Daugbjerg, N., Franco, J.M., 2003. Morphology, toxin composition and LSU rDNA phylogeny of *Alexandrium minutum* (Dinophyceae) from Denmark, with some morphological observations on other European strains. *Harmful Algae* 2, 317–335.
12. Hansen, G., Daugbjerg, N., Henriksen, P., 2000. Comparative study of *Gymnodinium mikimotoi* and *Gymnodinium aureolum*, comb. Nov. (= *Gyrodinium aureolum*) based on morphology, pigment composition, and molecular data. *J. Phycol.* 36, 394-410.
13. Filatov, D.A., 2002. ProSeq: a software for preparation and evolutionary analysis of DNA sequence data sets. *Mol. Ecol. Notes* 2, 621–624.
14. Thompson, J.D., Gibson, T.J., Plewniak, F., Jeanmougin, F., Higgins, D.G., 1997. The ClustalX windows interface: flexible strategies for multiple sequence alignment aided by quality analysis tools. *Nucleic Acids Research* 25, 4876–4882.
15. Kumar, S., Tamura, K., Nei, M., 2004. MEGA3.1: integrated software for molecular evolutionary genetics analysis and sequence alignment. *Brief. Bioinform.* 5, 150–163.
16. Ciminiello, P., Dell’Aversano, C., Fattorusso, E., Forino, M., Tartaglione, L., Grillo, C., Melchiorre, N., 2008. Putative Palytoxin and Its New Analogue, Ovatoxin-a, in *Ostreopsis*

- ovata* Collected Along the Ligurian Coasts During the 2006 Toxic Outbreak. *J. Am. Soc. Mass Spectrom.* 19, 111-120.
17. Ciminiello, P., Dell'Aversano, C., Fattorusso, E., Forino, M., Magno, G.S., Tartaglione, L., Grillo, C., Melchiorre, N., 2006. The Genoa 2005 outbreak. Determination of putative palytoxin in Mediterranean *Ostreopsis ovata* by a new liquid chromatography tandem mass spectrometry method. *Anal. Chem.* 78, 6153–6159.
  18. Tognetto, L., Bellato, S., Moro, I., Andreoli, C., 1995. Occurrence of *Ostreopsis ovata* (Dinophyceae) in the Tyrrhenian Sea during summer 1994. *Botanica Marina* 38, 291-295.
  19. Faust, M.A., Morton, S.L., Quod, J.P., 1996. Further SEM study of the marine dinoflagellates: the genus *Ostreopsis* (Dinophyceae). *J. Phycol.* 32, 1053–1065.
  20. Chang, F.H., Shimizu, Y., Hay, B., Stewart, R., Mackay, G., Tasker, R., 2000. Three recently recorded *Ostreopsis* spp. (Dinophyceae) in New Zealand: temporal and regional distribution in the upper North Island from 1995 to 1997. *NZ J. Mar. Freshwat. Res.* 34, 29–39.
  21. Penna, A., Vila, M., Fraga, S., Giacobbe, M.G., Andreani, F., Riobò, P., Vernesi, C., 2005. Characterization of *Ostreopsis* and *Coolia* (Dinophyceae) isolates in the Western Mediterranean Sea based on morphology, toxicity and internal transcribed spacer 5.8S rDNA sequences. *J. Phycol.* 41, 212–225.
  22. Monti, M., Minocci, M., Beran, A., Ivesa, L., 2007. First record of *Ostreopsis* cfr. *ovata* on macroalgae in the Northern Adriatic Sea. *Marine Pollution Bulletin* 54, 598–601.
  23. Bianco, I., Sangiorgi, V., Penna, A., Guerrini, F., Pistocchi, R., Zaottini, E., Congestri, R., 2007. *Ostreopsis ovata* in benthic aggregates along the Latium Coast (middle Tyrrhenian Sea). International Symposium on algal toxins, SITOX.
  24. Heil, C.A., Maranda, L., Shimizu, Y., 1993. Mucus-associated dinoflagellates: large scale culturing and estimation of growth rate. In: Smayda, T.J., Shimizu, Y. (Eds), *Toxic Phytoplankton Blooms in the Sea*. Elsevier Science Publishers B. V., Amsterdam, pp. 501-506.



## Chapter 8

### 42-Hydroxy Palytoxin: a new palytoxin analog from Hawaiian *Palythoa* spp.

An ancient Hawaiian legend refers to a mysterious *limu-make-o-Hana* (a deadly seaweed growing in an only fabled tidepool on the island of Maui near the harbor of Hana) that for centuries natives had “used to smear on the spear points to make them fatal”.<sup>1</sup>

Fascinated by the legend, Professor Paul Scheuer, a pioneer of the chemistry of marine metabolites, in collaboration with A.H. Banner and P. Helfrich, from the Hawaii Institute of Marine Biology, tried to locate the secret tidepool. Eventually, through a very elaborate chain of local Hawaiian informers the location of the legendary tidepool was disclosed.<sup>2</sup>

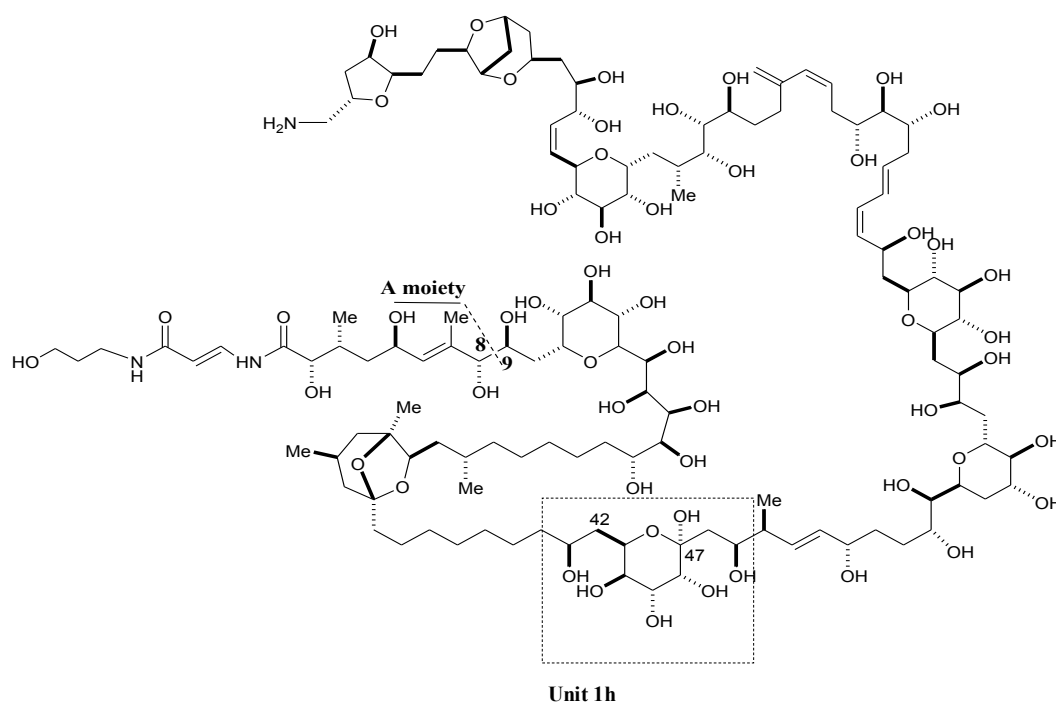
Analyses carried out on samples collected from the pool revealed that the toxic effects were not provoked by the seaweed but by an animal belonging to the phylum Coelenterata - possibly a new species - assigned to the genus *Palythoa*.<sup>3</sup> Scheuer succeeded also in offering some preliminary insights into the chemical structure of the molecule responsible for the high toxicity of the *Palythoa*, which was named palytoxin (PLTX).<sup>3</sup>

Successively, Walsh and Bowers<sup>4</sup> identified the marine coelenterate known to the Hawaiians as *limu-make-o-Hana* - from which palytoxin had been isolated for the first time - as *Palythoa toxica*, a very rare species sparingly found along the coasts of Hawaii.<sup>5</sup>

Toxins seemingly identical to palytoxin were isolated also from other species of zoanthids of the genus *Palythoa*, such as *P. mamillosa* from Jamaica<sup>3,6</sup> and an unknown species of *Palythoa* from Tahiti.<sup>6</sup> After its isolation in 1971, it took nearly 11 years before the correct chemical structure of palytoxin (**1**) was disclosed. Two research groups – one at the University of Hawaii led by R. E. Moore, and one at Nagoya University led by Y. Hirata – carried out monumental efforts to define the planar structure of this potent marine biotoxin. In 1980, using plasma desorption mass spectrometry with californium (<sup>252</sup>Cf), Hirata exactly established as 2680 the molecular weight of a palytoxin isolated from *P. tuberculosa* collected in Okinawa.<sup>7</sup> In 1981, independently and almost simultaneously, both the Hawaiian and the Japanese groups proposed two slightly different planar structures for palytoxin. The difference between the two structures suggested by the two competing groups resided basically in palytoxin unit 1h (Figure 1)<sup>8-10</sup>. In 1982, the absolute stereochemistry of palytoxin isolated from Okinawan *P. tuberculosa* encompassing 64 stereogenic centers in



addition to eight double bonds was eventually elucidated through degradation reactions and a chemical synthesis-based approach (Figure 1).<sup>11a-e</sup>



**Figure 1.** Stereostructure of palytoxin. In Unit 1h (enclosed in a dashed frame) resides the slight difference between the two planar structures proposed for palytoxin by Hirata and Moore, respectively. In particular, in palytoxin isolated from Okinawan *P. tuberculosis* Hirata located a hydroxyl group at position 44 and a hemiketal functionality at C47<sup>8</sup>; while Moore individuated a ketal bond connecting C44 with C47 in palytoxin isolated from a Tahitian *Palythoa* spp<sup>9</sup>.

Over the next years, Hirata's group isolated four minor palytoxin-like compounds from Okinawan *P. tuberculosis*, characterized as homopalytoxin, bishomopalytoxin, neopalytoxin, and deoxypalytoxin.<sup>12</sup>

Level and content of palytoxins in toxic *Palythoa* spp have been reported to vary significantly among species, populations of the same species and even seasonally.<sup>2,13</sup> The assumption that palytoxins are actually produced by bacteria<sup>2,14</sup> or microalgae presumably existing symbiotically with *Palythoa*.<sup>15</sup> has been also defended. Sporadic occurrence of palytoxins in algae,<sup>15</sup> crabs,<sup>16a,b</sup> and fish<sup>17</sup> alike, indicates that microorganisms could represent the real source of these toxins.

Recently, dinoflagellates belonging to the genus *Ostreopsis* have been proposed to be probable biogenetic originators of palytoxins. This follows from identification of three

palytoxin analogs from *Ostreopsis* spp., namely, i) ostreocin-D from *O. siamensis*,<sup>18</sup> ii) mascarenotoxins from *O. mascarensis*,<sup>19</sup> and iii) ovatoxin-a from *O. ovata*.<sup>20</sup>

In the wake of the scientific research on palytoxins, we have recently analyzed the toxin content from Hawaiian *P. tuberculosa* and *P. toxica*. The material we analyzed came from samples collected along the coasts of Hawaii and carefully stored by the U.S. Army Medical Research and Development Command.<sup>21</sup> These precious samples are unique, having been collected exactly from the legendary *Hana* tidepool. The isolation of toxins from Hawaiian *Palythoa* spp. was carried out by Bignami *et al.*<sup>22</sup> In the frame of this study, they also reported that at least two major palytoxin-like compounds were present in *P. tuberculosa* sample.<sup>23</sup> A number of experiments were then performed to rule out the possibility that the two detected major palytoxin-like compounds could undergo interconversion upon storage or be an artefact of the isolation procedure.<sup>23</sup>

Our work based on in-depth high resolution liquid chromatography-mass spectrometry (LC-MS) analysis along with extensive 1D- and 2D-NMR investigation led us to structurally characterize a never reported palytoxin-like compound, 42-hydroxy palytoxin (42-OH PLTX, **2**). This toxin and palytoxin itself appeared to be the major components of toxic extract from *P. tuberculosa* sample. Interestingly, 42-OH PLTX was proven to be by far the main palytoxin derivative present in *P. toxica*.

Even small structural differences on the complex architecture of palytoxin seem to induce quantitative differences in the biological activity.<sup>18,19,24</sup> Consequently, the effect of PLTX and its 42-OH derivative on  $[Ca^{2+}]_i$  levels was investigated in skeletal muscle cells, an important toxicity target of palytoxins,<sup>25-29</sup> to compare the potency of 42-OH PLTX to that of its parent compound. Furthermore, a competition assay was performed to define the binding affinity of the two compounds using  $[^3H]$ -ouabain bound to a well known palytoxin molecular target, the  $Na^+/K^+$  pump.<sup>30</sup>

## 8.1. Experimental

### 8.1.1. Extraction and isolation

Fractions containing palytoxins, namely compounds **1** and **2**, were obtained from *Palythoa tuberculosa* collected in Hawaii according to the procedure described by Moore and Scheuer and modified by Bignami *et al.*<sup>22</sup> Toxins were extracted from *P. tuberculosa* with 70% aqueous ethanol. The extract thus obtained was concentrated *in vacuo* and then extracted with dichloromethane. The toxic fraction was purified from the aqueous layer by column chromatography on Amberlite XAD-2, followed by chromatography on DEAE-Sephadex A-

25 and CM-Sephadex C-25. The toxic fraction was finally desalted on Bond Elut C18 eluted with 80% aqueous ethanol.

Compound **2** was isolated from *Palythoa toxica* collected in Hawaii as reported above.

### 8.1.2. Liquid chromatography-mass spectrometry (LC-MS)

All LC-MS analyses were performed on an Agilent 1100 LC binary system coupled to 1) an Applied Biosystems API 2000 triple-quadrupole MS equipped with a turbospray source (Foster City, CA, USA) for unit resolution spectra; 2) a 6210 time of flight mass spectrometer (TOF MS) equipped with an electrospray (ESI) source (Agilent, Palo Alto, CA, USA) for high resolution experiments. A 3  $\mu\text{m}$  Gemini C18 (150  $\times$  2.00 mm) column (Phenomenex, Torrance, CA, USA), maintained at room temperature, was used. Elution was accomplished with water (eluent A) and 95% acetonitrile/water (eluent B), both containing 30 mM acetic acid, at a flow rate of 0.2 mL min<sup>-1</sup>, by using a slow gradient system (20-50% B over 20 min, 50-80% B over 10 min, 80-100% B in 1 min, and hold 5 min).

Full scan MS experiments in the range  $m/z$  300–1400 were carried out in positive ion mode by using the following source settings: a turbogas temperature of 0 °C, an ionspray voltage of 5500 V, a declustering potential (DP) of 50 V, a focusing potential (FP) of 390 V, and an entrance potential (EP) of 11 V. Multiple reaction monitoring (MRM) experiments were carried out by monitoring the transitions  $m/z$  1340.7  $\rightarrow$  327.1, 1331.7  $\rightarrow$  327.1 for palytoxin and the transitions  $m/z$  1348.7  $\rightarrow$  327.1, 1339.7  $\rightarrow$  327.1 for 42-OH PLTX. A DP = 1 V, a collision energy (CE) = 50 eV, cell exit potential (CXP) = 10 V, EP = 11 V (for  $m/z$  1331.7  $\rightarrow$  327.1 and 1339.7  $\rightarrow$  327.1) and EP = 5 V (for  $m/z$  1340.7  $\rightarrow$  327.1 and 1348.7  $\rightarrow$  327.1) was used. The dwell time was set to achieve a total scan time of 1 sec. Palytoxin standards at four levels of concentration (2.0, 1.0, 0.5, and 0.25  $\mu\text{g mL}^{-1}$ ) were used to generate a calibration curve that was employed in quantitative analyses. Sum of MRM peak areas was used to express peak intensity. The average of duplicate measurements was used for plotting.

HRMS spectra were recorded in the range  $m/z$  100-3000 (positive ion mode) by using the following source settings: gas temperature = 300°C, drying gas flow = 11 L min<sup>-1</sup>, capillary voltage = 3000 V, fragmentor potential = 130 V, and skimmer potential = 60 V. Calculation of elemental formula of **2** was performed by using the mono-isotopic ion peaks for each ion cluster. The following bi-charged mono-isotopic ion peaks were observed:  $m/z$  1367.22320 (C<sub>129</sub>H<sub>224</sub>KN<sub>3</sub>O<sub>55</sub>,  $\Delta$  = 0.53 ppm),  $m/z$  1359.23216 (C<sub>129</sub>H<sub>224</sub>N<sub>3</sub>NaO<sub>55</sub>,  $\Delta$  = 2.46 ppm),  $m/z$  1339.23825 (C<sub>129</sub>H<sub>223</sub>N<sub>3</sub>O<sub>54</sub>,  $\Delta$  = 0.75 ppm),  $m/z$  1330.23485 (C<sub>129</sub>H<sub>221</sub>N<sub>3</sub>O<sub>53</sub>,  $\Delta$  = 0.66 ppm),

$m/z$  1321.222921 ( $C_{129}H_{219}N_3O_{52}$ ,  $\Delta = 0.39$  ppm),  $m/z$  1312.22478 ( $C_{129}H_{217}N_3O_{51}$ ,  $\Delta = 1.05$  ppm). The following tri-charged mono-isotopic ion peaks were observed:  $m/z$  919.47952 ( $C_{129}H_{225}KN_3NaO_{55}$ ,  $\Delta = 1.24$  ppm),  $m/z$  913.82099 ( $C_{129}H_{224}N_3Na_2O_{55}$ ,  $\Delta = 1.00$  ppm),  $m/z$  911.81531 ( $C_{129}H_{225}KN_3O_{55}$ ,  $\Delta = 2.30$ ),  $m/z$  900.48866 ( $C_{129}H_{223}N_3NaO_{54}$ ,  $\Delta = 0.64$  ppm),  $m/z$  881.15587 ( $C_{129}H_{220}N_3O_{52}$ ,  $\Delta = 1.12$  ppm),  $m/z$  875.15269 ( $C_{129}H_{218}N_3O_{51}$ ,  $\Delta = 1.51$  ppm). The base peak was present at  $m/z$  327.19117 (mono-isotopic ion) and corresponded to a  $C_{16}H_{27}N_2O_5$  part structure ( $\Delta = 0.85$  ppm).

### 8.1.3. Nuclear magnetic Resonance (NMR) experiments

NMR spectra were measured on a Varian Unity Inova 700 spectrometer equipped with a  $^{13}C$  Enhanced HCN Cold Probe. Shigemi 5 mm NMR tubes and  $CD_3OD$  as an internal standard ( $\delta_H$  3.31 and  $\delta$  49.0) were used. Standard Varian pulse sequences were employed for the respective classes of spectra; solvent signal suppression by presaturation was used when required. All NMR data reported in the text were derived from 2D  $^1H$ - $^1H$  COSY, Z-filtered TOCSY, ROESY, phase-sensitive HMBC, HSQC, and HSQCTOCSY spectra.

### 8.1.4. Functional studies

#### a) Materials

Palytoxin standard (from *P. tuberculosa*; purity grade > 90 %) was purchased from Wako Pure Chemical Industries Ltd (Osaka, Japan). Sample from *P. toxica* was used as 42-OH-PLTX (purity 91%). Fetal calf serum was from PAA Laboratories (Linz, Austria). [ $^3H$ ]-ouabain (specific activity 30 Ci/mmol) was from Perkin Elmer Italia (Monza, Italy).  $Na^+/K^+$ -ATPase from porcine cerebral cortex was purchased from Sigma Aldrich (St Louis, Mo, USA). Media and all other chemicals were from Sigma Aldrich (St Louis, Mo, USA).

#### b) Cell cultures

Cultures of skeletal muscle cells (i28) were established from mouse satellite cells isolated from hind leg muscles of 7-day-old male Balb/c mice killed by cervical dislocation as described elsewhere.<sup>27</sup> Cell cultures were maintained as exponentially growing myoblasts in medium consisting of HAM'S F-10 supplemented with 20% fetal calf serum, L-glutamine (4 mM), penicillin (100 units/ml) and streptomycin (100  $\mu$ g/ml). To induce cell differentiation and myoblast fusion into myotubes, the medium was replaced, 1 day after plating, with Dulbecco's modified Eagle's medium containing 2% horse serum and L-glutamine, penicillin

and streptomycin as above. Cells were maintained at 37 °C in CO<sub>2</sub> (5%)-enriched air. Experiments were performed on myotubes cultured up to 8 days of differentiation.

*c) Videoimaging technique*

[Ca<sup>2+</sup>]<sub>i</sub> was monitored in single cells by using the fluorescent calcium probe Fura2-AM (Sigma). Briefly, skeletal muscle cells were grown for 6-8 days on matrigel-coated glass coverslips and loaded with 5 μM Fura2-AM for 30 min at room temperature. Experiments were performed in a normal external solution (in mM: NaCl 140, KCl 2.8, MgCl<sub>2</sub> 2, CaCl<sub>2</sub> 2, glucose 10, HEPES-NaOH 10, pH 7.35) or in a Na<sup>+</sup>-free solution (in mM: N-methyl-D-glucamine 140, KCl 2.8, MgCl<sub>2</sub> 2, CaCl<sub>2</sub> 2, glucose 10, HEPES-NaOH 10, pH 7.35). A temperature-controlled microincubator chamber (Medical System Corporation, Greenwale, NY, USA) maintained the temperature at 37°C during the experiments. Toxins were gently applied to the bathing solution by loading appropriate volumes (x 200) of concentrated solution into a 2-ml syringe connected to the microincubator chamber. The videomicroscopy system was built around a Zeiss (Oberkochen, Germany) Axiovert 135 light microscope. Fura2 loaded cells were excited at 340 and 380 nm. The fluorescent images were collected by a CCD camera (Hamamatsu, Photonics, Hamamatsu, Japan). The image acquisition was performed at two frames/s. Determination of ratio images was performed pixel by pixel on pair of corresponding 340 and 380 images. Temporal plots corresponding to mean value of the fluorescence changes were calculated from ratio images at the single cell level. The fluorescent ratio at rest was assumed to be 1. Changes in fluorescent signal were measured relative to the fluorescent ratio at rest and expressed as percentage.

*d) Binding assay*

For competition experiments, increasing concentrations of palytoxin, 42-OH-palytoxin or ouabain (0.15-1000 nM) were added to a 96-well Multiscreen-FB microtiter plate in the presence of 5 nM (final concentration) [<sup>3</sup>H]-ouabain and 10 μg of purified Na<sup>+</sup>/K<sup>+</sup>-ATPase in 50 mM Tris-HCl buffer, pH 7.4, containing 5 mM MgCl<sub>2</sub>, 1 mM NaH<sub>2</sub>PO<sub>4</sub> and 1 mM H<sub>3</sub>BO<sub>3</sub>. The total volume was 250 μl. Nonspecific binding was defined in the presence of 100 μM ouabain. After 240 min at 37°C, the reaction was terminated filtering the plate under vacuum using the Millipore MultiScreen Vacuum Manifold; 25 μl SuperMix scintillation cocktail were added to each well and the plate counted in a MicroBeta Trilux counter (Wallac, Turku, Finland).

*e) Statistical analysis*

All data, when possible, are given as means  $\pm$  SEM. The Student's *t* test was used to examine statistical significance. Values were considered significantly different when  $P < 0.05$ .

## 8.2. Results and Discussion

Samples of palytoxins, obtained from *P. tuberculosa* and *P. toxica* according to the modified method of Moore and Scheuer<sup>3</sup> reported by Bignami *et al.*,<sup>22</sup> were provided by US Army Medical Research Institute of Infectious Diseases. Each sample was analyzed by LC-MS in full scan mode, using a triple quadrupole MS instrument equipped with a turbo ion spray source operating in the mass range 300-1400 amu. The chromatographic separation was accomplished by using a slow gradient elution system that, in our experience,<sup>20,31</sup> allows a good chromatographic resolution of palytoxins. Under the used conditions, the total ion chromatogram (TIC) of sample from *P. tuberculosa* contained two major peaks of similar intensity at 10.97 and 11.14 min (SI). This latter was assigned to palytoxin itself (**1**) on the basis of comparison of its retention time and associated mass spectrum with those of palytoxin standard injected under the same experimental conditions. Mass spectrum associated to peak at 10.97 min presented bicharged ion clusters which closely matched with palytoxin's for *m/z* absolute values but differed mainly for ion ratios.

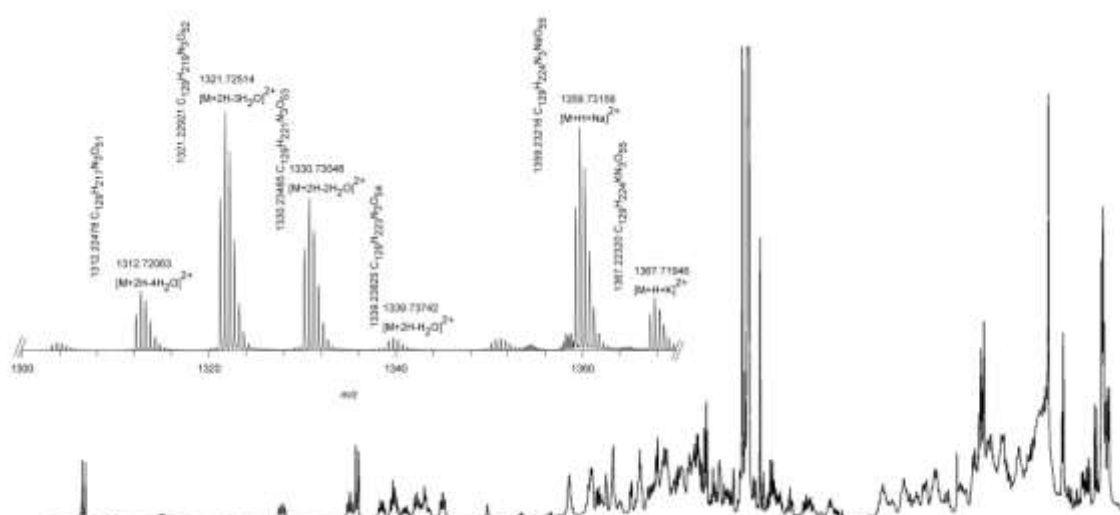
Under the same experimental conditions, TIC of sample from *P. toxica* was dominated by one major peak at 10.97 min and the associated MS spectrum was superimposable, in both *m/z* values and ion ratios of bicharged ions, to that emerging in the LC-MS trace of sample from *P. tuberculosa* at the same retention time. The whole of the above evidence suggested the presence of a palytoxin-like compound (**2**) eluting just earlier than palytoxin in both *P. toxica* and *P. tuberculosa* samples. The sample from *P. toxica*, which contained the potentially new compound **2** as the very major component, was used to gain some additional information on its molecular weight. In particular, full scan MS experiments were carried out on *P. toxica* sample and palytoxin standard by adding either NaCl or KCl to the mobile phase to a final concentration of 1 mM.

This resulted in an increased formation of either sodium or potassium adduct bicharged ions (SI) versus ions due to dehydration reactions. Under such conditions,  $[M+H+Na]^{2+}$  and  $[M+H+K]^{2+}$  ions appeared as very intense peaks at *m/z* 1351.7 and 1359.7 for **1**, respectively, and at *m/z* 1359.7 and 1367.7 for **2**, respectively. This suggested that **2** likely contained 16 mass units more than palytoxin (SI).

In order to establish the exact mass of the new compound **2**, high resolution (HR) LC-MS experiments were carried out on a LC-ESI-TOF MS instrument for both PLTX standard (**1**)

and sample from *P. toxica*. The HRMS spectra of **1** and **2** presented mono-charged ions too poor and unresolved to be used for assignment of molecular formulas. Much more informative was the comparative analysis of bi-charged ions.

In particular, all bi-charged ion clusters contained in HRMS spectrum of **2** were up-shifted of 8 mass units comparing to those of palytoxin standard. High resolution measurements were performed on the mono-isotopic ion peak of each bi-charged ion cluster (Figure 2, SI, and Methods) and all the obtained data pointed to the following molecular formula for **2**:  $C_{129}H_{223}N_3O_{55}$ . Further confirmation was provided by exact masses of the most abundant tri-charged ions (Experimental).



**Figure 2.** Mass scale expansion of the  $m/z$  1300-1370 region of the HRMS spectra of **2** (top).  $^1\text{H-NMR}$  spectrum registered in  $\text{CD}_3\text{OD}$  with one drop of deuterium oxide of **2** (bottom).

The obtained molecular formula indicated that **2** contains one more oxygen atom than PLTX ( $C_{129}H_{223}N_3O_{54}$ ). Some structural information on the new compound was provided by the presence of the base peak at  $m/z$  327.19117 ( $C_{16}H_{27}N_2O_5$ ) in HRMS spectrum of **2**. This ion dominates also HRMS spectrum of PLTX and was attributed to the cleavage between carbons 8 and 9 of **1** (Figure 1) and the additional loss of a water molecule.<sup>32-33</sup> Its presence suggested that **2** shares with palytoxin the western part of the molecule up to C-8, as reported also for mascarenotoxins<sup>19</sup> and ovatoxin-a.<sup>20</sup>

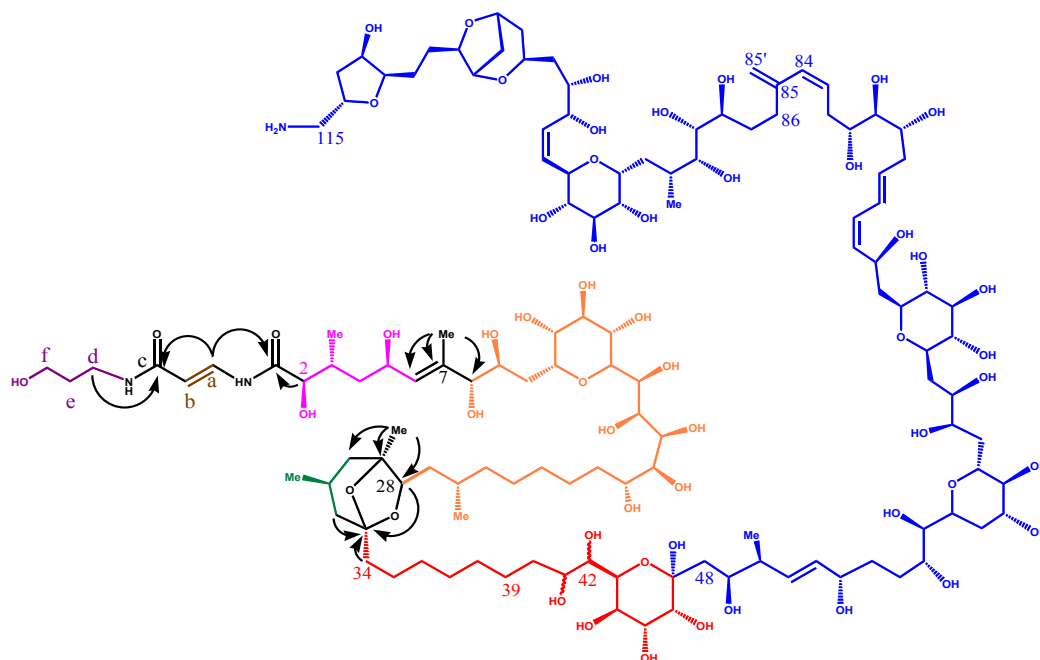
Quantitative analyses were carried out on both samples from *P. tuberculosa* and *P. toxica* in multiple reaction monitoring (MRM) mode by selecting two transitions (precursor ion  $\rightarrow$  product ion) for each toxin, namely  $[M+2H]^{2+} \rightarrow [A \text{ moiety}+H-H_2O]^+$  ( $m/z$  1340.7  $\rightarrow$  327.1

for **1** and  $m/z$  1348.7  $\rightarrow$  327.1 for **2**) and  $[M+2H-H_2O]^{2+} \rightarrow [A \text{ moiety}+H-H_2O]^+$  ( $m/z$  1331.7  $\rightarrow$  327.1 for **1** and  $m/z$  1339.7  $\rightarrow$  327.1 for **2**). On account of the evident structural similarities between the two compounds, we assumed that their molar responses were quite similar. Therefore, calibration curve for palytoxin standard at four levels of concentrations was used to calculate toxin content of both samples. Sample from *P. tuberculosa* contained a quite equal amount of **1** (1.43 mg) and **2** (1.46 mg), whereas sample from *P. toxica* contained 91% of **2** (3.00 mg). This latter sample was considered enriched enough in **2** to be employed as such in an in-depth NMR investigation aimed at determining the structure of the new palytoxin-like compound. We decided not to undertake purification of **2** from *P. toxica* sample that would have required multiple chromatographic separations on account of the extreme similarity between **1** and **2**. This would have caused a remarkable loss of such a rare and precious material without any advantage for the structural assignment studies.

Even though at first glance  $^1\text{H-NMR}$  spectra of both palytoxin and our compound appeared almost identical (Figure 2), we were barred from achieving the planar structure of **2** by merely comparing its NMR data with those reported in literature for palytoxin because of their high structural complexity resulting in hugely congested NMR spectra. In order to individuate all of the new molecule proton spin systems, we relied on an in parallel study of COSY and TOCSY spectra (SI). Successively, we associated every proton to its carbon thanks to both HSQC and HSQCTOCSY experiments (SI). In particular, this latter proved very useful in disentangling those spectral regions characterized by strong overlapping cross-peaks, thus leading to an unambiguous assignment of carbon and proton signals (Table1 and SI). At this point, comparing the spin systems of **2** –listed below - with those of palytoxin, we could pin down that all of them were mostly superimposable to those of palytoxin but one – namely F spin system (Figure 3): A spin system from Cd to Cf (violet); B spin system from Ca to Cb (brown); C spin system from C2 to C6 (pink); D spin system from C8 to C28 (orange); E spin system from C30 to C32 (green); F spin system from C34 to C46 (red); G spin system from C48 to C115 (blue).

Despite this last system may appear interrupted at position C85 - where an unprotonated  $sp^2$  carbon is located- long range correlations between H85'a and H<sub>2</sub>86 as well as between H85'b and H84, respectively, emerging from both COSY and zTOCSY experiments allowed us to consider it as a single system stretching as far as position C115 (Figure 3).





**Figure 3.** Structure 2. The seven spin systems (A-G) are depicted with different colors. Arrows highlight key HMBC correlations.

Once tracked down all of the above spin systems, we could connect them to each other on the basis of some key HMBC cross peaks (SI). In particular, HMBC correlations between H<sub>2</sub>d and C<sub>c</sub> as well as between H<sub>a</sub> and C<sub>c</sub> were conclusive for connecting A to B. Likewise, B was linked to C thanks to HMBC cross peaks between C1 and both H<sub>a</sub> and H<sub>2</sub>, respectively. Correlations of methyl at C7 with H<sub>6</sub> and H<sub>8</sub> were crucial to connect C spin system with D extending up to position C28.

HMBC correlations between CH<sub>3</sub>-29 and both C28 and C30 were definitive in order to relate D with E. At this point, carbon at position 33 turned out to be a crossroads for entwining D and E spin systems with each other thanks to its HMBC cross peaks with H<sub>28</sub> and H<sub>232</sub> (Figure 3).

With regard to F spin system, which contains the structural difference in comparison to palytoxin, its whole proton connectivity was achieved through COSY and TOCSY experiments; while an HSQC and HSQCTOCSY (SI) were crucial to correlate each proton to the respective carbon (Table1). F spin system appeared to be characterized by a series of –CH<sub>2</sub>– groups spanning from C34 through C40 followed by an uninterrupted sequence of oxymethine functionalities from C41 up to C46. In conclusion, F resulted basically superimposable to the corresponding palytoxin spin system with just a significant structural

difference: the C42 methylene typical of palytoxin ( $\delta_{\text{H}}$  1.86 and 1.44;  $\delta_{\text{C}}$  39.37 ppm) was found to be replaced by a –CHOH group ( $\delta_{\text{H}}$  3.70 and  $\delta_{\text{C}}$  77.34 ppm).

The last step of our NMR-based structural investigation of **2** was the location of the F spin system. HMBC correlations between C33 and H<sub>2</sub>34 allowed to connect F to E; while, HMBC cross peak between H<sub>2</sub>48 and C47 as well as ROE between H<sub>2</sub>48 and H46 led us to join F to the last spin system (G) spanning from C48 to C115 (Figure 3).

The careful NMR analysis performed on **2** allowed us to offer also some insights into its stereochemistry. In fact, considering that <sup>1</sup>H and <sup>13</sup>C chemical shifts of **1** and **2** were basically overlapping, we assumed that the two molecules shared the same stereochemistry at all the common chiral centers but at C41. At this position, in fact, significant differences in <sup>1</sup>H and <sup>13</sup>C chemical shifts were detected when comparing **2** with **1** (Table 1), so that at C41 in **2** we could neither confirm the same stereochemistry as **1** nor rule out a possible inversion of configuration.

**Table 1.**  $^1\text{H}$  and  $^{13}\text{C}$  NMR chemical shift data of Palytoxin (**1**) and 42-OH Palytoxin (**2**). Remarkable differences in chemical shifts between **1** and **2** are represented in bold.

No.	Palytoxin		42-OH Palytoxin		No.	Palytoxin		42-OH Palytoxin	
	$^{13}\text{C}$	$^1\text{H}$	$^{13}\text{C}$	$^1\text{H}$		$^{13}\text{C}$	$^1\text{H}$	$^{13}\text{C}$	$^1\text{H}$
1	175.92	-	175.76*	-	60	70.18	3.85	70.21	3.85
2	75.70	4.09	75.68	4.08	61	76.57	3.15	76.57	3.15
3	34.73	2.17	34.89	2.18	62	73.11	3.74	73.15 <sup>c</sup>	3.75
3-CH <sub>3</sub>	13.99	0.88	14.13	0.88	63	36.77	1.96; 1.70	36.89	1.96; 1.70
4	41.73	1.77; 1.40	41.82	1.76; 1.40	64	71.77	3.68	71.88 <sup>d</sup>	3.68
5	66.62	4.50	66.67	4.50	65	72.20	3.76	72.27	3.76
6	131.85	5.49	131.82	5.49	66	37.01	2.04; 1.53	37.16	2.04; 1.54
7	138.28	-	138.26*	-	67	77.22	3.44	77.16	3.44
7-CH <sub>3</sub>	13.17	1.72	13.34	1.72	68	76.04	3.12	76.04 <sup>e</sup>	3.12
8	80.91	3.92	80.97	3.92	69	79.74	3.36	79.81	3.36
9	72.34	3.81	72.30	3.82	70	75.85	3.09	75.95	3.09
10	29.23	2.12	29.36	2.13	71	77.08	3.44	77.08	3.43
11	76.19	4.18	76.26	4.17	72	41.51	2.04; 1.43	41.69	2.04; 1.40
12	73.88	3.64	73.68	3.65	73	64.99	4.84	65.03	4.84
13	75.17	3.54	75.18	3.55	74	133.47	5.37	133.45	5.37
14	71.68	3.60	71.82	3.59	75	130.04	6.00	129.99	6.00
15	72.91	3.62	72.91	3.62	76	128.87	6.46	128.87	6.46
16	71.28	4.03	71.35 <sup>a</sup>	4.03	77	133.88	5.78	133.95	5.78
17	71.68	4.04	71.64 <sup>a</sup>	4.04	78	38.64	2.42	38.81	2.41
18	73.27	3.54	73.29	3.54	79	71.20	3.93	71.22	3.93
19	71.35	3.79	71.30	3.79	80	76.29	3.27	76.34	3.26
20	71.11	3.87	71.19	3.88	81	73.04	3.71	73.10	3.71
21	27.38	1.48; 1.39	27.70	1.49; 1.37	82	34.35	2.75; 2.39	34.56	2.76; 2.39
22	26.93	1.47; 1.35	27.40	1.48; 1.35	83	130.18	5.69	130.26	5.69
23	35.03	1.64; 1.55	35.16	1.64; 1.55	84	132.64	5.95	132.67	5.95
24	28.44	1.36	28.70	1.36	85	146.73	-	146.63*	-

25	39.72	1.26	39.89	1.26	85'	114.86	5.07; 4.94	114.92	5.07; 4.94
26	29.70	1.67	29.83	1.68	86	34.30	2.34; 2.25	34.56	2.34; 2.25
26-CH <sub>3</sub>	19.30	0.92	19.50	0.92	87	33.13	1.72; 1.59	33.17	1.72; 1.58
27	40.78	1.47; 0.91	40.77	1.48; 0.90	88	74.19	3.71	74.29	3.71
28	80.17	3.97	80.22	3.97	89	74.02	3.50	74.09	3.50
29	82.31	-	82.27*	-	90	77.82	3.35	77.93	3.35
29-CH <sub>3</sub>	21.01	1.18	21.15	1.18	91	33.00	1.89	33.16	1.89
30	45.74	1.70; 1.14	45.92	1.70; 1.15	91-CH <sub>3</sub>	15.65	0.91	15.78	0.91
31	25.55	2.04	25.77	2.05	92	27.86	2.21; 1.30	27.97	2.22; 1.30
31-CH <sub>3</sub>	21.89	0.91	22.00	0.92	93	74.83	4.03	74.90	4.03
32	43.74	1.67; 1.09	43.94	1.68; 1.09	94	73.04	3.65	73.13	3.64
33	109.23	-	109.24*	-	95	74.73	3.61	74.74	3.61
34	38.64	1.60	38.69	1.60	96	76.01	3.15	76.01 <sup>e</sup>	3.15
35	23.98	1.41	24.23	1.43	97	69.71	4.32	69.74	4.32
36	30.98	1.31	30.84 <sup>b</sup>	1.29	98	132.43	5.55	132.41	5.54
37	30.93	1.31	30.84 <sup>b</sup>	1.29	99	135.28	5.71	135.31	5.70
38	30.81	1.31	30.84 <sup>b</sup>	1.29	100	71.90	4.36	71.94	4.37
39	<b>31.29</b>	<b>1.36</b>	<b>31.21</b>	<b>1.35</b>	101	71.77	3.68	71.88 <sup>d</sup>	3.68
40	<b>39.20</b>	<b>1.48</b>	<b>38.69</b>	<b>1.58</b>	102	40.21	1.58	40.33	1.59
41	<b>69.26</b>	<b>3.80</b>	<b>71.92</b>	<b>3.65</b>	103	68.39	4.22	68.38	4.22
42	<b>39.37</b>	<b>1.86; 1.44</b>	<b>77.34</b>	<b>3.70</b>	104	40.53	1.74; 1.38	40.72	1.74; 1.38
43	<b>64.86</b>	<b>4.39</b>	<b>66.10</b>	<b>4.32</b>	105	76.14	4.51	76.21	4.51
44	<b>73.88</b>	<b>3.65</b>	<b>74.08</b>	<b>3.910</b>	106	36.83	1.84; 1.78	36.96	1.84; 1.79
45	<b>74.28</b>	<b>3.95</b>	<b>74.28</b>	<b>3.915</b>	107	79.62	4.21	79.61	4.21
46	<b>68.25</b>	<b>3.67</b>	<b>67.75</b>	<b>3.78</b>	108	82.74	4.35	82.80	4.36
47	<b>101.24</b>	<b>-</b>	<b>101.59*</b>	<b>-</b>	109	26.59	1.78; 1.67	26.83	1.78; 1.66
48	41.95	1.83	41.92	1.77	110	32.30	1.47	32.47	1.48
49	72.40	3.94	72.45	3.92	111	83.81	3.89	83.87	3.89
50	44.07	2.26	44.41	2.25	112	73.27	4.27	73.31	4.27
50-CH <sub>3</sub>	16.58	1.03	16.72	1.03	113	39.78	2.10; 1.86	39.89	2.11; 1.86

51	134.46	5.62	134.59	5.64	114	75.31	4.36	75.14	4.37
52	134.74	5.51	134.69	5.50	115	45.13	2.99; 2.87	45.13	3.03; 2.90
53	74.06	4.05	74.06	4.06	a	134.82	7.79	134.76	7.80
54	34.93	1.77; 1.61	35.09	1.78; 1.61	b	106.82	5.95	106.79	5.95
55	27.79	1.69; 1.46	27.89	1.69; 1.46	c	169.66	-	169.57*	-
56	73.11	3.74	73.15 <sup>c</sup>	3.75	d	37.42	3.33	37.51	3.33
57	72.81	3.85	72.86	3.86	e	33.28	1.74	33.46	1.74
58	74.19	3.87	74.11	3.87	f	60.40	3.60	60.60	3.59
59	33.05	2.27; 1.66	33.16	2.26; 1.66					

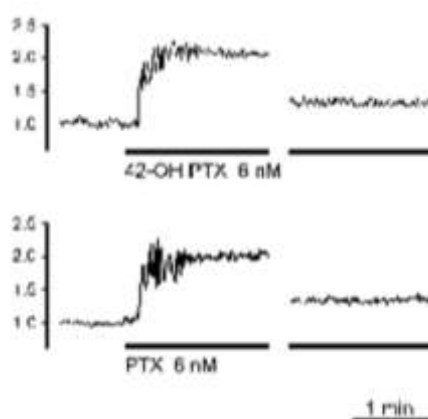
NMR spectra were run in CD<sub>3</sub>OD with one drop of D<sub>2</sub>O. \* these carbon chemical shifts emerged from a HMBC spectrum. <sup>a, c</sup> these two sets of carbons resonate partially overlapped in the HSQC spectrum and are exchangeable each other. <sup>b, c, d</sup> these three sets of carbons resonate totally overlapped in the HSQC spectrum. Significant chemical shift divergences between **1** and **2** have been printed in red.

It is to be noted that with regard to dihydropyrane moiety spanning from C43 through C47 some slight differences in <sup>1</sup>H and <sup>13</sup>C chemical shifts at positions 43 and 44, respectively, also were revealed between **1** and **2**; but they seemed reasonably coherent with the presence of the hydroxyl group at C42 in **2** (Table 1). We tried to gain further experimental NMR evidence consistent with the same stereochemistry as **1** at both C43 and C44 in **2**. With regard to this, the following data proved crucial. Multiplicity of H43 extrapolated from a z-filtered TOCSY was indicative of small <sup>3</sup>J<sub>H-H</sub> between such a proton and both H42 and H44. This pointed out a cis axial-equatorial relationship between H43 and H44. Likewise, multiplicity of H46 was indicative of a cis axial-equatorial relationship between H46 and H45 (SI). Moreover, absence of NOEs among H43, H44, H45, and H46 reasonably pointed out to no 1,3-diaxial orientation among them. And eventually, a strong HMBC correlation between H45 and C47 deriving from a large <sup>3</sup>J<sub>C-H</sub> indicated a preferential dihedral angle between H45 and C47 implying an anti relationship between these two atoms. In conclusion, apart from stereochemistry at C41 – which remains to be determined - our new compound was unambiguously defined as 42-hydroxy palytoxin.

A set of experiments was carried out to check the *in vitro* effect of 42-OH PLTX on skeletal muscle. To this end, 42-OH PLTX was applied to the bathing solution of isolated skeletal

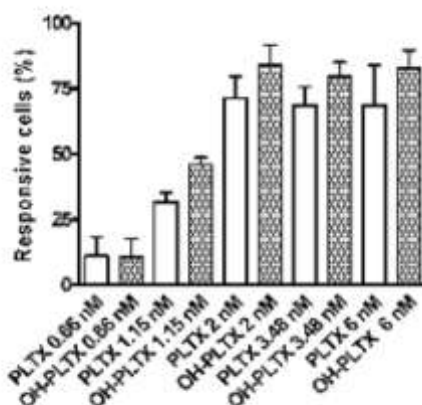
muscle cells, and the intracellular  $\text{Ca}^{2+}$  concentration ( $[\text{Ca}^{2+}]_i$ ) was measured by video-imaging.

Upon application of 42-OH PLTX (6 nM) to the bathing solution of skeletal myotubes, an increase of the  $[\text{Ca}^{2+}]_i$  was detected in  $82.5 \pm 7.0$  % of the observed cells ( $n = 4$  fields, 33 cells). The  $[\text{Ca}^{2+}]_i$  increase reached the maximum value within 30 s ( $113.3 \pm 3.8$  %) and it was still detectable 30 min after the toxin application, when the  $[\text{Ca}^{2+}]_i$  level reached a plateau and was  $16.1 \pm 1.9$  % higher than the  $[\text{Ca}^{2+}]_i$  at rest ( $n = 27$  cells; Figure 4). A similar effect was observed after application of 6 nM PLTX: the responsive cells were  $68.6 \pm 15.4$  % ( $n = 4$  fields; 38 cells), the peak of the  $[\text{Ca}^{2+}]_i$  transient was  $106.1 \pm 3.6$  % and the  $[\text{Ca}^{2+}]_i$  level was  $17.5 \pm 1.9$  % higher than that in control conditions after 30 min exposure to the toxin ( $n = 20$  cells; Figure 4).



**Figure 4.** Effect of **1** and **2** on the  $[\text{Ca}^{2+}]_i$ . Representative temporal plots of  $\text{Ca}^{2+}$  responses elicited in two different skeletal mouse myotubes by **1** and **2** (6 nM). Trace interruptions represent an interval of 30 min. Both **1** and **2** exhibited a long-lasting effect on  $[\text{Ca}^{2+}]_i$ .

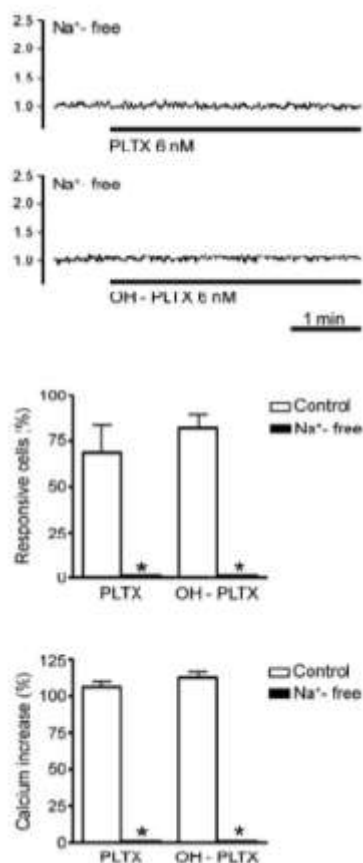
We also tested the effect of 42-OH PLTX on skeletal myotubes at different concentrations (0.67, 1.15, 2, and 3.48 nM). Although kinetics of the  $[\text{Ca}^{2+}]_i$  increases did not change, the number of responsive cells increased in a concentration-dependent manner. The effect saturated at concentrations higher than 2 nM. A similar concentration-dependency was observed when the effect of PLTX was investigated in the same experimental conditions (Figure 5).



**Figure 5.** Concentration-response curves for **1** and **2** induced  $[Ca^{2+}]_i$  response. The number of responsive cells showed the same dose-dependency in the presence of **1** and **2**. Each experimental point was carried out in 2 different cell preparations. For each experimental point, the minimum number of analyzed optical fields was 4 and the minimum number of observed cells was from 36.

PLTX is known to switch the  $Na^+/K^+$  pump in a channel permeable to monovalent cations, leading to potassium leak and concomitant sodium influx.<sup>34-35</sup> The increase of intracellular sodium concentration could cause an increase in  $[Ca^{2+}]_i$  by at least two mechanisms: 1) inducing an activation of voltage-gated calcium channels<sup>26, 36</sup>, 2) activating the  $Na^+/Ca^{2+}$  exchangers<sup>37-38</sup>.

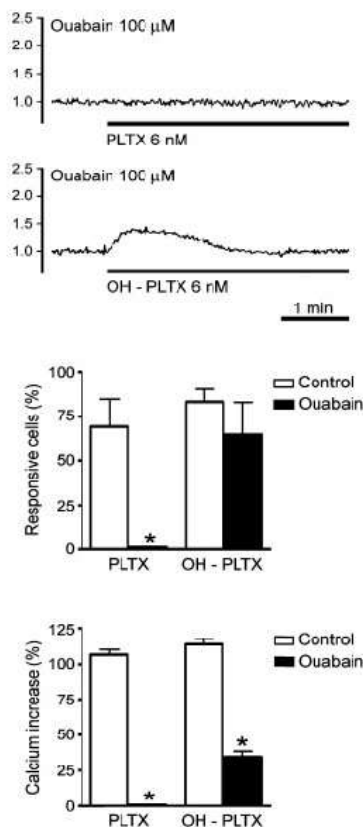
In order to evaluate how the effects of PLTXs on  $[Ca^{2+}]_i$  are related to the  $Na^+$  influx, some experiments were performed in a  $Na^+$ -free solution. In these conditions, neither PLTX (6 nM; n = 3 fields, 15 cells), nor 42-OH-PLTX (6 nM; n = 3 fields, 15 cells) were able to induce an  $[Ca^{2+}]_i$  variation, demonstrating that  $Na^+$  influx is a key event for the PLTXs induced  $Ca^{2+}$  influx into myotubes (Figure 6).



**Figure 6.** Effect of **1** and **2** on the  $[Ca^{2+}]_i$  in  $Na^+$ -free solution. Representative temporal plots of  $Ca^{2+}$  responses elicited by **1** and **2** (6 nM) in absence of extracellular  $Na^+$ . In all of the observed cells, neither **1** nor **2** was able to elicit an  $[Ca^{2+}]_i$  increase.

To test the role of  $Na^+/K^+$ -ATPase in the palytoxins induced effect on  $[Ca^{2+}]_i$ , we performed some experiments also in the presence of 100  $\mu$ M ouabain, a well-known blocker of  $Na^+/K^+$ -ATPases. The results of these experiments showed that the two toxins exhibit a different sensitivity to ouabain. Ouabain abolished  $[Ca^{2+}]_i$  increase induced by PLTX (6 nM;  $n = 3$  fields, 19 cells) and reduced from  $113.3 \pm 3.8\%$  to  $34.5 \pm 4.0\%$  the amplitude of  $[Ca^{2+}]_i$  transient elicited by 42-OH-PLTX (6 nM;  $n = 3$  fields, 25 cells). In spite of that, ouabain did not affect the number of responsive cells to 42-OH-PLTX ( $64.3 \pm 18.0\%$ ;  $n = 3$  fields, 25 cells) (Figure 7).





**Figure 7.** Effect of **1** and **2** on the  $[Ca^{2+}]_i$  in the presence of ouabain. Representative temporal plots of  $Ca^{2+}$  responses elicited by **1** and **2** (6 nM) in cells incubated with ouabain (100  $\mu M$ ). Ouabain prevented the  $[Ca^{2+}]_i$  increase induced by **1**. Although the glycoside did not significantly affect the number of cells responsive to **2**, it caused a remarkable reduction in the amplitude of the  $[Ca^{2+}]_i$  increase in all of the observed cells.

These results suggest the coexistence of a  $Na^+$ -dependent mechanism of action for 42-OH-PLTX independent from the  $Na^+/K^+$  pump.

To determine the degree of affinity of palytoxin and its 42-OH derivative towards the  $Na^+/K^+$  pump, molecular target of PLTX, competition experiments were performed using a purified porcine  $Na^+/K^+$ -ATPase and  $[^3H]$ -ouabain as a ligand. The two toxins inhibited the binding of 5 nM  $[^3H]$ -ouabain in a concentration-dependent manner and within the same concentration range. The calculated  $IC_{50}$  values were  $29.4 \pm 3.1$  and  $28.2 \pm 7.0$  nM for PLTX and 42-OH-PLTX, respectively.

As previously reported,<sup>30</sup> unlabelled ouabain displaced 5 nM  $[^3H]$ -ouabain bound showing a slightly higher affinity for the binding site with respect to the toxins, with a calculated  $IC_{50}$  value of  $9.0 \pm 0.9$  nM. Results are summarized in Table 2.

**Table 2.** Displacement of ouabain, **1** and **2** against [<sup>3</sup>H]-ouabain binding to purified Na<sup>+</sup>/K<sup>+</sup>-ATPase.

Substance	IC <sub>50</sub> (nM)	n <sub>H</sub>
Ouabain	9.0 ± 0.9	0.9 ± 0.1
Palytoxin	29.4 ± 3.1	0.8 ± 0.1
42-OH-Palytoxin	28.2 ± 7.0	0.8 ± 0.1

Values are the mean ± S.E.M. of three separate determinations performed in triplicate. IC<sub>50</sub> values and Hill's coefficients (n<sub>H</sub>) were calculated by nonlinear regression using a four parameters curve-fitting algorithm of the SigmaPlot software.

Although the two toxins exhibit the same binding affinity to a purified Na<sup>+</sup>/K<sup>+</sup>-ATPase and a similar effect on [Ca<sup>2+</sup>]<sub>i</sub> levels in skeletal muscle cells, Na<sup>+</sup>/K<sup>+</sup>-ATPase does not seem to be the unique target for 42-OH-PLTX because of the different sensitivity to ouabain detected using videoimaging studies. Nevertheless, the acute oral toxicity studies performed in mice indicate a similar lethal potency for PLTX and 42-OH-PLTX with LD<sub>50</sub> of 767 µg/kg (C.L. 549-1039 µg/kg)<sup>29</sup> and 652 µg/kg (C.L. 384 – 1018 µg/kg) (Sosa et al. unpublished results), respectively.

In conclusion, a new palytoxin congener 42-OH-PLTX was characterized in *P. toxica*. The new compound shows *in vitro* and *in vivo* effects similar to that of PLTX, although an additional mechanism of action can be hypothesized. Studies are in progress to fully characterize the peculiar mechanism of action of 42-OH-PLTX.

Bearing in mind that *P. toxica* sample we analyzed had been collected exactly from the legendary tide pool located in Hana district and considering that 42-OH PLTX and PLTX itself seem to share the same biological effects, we were tempted to venture an answer to the ancient mystery concerning the famous *limu-make-o-Hana*. Might 42-hydroxy palytoxin play a role in toxicity of the “deadly seaweed” Hawaiians used for making their spears fatal?

### 8.3. References

1. Malo, D. (1951) In *Hawaiian Antiquities* (B. P. Bishop Museum Special Publication 2, ed. 2, Honolulu) pp 201-226.
2. Moore, R. E., Helfrich, P., and Patterson, G. M. L. (1982) The deadly seaweed of Hana. *Oceanus* 25, 54-63.
3. Moore, R. E., and Scheuer, P. J. (1971) Palytoxin: a new marine toxin from a Coelenterate. *Science (Washington, D.C.)* 172, 495-498.

4. Walsh, G. E., and Bowers, R. E. (1971) A review of Hawaiian zoanthids with descriptions of three new species. *Zool. J. Linn. Soc.* 50, 161-180.
5. Wiles, J. S., Vick, J. A., and Christensen, M. K. (1974) Toxicological evaluation of palytoxin in several animal species. *Toxicon* 12, 427-433.
6. Moore, R. E., Dietrich, R. F., Hatton, B., Higa, T., and Scheuer P. J. (1975) The nature of the  $\lambda$  263 Chromophore in the Palytoxins. *J. Org. Chem.* 40, 540-542.
7. Macfarlane, R. D., Uemura, D., Ueda, K., and Hirata, Y. (1980) Californium-252 plasma desorption mass spectrometry of palytoxin. *J. Am. Chem. Soc.* 102, 875-876.
8. a) Uemura, D., Ueda, K., Hirata, Y., Naoki, H., and Iwashita, T. (1981) Further studies on palytoxin. I. *Tetrahedron Lett.* 21, 1909-1912 b) Uemura, D., Ueda, K., Hirata, Y., Naoki, H., and Iwashita, T. (1981) Further studies on Palytoxin. II. Structure of Palytoxin. *Tetrahedron Lett.* 21, 2781-2784.
9. Moore, R. E., and Bartolini, G. (1981) Structure of Palytoxin. *J. Am. Chem. Soc.* 103, 2491-2494.
10. Nakamura, K., Kitamura, M., and Uemura, D. (2009) Biologically active marine natural products. *Heterocycles* 78, 1-17.
11. a) Klein, L. L., McWhorter Jr, W. W., Ko, S. S., Pfaff, K. P., Kishi, Y., Uemura, D., and Hirata, Y. (1982) Stereochemistry of palytoxin. Part 1. C85-C115 segment. *J. Am. Chem. Soc.* 104, 7362-7364. b) Ko, S. S., Finan, J. M., Yonaga, M., Kishi, Y., Uemura, D., and Hirata, Y. (1982) Stereochemistry of palytoxin. Part 2. C1-C6, C47-C74, and C77-C83 segments. *J. Am. Chem. Soc.* 104, 7364- 7367. c) Fujioka, H., Christ, W. J., Cha, J. K., Leder, J., Kishi, Y., Uemura, D., and Hirata, Y. (1982) Stereochemistry of Palytoxin. Part 3. C7-C51 segment. *J. Am. Chem. Soc.* 104, 7367- 7369. d) Cha, J. K., Christ, W. J., Finan, J. M., Fujioka, H., Kishi, Y., Klein, L. L., Ko, S. S., Leder, J., McWhorter Jr, W. W., Pfaff, K. P., Yonaga, M., Uemura, D., and Hirata, Y. (1982) Stereochemistry of palytoxin. Part 4. Complete Structure. *J. Am. Chem. Soc.* 104, 7369-7371. e) Moore, R. E., Bartolini, G., Barchi, J., Bothner-By, A. A., Dadok, J., and Ford, J. (1982) Absolute stereochemistry of palytoxin. *J. Am. Chem. Soc.* 104, 3776-3779.
12. Uemura, D., Hirata, Y., Iwashita, T., and Naoki, H. (1985) Studies on palytoxins. *Tetrahedron* 41, 1007-1017.
13. Kimura, S., Hashimoto, Y., and Yamazato, K. (1973) Toxicity of the zoanthid *Palythoa tuberculosa*. *Toxicon* 10, 611-617.

14. Seemann, P., Gernert, C., Schmitt, S., Mebs, D., and Hentschel, U. (2009) Detection of hemolytic bacteria from *Palythoa caribaeorum* (Cnidaria, Zoantharia) using a novel palytoxin –screening assay. *Antonie van Leeuwenhoek* (DOI: 10.1007/s10482-009-9353-4).
15. Maeda, M., Kodama, T., Tanaka, T., Yoshizumi, H., Nomoto, K., Takemoto, T., and Fujiki, T. (1985) Structure of insecticidal substances isolated from a red alga, *Chondria armata*. In Symposium Papers, 27<sup>th</sup> Symposium on the Chemistry of Natural Products, Hiroshima, Japan, pp 616-623.
16. a) Yasumoto, T., Yasumura, D., Ohizumi, Y., Takahashi, M., Alcalá, A. C., and Alcalá, L. C. (1986) Palytoxin in two species of xanthid crab from the Philippines. *Agric. Biol. Chem.* 50, 163-167. b) Alcalá, A. C., Alcalá, L. C., Garth, J. S., Yasumura, D., and Yasumoto, T. (1988) Human fatality due to ingestion of the crab *Demania reynaudii* that contained a palytoxin-like toxin. *Toxicon* 26, 105-107.
17. Fukui, M., Murata, M., Inoue, A., Gawel, M., and Yasumoto, T. (1987) Occurrence of palytoxin in the trigger fish *Melichthys vidua*. *Toxicon* 25, 1121-1124.
18. Usami, M., Satake, M., Ishida, S., Inoue, A., Kan, Y., and Yasumoto, T. (1995) Palytoxin analogs from the dinoflagellate *Ostreopsis siamensis*. *J. Am. Chem. Soc.* 117, 5389-5390.
19. Lenoir, S., Ten-Hage, L., Turquet, J., Quod, J. P., Bernard, C., and Hennion, M. C. (2004) First evidence of palytoxin analogues from an *Ostreopsis mascarenensis* (Dinophyceae) benthic bloom in southwestern Indian Ocean. *J. Phycol.* 40, 1042-1051.
20. Ciminiello, P., Dell'Aversano, C., Fattorusso, E., Forino, M., Tartaglione, L., Grillo, C., and Melchiorre, N. (2008) LC-MS/MS and HRMS/MS data demonstrated the presence of putative palytoxin and the novel ovatoxin-a in plankton collected during the Ligurian 2006 toxic outbreak. *J. Am. Soc. Mass Spectrom.* 19, 111-120.
21. Raybould, T. J. G. (1991) Toxin production and immunoassay development I. Palytoxin (Annual/Final report, Hawaii). DTIC Accession Number: ADA239837. U.S. Army Medical Research and Development Command, Fort Detrick, Frederick, Maryland, pp 21702-5012.
22. Bignami, G. S., Raybould, T. J. G., Sachinvala, N. D., Grothaus, P. G., Simpson, S. B., Lazo, C. B., Byrnes, J. B., Moore, R. E., and Vann, D. C. (1992) Monoclonal antibody-based enzyme-linked immunoassays for the measurement of palytoxin in biological samples. *Toxicon* 30, 687-700.
23. Corpuz, G. P., Grothaus, P. G., Waller, D. F., and Bignami, G. S. In: Hokama Y, Scheuer P, J, Yasumoto T (1995) in Proceedings of the international symposium on ciguatera marine natural product- Asian Pacific Research Foundation- Honolulu, pp145-153.

24. Bellocchi, M., Ronzitti, G., Milandri, A., Melchiorre, N., Grillo, C., Poletti, R., Yasumoto, T., and Rossini, G. P. (2008) A cytolytic assay for the measurement of palytoxin based on a cultured monolayer cell line. *Anal. Biochem.* 374, 48-55.
25. Munday, R. (2008) in *Seafood and Freshwater Toxins: Pharmacology, Physiology, and Detection*, Second Edition, ed Botana L-M (CRC press), pp 693-713.
26. Ecault, E., and Sauviat, M-P. (1991) Characterization of the palytoxin-induced sodium conductance in frog skeletal muscle. *British Journal Pharmacology* 102, 523-529.
27. Lorenzon, P., Bernareggi, A., Degasperis, V., Nurowska, E., Wernig, A., and Ruzzier, F. (2002) Properties of primary mouse myoblasts expanded in culture. *Experimental Cell Research* 278, 84-91.
28. Frelin, C., and van Renterghem, C. (1995) Palytoxin. Recent electrophysiological and Pharmacological evidence for several mechanisms of action. *General Pharmacology* 26, 33-37.
29. Sosa, S., Del Favero, G., De Bortoli, M., Vita, F., Soranzo, M. R., Beltramo, D., Ardizzone, M., Tubaro, A. (2009) Palytoxin toxicity after acute oral administration in mice. *Toxicology Letters*, doi: 10.1016/j.toxlet.2009.09.009
30. Habermann, E., and Chatwal, G. S. (1982) Ouabain inhibits the increase due to palytoxin of cation permeability of erythrocytes. *Naunyn-Schmiedeberg's Arch Pharmacol* 319, 101-107.
31. Ciminiello, P., Dell'Aversano, C., Fattorusso, E., Forino, M., Magno, G. S., Tartaglione, L., Grillo, C., and Melchiorre, N. (2006) The Genoa 2005 outbreak. Determination of putative palytoxin in Mediterranean *Ostreopsis ovata* by a new liquid chromatography tandem mass spectrometry method. *Anal. Chem.* 78, 6153-6159.
32. Taniyama, S., Arakawa, O., Terada, M., Nishio, S., Taktani, T., Mahmud, Y., and Noguchi, T. (2003) *Ostreopsis* sp., a Possible Origin of Palytoxin (PTX) in Parrotfish *Scarus ovifrons*. *Toxicon* 41, 605-611.
33. Ukena, T., Satake, M., Usami, M., Oshima, Y., Naoki, H., Fujita, T., Kan, Y., and Yasumoto, T. (2001) Structure Elucidation of Ostreocin D, a Palytoxin Analog Isolated from the Dinoflagellate *Ostreopsis siamensis*. *Biosci. Biotechnol. Biochem.* 65, 2585-2588.
34. Scheiner-Bobis, G., Zu Heringdorf, D. M., Christ, M., Habermann, E. (1994) Palytoxin induces K<sup>+</sup> efflux from yeast cells expressing the mammalian sodium pump. *Mol. Pharm.* 45, 1132-1136.

- 
35. Redondo, J., Fiedler, B., Scheiner-Bobis, G. (1996) Palytoxin-induced  $\text{Na}^+$  influx into yeast cells expressing the mammalian sodium pump is due to the formation of a channel within the enzyme. *Mol. Pharm.* 49, 49-57.
  36. Vale, C., Alfonso, A., Sunol, C., Vieytes, M., Botana, L. (2006) Modulation of calcium entry and glutamate release in cultured cerebellar granule cells by palytoxin. *Journal of Neuroscience Research*, 83, 1393-1406.
  37. Ishii, K., Ito, K. M., Uemura, D., Ito, K. (1997) Possible mechanism of palytoxin-induced  $\text{Ca}^{2+}$  mobilization in porcine coronary artery. *JPET* 281, 1077-1084.
  38. Ishii, K., Ikeda, M., Ito, K. (1997) Characteristics of palytoxin-induced cation currents and  $\text{Ca}^{2+}$  mobilization in smooth muscle cells of rabbit portal vein. *Naunyn-Schmiedeberg's Archives of Pharmacology*, 355, 103-110.

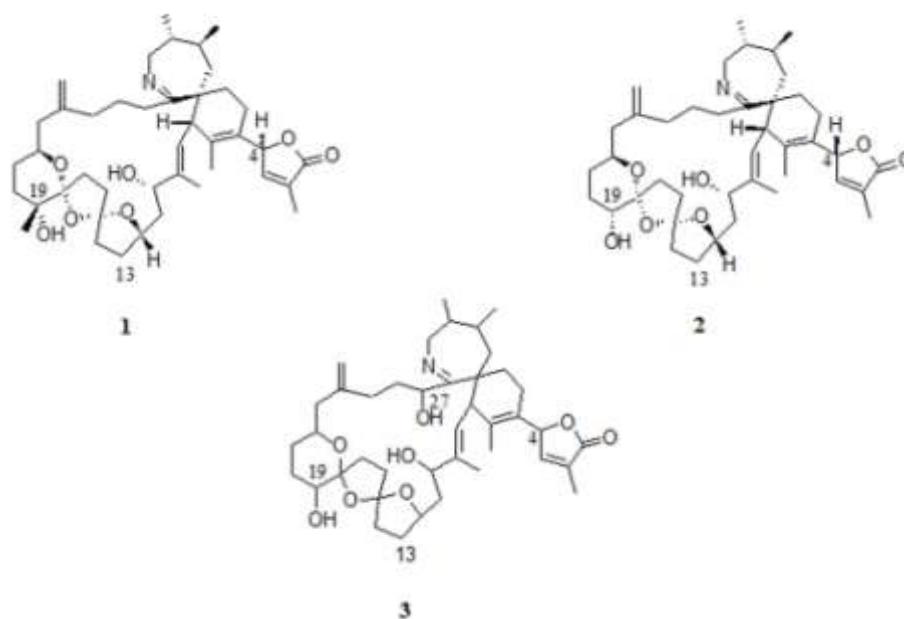


## Chapter 9

**27-hydroxy-13-desmethylspirolide C and 27-oxo-13,19-didesmethylspirolide C: two new spirolides from Adriatic *Alexandrium ostenfeldii***

The widespread toxic dinoflagellate *Alexandrium ostenfeldii* produces different classes of marine biotoxins depending on its geographical origin. Canadian *A. ostenfeldii* is reported as the producer of spirolides (SPXs);<sup>1</sup> while paralytic shellfish poisoning (PSP) toxins have been detected in *A. ostenfeldii* strains isolated from New Zealander seawater.<sup>2</sup> Even more complex resulted the toxin content of Scandinavian *A. ostenfeldii* extracts, in which both spirolides and PSP toxins have been individuated.<sup>3</sup>

Around the onset of the new millennium, a massive bloom of *A. ostenfeldii* across the Adriatic Sea prompted us to investigate its toxin profile. Our initial studies based on combination of liquid chromatography with tandem mass spectrometry (LC-MS/MS) identified the Adriatic *A. ostenfeldii* as the producing organism of only spirolide toxins.<sup>4</sup> Among the spirolides known at the time of our first analyses, 13-desmethyl spirolide C (**1**, Figure 1) was unambiguously detected as the major component of the *A. ostenfeldii* toxic extract.



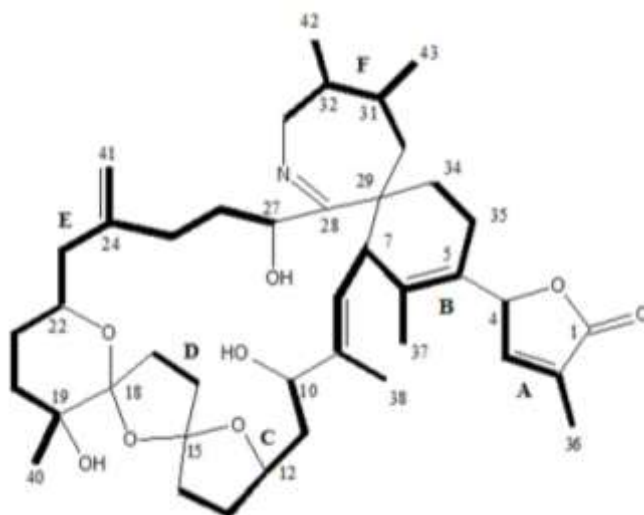
**Figure 1.** Stereostructure of 13-desmethyl spirolide C (**1**) devoid of configuration at C4; full stereostructure of 13,19-didesmethyl spirolide C (**2**); planar structure of 27-hydroxy-13,19-didesmethyl spirolide C (**3**).



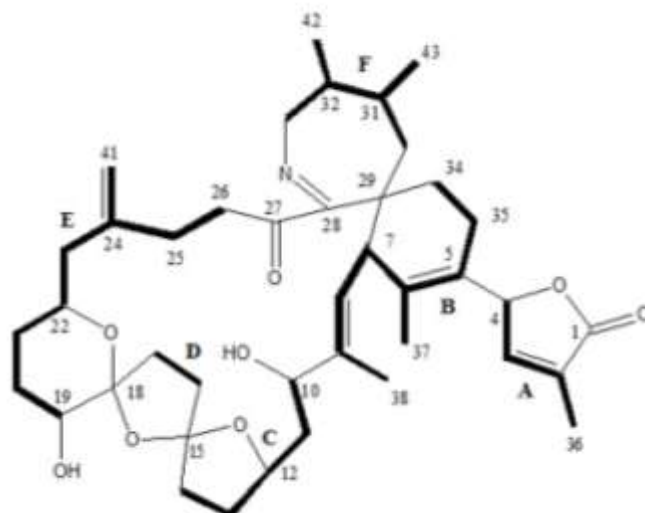
Successive LC-MS/MS- and NMR-based studies<sup>6</sup> - carried out on much larger extracts obtained from Adriatic *A. ostentfeldii* cultures – along with **1** led us to isolate and structurally characterize two further major spirolides, identified as 13,19-didesmethyl spirolide C (**2**, Figure 1) and 27-hydroxy-13,19-didesmethyl spirolide C (**3**, Figure 1), respectively. The former (**2**) had been isolated and structurally characterized by MacKinnon in 2006,<sup>5</sup> while the latter (**3**) emerged as an unreported compound. In the frame of this study, we have recently elucidated the whole relative stereochemistry of **2** as well as shed some light on its conformational behavior in solution.<sup>7</sup> This study can be instrumental for a better understanding of the molecular bases of spirolide biological activity, which is far from being totally and unambiguously defined. To this day, in fact, pharmacological studies have defined spirolides as fast-acting toxins, considering that in the mouse bioassay they induce rapid onset of symptoms akin to those reported for the acute toxicity of PSP-toxins, followed by death within minutes from the intraperitoneal injection.<sup>8-10</sup>

In addition to the above mentioned spirolides (**1-3**), our LC-MS/MS investigation of the Adriatic *A. ostentfeldii* toxin profile highlighted the presence of a number of co-occurring minor spirolides, for which we could only venture MS-based structural hypotheses, as they had been isolated in too small amounts for any NMR investigation.<sup>6</sup>

In the present paper, we report on isolation and structural characterization of two among the above minor spirolides. High resolution MS (HRMS), HRMS/MS and NMR experiments were used to identify them as the new 27-hydroxy-13-desmethylspirolide C (**4**, Figure 2) and 27-oxo-13,19-didesmethylspirolide C (**5**, Figure 3), respectively.



**Figure 2.** Planar structure of 27-hydroxy-13-desmethylspirolide C (**4**). Bold lines represent the six spin systems (A-F) emerging from COSY and z-TOCSY experiments.



**Figure 3.** Planar structure of 27-oxo-13,19-didesmethylspirolide C (**5**). Bold lines represent the six spin systems (A-F) emerging from a TOCSY experiment.

## 9.1. Experimental

### 9.1.1. Chemicals

All organic solvents were of distilled-in-glass grade (Carlo Erba, Milan, Italy). Water was distilled and passed through a MilliQ H<sub>2</sub>O purification system (Millipore Ltd., Bedford, MA, USA). Formic acid (95-97%, Laboratory grade) and ammonium formate (AR grade) were purchased from Sigma Aldrich (Steinheim, Germany). Spirolide 13-desMeC standard solution was kindly provided by Dr Michael A. Quilliam (Institute for Marine Biosciences, National Research Council of Canada, Halifax, NS, Canada).

### 9.1.2. Cultures of *Alexandrium ostenfeldii*

*Alexandrium ostenfeldii* (Paulsen) Balech et Tangen (1985)<sup>12</sup> was collected in the North-Western Adriatic Sea along the Emilia-Romagna coast (Italy) in November 2003. The dinoflagellate was isolated by the capillary pipette method<sup>13</sup> and after an initial growth in microplates, unialgal cultures were grown in sterile Erlenmeyer flasks sealed with cotton plugs at 20 °C under a 16:8 h LD cycle (ca. 90 μmol m<sup>-2</sup> s<sup>-1</sup> from cool white lamps); nutrients were added at the f/2 concentration,<sup>14</sup> and H<sub>2</sub>O salinity was adjusted to 30 Practical Salinity Units (psu, which corresponds to grams of salts per liter of solution). Cells from a total culture volume of 60 L were collected at stationary phase on the 30<sup>th</sup> day of growth first by gravity filtration through 0.45 μm Millipore filters and then by centrifugation at 3000 g for 15 min at 10 °C. Both cell pellets and growth mediums were saved for analyses. Cell counts were made every other day in settling chambers by the Utermöhl method.<sup>15</sup>

### 9.1.3. Extraction and isolation

Cultured cell pellets ( $40 \times 10^7$  cells) were suspended in a MeOH/H<sub>2</sub>O (8:2, v/v) solution (20 mL) and sonicated for 5 min in pulse mode while cooling in an ice bath. The mixture was centrifuged at 5000 rpm for 10 min and the pellet was washed twice with 20 mL of MeOH/H<sub>2</sub>O (8:2, v/v). The supernatants were combined and the volume was adjusted to 60 mL with the extraction solvent. The growth medium fraction (60 L) was separately filtered through 0.45  $\mu$ m filters (Millipore, Molsheim, France). The filtrate was loaded on Sep-Pak C-18 plus cartridges (Waters Corporation, Milford, MA, USA) equilibrated with H<sub>2</sub>O. The columns were eluted each with 15 mL H<sub>2</sub>O, 15 mL H<sub>2</sub>O/CH<sub>3</sub>CN (7:3, v/v), 15 mL of H<sub>2</sub>O/CH<sub>3</sub>CN (1:1, v/v) and 15 mL CH<sub>3</sub>CN. The pellet extract and all the SPE eluates were combined up to a total volume of 500 mL. A 1 mL aliquot was saved for LC-MS analyses and the remaining part was evaporated to dryness. The residue was dissolved in 4 mL of H<sub>2</sub>O/CH<sub>3</sub>CN (9:1, v/v), and the solution was loaded on a ODS column equilibrated with the same solution. The column was sequentially eluted with 150 mL of H<sub>2</sub>O/CH<sub>3</sub>CN (9:1, 7:3, 1:1, v/v) solutions and CH<sub>3</sub>CN 100%. The spiroolides eluted in the H<sub>2</sub>O/CH<sub>3</sub>CN (1:1, v/v) and CH<sub>3</sub>CN 100% fractions. The successive clean-up step was carried out by injecting the spiroolides-containing fractions on a 10  $\mu$ m Luna C18 250  $\times$  10 mm column (Phenomenex, Torrance, CA, USA) isocratically eluted with H<sub>2</sub>O/CH<sub>3</sub>CN (8:2, v/v), 0.1% trifluoroacetic acid. The flow rate was 2 mL min<sup>-1</sup> (UV detector, 210 nm). Final purification was accomplished by a 3  $\mu$ m Hypersil C8 BDS, 50  $\times$  4.60 mm column (Phenomenex, Torrance, CA, USA) eluted with H<sub>2</sub>O (eluent A) and CH<sub>3</sub>CN (eluent B). A gradient elution was used, namely 10 to 30 % B in 4 min, 30 % to 80 % B in 24 min, 80 % to 100 % B in 4 min, 100 % B for 15 min. The flow rate was 750  $\mu$ L min<sup>-1</sup> (UV detector, 210 nm). Finally, 30  $\mu$ g of **4** and 20  $\mu$ g of **5** were obtained as pure compounds. LC-MS analyses were carried out throughout the purification procedure in order to check for the presence of spiroolides in each fraction.

### 9.1.4. Liquid chromatography-mass spectrometry (LC-MS)

LC-MS analyses were accomplished by using a 3  $\mu$ m Hyperclone C8 BDS, 50  $\times$  2.00 mm column (Phenomenex, Torrance, CA, USA) at room temperature. Eluent A was H<sub>2</sub>O and B was a 95% CH<sub>3</sub>CN/H<sub>2</sub>O solution, both eluents containing 2 mM ammonium formate and 50 mM formic acid. The flow rate was 200  $\mu$ L min<sup>-1</sup>. A gradient elution (10 to 100% B in 10 min followed by 100% B for 15 min) was used. High resolution (HR) MS and MS/MS spectra were acquired by using an Agilent HPLC model 1100 (Palo Alto, CA, USA) coupled to a linear ion trap LTQ Orbitrap XL<sup>TM</sup> hybrid Fourier Transform MS (FTMS) equipped with an

ESI ION MAX<sup>TM</sup> source (Thermo-Fisher, San José, CA, USA). MS experiments (positive ions) were acquired in the range  $m/z$  500-800 at the 100,000 resolving power setting. The following source settings were used: a source voltage of 4.2 kV, a capillary temperature of 350°C, a capillary voltage of 2.0 V, a tube lens voltage of 75 V, a sheath gas and an auxiliary gas flow of 32 and 9 (arbitrary units), respectively. MS/MS spectra were acquired in high collision dissociation (HCD) mode at the 60,000 resolving power setting by fragmenting the  $[M+H]^+$  ion of both **4** ( $m/z$  708.5) and **5** ( $m/z$  692.5) with a collision energy of 50% and an activation time of 30 msec. Calculation of elemental formulas of relevant  $[M+H]^+$  ions as well as of fragment ions contained in the MS/MS spectra was performed by using the Xcalibur software.

### 9.1.5. Nuclear Magnetic Resonance (NMR)

NMR spectra were measured on a Varian Unity Inova 700 spectrometer equipped with a 13C Enhanced HCN Cold Probe. Shigemi 5 mm NMR tubes and CD<sub>3</sub>OD as an internal standard ( $\delta_H$  3.31 and  $\delta_{49.0}$ ) were used. Standard Varian pulse sequences were employed for the respective classes of spectra; solvent signal suppression by presaturation was used when required. Assignments were checked from 2D <sup>1</sup>H COSY, TOCSY, and ROESY spectra.

Quantification of 27-hydroxy-13-desmethylspiroside C (4  $\mu$ g) and 27-oxo-13,19-didesmethylspiroside C (6  $\mu$ g) was carried out by running an <sup>1</sup>H NMR spectrum for each of the two spiroside employing pyridine as an internal standard. The <sup>1</sup>H NMR spectrum for each spiroside was performed setting a d1 value at 7.0 sec in order to allow a complete relaxation of the pyridine standard to equilibrium. The T<sub>1</sub> (0.70 sec) of pyridine was evaluated through the inversion-recovery T<sub>1</sub> experiment. The amount of each spiroside was then quantified utilizing the area per proton (determined by integration). In particular, quantification of each spiroside was carried out measuring the area of the well isolated olefinic protons at C-3.

### 9.1.6. 27-hydroxy-13-desmethylspiroside C

HRMS (positive mode)  $m/z$  708.4466 (calcd for C<sub>42</sub>H<sub>61</sub>NO<sub>8</sub>  $[M+H]^+$  708.4470). HRMS/MS data are contained in Figure 4. NMR chemical shifts are reported in table 1. Significant ROE correlations: H-3/H<sub>3</sub>-37; H-4/H-35a; H-7/H-27; H-7/H<sub>3</sub>-38; H-8/H-10; H-8/H-43; H-8/H-25a; H-10/H-43; H-12/H-16a; H-17a/H-40; H-17b/H-40; H-20a/H-42; H-21b/H-40; H-22/H-25b; H-25a/H-43; H-33b/H-34b.

### 9.1.7. 27-oxo-13,19-didesmethylspirolide C

HRESIMS (positive mode)  $m/z$  692.4148 (calcd for  $C_{41}H_{57}NO_8$   $[M+H]^+$  692.4157). HRMS/MS data are contained in Figure 4. NMR chemical shifts are reported in table 1. Significant ROE correlations: H-3/H<sub>3</sub>-37; H-4/H-35a; H-7/H<sub>3</sub>-38; H-8/H-10; H-8/H-43; H-8/H-25a; H-10/H-43; H-12/H-16a; H-17b/H-19; H-20a/H-42; H-21b/H-40; H-22/H-25b; H-25a/H-43; H-33b/H-34b.

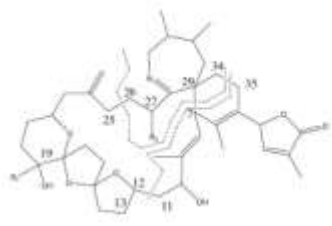
## 9.2. Results and Discussion

From large scale cultures of Adriatic *A. ostefeldii* we isolated and structurally defined two of the minor SPXs detected in our previous study, basing on LC-MS/MS data acquired at unit resolution:<sup>6</sup>

- 1) **4**: a compound at  $m/z$  708.5 eluting 0.48 min later than **3** and originating A-type fragments shifted 14 amu higher than **3** but the same B-type fragment as **3** in its MS/MS spectrum;
- 2) **5**: a compound with a protonated ion at  $m/z$  692.5, an isobaric analog of **1**, eluting 2.3 min later and paralleling **1** in A-type fragments but with a different B-type fragment (at  $m/z$  178 versus  $m/z$  164 in **1**) in its MS/MS spectrum.

To this regard, it is worth recalling that SPXs give rise to typical MS/MS fragmentation pattern<sup>11</sup> (Figure 4) characterized by:

- Ions due to loss of a number of water molecules from the  $[M+H]^+$ ;
- A-type fragment ions deriving from the pseudo-molecular ion by cleavage between C-11/C-12, C-29/C-7, C-34/C-35, and associated water losses;
- B-type fragment ion deriving from the A-type fragment by cleavage between C25/C26.



Spirolide	R <sub>1</sub>	R <sub>2</sub>	[M+H] <sup>+</sup> ( <i>m/z</i> )	A-type Fragments		B-type Fragments	
				( <i>m/z</i> )	Elemental formula	( <i>m/z</i> )	Elemental formula
<b>1</b> 13-desMeC	CH <sub>3</sub>	H	692.4492	462.3194	C <sub>27</sub> H <sub>44</sub> NO <sub>3</sub>	164.1427	C <sub>11</sub> H <sub>18</sub> N
				444.3090	C <sub>27</sub> H <sub>42</sub> NO <sub>4</sub>		
				426.2985	C <sub>27</sub> H <sub>40</sub> NO <sub>5</sub>		
<b>3</b> 27-OH-13,19-didesMeC	H	OH	694.4319	464.3004	C <sub>26</sub> H <sub>42</sub> NO <sub>6</sub>	180.1383	C <sub>11</sub> H <sub>18</sub> NO
				446.2900	C <sub>26</sub> H <sub>40</sub> NO <sub>5</sub>		
				428.2794	C <sub>26</sub> H <sub>38</sub> NO <sub>4</sub>		
				410.2689	C <sub>26</sub> H <sub>36</sub> NO <sub>3</sub>		
<b>4</b> 27-OH-13-desMeC	CH <sub>3</sub>	OH	708.4466	478.3160	C <sub>27</sub> H <sub>44</sub> NO <sub>6</sub>	180.1381	C <sub>11</sub> H <sub>18</sub> NO
				460.3053	C <sub>27</sub> H <sub>42</sub> NO <sub>5</sub>		
				442.2948	C <sub>27</sub> H <sub>40</sub> NO <sub>4</sub>		
<b>5</b> 27-oxo-13,19-didesMeC	H	O=	692.4148	444.2744	C <sub>26</sub> H <sub>38</sub> NO <sub>5</sub>	178.1223	C <sub>11</sub> H <sub>16</sub> NO

**Figure 4.** Accurate mass measurements, and elemental formulae for pseudo-molecular and diagnostic fragment ions of spiroldes **1**, **3**, **4**, and **5**.

Determination of the planar structure of the two novel spiroldes was achieved through HRMS/MSMS- and NMR-based techniques. Carbon chemical shifts of both compounds were not provided, as their very small amount (Experimental Section) kept us from obtaining neither reliable 1D-NMR <sup>13</sup>C spectra nor more sensitive 2D-NMR heteronuclear experiments, such as HMQC and HMBC. Nevertheless, basing on the experimental data in our hands we could confidently suggest the planar structure of the two novel spiroldes as 27-hydroxy-13-desmethyl spirolide C (**4**), and 27-oxo-13,19-didesmethyl spirolide C (**5**), respectively.

#### 9.2.1. 27-hydroxy-13-desmethylspirolide C: Structure determination (**4**)

The HRMS spectrum of **4** showed an [M+H]<sup>+</sup> ion at *m/z* 708.4466, which allowed to infer the molecular formula C<sub>42</sub>H<sub>61</sub>NO<sub>8</sub> to the molecule ( $\Delta = -0.557$  ppm).

Preliminary NMR investigation was instrumental for assessing a strict structural analogy of this new compound with 27-hydroxy-13,19-didesmethyl spirolide C (**3**), in comparison to which **4** possessed an extra carbon and two more hydrogen atoms. Hence, we could refer to the NMR data of **3** as a guide in elucidating the planar structure of **4** (Table.1).

**Table 1.** NMR spectroscopic data (700 MHz, CD<sub>3</sub>OD) for 13-desmethyl spiroside C (1), 27-hydroxy-13, 19-didesmethyl spiroside C (3), 27-hydroxy-13-desmethyl spiroside C (4), and 27-oxo-13,19-didesmethyl spiroside C (5)

position	13-desmethyl spiroside C (1)	27-hydroxy-13,19- didesmethyl spiroside C (3)	27-hydroxy-13- desmethyl spiroside C (4)	27-oxo-13, 19- didesmethyl spiroside C (5)
	$\delta_{\text{H}}$	$\delta_{\text{H}}$	$\delta_{\text{H}}$	$\delta_{\text{H}}$
1	-	-	-	-
2	-	-	-	-
3	7.11	7.15	7.15	7.14
4	5.94	5.97	5.96	5.94
5	-	-	-	-
6	-	-	-	-
7	3.58	3.87	3.86	4.10
8	5.17	5.20	5.21	5.12
9	-	-	-	-
10	4.10	4.11	4.13	4.06
11	1.37, 2.24	1.41, 2.33	1.42, 2.30	1.53, 2.16
12	4.28	4.35	4.31	4.39
13	1.70, 2.30	1.77, 2.30	1.75, 2.30	1.78, 2.29
14	1.94, 2.30	1.98, 2.29	1.97, 2.30	1.91, 2.20
15	-	-	-	-
16	2.04, 2.20	1.92, 2.22 <sup>a</sup>	2.06, 2.16 <sup>a</sup>	1.91, 2.21
17	1.79, 2.20	2.06, 2.12 <sup>a</sup>	1.86, 2.08 <sup>a</sup>	2.05, 2.07
18	-	-	-	-
19	-	3.37	-	3.36
20	1.43, 1.81	1.56, 1.71	1.45, 1.83	1.65, 1.70
21	1.29, 1.54	1.16, 1.68	1.21, 1.50	1.19, 1.65
22	4.01	3.94	4.00	3.89
23	2.00, 2.36	2.06, 2.35	2.03, 2.38	2.02, 2.31
24	-	-	-	-
25	1.59, 2.07	1.66, 1.89	1.60, 1.81	2.18, 2.20
26	1.38, 2.03	1.45, 2.42	1.41, 2.42	2.60, 3.06
27	2.31, 2.31	4.22	4.20	-
28	-	-	-	-
29	-	-	-	-
30	1.54, 1.71	1.61, 1.68	1.64, 1.69	1.65, 1.72
31	1.11	1.06	1.00	1.21
32	1.37	1.44	1.41	1.54
33	3.45, 3.78	3.57, 3.89	3.56, 3.86	3.69, 3.89
34	1.71, 1.94	1.87, 1.96	1.93, 2.07	1.96, 2.20
35	1.55, 2.24	1.55, 2.14	1.55, 2.15	1.54, 2.06
36	1.89	1.94	1.92	1.90

<b>37</b>	1.71	1.77	1.75	1.66
<b>38</b>	1.87	1.93	1.91	1.62
<b>39</b>	-	-	-	-
<b>40</b>	1.19	-	1.19	-
<b>41</b>	4.75, 4.76	4.78, 4.80	4.77, 4.79	4.77, 4.79
<b>42</b>	1.03	1.05	1.00	1.04
<b>43</b>	1.01	1.01	1.03	1.11

<sup>a</sup> Slight differences in chemical shifts between **3** and **4**, essentially at position C16 and C17, appear fully consistent with the different substitution pattern at C19 of the two spiroptides.

Firstly, the occurrence of a singlet accounting for three protons at  $\delta$  1.19 ppm in the <sup>1</sup>H-NMR spectrum of **4** was diagnostic of the presence of an extra methyl group, in accordance with its molecular formula in comparison to that of **3**. An in parallel study of COSY and z-TOCSY spectra led to the individuation of six spin systems represented in bold in figure 2:

A spin system: C-1/C-4 including C-36

B spin system: C-5/C-9 including C-37, C-38, and the segment C-34/C-35

C spin system: C-10/C-14

D spin system: C-16/C-17

E spin system: C-19/C-27 including C-40 and C-41

F spin system: C-30/C-33 including C-42 and C-43

Despite the fact that A, B, and E spin systems featured some quaternary carbons (namely, C-2, C-5, C-6, C-19, and C-24) key long-range correlations emerging from the z-TOCSY spectrum allowed us to unambiguously define the complete connectivity of each of the spin systems. As for E spin system – where only some remarkable differences in comparison to **3** had been detected (Table.1) - we individuated a connectivity from H-20 through H-27 that included also H<sub>3</sub>-40. This way, the extra methyl - highlighted by <sup>1</sup>H-NMR spectrum- was located at position C-19. Eventually, the six spin systems of **4** were connected to each other on the basis of some crucial ROE correlations reported in the Experimental Section.

The planar structure of **4** was further corroborated by HRMS/MS experiments. Accordingly to the characteristic MS/MS fragmentation pattern of spiroptides, the HRMS/MS spectrum of **4** (Figure 4) contained:

- 1) ion peaks due to subsequent loss of three water molecules from the [M+H]<sup>+</sup> ion;
- 2) A-type fragment ions at  $m/z$  478.3160, 460.3053, and 442.2948 corresponding to C<sub>27</sub>H<sub>44</sub>NO<sub>6</sub> ( $\delta$  = -0.658 ppm ) and subsequent loss of two water molecules, respectively;



3) an abundant peak at  $m/z$  180.1381 inferring the molecular formula  $C_{11}H_{18}NO$  ( $\delta = -1.059$  ppm) to the B-type fragment. Such results, once compared with the MS/MS fragmentation pattern of **3**, confirmed that the extra methyl group - located at C-19 in **4** on the basis of NMR evidence - was indeed housed in the region encompassing C12/C25.

In conclusion, we confidently identified **4** as 27-hydroxy-13-desmethyl spiroside C (**4**). It is to be noted that the above HRMS data of **4** were superimposable with those obtained by Sleno et al. for a spiroside at  $m/z$  708.5 detected in a Canadian *A. ostensfeldii* culture and whose structure had not been completely assigned.<sup>11</sup>

### 9.2.2. 27-oxo-13,19-didesmethylspiroside C: Structure determination (**5**)

The HRMS spectrum of **5** showed an  $[M+H]^+$  ion at  $m/z$  692.4148, which allowed to infer the molecular formula  $C_{41}H_{57}NO_8$  to **5** ( $\delta = 1.291$  ppm). This pointed out that **5** presented 2 hydrogen atoms less than **3** ( $C_{41}H_{59}NO_8$ ). The HRMS/MS spectrum of **5** contained:

- 1) ion peaks due to two subsequent losses of water molecules from the  $[M+H]^+$  ion;
- 2) one A-type fragment ion at  $m/z$  444.2744, corresponding to  $C_{26}H_{38}NO_5$  ( $\delta = -0.112$  ppm);
- 3) an abundant peak at  $m/z$  178.1223 inferring the molecular formula  $C_{11}H_{16}NO$  ( $\delta = -1.913$  ppm) to the B-type fragment. Comparison between fragmentation patterns of **5** and **3** suggested that in the B-type fragment of **5** there was an additional unsaturation.

Structural elucidation of **5** was essentially carried out as reported above for 27-hydroxy-13-desmethyl spiroside C. Once individuated the six spin systems (A-F) displayed in bold in figure **3** through an in parallel analysis of COSY and z-TOCSY experiments, we noticed that all but one of the six systems turned out basically superimposable with the corresponding spin systems of **3** (Table.1). Significant differences in chemical shifts were indeed detected only in E spin system and in particular along the C-25/C-26 segment. Unlike **3**, this latter spin system did not include H-27. So, we concluded that the C-27 had to be a ketone functionality as deduced by the remarkable downfield shift of the proton resonating values of both H<sub>2</sub>-25 and H<sub>2</sub>-26 in comparison to **3** that features a -OH group at C-27.

In conclusion, we identified this new spiroside as 27-oxo-13,19-didesmethylspiroside C (**5**).

### 9.3. References

1. Balech, E., Tangen, K., 1985. Morphology and taxonomy of toxic species in the Tamarensis group (Dinophyceae): *Alexandrium excavatum* (Braarud) comb. nov. and *Alexandrium ostensfeldii* (Paulsen) comb. nov. Sarsia 70, 333–343.

2. Cembella, A.D., Lewis, N.I., Quilliam, M.A., 1999. Spirolide composition of micro-extracted pooled cells isolated from natural plankton assemblages and from cultures of dinoflagellate *Alexandrium ostenfeldii*. *Nat. Toxins* 7, 197–206.
3. Cembella, A.D., Quilliam, M.A., Lewis, N.I., 2000. The marine dinoflagellate *Alexandrium ostenfeldii* (Dinophyceae) as the causative organism of spirolide shellfish toxins. *Phycologia* 39, 67–74.
4. Ciminiello, P., Dell'Aversano, C., Fattorusso, E., Magno, S., Tartaglione, L., Cangini, M., Pompei, M., Guerrini, F., Boni, L., Pistocchi, R., 2006. Toxin profile of *Alexandrium ostenfeldii* (Dinophyceae) from the northern Adriatic Sea revealed by liquid chromatography-mass spectrometry. *Toxicon* 47, 597–604.
5. Ciminiello, P., Dell'Aversano, C., Fattorusso, E., Forino, M., Grauso, L., Tartaglione, L., Guerrini, F., Pistocchi, R., 2007. Spirolide toxin profile of Adriatic *Alexandrium ostenfeldii* cultures and structure elucidation of 27-hydroxy-13,19-didesmethyl spirolide C. *J. Nat. Prod.* 70, 1878–1883.
6. Ciminiello, P., Catalanotti, B., Dell'Aversano, C., Fattorusso, C., Fattorusso, E., Forino, M., Grauso, L., Leo, A., Tartaglione, L., 2009. Full relative stereochemistry assignment and conformational analysis of 13,19- didesmethyl spirolide C. via NMR- and molecular modeling-based techniques. A step towards understanding spirolide's mechanism of action. *Org. Biomol. Chem.* 7, 3613–3880.
7. Ciminiello, P., Dell'Aversano, C., Fattorusso, E., Forino, M., Tartaglione, L., Boschetti, L., Rubini, S., Cangini, M., Pigozzi, S., Poletti, R., 2010. Complex toxin profile of *Mytilus galloprovincialis* from the Adriatic Sea revealed by LC-MS. *Toxicon* 55, 280–288.
8. Guillard, R.R.L., 1975. Culture of Phytoplankton for Feeding Marine Invertebrates. In: Smith, W.L., Chanley, M.H. (Eds.), *Culture of Marine Invertebrates Animals*. Plenum Press, New York, pp. 26–60.
9. Hoshaw, R.W., Rosowski, J.R., 1973. Culture Methods and Growth Measurements. In: Stein, J.R. (Ed.), *Handbook of Phycological Methods*. Cambridge University Press, New York, pp. 53–67.
10. Hu, T., Curtis, J.M., Oshima, Y., Quilliam, M.A., Walter, J.A., Watson- Wright, W.M., Wright, J.L.C., 1995. Spirolides B and D, two novel macrocycles isolated from the digestive glands of shellfish. *J. Chem. Soc. Chem. Commun.* 20, 2159–2161.
11. Hu, T., Curtis, J.M., Walter, J.A., Wright, J.L.C., 1996. Characterization of biologically inactive spirolides E and F: identification of the spirolide pharmacophore. *Tetrahedron Lett.* 37, 7671–7674.

12. Mackenzie, L., White, D., Oshima, Y., Kapa, J., 1996. The resting cyst of *Alexandrium ostenfeldii* (Dinophyceae) in New Zealand. *Phycologia* 35, 148–155.
13. MacKinnon, S.L., Walter, J.A., Quilliam, M.A., Cembella, A.D., LeBlanc, P., Burton, I.W., Hardstaff, W.R., Lewis, N.I., 2006. Spirolides isolated from Danish strains of the toxicogenic dinoflagellate *Alexandrium ostenfeldii*. *J. Nat. Prod.* 69, 983–987.
14. Richard, D., Arsenault, E., Cembella, A.D., Quilliam, M.A., 2001. Investigations into the Toxicology and Pharmacology of Spirolides, a Novel Group of Shellfish Toxins. In: Hallegraeff, G.M., Blackburn, S.I., Bolch, C.J., Lewis, R.J. (Eds.), *Intergovernmental Oceanographic Commission of UNESCO. Harmful Algal Blooms 2000*, Paris, pp. 383–386.
15. Sleno, L., Chalmers, M.J., Volmer, D.A., 2004. Structural study of spirolide marine toxins by mass spectrometry. Part II. Mass spectrometric characterization of unknown spirolides and related compounds in a cultured phytoplankton extract. *Anal. Bioanal. Chem.* 378, 977–986.
16. Utermöhl, H., 1958. Zur Vervollkommnung der quantitativen Phytoplankton- Methodik. *Mitt. Int. Verein. Limnol.* 9, 1–38.

*Alla mia famiglia, che mi ha donato tutto e mi ha insegnato a vivere;*

*Alla Prof.ssa Ciminiello, che mi ha permesso di far parte del suo gruppo di ricerca, arricchendomi tante volte, non solo scientificamente, ma anche umanamente;*

*Al Prof. Fattorusso, che mi ha insegnato a guardare sempre oltre;*

*Al Dott. Forino e alla Dott.ssa Dell'Aversano, per avermi insegnato molto e dedicato tanto del loro prezioso tempo;*

*Alla Dott.ssa Tartaglione, con la quale ho condiviso le piccole vittorie e le piccole sconfitte di ogni giorno, che mi ha insegnato tantissimo e alla quale ho imparato a volere un gran bene;*

*A Lairetta, diventata per me un'amica preziosa;*

*A tutti gli interni del LAB 515, che mi sono entrati nel cuore;*

*A Rocco, amico fraterno;*

*Alla Dott.ssa Imperatore, amica e confidente;*

*A Paolo, Ciro I. e Ciro P., che mi hanno sostenuta e aiutata in questo lavoro di tesi;*

*A Cristina e Carmen, colleghe di dottorato, ma soprattutto amiche, con le quali ho condiviso ogni piccolo passo verso questo traguardo;*

*A tutti i Prof, ricercatori e dottori del Dipartimento di Chimica delle Sostanze Naturali, dove mi sono sempre sentita a casa;*

*A chi mi vuole bene e ha gioito con me di ogni piccolo e grande traguardo raggiunto;*

*A chi ha sempre creduto in me...*

**Grazie di cuore!**  
**Emma**